NANO-STRUCTURAL MODIFICATION OF g-C_3N_4 WITH V_2O_5 AND La_2O_3 EMBEDDED WITH GRAPHENE OXIDE FOR PHOTOCATALYTIC MINERALIZATION OF PESTICIDES

Thesis

Submitted for the Award of the Degree of

DOCTOR OF PHILOSOPHY

in

Environmental Sciences

By

Sahima Tabasum

Registration Number: 11916600

Supervised By

Dr. Ajit Kumar Sharma (24338)

Associate Professor, Department of Chemistry

Lovely Professional University

LOVELY PROFESSIONAL UNIVERSITY, PUNJAB

2023

DECLARATION

I, hereby declared that the presented work in the thesis entitled " **Nano-structural modification of g-C_3N_4 with V_2O_5 and La_2O_3 embedded with graphene oxide for photocatalytic mineralization of pesticides**" in fulfilment of the degree of **Doctor of Philosophy (Ph. D.)** is the outcome of research work carried out by me under the supervision Dr. Ajit Kumar Sharma, working as Associate Professor in the Department of Chemistry, School of Chemical Engineering and Physical Sciences, Lovely Professional University, Punjab, India. In keeping with general practice of reporting scientific observations, due acknowledgements have been made whenever work described here has been based on findings of other investigator. This work has not been submitted in part or full to any other University or Institute for the award of any degree.

(Signature of Scholar)

Sahima Tabasum

Registration No.: **11916600**

Department/School: School of Chemical Engineering and Physical Sciences

Lovely Professional University,

Punjab, India

CERTIFICATE

This is to certify that the work reported in the Ph. D. thesis entitled "**Nano-structural modification of g-C_3N_4 with V_2O_5 and La_2O_3 embedded with graphene oxide for photocatalytic mineralization of pesticides**" submitted in fulfillment of the requirement for the reward of degree of **Doctor of Philosophy (Ph.D.)** in the Department of Environmental Sciences, School of Chemical Engineering and Physical Sciences, Lovely Professional University, Punjab, India is a research work carried out by Sahima Tabasum, (**11916600**), is bonafide record of his/her original work carried out under my supervision and that no part of thesis has been submitted for any other degree, diploma or equivalent course.

(Signature of Supervisor)

Dr. Ajit Kumar Sharma

Associate Professor

School of Chemical Engineering and Physical Sciences

Lovely Professional University, Punjab, India

ABSTRACT

Pesticides are among the most dangerous toxins to which humans have ever been exposed. Due to the excessive and frequent use of pesticides, as well as a lack of information, the ecosystems of the soil and water have been significantly damaged. This has resulted in severe problems for humans. Even though there is a wide variety of remediation technology that may be utilized for cleaning up pesticide contamination in soil and water, selecting the approach that will be most effective can be a tough job. Photocatalysis appears to be the ideal strategy that can overcome the limits of the other approaches that can be employed to get rid of the persistent pesticide. This is because photocatalysis can convert light energy into chemical energy. The photocatalytic process transforms potentially hazardous organic pollutants into CO_2, H_2O, and a number of other simple acids and salts. One of the advantages of employing photocatalysis is that it eliminates the need for a secondary method of waste disposal. This is one of the many benefits of using photocatalysis. Lately, g-C_3N_4 has been receiving a lot of interest because of its many useful properties.

The graphitic carbon nitride is a fascinating metal-free semiconductor that, as a result of its polymeric-conjugated structure, possesses synergistic adsorption capabilities. These qualities make it a viable photocatalyst for use in the purification of water. Due to their low band gap (2.7 eV), which is sufficient for catalyzing a wide range of photocatalytic degradation in environmental remediation and (ii) production of electron (e-) and hole (h+) pairs, g-C_3N_4 -based nanocomposites have recently attracted a great deal of attention and made significant progress in the field of photocatalysis. This is due to the fact that in recent times, these nanocomposites have been used. Unfortunately, g-C_3N_4 has significant limitations that prevent it from being used effectively in photocatalysis. Because of this, the recombination rate of the photogenerated charge is high, and g-C_3N_4 also has a poor specific surface area. To this day, ongoing research efforts have been performed in an effort to boost the degrading efficiency of g-C_3N_4. These efforts have included grafting nonporous g-C_3N_4, metal doping, non-metal doping, and other similar strategies.

Combining g-C_3N_4 with other materials that have band gaps that are suited for the purpose of expanding the absorption range of g-C_3N_4 is the most promising solution. In the meantime, hetero-junctions may be established between the g-C_3N_4 and the other material introduced. These hetero-junctions have the potential to distribute a potential driving force for the separation of

photogenerated charges at the interfaces. It is possible to increase the photocatalytic activity of g-C_3N_4 through the preparation of g-C_3N_4 composites, which, due to their increased photocatalytic efficiency, also increase the catalytic activities of the material. As a result, the primary focus of this thesis is on the development of a novel photocatalysis that may degrade pesticides i.e Chlorpyrifos and Carbofuran and that is activated by irradiation with visible light and possesses photocatalytic capabilities.

In light of this, a number of different g-C_3N_4 nanocomposites, including g-C_3N_4/GO, g-C_3N_4 /V_2O_5, g-C_3N_4/GO/V_2O_5, g-C_3N_4/La_2O_3, and g-C_3N_4/GO/La_2O_3, were manufactured by using the calcination method and hydrothermal method. XRD, FT-IR, SEM, DRS-UV, and TGA were among the physio-chemical techniques that were utilized in the process of characterizing every material that was synthesized.

XRD and FTIR results revealed the formation of nanocomposite and also confirm the co-existence of bare material with g-C_3N_4. From the XRD results, it was observed that g-C_3N_4 remains in the same phase in the prepared nanocomposites. The band gap energy of the nanocomposites was determined by using DRS-UV spectroscopy and shows the active absorption in the visible region.

The adsorption efficiency and photocatalytic activity of prepared nanocomposites were examined for Chlorpyrifos and Carbofuran under visible light as irradiation sources at optimized reaction conditions. However, the removal of both pesticides was achieved maximum by ternary nanocomposites i.e. 87 to 88%. From the overall results, g-C_3N_4 with ternary nanocomposites efficiently removes the pesticides through the photodegradation process.

This is due to the fact that it is simple to produce, that it possesses a controllable electronic structure, that it possesses an adequate response to visible light, and that it possesses an appropriate optical bandgap. In addition to this, g-C_3N_4 possesses a correct optical bandgap, and the sp^2-hybridized nitrogen (N) and carbon (C) atoms inside its structure have conjugated electronic structures. These configurations are also consistent with the existence of long-lasting covalent connections between the N and C atoms, which can be found between them. In addition to this, the sp^2 hybridized-conjugated electronic structure was responsible for the presence of unsaturated nitrogen (N) atoms in the tri-s-triazine-linked amino-group layers.

Dedicated to

my Loving Parents

and Siblings

This humble work is a sign of my love, and affection for them.

ACKNOWLEDGEMENT

All praises to Allah the Almighty, the Most Gracious, and the Most Merciful for his blessing. I thank Almighty for all the opportunities, challenges, and perseverance that have enabled me to complete this project.

My humble gratitude to the Prophet Mohammed PBUH, Prophet Isa (Jesus) PBUH and all Prophets their way of life has been an unending inspiration for me.

It gives me immense pleasure and happiness to express my gratitude to all those people who have been part of this journey.

First and foremost, I would like to sincerely thank my advisor, **Dr. Ajit Kumar Sharma** (Associate Professor, School of Chemical Engineering and Physical Sciences), for his continuous guidance, understanding, and most importantly, for providing me with positive encouragement and a welcoming spirit to complete this project. It has been an honor and a pleasure to have him as my guide.

I am highly thankful to all my Doctoral Advisory Committee members for their valuable suggestions and scientific input in my Ph.D. work. Sincere thanks to **Dr. Navdeep Singh, Dr. Harminder Pal Singh, Dr. Gurpinder Singh, Dr. Harminder Singh, Dr. Rekha, Dr. Nupur** and **Dr. Ragini Gupta**. Their critical feedback has been instrumental in improving the quality of this thesis. I would like to express my sincere gratitude to **Dr. Neelam Verma**, for helping me in the initial phase of my Ph.D.

I am thankful to **Monika, Riya, Ashima, Suman, Neetu, Upasana, Saima, Karan**, and all the lab mates for their support during this project. I am very much thankful to **Manoj sir** for providing all chemicals and apparatus on time and **Sandeep sir** for always helping me in the lab.

I sincerely thank LPU for providing all the infrastructure for my research work and a good learning environment.

I grateful to GOI and Waste to Wealth Mission for providing financial support during my Ph.D.

Furthermore, a number of people have knowingly and unknowingly helped me in completing this project. Perhaps, I forgot someone. I owe my loving thanks to whom it concerns.

Words are inadequate to thank my friends **Savita, Qurat-ul-Ain, Tunisha, Nancy George**, and **Monika** who were always with me in the good and bad phases of my research period, helping me in writing the manuscript, thesis, in experimental work, and for all the fun we have had in all these four years. I express special thanks to my twin soul **Asma** for all the gossip, discussions, and time spent together.

The love, support, and blessing of one's family are essential to every successful endeavor. I would like to express my profound love for my parents, **Rayaz Anjum** and **Mohammad Iqbal**. To my father, I am truly blessed to have you as my father, your belief in me and my abilities has been a constant source of inspiration throughout my academic journey. Your encouragement, financial help, guidance, and wisdom have been invaluable in helping me to navigate the challenges of pursuing a Ph.D. To my mother, your sacrifices, both big and small, have made it possible for me to pursue my dreams to reach this significant milestone. I am truly grateful for your endless patience, your listening ear, and your unwavering support.

My life would not be possible without my beloved siblings, I would like to express my sincerest gratitude to **Tehseen, Attia, Sadhia**, and **Danish** who is my favorite for your disagreement, criticism, fights, and quality time spent the over years. Your unwavering support, help, encouragement, and belief in me have been a constant source of inspiration throughout my academic journey. Thank you for always reminding me of my strengths and pushing me to reach my full potential. I want to thank you all for being my biggest supporters and my driving force. You all were the source of happiness, positive vibes and love throughout my journey. In short, I am privileged to say that I have the **"Best Family"** anyone can ask for and owe my existence and survival to them.

Sahima Tabasum

TABLE OF CONTENTS

LIST OF CONTENT

LIST OF ABBREVIATION

g-C_3N_4	Graphitic carbon nitride
GO	Graphene oxide
V_2O_5	Vanadium pentoxide
θ	Theta
La_2O_3	Lanthanum oxide
cm^{-1}	Centimeter inverse
CBF	Carbofuran
OP	Organophosphorus
OC	Organochlorine
OH	Organohalogen
OCPs	Organochlorine pesticides
DDT	Dichlorodiphenyltrichloroethane
HCH	Hexachlorocyclohexane
HCB	Hexachlorobenzene
P	Phosphorus atom
ACh	Neurotransmitter acetylcholine
CNS	Central Nervous System
AChE	Acetylcholine esterase enzyme
ARfD	Acute Reference Dose
MRL	Maximum residue limit
FDA	Food and drug administration
CP	Chlorpyrifos
USEPA	United states environment protection agency
mg/l	Milligram per liter
ug/l	Microgram per liter
CYP2B6	Cytochrome P450
TCP	3,5,6-trichloro-2-pyridinol
DEP	Diethyl phosphate

DETP	Diethyl thiophosphate
RfD	Dietary reference dose
AOEL	Acute oral exposure limit
CO_2	Carbon dioxide
(HUVECs)	human umbilical vein endothelial cells
MTT assay	3-[4,5-dimethylthiazol-2-yl]-2,5 diphenyl tetrazolium bromide
Bt cotton	Bacillus thuringiensis
BHC	Benzene Hexachloride
HYVs	High-yielding varieties
CIBRC	Central Insecticides Board and Registration Committee of India
AOPs	Advanced oxidation processes" (AOPs)
OH	Hydroxyl radicals
CB	Conduction band
VB	Valence band
eV	Electron volt
N	Nitrogen
$La(NO_3)_3.6H_2O$	Lanthanum nitrate
C_3N_4	Cyanide nitrogen
PCs	Photocatalysis
AU	Gold
P-N bond	Phosphorous mononitride
H_2O_2	Hydrogen peroxide
MNPs	Metal oxide nanoparticles
NPs	Nanoparticles
PSF substrate	Polysulfone
SMX	Sulfamethoxazole
CNT	Carbon nanotubes
Fc	Ferrocene carboxaldehyde (Fc)

TBT	Tebuthiuron
QTAIM	Quantum theory of atoms in molecules
BCP	Bond critical point
EHB	European Hydrogen Backbone
TMX	Thiamethoxam
COOH	Carboxylic acid
XRD	X-Ray diffraction
FT-IR	Fourier Transform-infrared spectroscopy
SEM	Scanning electron microscopy
EDX	Energy Dispersive X-ray spectroscopy
TGA	Thermogravimetric Analysis
DRS	Diffused Reflectance Spectroscopy
KOH	Potassium hydroxide
RGO	Reduced graphene oxide
NCDS	N-doped Cadmium sulfide
IDM	Indomethacin
HCL	Hydrochloric acid
NaOH	Sodium Hydroxide
KBr	Potassium Bromide
ATR sampling	Attenuated total reflection
IR spectrum	Infrared
FWHM	Full width and half maximum
hkl	Miller index
CuKα radiation	Copper K-alpha
MoKα	Molybdenum K-alpha
TiO_2	Titanium dioxide
ZnO	Zinc oxide
CeO_2	Cerium dioxide
Ag_3PO_4	Silver phosphate
Bi_2WO_6	Bismuth tungstate

NiO/WO_3	Nickel oxide/tri tungsten oxide
Fe_3O_4	Iron (II, III) oxide

LIST OF TABLES

LIST OF FIGURES

CHAPTER-1

INTRODUCTION

Protecting and developing the human environment has become a major priority, for global economic development. Every individual must preserve and improve the environment for the benefit of all the people and their prosperity. Since the beginning of life on earth, human actions have been the primary cause of pollution of the environment. Discharging industrial wastewater containing dyes, heavy sources of pesticide. The wastewater that is produced by agricultural sectors as well as manufacturing and formulation factories for pesticides is the most significant point cause of insecticide pollution. As a result, the waste coming from these sources needs to be cleaned up or broken down before it can be released into bodies of water. The removal of pesticides from wastewater is now accomplished through a variety of processes. On the other hand, the vast majority of them are both expensive and unable to provide a particular level of fulfillment.

1.1 INTRODUCTION

One of the most significant activities worldwide is agriculture. It occupies the most significant position on the Indian economy's socioeconomic front and is also the major component of the world economy. Because of the increased need for food caused by the growing global population over the past few decades, pollution from agricultural practices has become an issue. Conventional farming practices are modified to include the use of supplemental chemical fertilizers, insecticides, weedicides, and many other similar products and methods in order to protect fields and farms from damage and increase their overall productivity. The advancement of contemporary technology, which is dependent on artificial fertilizers, has led to the development of agrochemicals. The excessive use of agrochemicals also contributes to agricultural pollution, which contaminates the surrounding environment. The overuse of these substances causes ecological imbalance and produces unexpected, deadly effects (Subash et al., 2017).

The usage of pesticides to protect crops against insects and pests that reduce crop yield and quality has been a major driver in the evolution of agricultural techniques over the past few decades. Plant protection products (PPP) have been used in agriculture for a while; shortly after the green revolution, these pesticides were widely used throughout the world. Pests in the field are thought to be causing more than 40% of crops (Jacob, 2018). To maintain their efficiency after application, these chemicals are therefore created and intended to persist for longer.

1.2 Pesticides:

In general, the term pesticides refer to the group of synthetic compounds employed to ensure food security and meet the world population's demand. The chemical that is used to eradicate pests is commonly referred to as 'pesticides' (Ahmad et al., 2011, Fenoll et al., 2013). Pesticides are made up of inorganic and organic molecules to manage weeds in lawns and fields and undesired or dangerous pests like insects and mites that feed on crops. In terms of their chemical composition, pesticides are an extremely complicated class of substances occasionally, a breakdown product or intermediary is more deadly than the original component. The four detrimental effects of pesticides are so awful that they have the potential to change the course of evolution (Abhilash et al., 2009).

According to the findings of a number of studies, more than 98% of the pesticides that are used in agricultural settings do not degrade quickly at the site of application and, as a consequence, end up damaging the environment (Fenoll et al., 2011). Concerns have been raised regarding the potential adverse impact that the widespread use of a wide range of pesticides through a variability of chemical structures may have on both the health of humans and the health of the environment. Concerns about potential neurological impairments in children have been raised as a result of the prenatal or early postnatal exposure of pregnant women or newborns to pesticides (Anand et al. 2021, Muhamad, 2010).

1.2.1 Pollution of pesticides

The invention of pesticides to control a wide range of pests was a major contributor to the Green Revolution, which changed society thereafter. To this day, the pesticide is recognized as the most dangerous toxin ever exposed to humans.

Because of the excessive use of pesticides in agricultural production, these chemicals can now be found in both surface water and groundwater sources. Most of this pollution came from runoff, drainage, and other things that happened at industrial sites and other places. Because pesticides stay in earth soil and water for longer periods and build up in the food chain, the pollution they cause has become a major problem for the ecosystem. The existence of organic pollutants in water is an indication that the majority of these compounds are non-biodegradable, resistant, and persistent; as a result, they have the potential to persist in the environment for huge time period. Despite physicochemical and biological pesticide treatment, residual pesticide wastes have been observed to persist in terrestrial and aquatic environments Xue et al., 2014, Mubushar et al., 2019). Higher concentrations of these compounds exacerbate pollution in the soil and water. Most synthetic pesticides are fat soluble, which allows them to easily bind to creatures' bodies and promote biomagnification of these substances in the food chain. Compounds of insecticides such as imidacloprid and acetamiprid, which pose a threat to all organisms (earthworms, bees), are highly dangerous to food webs in terrestrial ecosystems. (Kenko et al., 2023).

Pesticides attack the neurological system and mimic hormones, causing cancer in many cases and even death in extreme circumstances (US Environment Protection Agency, 2014). According to Miller (2004), more than a million agricultural laborers experience pesticide poisoning symptoms each year.

The overall value of pesticides used across the globe is estimated to be 6 million tonnes, but only 1% to 3% of the pesticides that are applied to crops actually reach their intended targets. The remaining pesticides either have an effect on non-intended organisms or are released into the environment, where they contaminate the water, soil, and air. There are about 1500 different kinds of chemicals that are used as pesticides around the world (Bolognesi and Merlo, 2011). Due to the chemical nature of pesticides, they can result in major issues for both the environment and human health. There are a total of 108 pesticide distinct types, 39 herbicide types, 30 fungicide types, 6 rodenticides types, and 5 acaricides types that are utilized in Pakistani agriculture (Anwar et al., 2011; Muhammad et al., 2021). It is estimated that the total amount spent worldwide on pesticides saw a considerable increase between the years 2008 and 2012. Between 2008 and 2012, the entire amount spent on pesticides came to almost $56 billion (Mubushar et al., 2019). Because it is not very specific, a pesticide can kill both the pests it is meant to kill and other animals and people. Still, the pesticide should only be harmful to the pests it is meant to kill, not to people or other animals (Sharma et al., 2020).

The extensive use of chemical pesticides in intensive agricultural methods has led to an increase in the presence of pesticides and their five intermediary chemicals in soil, surface water, and groundwater over the past few years. The fact that another insecticide i.e. Organochlorine was found in water 20 years after its usage of the pesticide in question is evidence that pesticides can persist for long periods in the environment (Ullah et al., 2012). Some pesticides can accumulate in the food chain, be able to penetrate the deepest layers of soil, be absorbed by roots, and be biologically active. Figure 1.1 shows pesticide pollution.

Figure 1.1 Pesticide pollution

(Source-Google images)

1.2.2 Pesticide Pollution source

Industrial compounds, organic cleaners, insecticides, and cleansing agent are some examples of the many different types of persistent pollutants that can be found in an environment. Water-soluble pesticides are a major cause for concern as a result of this (Ollera et al., 2006, Blankson et al., 2016). The improper management of pesticides, particularly their application, and removal on farms, is the primary cause of contamination with these chemicals (Anderson and Yerraguntla, 2002). Through the process of biomagnification, pesticides that come from a different source, an make a major contribution to the poisoning of the environment. Both, directly and indirectly, introducing pesticides into the ecosystem are two conceivable pathways for their introduction (Duirk et al., 2005; Devi et al., 2009). There is a different source of contamination of insecticides, i.e. non point and point sources. Some of these sources are more widespread than others. Point sources are a type of pollution that comes from specific locations that can be pinpointed and located. Inappropriate management also discarding of waste near aquatic environment, soil leaching, wastewater from spray tank rinsing, and pesticide-contaminated crop debris are the most common releases of pesticides into the environment.

Other common pathways are farmland emissions, municipal solid waste, pesticide use in agriculture, effluents from agribusiness (fruit and vegetable washing), and pesticide contamination. crop residue. Soil penetration, wastewater from washing spraying containers, and discharge from agricultural sources are three other frequent ways. Yet, the washing of spraying containers is by far the most common cause of pollution caused by pesticides. One example of pollution from a non-point source is the contamination of water by pesticides, which affects both aquatic and terrestrial ecosystems. This type of source originates from a broad region, so it is impossible to determine exactly where the contamination originated. Pesticides that move from surface water to groundwater from more than one source are an example of a non-point source. Because agricultural waste disposal, companies that make pesticides, and runoff posed the biggest threat to water bodies, and because agricultural waste and runoff can sometimes form toxic intermediates that are much more dangerous than the compounds from which they came (Herrmann and Guillard, 2000). The amount of this contaminant that can be found in water can range anywhere from ng/l^{-1} to mg/l^{-1}. There have been many different treatment technologies used up to now, but most of them have not been successful in achieving sufficient degradation (Gaya and Abdullah, 2008).

1.3. Pesticides in the Environment

Pesticides can pollute atmospheric pollution. When pesticides are in the form of particles that are floating in the air, a process known as pesticide drift can take place. This occurs when these particles are carried by the wind to other locations, where they could possibly pollute other areas. It is possible for pesticides that have been sprayed on crops to volatilize and be carried by the wind to places nearby, where they could pose a risk to the local wildlife population. As a result of this, the quantity of inhalable pesticides that are present in the external environment varies significantly from one season to the next. In addition, according to a report that was published by the United States Environmental Protection Agency in 2007, droplets of pesticides that have been sprayed or particles of pesticides that have been treated as dust may be carried by the wind to other regions.

The contamination of groundwater with pesticides is an issue that is of national relevance since almost half of the population of India drinks water that comes from groundwater sources. Because about a million people who live in agricultural areas, where pesticides are most often

used, get their drinking water from the ground, this is a very important issue for them (Hashmi et al., 2012). The five agricultural herbicides, the five non-agricultural herbicides, and the three insecticides were the most frequently found pesticides in rivers and groundwater. Pesticides can get into water-bearing aquifers below the ground in a number of ways, such as when they are put on crop fields, when contaminated surface water seeps down, when there are spills or leaks, when they are not thrown away properly, or when waste is put into wells.

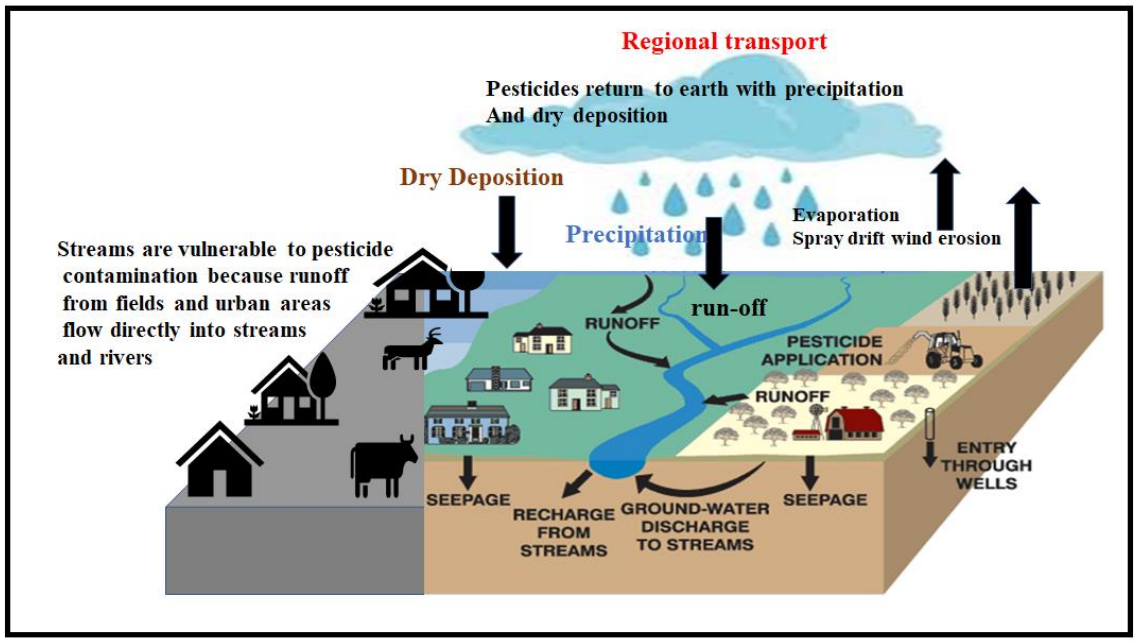

Figure 1.2. Movement of Pesticides in the Environment

(Images modified: source Google image)

The application of pesticides on Earth can have a number of different outcomes, and the diagram in figure 1.2 provides an overview of those outcomes as they occur in the natural world. Adsorption, volatilization, leaching, runoff, absorption, and degradation are the primary pathways by which the substance can be eliminated (chemical degradation, biodegradation, and photodegradation). The solubility of the pesticide in water, its mobility in the soil, and its volatility are all factors that influence the physicochemical qualities of the chemical (Muszkat et al., 2002). In spite of the low concentration of this contaminant, it poses a significant threat to both human and environmental health due to the fact that it is not completely removed during the treatment process (Sivaperumal et al., 2022).

The effects of pesticides on aquatic systems are frequently investigated with the help of a hydrological transport model, which is used to investigate the destiny of substances in waterways. Quantitative analyses of pesticide runoff have been performed as far back as the 1970s in order to provide predictions about the amounts of pesticide that will end up in surface waters (Hogan et al., 1973). Pesticides can enter bodies of water in one of four primary ways: they can permeate or seep into the earth, runoff to waterbodies, or they can be discharged for a variety of reasons, such as intentionally or through negligence. These are the primary ways that pesticides can enter bodies of water. Erosion of the soil can also transport them to bodies of water. Pesticides can pollute water in a number of ways, depending on how well others solve in water, how far they are from a body of water, the type of soil, the weather, whether or not a crop is growing, and how they were applied (Pedersen, 1997). If water is contaminated with pesticides, it could be harmful to fish and another aquatic biota. The runoff of pesticides from land to waterbodies can be extremely harmful, and can even wipe out an entire stream's fish population. The use of herbicides in bodies of water has the potential to eradicate plant life, including that upon which fish depend for their habitat. It is possible for pesticides to build up in water bodies and are lethal to zooplankton, which is the primary food supply for younger fish. Pesticides have the potential to kill off insects that certain species of fish feed on, (Helfrich et al., 1996). The food chain is responsible for the accumulation of more than 80 percent of the pesticide residues found in humans (Ashesh et al., 2022). It would appear that frogs are subject to a cumulatively harmful effect from pesticide combinations. Tadpoles that grow in ponds that are contaminated with many types of pesticides take longer to develop into frogs and are smaller when they do so, which reduces their capacity to hunt and avoid being eaten (Science Daily, 3 Feb 2006).

The presence of insecticides in the body of water is exacerbated by both the runoff that comes from agricultural areas and the wastewater that comes from industrial processes. The matrix of the soil can serve as a storage space for pesticides and other chemicals because of the strong affinity that these substances have with the ground. On the other hand, due of the close relationship that the soil has with the bodies of water, both the surface water resources and the groundwater are vulnerable to being contaminated by pesticides (Syafrudin et al., 2021, Subash et al., 2018). Via agriculture and other means, the Ganga, which is the country's second largest river, is directly or indirectly responsible for the well-being of 36.1% of nation's over-all people

(Shah and Parveen, 2021). Large-scale human activities, such as the disposal of industrial and household waste, the building of dams and barrages, the use of fertilizers and pesticides in agricultural areas, and so on, have had a big effect on the biological processes that took place in the Ganga in the past. In the past, these activities had a big effect on the biological processes that happened in the Ganga. The increased use of pesticides in the agricultural fields along the river basin led to their bioaccumulation in the environment through a variety of different ways (Dar et al., 2023).

1.4. Classification of pesticide

Since the first synthetic pesticide was developed in 1940, there has been a rapid expansion in the usage of these substances; at the present time, more than 10,000 unique formulations of around 1500 distinct pesticides are registered across the globe (Ecobichon, 2001, Kaur et al., 2019). It is possible to classify pesticides into two main categories: (a) the kind of pest that they are designed to eradicate, and (b) the chemical family to which they belong. Insecticides, herbicides, rodenticides, algaecides, fungicides, and bactericides are the many types of pesticides that may be classified according to the target species that they are intended to kill. Herbicides harm plants, insecticides kill insects and rodenticides kill rodents. Based on their chemical makeup, pesticides can be put into the following groups: (Dehghani and Fadaei, 2012).

Pyrethroids

Pyrethroids were first identified by a group of researchers working at the Rothamsted Research Centre in the United Kingdom. Subsequently, the structures of pyrethrin I and II were found. Pyrethroids have become a well-established constituent of the pesticide industry. They have notable benefits in terms of cost-effectiveness, low toxicity to mammalian organisms, and the control of insect populations that are resistant to other classes of pesticides (Elliott et al, 1978). Pyrethroids are created by synthesizing pyrethrins, which are found in pyrethrum. These pyrethroids include permethrin, cyfluthrin, cypermethrin, fenvalerate, deltamethrin, bifenthrin, and others (Matsuo).

As a result of using pyrethroids as pesticides, some insect populations, especially mosquitoes, have become very resistant to them. This is a trait that has been passed down from generation

to generation. More and more people started to use pyrethroids to kill bedbugs, but bedbugs have since learned to avoid these chemicals as well (Goddard et al., 2009). Allethrin, Bifenthrin, Cyfluthrin, Cypermethrin, Esfenvalerate, Etofenprox, Fenpropathrin, Fenvalerate, Flucythrinate, Flumethrin, Imiprothrin, etc. are all examples of pyrethroids.

Pyrethroids are somewhat less hazardous to mammals as a result of the rapid biodegradation that occurs in mammalian livers when these chemicals are exposed to them; nonetheless, insects are more sensitive to the effects of these chemicals (Reigart and Roberts, 1999). They have the ability to cause neurotoxicity by preventing the voltage-gated sodium channels in the axon membranes from shutting. This results in the sodium channels being permanently activated, which leaves the membrane of the axons in a permanently depolarized condition. This results in the target organism being attacked by paralyzing agents, which ultimately results in death (Soderlund et al., 2012). The spread of insects that are harmful to crops like alfalfa, cotton, and lettuce, as well as orchards like almonds, pistachios, and peaches, can be stopped by applying these pesticides to the fields where the crops are grown. The realization that DDT and other organochlorine pesticides had undesirable effects led to a rise in the utilization of pyrethroids as a pest control method.

Organochlorine pesticides

Organochlorine pesticides, often known as OCPs, are compounds that have been chlorinated with a number of chlorine atoms in various places. These chemicals have the ability to kill insects. OCPs were originally introduced in the 1940s, and their use became widespread throughout the 1950s through the 1970s for the purpose of eradicating agricultural pests. These OCPs are well-known chemicals (Abhilash and Singh, 2009; Zhang et al.,2011). The majority of the organic chlorinated pesticides (OCPs) that are utilized include chlordane, dieldrin, aldrin, DDT, HCH, benzoepin, mirex, HCB, toxaphene, methoxychlor, and metolachlor. A person may have a multitude of symptoms if they are subjected to organochlorine for a short period of time. Some of these symptoms include head pains, wooziness, nausea, vomiting, tremors, disorientation, general weakness, muscular pain, slurred speech. These symptoms may develop as a direct consequence of organochlorine pesticides. When exposed for extended periods of time, organochlorine pesticides have the potential to cause damage to several organs and systems, including the thyroid, the bladder, the liver, and the central nervous system. It has

been found that exposure to a substantial number of these pesticides can lead to an elevated risk of cancer developing in the livers or kidneys of animals. Some data indicates that organochlorine insecticides may potentially cause cancer in humans. This data comes in the form of animal studies. There is a tendency for pesticides that include organochlorines to accumulate in the environment (Sultan et al., 2023). They are extremely hard to eradicate and can travel significant distances through surface runoff or groundwater. Prior to the middle of the 1970s, organochlorines were the cause of widespread reproductive failure in birds. This was due to the fact that birds deposited eggs with thin shells, which resulted in the eggs breaking before they could hatch.

The half-lives of different substances can be a few months to many years, and even ten years. OCPs are non-polar and readily soluble in lipids, and because they are non-biodegradable, they have a tendency to accumulate in magnified concentrations within the food chain. This is a problem because OCPs have the potential to cause health problems. As a result, they are able to bio-accumulate in the adipose tissue of organisms, as well as in breast milk, blood, and other bodily fluids. They are extremely stable in the environment, which makes it difficult for any kind of treatment system, whether it be chemical, physical, or biological, to break them down. OCPs can enter the bodies of people and other animals that are not their intended targets through a variety of different mediums, including food, dust, dirt, and other things. OCPs have also been shown to be transmitted from nursing moms to their children through the consumption of breast milk by the children. Because of their potential to interact with the endocrine and neurological systems of humans and other animal groups, they have an impact on human health. These pesticides, in addition to causing serious illness in humans, are also exceedingly harmful to the flora and fauna that live in water environments (Jayaraj et al., 2016).

Organophosphorus Pesticide (OPs)

Gerhard, a German chemist, is credited with the creation of the first organophosphate (OP) pesticide and with its subsequent commercialization under the brand name Bladan. Later on, in 1944, he also created another organophosphate insecticide called parathion. Among the many different types of pesticides, organophosphates (OPs) are the most well-known, broadly recognized, and frequently used insecticides all over the world. These insecticides have a broad spectrum of activity against multiple groups of plant pathogens that can cause damage to crops

(Marrs, 1993). OPs are responsible for roughly more than 38 percent of the overall usage of pesticides around the globe (Zhang et al., 2008). In addition, the 1930s and early 1940s were the years in which they were initially developed as insecticides. Later on, with the passage of time, a number of different organophosphorus pesticides were produced, and at the current time, these are the agents that are most commonly employed for pest management worldwide (Kumar, et al., 2016).

Prior to the 1970s, organochlorine pesticides were generally acknowledged as the primary type of pesticide composition. Over time, it was discovered that they also had a number of drawbacks, such as long-term persistence, a tendency to bioaccumulate in bodily tissues, and the ability to impose acute toxicological effects on other living forms that were not their intended target. In addition, OPs were initially utilized as an appealing alternative to organochlorine pesticides due to the fact that they are less persistent in ecosystems and have other advantageous qualities (Sidhu et al., 2019). Over the course of time, widespread use of organophosphates causes effects that are lethal to a wide variety of insect populations, as well as mammalian and other animal populations. OPs can make bonds with acetylcholine esterase, which is an enzyme in the central nervous system that helps send nerve impulses (Theriot and Grunden, 2011). These pesticides are used all over the world.

Despite anticholinergic treatment and the availability of modern comprehensive care facilities, the death rate for severe OP poisoning is from 25–40 percent. As a consequence of this, it is essential, while dealing with OP toxicity, to have sufficient knowledge of the pathophysiology induced by OPs and to promote creative therapeutic strategies (Dar et al., 2023).

In a single year, around 15,730 cases of severe poisoning caused by these insecticides were documented across India and Sri Lanka. These countries share a common language and culture. There was a total of 1,571 deaths as a result of these acute poisonings. According to the findings of epidemiological studies, India and Sri Lanka are two of the key countries where OP poisoning is a problem. According to the findings of a study that was conducted at the Kasturba Hospital in Manipal, India, on a total of one hundred patients who had been poisoned by OP, the age group that was most afflicted was between the ages of 21 and 30. The number of guys who were afflicted with the illness was significantly larger (68) than the number of

girls who were affected. The fatality rate reached as high as 25%, and 64.5% of those affected lived in rural areas, while 35.5% resided in urban areas. (Dar et al., 2023).

Approximately 80% of pesticide-related hospitalizations throughout the globe and serious human toxicities are associated with OPs poisonings (Eddleston et al., 2008). (Eddleston et al, 2008). The indiscriminate use of OPs is a global health concern that is responsible for around 3 million cases of poisoning and 200,000 fatalities per year. The contamination of agricultural areas brought on by the use of OPs chemicals and the subsequent entrance of those compounds into food chains is a source of serious and persistent toxicity to humans. Contamination of soil, crops, sediments, air, and groundwater with OPs compounds continues to be a problem on an international level (Ghosh et al., 2010). It has been determined that the majority of OPs are very hazardous to mammals and that they specifically target the endocrine system, the neurological system, the reproductive system, and other similar systems (Rezg et al., 2010).

Organophosphates can be taken in by humans in many different ways, including through the skin, the lungs, and the stomach. They may infiltrate the central nervous system and the muscles, and they can build up in different organs of human body. Additionally, they are able to reach high concentrations in the thyroid, the pancreas, the lungs, and the lungs. Even though organophosphates do not accumulate very much in the human body and are bio-transformed in the liver, being exposed to larger amounts of them can still have life-threatening effects. These substances removed from the body primarily through the urine, with only a trace amount passing through the skin of the face. Because of the issues that have been described above, in addition to the additional issues that are linked to the use of organophosphorus pesticides, it is crucial that these pesticides be found early and removed effectively from the contaminated sites (Kumar et al., 2016). In 2017, the maximum total amounts of each class of OPs that were used were as follows: 32,607 tonnes for OP insecticides; 10,018 tonnes for OP herbicides; and 20,646 tonnes for OP fungicides and bactericides combined. Insecticides, fungicides, and herbicides are just a few of the pesticides that are frequently used in agricultural settings. In India, on the other hand, insecticides are used more than any other kind of pesticide. Many people also use herbicides (Dar et al., 2023). In 2019, 31,731 tonnes of insecticides were used, which is about ten times as much as was used in 2008. In 2019, 9749 tonnes of herbicide were used, which is more than three times as much as was used in 2008. Fungicides are being used

more often because they are used in so many ways to grow fruit and vegetables (Subash et al., 2018). The combined use of fungicides and bactericides reached 20,092 tonnes in 2019, which is over three times as much as the amount used in 2005 (Subash et al., 2018).

1.5. Chemistry and toxicology of Organophosphorus compounds

At its 38th session in 2006, held in Fortaleza, Brazil, the Codex Committee on Pesticide Residues authorized an ARfD for OP in the range of 0.01–0.3 mg kg^{-1} bw day^{-1}. Any MRL value that falls outside of this range poses a threat to human health (Dar et al., 2023).

OPs are esters or thiol derivates of phosphoric acid, and they also comprise phenyl, aliphatic, and heterocyclic derivatives of substances. Phosphoric acid can also be used as a starting material to make OPs. The characteristic phosphoric (P=O) or thiophosphoric (P=S) link is a component of the overall chemical structure of organophosphates. Organophosphates also have a phosphorus atom (P) in their central position. The aryl or alkyl group that linked to a phosphorous atom to form phosphinates, or they can be attached to an oxygen atom to form phosphates, or they can be attached to a sulphur atom to form phosphothioates. All three of these attachment methods are possible. The group X is an exit group as it may be freed from the phosphorous atom during hydrolysis of the ester bond and because it can belong to a broad range of aliphatic, aromatic, and heterocyclic groups. (Sogorb and Vilanova, 2002).

During the process of nerve impulse transmission at a synapse, OPs are able to prevent the breakdown of the neurotransmitter acetylcholine (ACh). Acetylcholine is a molecule that is involved in nerve conduction in the CNS, skeletal muscles, and other regions of the body. It also works as a neurotransmitter. Following the passage of the nerve impulse at the synapse, the acetylcholine that has accumulated in the synaptic cleft is hydrolyzed so that the nervous system does not experience an excessive amount of stimulation. The acetylcholine esterase (AChE) enzyme is responsible for catalyzing the hydrolysis of acetylcholine, which results in the formation of choline and acetyl coenzyme A. After some time has passed, choline is liberated from the enzymes' substrate complex, and the synthesis of acetic acid occurs as a result of the combination of acetyl CoA and water. Figure 1.3 shows a diagrammatic representation of the activities of AChE enzyme. When the chemical reaction is complete, the acetylcholine esterase will have been regenerated. One molecule of the AChE enzyme is

capable of hydrolyzing up to 300,000 molecules of acetylcholine every single minute, according to some reports (Ragnarsdottir,2000).

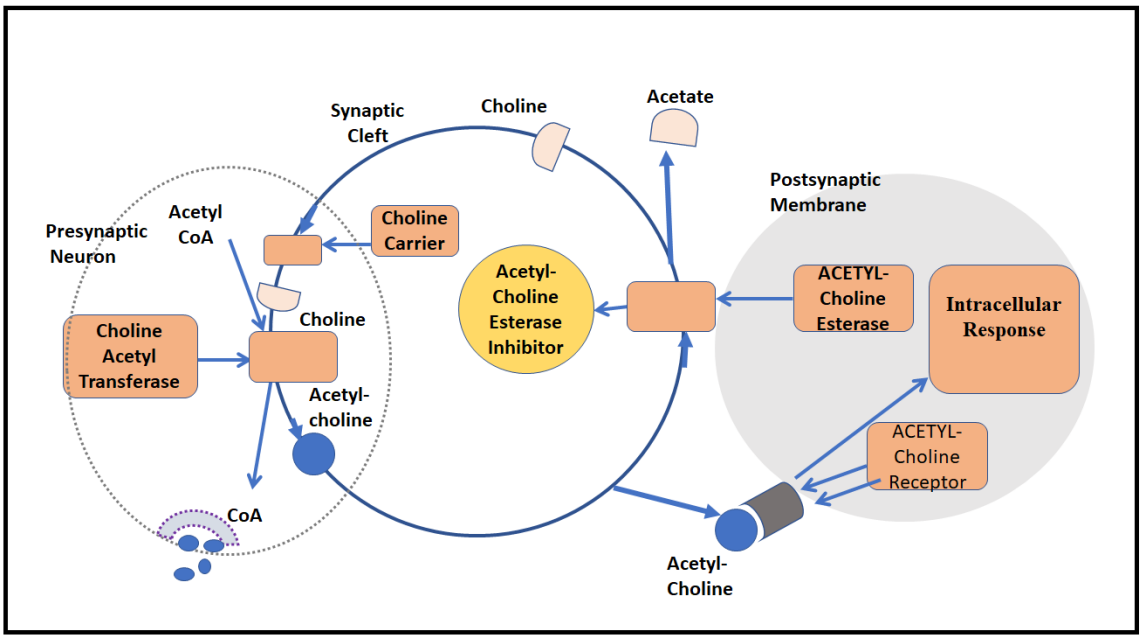

Figure 1.3 Mechanism of AChE enzyme working during nerve impulse transmission

(Images recreated: source Ragnarsdottir, 2000)

The majority of the members that are a part of the OPs group are what prevent the hydrolysis of acetylcholine (Toole and Toole,1995). OPs compounds modify the structure of acetylcholine esterase, which in turn causes the activity of the enzyme to be inhibited. This is accomplished by creating a covalent link with the enzyme. The OP attaches to the serine (203) amino acid that is located in the active site of the enzyme, and the leaving group binds to the positive hydrogen that is located in the histidine (447). This results in the phosphate being broken off, which causes the enzyme to become phosphorylated. Because of this, the regeneration of the phosphorylated enzyme is slow, which ultimately results in a buildup of neurotransmitters at synapses. It causes the nerves to be highly stimulated and generates impulses that are garbled. Because of this inhibition, insects and other animals that are not the intended target suffer from convulsions, paralysis, and eventually death (Ragnarsdottir, 2000).

Other major effects of OPs on humans include disruption of the endocrine system, birth deformities, neurological system diseases, and aberrations in the immunological system

(Furlong et al., 2006; Rauh et al.,2011). There are around one hundred different types of organophosphate chemicals that have been produced and documented up until this point. Due to the severe toxicity of many of these compounds, several of them have been outlawed (Cycon et al., 2013)

1.5.1 Chlorpyrifos- An organophosphorus insecticide

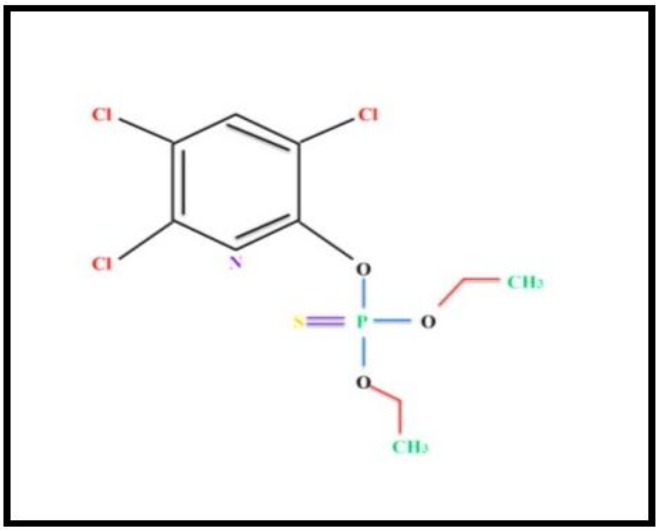

Figure 1.4 Structure of Chlorpyrifos

Chlorpyrifos is an OP insecticide or $C_6H_{11}Cl_3NO_3PS$ is widely used pesticide in the world and is thought to be moderately toxic in how it works. It is a pesticide used on crops, including grains, cotton, fruits, and vegetables, to keep pest populations down. It is one of the most common pesticides used around the world and has been for the better part of the last six decades. Because of its insecticidal activity against a diverse range of organisms that are harmful to crops, CP has the potential to cut down on agricultural losses (Rani et al., 2008; Harris et al., 2017). In terms of its chemical composition, it is a non-volatile, neutral, organic poison that is derived from thiophosphoric acid. Its primary functions are as an insecticide, acaricide, and nematicide. It smells a little bit like skunk or mild mercaptan, which is similar to the smell of rotten eggs, onions, garlic, and other foods that contain sulfur compounds (Christensen et al., 2009). It is estimated that approximately 8.5 million acres of cropland are treated with chlorpyrifos each year. The chemical has been approved for use in more than one hundred countries. Because of its superior cost-effectiveness and accessibility in comparison to other pesticides Chlorpyrifos is a frequently selected option among customers (Murphy et al., 2012; Phung et al., 2012).

Standard Chlorpyrifos is manufactured and distributed in India in accordance with the provisions outlined in the Insecticide Act and Rule of 1968. (FDA 1, 2006). It is available for purchase and distribution in a large number of different physical forms (Singh and Walker, 2006). CP is the pesticide that is found in environmental samples the second most frequently, and the World Health Organization (WHO) classifies it as being a pesticide that is only moderately dangerous to human health. Acetyl cholinesterase is the primary target of CP poisoning in species that are not its intended victims. In addition to this, it inhibits an enzyme known as neuropathy target esterase, and as a result, there is a degeneration of the myelin sheath that is located over the axon fibers of the peripheral and central nervous systems (Christensen et al., 2009). CP has been approved for use in a number of countries for the purpose of preventing the reproduction of a extensive variation of different pests (Romeh and Hendawi, 2013). It has also been observed that CP inhibits the development of soil-dwelling bacterial, fungal, and actinomycete populations, which is thought to hinder the nitrogen mineralization process. (Menon et al.,2004; Shan et al., 2008).

TABLE 1.1 Physio-chemical properties of Chlorpyrifos

Name	O,O-diethyl-0-(3,5, 6-trichloro-2-pyridyl) phosphorothioate
Common Name	Chlorpyrifos
Molecular formula	$C_9H_{11}CI_3NO_3PS$
Molecular weight	350.6
Trade names	Brodan, Detmol UA, Dowco 179, Dursban, Empire, Eradex, Lorsban, Paqeant, Piridane, Scout and Stipend.
Pesticide type	insecticide
Class	Organophosphate
Mechanism of action	cholinesterase inhibitor
CAS number	2921-88-2

TABLE 1.2 Other relevant physio-chemical properties

State	white, granular, crystalline solid with a mild sulphur odour.
Melting point	42 - 43.5° C
Vapour pressure	1.87x 10'" mm Hg (at 25° C) 8.87x10-^ mm Hg (at 35° C)
Purity	99.5 %
Partition coefficient	Pow = 50,000; log P = 4.7 (n-octanol / water)
Solubility	Readily soluble in acetone, benzene, chloroform, methanol, and iso-octane; slightly soluble (1.4 mg/L) in water at 25° C.
Acidity	0.15 % w/w (max) as H_2SO_4
Alkalinity	Not applicable
pH value	6-8

1.5.2 Chlorpyrifos production and application

According to a survey by the GOI's Direction of Plant Protection and Storage, CP is one of the top ten most often used pesticides in India. After phorate, methyl parathion, and monocrotophos, CP was the fourth most consumed organophosphorus pesticide in India between the years 2005 and 2010, and in 2015 and 2016, it was recorded as the second most used agricultural insecticide, with 9540 tonnes of consumption (Ministry of Chemicals and Fertilizers, Government of India). In 2015, CP was the fourth most consumed organophosphorus pesticide in India (2015). The rising use of CP that can be seen around the world can be attributed to the fact that it is utilized in a variety of settings, including residential, commercial, and most notably agricultural settings. Asia was regarded as the continent with the highest level of CP technical production during the years 2009-2010, and it was responsible for 79% of the world's total CP technical supply. At the moment, China and India are the most important participants in the field of CP production, with China now in the lead position due to its status as the world's largest producer both in terms of output and capacity. Because of the stringent controls that are being implemented to CP, there is a declining market for it in both the United States and Israel. Because of the increased emphasis placed on research and development by Chinese manufacturers, the production technology of CP has been enhanced.

The Companies such as Dow Chemical Company, Dow Agrosciences LLC (USA), Platte Chemical Company (USA), Xianlong Chemical Industry (China), Zhejiang Xinnog Chemical Corporation Limited (China), and Shandong Tiancheng biological technology corporation limited

are among the world's top producers of CP (China). In India Sabero organics Limited (Gujarat), Nanjing Redsum group and Bhagiradha chemicals and industries limited (Hyderabad), Maghmani organics limited and Gharda corporation (Gujrat), Makhteshim Agan Group (Hyderabad), Punjab chemicals and crop protection limited (Punjab), Biostadt India Limited (Mumbai), and Indiclay excel crop corporation limited (Mumbai), and many more. AIMCO Pesticides Ltd. Is headquartered in Mumbai and is one of the largest CP-producing factories in the country. When applying a granular or liquid form of CP, it is suggested by government officials that the person doing the application either be an approved handler themselves or be under the direct observation of an approved handler.

1.5.3 Chlorpyrifos pollution and Contamination

In 2007, the US Department of Agriculture's Pesticide Data Program gathered information on the existence of insecticide residues in diet products. Additionally, 9734 samples of fruits and vegetables were evaluated to determine whether or not CP residues were present. It was revealed that CP was found in 339 samples, which constitutes 3.48 percent of the total. CP allows for a max. residual level of 0.1 mg/l in any and all food items, regardless of whether the food products are being held, processed, cooked, or served. According to the WHO's pesticide e-value scheme, CP is not approved for addition to the water for the purposes of cleansing and public health; however, it can be used in some nations to restrict the growth of mosquito larvae. This is because CP inhibits the development of mosquitoes. According to the report, the majority of fruit samples collected from both the control and affected areas confirmed the presence of CP residues at levels (0.05mg/l) that were higher than the recommended limits (30 ug/l) set by the USEPA. This may have been the result of negligence on the part of the applicators or a lack of adequate information regarding pesticide applications (Qamar et al.,2017).

In the Indian state of Punjab, it was discovered that CP was present in both drinking water bottles, and blood samples were taken from local farmers (The Hindu,2005). The study of urine samples taken from volunteers who were exposed to CP revealed that the oral route resulted in the greatest amount of exposure to CP, whereas the dermal route resulted in the least amount of exposure. There was evidence of CP contamination in the samples of Limca and Coca-Cola soft beverages that were taken in the states of Gujarat and Maharashtra. The chemical was found in concentrations ranging from 0.17 to 20.43 parts per billion. It has also been hypothesized that inhaling CP causes

toxic effects to appear more quickly than when the substance is either orally or applied topically (on the skin). In the course of an examination that took place in Punjab, it was discovered that fortified samples of cauliflower, also known as Brassica oleracea (cauliflower), which is a vegetable crop in India, were tainted with CP (Mandal and Singh, 2010).

An investigation was conducted on soil samples obtained from agricultural fields in Haryana that were cultivated with paddy-wheat, paddy-cotton, and sugarcane. The results of the investigation discovered that the soil samples were contaminated with the residues of OP pesticides such as CP, quinalphos, and malathion in high concentrations (Kumari et al.,2008). The soils of tea fields in the West Bengal region have also been found to have traces of the pesticides ethion and CP (Bishnu et al., 2009). Additionally, CP was found in agricultural land in the Idukki district of Kerala at a concentration that was higher than the maximum residue limit (MRL) (Jacob et al., 2014). According to a number of studies, the most significant contributors to water pollution come from agricultural fields. These are the areas where pesticides are used to keep populations of pests under control for crops such as cotton, vegetables, and other horticultural commodities (Kumari et al., 2008. Lakes in the state of Karnataka were discovered to have extremely high levels of CP pollution (Punjeri et al., 2011). Similarly, surface and grounded water samples taken in the Vidarbha region of Maharashtra were found to include OPs such as dichlorvos, ethion, parathion-methyl, phorate, Chlorpyrifos, and profenofos. These OPs were shown to be polluting the water (Yadav et al., 2015; Pirsaheb et al., 2017).

The presence of CP pollution has been documented in the living tissues of organisms of both plant and animal origin, in addition to other abiotic components. A study on farm gate and market vegetables in Rajasthan discovered contamination with CP, monocrotophos, quinalphos, and dimethoate at levels ranging from below to beyond their respective residual limits. The research was carried out by the University of Rajasthan (Singh and Gupta, 2002). It was discovered that the levels of monocrotophos and cp in some of the samples of seasonal vegetables were greater than the MRL value (Kumari et al., 2004). Consumption of contaminated vegetables in a continuous manner can lead to accumulation of the toxins in the body, which poses a serious risk to one's health (Bhanti and Taneja, 2007). According to the findings of a study that was conducted by Srivastava et al., (2011), various types of vegetables that were purchased from a local market in Lucknow were found to be contaminated with CP and monocrotophos (Chandra et al., 2014).

Residues of CP have been found not only in plants and other agricultural goods but also in a wide variety of animal and food products, as well as in the fluids of human bodies. This indicates that their presence is widespread. Breast milk samples collected in Bhopal, Madhya Pradesh, also contained traces of the pesticides CP and methyl parathion (Sanghi,2003).

1.5.4 Environment persistence and movement of CP

Because of improper pesticide storage facilities and labelling, members of the human population are at risk of being exposed to CP, which also contributes to the degradation of the environment. The leakage of contaminated pesticide containers and the burning of those containers contribute to the contamination of the environment, which puts human health and safety at risk (Curtis and Olsen, 2004). In addition, the use of empty, used pesticide containers for home uses, such as the storage of crops, fuel, food, and water, as well as the disposal of these containers near water bodies, is directly responsible for the introduction of human populations to pesticides. (Dalvie et al., 2006).

The adsorption and movement of CP in soil and water are both greatly influenced by the nature of the adsorbents, as well as the water solubility of the compound. CP is capable of adsorbing to a wide variety of soils, although the extent to which it does so varies considerably. Adsorption is enhanced in soils that are high in organic matter (Gebremariam et al., 2012). Because cp is not mobile in soil and tightly attaches to it, adsorption considerably lowers the mobility of cp and increases its persistence in the soil. There is a wide range of values for CP's half-lives that have been reported, and these values depend entirely on a variety of factors such as the application rate, the type of ecosystem, the microflora that is present in the soil, and the climatic conditions (Sasikala et al., 202. When compared to the concentration of the original application, the amount of CP in the soil was determined to remain unchanged after seven years. The rate of application is the single most critical element that determines CP persistence, and it reaches its maximum at greater concentrations due to the fact that the soil degradation half-life increases with increasing application rates.

Two processes that lead to the loss of CP in soil and other ecosystems are biotic degradation and abiotic degradation. In tropical settings, CP degrades at a somewhat faster rate than in temperate ones (Chai et al., 2013). CP degradation is also accelerated in organic soils in comparison to mineral-rich soils, and this difference is significant (Gebremariam et al., 2012). The moisture content of the soil and its pH are also key factors that influence the degradation process, and the

rate of degradation is accelerated in alkaline conditions. The increased stability of CP and its metabolites in the environment is attributed to the aforementioned conditions of temperature, pH, and reduced light intensity (Yadav et al., 2015).

The findings of the risk assessment showed that dichlorvos and CP provide considerable dangers to the aquatic ecosystem of the Indian subcontinent (Dar et al., 2023).

Although it has been reported that CP will break down through photolytic hydrolytic and photolytic processes within a neutral pH range, its persistence in natural water has been found. It was discovered in California that the half-life of CP in seawater is 49.5 days at 10 degrees Celsius, whereas the half-life of CP in freshwater is 18. 7 days. This led researchers to the conclusion that degradation occurs far more slowly in marine water than in freshwater (Bondarenko et al., 2004).

A significant concentration of CP has also been documented in the air (Mills and Kegley, 2006). According to Haryward et al research .'s from 2009, CP degrades more quickly in the air, which also results in a shorter occupancy time period in the atmosphere. When compared to soils, CP showed a significantly stronger affinity for the sediments found in aquatic environments (Gebremariam et al., 2012).

1.5.5 Chlorpyrifos effect on humans

The use of pesticides in India has been successful in reducing the incidence of a number of diseases, including cholera, dengue fever, Japanese encephalitis, malaria, and filariasis, among others. Despite this, the most common way that people are exposed to pesticides is through the agricultural industry. The human body may exhibit signs of CP poisoning if it is subjected to a high amount of the substance. These symptoms include headache, fatigue, dizziness, nausea, stomach cramps, and diarrhea. The pollution caused by CP is a global health problem that is responsible for around 200,000 fatalities and 3 million cases of poisoning each year (Karalliedde and Senanayake, 1989; Sogorb et al., 2004). Some studies have documented the possibility for human beings to be exposed to CP in a variety of ways, including through the ingestion of contaminated food products, through breathing (inhalation) during the application of fume forms, through the skin, during its application, and in other ways. One of the studies that described the potential for human beings to be exposed to CP in this manner was published in the journal Environmental Health Perspectives. The following are examples of some of these methods: (Christensen et al., 2009). Despite this, the hydrological system is one of the most significant

vectors that contributes to the spread of pesticides across the ecosystem. This is as a result of the fact that it serves as the primary supply of water for all forms of life, including people. CP contamination of agricultural land, water bodies notably groundwater, and several other natural places continue to be a problem in India and in the world in general (Ghosh et al., 2010). The primary reason for the potential for harm to one's health is the substance's toxicity, which poses a threat both to the person who applies it and to the population that is either directly or indirectly exposed to it (John and Shaike,2015).

CP has a harmful effect not just on creatures that it targets, but also on organisms that it does not target (Singh et al., 2004). Less than 0.1% of the pesticide that is applied actually makes it to its intended victims; this means that the vast majority of it is wasted, where it continues to build up and negatively impact the ecosystem. The effect that CP has on humans is mostly contingent upon the amount taken, the length of time it is taken, and certain other environmental conditions. Because CP is most commonly found in liquid form, its absorption through the skin has the potential to result in systemic toxicity. Poisoning with CP causes a variety of signs and symptoms in humans, and it has been hypothesized that humans may be more vulnerable to the effects of CP exposure than other species. It has been theorized that CP is a strong neurotoxic during development (Slotkin, 2004). Also, it has been hypothesized that CP interferes with the regular hormone secretion process that takes place in the many endocrine glands found throughout the body (Slotkin et al., 2004; De Angelis et al., 2009; Haviland et al., 2010). Even if only exposed to its tiniest possible concentrations, chlorpyrifos has the potential to have a deleterious effect on the development of the brain by inhibiting mitosis, encouraging apoptosis, and producing changes in neuronal activity in the CNS (John and Shaike, 2015).

The cardiovascular system, skeletal system, central nervous system, and respiratory system of an individual are all impacted by the substance in the event that it is ingested orally during an attempt at suicide or inhaled unintentionally and indirectly during an accident, both of which result in fatalities caused by the substance (Rangnarsdottir, 2000). According to the findings of epidemiological studies, people who worked with CP had a significantly increased risk of developing a variety of cancers. Some of the diseases that are included in this category include cancers of the prostate (Alavanja et al., 2003), hematopoietic, leukemia, brain tumors (Lee et al., 2007), colorectal breast (Engel et al., 2005), (Lee et al., 2007), lymphoma, and so on. Other diseases that are included in this category include: (Karunayake et al., 2012). According to studies

that were conducted in a controlled environment, acute and chronic exposures to CP can induce genotoxic and mutagenic consequences in rats and mice (Cui et al., 2011; Ojha et al., 2013), as well as in the human population. These findings come from research that was conducted in a laboratory setting. These findings were supported by the findings of Ojha et al., 2013. (Sandal and Yilmaz, 2011). To birds, it is thought to be anything from moderately to severely harmful; however, there are no such toxicity data available for reptiles (Watts, 2012; Boedeker et al., 2020).

There is evidence to show that CP is immune-toxic in a variety of ways, such as the fact that it causes autoimmunity, affects lymphocytes and tumor necrosis factor, T-cells (Thrasher et al., 2002), and thymocytes (Prakash et al., 2009), and so on. In addition, CP exposure can result in a variety of difficulties with reproduction, including abnormalities in birth, DNA damage in the reproductive cells of men, and a reduction in the production of body fluids. In addition to this, there is a correlation between CP poisoning and a reduction in the motility and concentration of sperm (Watts, 2012). According to the USEPA, there is evidence that children who are exposed to even lower amounts of CP still suffer from neurodevelopmental abnormalities.

However, in order to conduct an accurate assessment of the toxicity and behavioral consequences caused by CP, long-term research and assessments are required. CP has been found in a variety of environmental samples, and its half-life has been reported by a variety of researchers to range anywhere from 360 days to 17 years (Sasikala et al., 2012). In their review, Chishti et al. provide a succinct explanation of what ultimately happens to CP (2013). John and Shake (2015) conducted a study to investigate the toxicity risks associated with CP with regard to higher animals, aquatic systems, plants, and microorganisms.

1.5.6 Chlorpyrifos toxicity cases- an Indian Scenario

Over-the-counter pain relievers (OPs) are the leading source of serious human toxicities and are responsible for 80 percent of hospitalized cases (Kumar et al., 2010) The most significant symptoms of acute ops poisoning, as described by patients, were vomiting (96% of cases), nausea (82% of cases), increased thirst (61% of cases), and decreased eyesight (54% of cases). These findings are from a study that was conducted. Several patients also exhibited symptoms that are related with the CNS, such as giddiness (93% of cases), headache (84% of cases), and disruption in consciousness (44% of cases) (Agrawal et al., 2015, Anju et al., 2010). The potential detrimental effects of CP exposure on human health are anticipated to be more pronounced in India because

to the ready availability of extremely hazardous chemicals, the lack of knowledge among children and women, and the low level of education among agricultural workers. Moreover, the potential detrimental health effects of CP exposure in India are likely to be more severe (Singh and Khurana, 2009; Kumar et al.,2010).

According to the findings of study that was carried out by S. N. Meyyanathan in the Nilgiris, it was discovered that the production of fruits and vegetables involved the use of organophosphate pesticides such as acephate, malathion, profenofos, chlorpyrifos, and quinalphos. The fruits and vegetables that are native to that region served as the subjects of the study. The levels of these pesticides were determined by analyzing 659 samples of fresh fruit and vegetables that were gathered throughout the agricultural season of 2018-2019 in order to participate in the study. Only 53 of the total of 659 samples revealed significantly higher amounts of the pesticide. The majority of these were found in strawberries, potatoes, cabbage, cauliflower, carrots, broccoli, and garlic. "About 85% of these samples included chlorpyrifos, making it the most prevalent pesticide. This was followed by quinalphos with 72%, acephate with 56.6%, profenofos with 54%, and malathion with 17%. (The Hindu, January 25, 2020).

Twenty blood samples were collected from residents of several villages in the state of Punjab, Of these blood samples, CP residues made up 80% of the total, which was more than the percentage found in any other OP (Mathur et al., 2005). According to the findings of a study conducted at Kasturba Medical College in Manipal, India, organophosphate insecticides were responsible for roughly 65 percent of all deaths that occurred within a period of two years (Singh and Unnikrishnan, 2006). When CP was diagnosed based on the blood samples of 94 individuals, it was discovered that it was present in the majority of instances. It was discovered that the vast majority of these patients, around 27.7%, were involved in agricultural activities.

Over one thousand cases of pesticide poisoning are reported each year at the Mahatma Gandhi Memorial, which is a government hospital at the district level and located in the Warangal district of Andhra Pradesh. Between the years 1997 and 2002, hundreds of people lost their lives as a result of pesticide poisoning (Rao et al., 2005). In the year 2002, there were a total of 1035 cases of pesticide poisoning were registered. Of those patients, 653 were presumed to have consumed OP based on clinical symptoms. The OPs monocrotophos (257 patients), CP (119 patients), and quinalphos were the ones that were used the most frequently (78). In a similar fashion, CP residues

were found in blood samples taken from persons living in the vicinity of Dal Lake in Jammu and Kashmir (Bandey et al., 2012). More than eighty percent of the blood serum samples contained traces of CP, and it was discovered that the population being investigated had a higher concentration of CP than the population serving as a control.

Spray farmers in the Sehore district of Madhya Pradesh were found to have experienced biochemical shifts as a result of their prolonged exposure to CP. It was stated that a male farmer who worked in agricultural fields and used to spray CP suffered from a variety of symptoms, including weakness, loose stools, and numbness over the legs. This farmer was 53 years old. After a comprehensive medical examination, it was found that the patient had an increased respiratory and pulse rate, cyanosis, acute pancreatitis, and frothing from the mouth (Agarwal et al., 2013). During the span of time between August 2001 and July 2002, a total of 165 individuals who had been poisoned by organophosphates were examined at Stanley hospital in Chennai. It was determined that there were three operations that occurred most frequently, and CP was one of them (Shivakumar et al., 2013). According to the findings of a study that was conducted at the Shri Aurobindo Medical College Hospital in Indore between dates of January 1, 2012, and August 20, 203. One hundred cases with a history of pesticide poisoning were diagnosed, and the majority of them were connected with ops, including CP (Waghmare et al., 2014).

1.5.7 Toxic-kinetics of CP in the human body

Once CP has entered the body, it is dispersed, and a portion of it is stored in adipose tissue. However, significant bioaccumulation is not anticipated because CP has a half-life of fewer than three days in humans (Christensen et al., 2009). Both aerobic and anaerobic methods of CP dissipation have been shown to be effective in human studies (Pawar et al., 2015). The liver cells contain an enzyme called CYP2B6, a member of the cytochrome P450 (CYP) group. This enzyme changes CP into chlorpyrifos-oxon by exchanging the sulfur group for an oxygen group. Figure 1.5

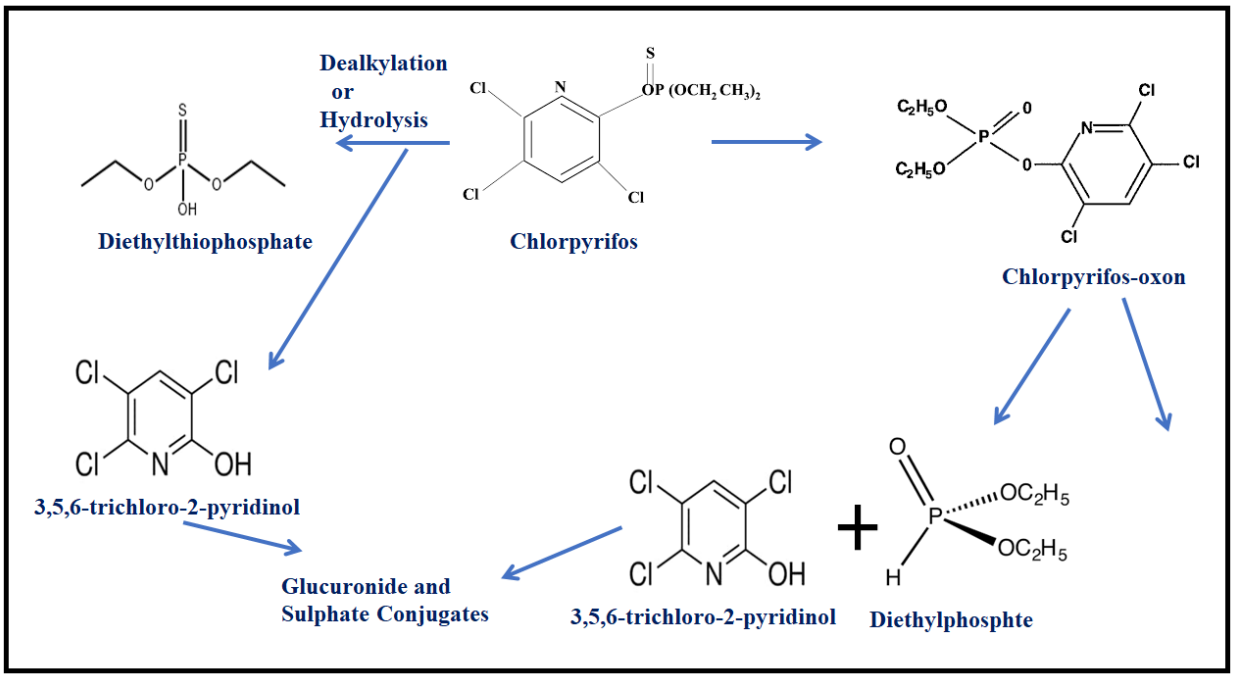

Figure 1.5 Different routes of CP transformation in the human body (Pawar et al., 2015)

In the later stages, the liver makes TCP from CP and CP-oxon with the help of more cytochrome P450 (CYP) enzymes (Eaten et al., 2008). Chlorpyrifos-oxon makes TCP, which is more water-soluble than CP. TCP then binds to glycine or glucuronide conjugates and is passed out of the body in the urine. Chlorpyrifos-oxon also has a higher molecular weight than CP. In acute exposure, the biological half-life of CP is only up to 24 hours in the blood and 60 hours in adipose tissues (Pawar et al., 2015).

In addition, an additional group of liver enzymes known as oxidase is responsible for detoxification. These enzymes convert Chlorpyrifos-oxon into the metabolites diethylphosphate (DEP), DETP, and TCP in humans (Smegal, 2000; Pawer et al., 2015). The most typical method of detoxification is accomplished through the hydrolysis of CP-oxon by A-esterase. Although other metabolites of chlorpyrifos are believed to be less hazardous in humans, Chlorpyrifos-oxon nevertheless promotes the inhibition of the AChE enzyme in the same way that CP does. It has a quick effect on the human nervous system, causes toxic consequences, and if even a very tiny amount of it reaches the liver and tissues, it will slowly hydrolyze into metabolites that are not hazardous. If CP is exposed to higher concentrations, the substance excretes in the urine as almost totally non-toxic metabolites.

When Chlorpyrifos is taken orally, some of it is eliminated unaltered through the bowels. However, as soon as it is absorbed into the bloodstream, it is swiftly converted in the liver into a less harmful component and then promptly eliminated by the urine. The kidneys are primarily responsible for the elimination of Chlorpyrifos. Humans eliminate this insecticide in their urine as TCP, DEP, and DETP (Risher, 1997). There are presently exposure limits for the pesticide chlorpyrifos. The tolerable everyday intake value is 0.01 mg/kg/day, the acute oral exposure limit is 0.01 mg/kg/day, the acute dietary reference dose is 0.0036 mg/kg/day, and the chronic dietary reference dose is 0.0003 mg/kg/day (Mishra and Devi, 2014).

1.6 Carbamates:

1.6.1 Chemistry and toxicology of Carbamate compounds

As an alternative to the persistent organochlorine pesticides, carbamate insecticides have been created. In the 1950s, commercial insecticides containing carbamates were created and introduced. Compounds such as insecticides, fungicides, and herbicides with a high level of activity are included in this group (Khur et al., 1976). As a result, enhanced new analytical approaches for their regulation have been developed as a result of this stimulus. However, the only compounds that have been shown to be effective against insects are esters of N-alkyl carbamic acids. Carbamates have a high level of biological activity and a polarity ranging from medium to high; nevertheless, some of them are transformed into products in the environment with a higher level of both polarity and toxicity than the parent molecules (Vale et al.,2015). The aryl esters of N-methyl carbamic acid have been shown to have the highest level of activity. These pesticides have a wide range of effects and are extremely active both on contact and in the stomachs of their targets. The inhibition of the activity of the enzyme acetylcholinesterase in the nerve tissue is the mechanism of action that these chemicals have on animals and insects. It has been demonstrated that carbamates and other anti-cholinesterases interfere with the learning and memory processes. The accumulation of acetylcholine as a result of the suppression of the activity of acetylcholinesterase in the nerve tissue causes a disruption in the function of the nervous system. The end outcome is that the insects are rendered unable to move and die. Pesticides containing carbamates are extremely harmful to both humans and animals (the lethal dose for rats ranges from 16-250 mg/kg). Carbamates have a deleterious effect on the neurohumoral and endocrine systems when injected into animals and humans, even in low doses, and they also have an embryotoxic and mutagenic effect. The carbamates were first

discovered in extracts of the bean that comes from the Calabar plant, also known as Phyto stigma venomous, which is native to West Africa. These extracts were shown to have a substance known as physostigmine, which is an ester of methylcarbamate (Bolognesi 1994). The research on naturally occurring compounds and their derivatives has uncovered a great deal of information regarding the impacts of carbamates.

There is a wide variety of carbamate chemicals that have been put to use in the pharmaceutical and pesticide industries. There is evidence that carbamate insecticides pose a significant threat to the populations of numerous species of birds, fish, and bees, as well as earthworms (Vale 2015).

The majority of carbamates are used for different purposes. In addition to this, they have the potential to be exploited as biocides in a variety of settings, including residences, industries, and other applications. One of these applications is in the realm of controlling vectors that pose a threat to public health. These pesticides have been developed, produced, and utilized in order to combat a wide variety of pests, including insects, weeds, and rodents.

1.6.2 Sources, environmental transport, and distribution

Even though most carbamates have a low vapor pressure, they still evaporate or sublimate slowly at normal temperatures. This can cause carbamates to be released from water and soil. Though, dissemination through the air will only play a supporting role. It is anticipated that highly soluble carbamates will go a significant distance across aqueous environments. Carbamate insecticides are typically sprayed on the plants, but they have the potential to travel down into the soil as well. On the other hand, carbamate nematicides and herbicides are administered straight to soil.

The biodegradation of carbamates in the soil is affected by a number of parameters, including volatility, the type of soil, the moisture content of the soil, adsorption, pH, temperature, and photodecomposition. According to the data that is currently available, it appears that there will only be a negligible amount of bioaccumulation across all of the different species and food chains. It's possible for certain carbamates to make their way down into the groundwater, and as a result, they could end up in the water supply.

1.6.3 Toxic-kinetics and Metabolism

The end result of the metabolism of Carbamates is fundamentally the same in plants, insects, and mammals. There are certain rare cases in which carbamates do not readily absorb via the

skin, mucosal membranes, respiratory, or digestive systems; nonetheless, this is the rule rather than the exception. In most cases, the metabolites are significantly less hazardous than the parent substances. On the other hand, there are circumstances in which the metabolites are either equally as hazardous as the parent Carbamate or much more so (Vale et al., 2015). In the majority of mammalian species, the metabolites are flushed out of the body primarily and quite swiftly through the urine. It would appear that the dog is an outlier in this regard. In some instances, accumulation occurs; however, due to the high metabolic rate, this phenomenon is of relatively little consequence.

Carbamates are broken down into carbamic acid in the first step of their metabolism. After that, carbamic acid breaks down into carbon dioxide (CO_2) and the amine that corresponds to it.

Both N-methyl and N-dimethyl derivatives undergo hydrolysis, although the mechanism by which they do so is distinct for each. When N-methyl carbamates are broken down by water, an isocyanate intermediate is made. When N-dimethyl carbamates are broken down by water, an addition product with a hydroxyl ion is made, which leads to alcohol and N-dimethyl substituted acid. When compared to plants and insects, mammals have a much faster rate of hydrolysis caused by esterase. There is also hydrolysis going on. The process of oxidation is done with the help of enzymes called mixed-function oxidases.

In mammals, the process of conjugation results in the creation of O- and N-glucuronides, as well as sulfates and derivatives of mercapturic acid. Conjugation can produce a variety of compounds, the most frequent of which are glycosides and phosphates (Risher et al 1987; Fukuto et al.,1990; Fikes et al.,1990; Mohammad et al.,2023).

Carbamates are a type of insecticide that works very well because they can block AChE in the nervous system. The enzyme acetylcholine esterase (AChE) breaks down the neurotransmitter acetylcholine (ACh) into choline and acetic acid. In the nervous systems of mammals and insects, ACh helps send nerve impulses from one nerve cell to another. It accomplishes this function in the following ways:

(a) in the brains of mammals and in the CNS of insects as a neurotransmitter;

(b) in mammalian autonomic nerve systems as a pre-ganglionic neurotransmitter;

(c) at the terminals of post-ganglionic nerves found inside the autonomic nervous system; and

(d) at the point where the nerves and muscles of skeletal muscle are joined together.

Similar to organophosphates, carbamates have the ability to inhibit the activity of enzymes that have serine located at their catalytic site. These enzymes are called serine esterases or beta-esterases. Even though blocking serine esterases other than AChE doesn't affect how dangerous the drugs are, it could affect how dangerous other chemicals become after being exposed to low levels for a long time.

When a nerve impulse travels along the length of a neuron, it eventually reaches the nerve ending. At this point, the vesicles at the ends of nerves release the AChE that has been stored there. Within 2–3 ms, the acetylcholine gets to the receptor side of the muscle.

1.6.4 Carbofuran- A Carbamate insecticide

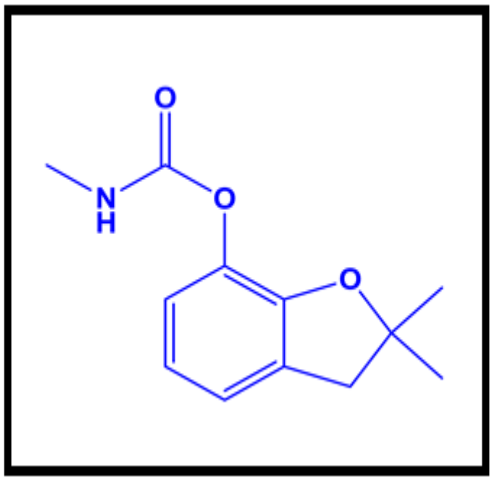

Figure 1.6 Carbofuran Structure

Carbofuran, also known as 2, 3-dihydro-2, 2-dimethyl-7-benzofuranol N-methyl carbamate, is a pesticide that belongs to the carbamate family and is frequently employed in agricultural practices all over the world (Mdeni et al.,2022). It kills insects, nematodes, and ticks by getting into their bodies. It is used a lot to get rid of stem borers in rice, sugarcane, fruits, and vegetables. It is a carbamate insecticide with a wide range of effects. Nematodes, nematode mites, and insects die when they touch it or eat it. When used to fight soil and leaf pests, they help protect field, fruit, vegetable, and forest crops. You can choose between granules and liquid forms of the formula. Since it is a systemic insecticide, this implies that it kills insects throughout the plant. Carbofuran is one of the insecticides that is used on field crops the most frequently, and it has one of the highest acute toxicity ratings for people (only aldicarb and parathion are more toxic). The vast majority of carbofuran is administered by commercial applicators who make use of closed systems and

sophisticated controls. This ensures that no one is exposed to the chemical while it is being prepared. It is recognized as a neurotoxic pesticide due to the fact that its toxic effects are brought on by the fact that it acts as a cholinesterase inhibitor. Carbofuran is not only a powerful neurotoxin, but it is also a powerful endocrine disruptor. This means that even when given in very small amounts, it can temporarily change the levels of many hormones in both animals and people. As a consequence of these modifications, there is a potential for major reproductive issues to arise after repeated exposure (Mishra et al., 2020).

TABLE 1.3: Physical and Chemical Properties of Carbofuran

Name	2,2-Dimethyl-2,3-dihydro-1-benzofuran-7-yl methylcarbamate
Common Name	Carbofuran
Molecular formula	$C_{12}H_{15}NO_3$
Molecular weight	221.256 $g.mol^{-1}$
Trade names	Furadan, Curater, Furacarb
Pesticide type	insecticide
Class	Carbamate
Mechanism of action	Acetylcholinesterase (AChE)
CAS number	1563-62-2

TABLE 1.4: Other relevant physio-chemical properties

State	White, crystalline solid
Melting point	151 ºC
Boiling Point	313.3 ºC
Solubility	320 mg/L
Density	1.18 g/cm^3

Carbofuran is also sold under the brand names Furadan, Bay 70143, Carbodan, Carbosip, Chinofur, Curaterr, D 1221, ENT 27164, Furacarb, Kenafuran, Pillarfuron, Rampart, Nex, and Yaltox. Other names for this chemical include ENT 27164. Over the past few years, the use of

Carbofuran has gone up because it is one of the few insecticides that works against soybean aphids. Since 2002, soybean aphids have spread to most of the places in India where soybeans are grown. It has been discovered that carbofuran has contaminated the land, the air, the food, the water, and the fauna. However, carbofuran is widely used by farmers in the southernmost region of India as an insecticide for the control of grasshoppers and other insect pests (Gupta, 1994). As a result, the effects of the pesticide on both the organisms it is intended to kill and other organisms must be considered in terms of their potential impact on public health. Carbofuran can be dissolved in water and has only a somewhat long half-life in soil. Between 30 and 120 days pass before it reaches half-life. Chemical hydrolysis and microbiological activities both contribute to the breakdown of carbofuran in soil. The rate of hydrolysis is significantly increased in alkaline soils (Howard,2018). Carbofuran degrades when exposed to sunshine. There is a significant risk of carbofuran contaminating groundwater with its presence (Howard,2018). In different soils, the mobility of carbofuran varies from mobile to highly mobile; in silty clay loam soils, its mobility is moderate; and in muck soils, its mobility is only slightly higher. In the presence of alkaline circumstances, carbofuran is degraded through the process of chemical hydrolysis when it is dissolved in water. In addition to photodegradation, the potential involvement of aquatic bacteria in the degradation process should not be discounted. Carbofuran doesn't evaporate from water, and it doesn't stick to silt or other particles in water (Howard,2018). When carbofuran is put on the roots of plants, it lasts about four days. When it is put on the leaves, it lasts longer than four days. Carbofuran is extremely poisonous to a wide variety of fish. 0.38 micrograms per liter is the 96-hour LD50 for rainbow trout, while 0.24 micrograms per liter are the LD50 for bluegill sunfish. The possibility of the chemical becoming accumulated in aquatic creatures is very minimal. The bioconcentration factor might range anywhere from ten for snails to more than one hundred for fish (Howard, 2018). According to the evidence that is now available, carbofuran is capable of disrupting the normal functions of neurons in both the CNS and the peripheral nervous system when administered to test animals through the oral route (Ray, 2006). The reported toxicity of carbofuran, like that of many other compounds belonging to the carbamate family, varies not only with the concentration of the active ingredient but also with the solvent vehicle. This is the case. This may manifest itself as the stable repetitive firing of the neuron at lesser dosages, but at higher concentrations, it has the potential to cause depolarization of the nerve cell as well as an obstruction of conduction (Ray, 2006).

1.6.5 Carbofuran pollution and Contamination

Carbofuran and its usual technical form, Furadan, are both very dangerous to animals that are not the target, especially birds. Carbofuran is a good example of this. Oral LD50 values for furadan have been found to range from 0.238 mg/kg (in the case of whistling ducks) to 1.3 mg/kg (in the case of mallards) (house sparrow). In the past, Furadan has been linked to a large number of poisonings and deaths of birds in many countries, including the United States and Canada. Even though Furadan works well as a pesticide for crops, this is the case. In the past, Furadan has been used in many cases where birds were poisoned and died in large numbers (Allen et al., 1996; Elliott et al., 1996; Otieno et al., 2010). These cases were investigated and found to involve Furadan. These incidents include poisonings that occurred through the food chain, through secondary exposure, and through the use of laced baits for direct poisoning (Vyas et al., 2005). Because of the severe acute toxicity of the substance and the danger it poses to birds, its usage has been limited or prohibited in many nations.

In South Africa and Uganda, there have been reports of Furadan being a concern to animals, particularly birds. In several of these incidents, different vulture species have been poisoned either directly or indirectly (Otieno 2011; 2010). The overuse of the Furadan by farmers and herders in Kenya has caused a large number of poisonings in recent years. This has led to a strong movement to ban Furadan in the country, which is being led by wildlife conservationists. (Otieno, 2010).

1.6.6 Environment persistence and movement of Carbofuran

Carbofuran can be dissolved in water and has a moderately long half-life in soil (half-life of 30–120 days). Chemical, photochemical, and microbiological mechanisms all contribute to the degradation of carbofuran. In alkaline settings, hydrolysis proceeds at a faster rate. Carbofuran degrades when exposed to sunshine. Carbofuran has a significant risk of seeping into groundwater if it is not properly managed. Carbofuran may move through soft texture soils with relative ease. In waters, carbofuran is susceptible to hydrolysis, and this process is accelerated in alkaline environments. The rate of hydrolysis of carbofuran in water (measured in half-lives) is 690 weeks, 8 weeks, and 1 week, respectively, with pH values of 6, 7, and 8. Photodegradation and microbial transformation may both play a role in the degradation process, much as they do in soils. Carbofuran does not evaporate and does not bind to silt or particles in the environment.

1.6.7 Effect on humans

The cholinergic crisis is a potentially life-threatening condition that can be brought on by exposure to carbofuran. It is possible that the sickness cannot be differentiated from the one that occurs following organophosphate exposure. There is a possibility that the individual will experience seizures, unconsciousness, diaphoresis, muscle weakness, fasciculation, bradycardia, and tachycardia. There is a chance that death will happen because of severe bronchoconstriction and/or paralysis of the breathing muscles. After being exposed to carbofuran, workers at a plant in China that makes pesticides got dizzy, weak, had blurry vision, felt sick and sweated, turned pale, had pain in their stomachs, threw up, and felt pressure in their chests. The detection of miosis was fairly common. Some of the workers had signs of muscle fasciculations, specifically in the gastrocnemius and orbicularis oculi muscles. There was a correlation between the suppression of blood cholinesterase and clinical symptoms. The consumption of carbofuran resulted in severe poisoning for a pregnant woman. She made a full recovery, but the baby did not survive. Carbofuran is able to penetrate the human placenta and hurt the growing fetus. This was shown by the fact that the fetal organ have carbofuran percentage that were similar to those in the mother's blood. Tobin (1970) wrote about three different times when carbofuran was used to poison people. Two people at a formulation facility were making 10% granules, and a third person, an entomologist, was weighing a 50% water-dispersible powder formulation when he or she started to feel uneasy. Both of the formulators started having signs of carbamate poisoning, like a lot of sweating, feeling weak, having blurry vision, and feeling sick. (Tobin, 1970).

1.6.8 Carbofuran toxicity cases- an Indian Scenario

A farmer in Narishu village, near Niali in Cuttack district, was spraying Carbofuran pesticide but got staggered and collapsed. After burying the remaining amount of carbofuran in a hole in one of his fields, he looked down and saw dead snails, snakes, and frogs floating in the water that had pooled in the hole (The Hindu,16 Nov 2021).

1.6.9 Toxic-kinetics of Carbofuran in the human body

In both target and non-target organisms, carbofuran exerts its toxic effects by inhibiting an enzyme known as acetylcholine esterase (AChE). This causes acetylcholine to build active at the point where the nerve cell meets the receptor site. This causes the nerve to fire constantly, which causes

tremors, fits, and eventually death (Ecobischon 2019; Hayes 2001). In this step, the pesticide molecule's phenyl ring part is attached to AChE, and then carbamylation is done. This gives rise to an unstable enzyme-pesticide (inhibitor) complex that is covalently bound. This is ultimately followed by decarbamylation, because of hydrolysis, resulting in the release of an actetylcholine esterase enzyme that has been inhibited in addition to a hydroxylated pesticide molecule (Hodgson et al. 1991; Ecobischon 2019). Due to the highly rapid pace at which the enzyme is able to undergo decarbamylation after it has been inhibited, the carbamate-induced inhibition of AChE is only partially reversible. This is because of the incredibly rapid rate at which the enzyme is able to undergo decarbamylation. In contrast, the process of decarbamylation with OPs is very slow because they also function by blocking the AChE. Because of this irreversible nature of the inhibition mechanism, the term "irreversible inhibition mechanism" is used to describe the phenomenon. (Hill 1989; Ecobischon 2019; Hill and Fleming 1982; Brown 1997; Mineau 2003). During their AChE-inhibition experiments, carbamates' modest reversibility as an inhibiting agent typically causes issues and ambiguity to the researchers (Mineau and Tucker 2002; Hopkins and Scholz 2006). Carboxyfuran undergoes a rapid and intracellular metabolism that is catalyzed by both Phase I and Phase II P450 systems (McRae 1989).

Carboxylesterases (CarbEs) and butyrylcholine esterases are two examples of non-selective serine-containing enzymes that are inhibited by carbofuran. Carboxylesterases and butyrylcholinesterases (BuChE) are inhibited in addition to the target enzyme acetylcholinesterase (AChE). This made it seem like there was a lot of carbofuran binding that wasn't said. Carboxylesterases (CarbEs) was shown to be stopped in both neuronal (brain) and nonneuronal (skeletal muscle, liver, and plasma) tissues. The brain is made up of neuronal tissues. The effects of carbofuran on this enzyme were much stronger in the plasma and other tissues outside of the brain than in the brain itself. This shows that a protective mechanism in peripheral tissues is a kind of binding that doesn't target anything in particular. Because of this, there isn't much free carbofuran left in the brain to stop AChE from working.

Carbofuran is a carbamate insecticide that is efficient against a large number of different pests. It has a wide spectrum of activity. Acetylcholinesterase, also known as AChE, is an enzyme that is found in the nervous system. This medication works by blocking the activity of AChE, which is its primary method of action. Nonetheless, their behavior of selection is not limited to a single

species; rather, it has been extended to include people of all species. Using the MTT assay, Saquib et al. in 2021 found that exposing human umbilical vein endothelial cells (HUVECs) to carbofuran for 24 hours drastically decreased the cell survival rate to 25.16 and 33.48 percent, respectively, at 500 and 1,000 μM analyzed by MTT assay.

Carbofuran is absorbed well through breathing and eating, but not through healthy skin. About 75% of the carbofuran that is taken in is made up of proteins. Through oxidation, 3-hydroxy carbofuran and 3-keto carbofuran are made from carbofuran. By hydrolysis, 3-hydroxy-7-phenol, 3-keto-7-phenol, and 7-phenol are generated from carbofuran. The vast majority of metabolites exist in the form of glucuronides or sulphate conjugates, both of which are eliminated from the body via the urinary tract. In rats, the half-life of the parent molecule is twenty minutes, but the half-life of the 3-hydroxy carbofuran metabolite is sixty-four minutes. (Lau et al., 2007).

Major Sections of Present Thesis

In this thesis, graphitic carbon nitride and other nanocomposite materials are investigated for their potential to advance the performance of g-C_3N_4 in terms of doping with a variety of different doped materials, as well as for the investigation of the influence of doping on the applications. This particular thesis focuses on the synthesis and characterization of graphitic carbon nitride-based nanocomposite materials, including g-C_3N_4/GO, g-C_3N_4/V_2O_5, g-C_3N_4/GO/V_2O_5, g-C_3N_4/La_2O_3, and g-C_3N_4/GO/La_2O_3, for the photocatalytic degradation of organophosphate and carbamate pesticides. The thesis is divided up into five different chapters, and their contents are as follows:

Chapter-1 discuss the introduction of pesticide pollution and its impact on human and the environment. In addition, pesticide classification, chemistry, usage, and distribution in the world.

Chapter-2 includes an overview of the literature survey that described in detail photocatalysis and g-C_3N_4 as a photocatalyst with other doped material for water treatment finally the objective of the thesis was to discuss the present work in a detailed study.

Chapter-3 contains the material, methods, and techniques used for this study. It will explain the materials used to synthesize the photocatalyst, instrument, and analysis method was also discussed in this chapter. In this work, we used Thiourea (99%), ethanol, sodium hydroxide, hydrogen peroxide, graphite flakes, sodium nitrate (98 percent), potassium permanganate (99 percent), ammonium metavanadate, hydrogen peroxide (40 percent wt), sulphuric acid (98 percent), and

hydrochloric acid DI water was used for the research of the photocatalyst. All reagents were analytical grade and were not purified further. DI water was used to prepare the stock solution.

Chapter-4 includes results and discussion. g-C_3N_4 was prepared by using a simple calcination method and other binary and ternary neon composites by using the hydrothermal method. As prepared pure, binary, and ternary nanocomposite was confirmed and characterized by XRD, FT-IR, UV-DRS, TGA, and FE-SEM, compared to pure g-C_3N_4, ternary nanocomposite efficiently degrades Chlorpyrifos and Carbofuran insecticide under visible light irradiation within 120 minutes.

Chapter-5 The overview and recommendations of g-C_3N_4, g-C_3N_4/GO, g-C_3N_4/V_2O_5, g-C_3N_4/GO/V_2O_5, g-C_3N_4/La_2O_3 and g-C_3N_4/GO/La_2O_3 was discussed in chapter V Relevant references and articles presented/published in journals were also included at the conclusion of the thesis.

CHAPTER-2:

REVIEW OF LITERATURE, SCOPE, AND OBJECTIVE

One of the most lethal toxins to which mankind has ever been exposed is pesticides. The researcher attempted to address the deadly issue of pesticide pollution by employing advances in nanotechnology. The use of g-C_3N_4 nanoparticles for the photocatalytic destruction of different insecticides is highlighted in this chapter. The mechanism and principle of photocatalysis are also highlighted, with particular attention paid to the degradation of various pesticides and intermediate compounds on a g-C_3N_4 basis while taking into account the many parameters influencing the process and the mechanism of photodegradation. The chapter provides deep information on the integrated strategy for pesticide degradation and their limitations. Based on literature review Objectives of present study has been design to fill the existing knowledge gap.

2.1 Overview of Pesticides

Ever since the beginning of civilization, it has been the major assignment of the human population to engage in a continuous endeavor to fulfill nutritional requirements. One of the fundamental human needs in which man has been betrothed is securing relief from hunger and shortage of food commodities. The world human population has increased from 2.5 billion in 1950 to 7.7 billion in the year 2018 which suggested that it has doubled in the past 50 years. Furthermore, it has been also proposed that by 2050, the world human population will cross the mark of 9.1 billion (Carvalho, 2006), and India and china are in the leading role. Therefore, the urgency to increase global food production and to accommodate the needs of a rapidly growing population is well recognized and documented (Agoramoorthy, 2008). In India, fulfillment of food needs would have not been possible without the miracle called the 'Green Revolution' that happened in the early 1960s.

This rebellion gave reasonable anticipation to the country being not only self-sufficient for adequate food but also for fodder production for feeding the animal population. The green revolution has brought a tremendous increase in worldwide crop production and has also made India one of the largest producers of some important agricultural products. In the current scenario, the important necessity is not only to increase food production but also to maintain the security of cultivated food. This increasing demand for food production per capita could be accomplished by the combination of various approaches like increasing land area for crop cultivation, improving soil water management systems, focusing more on organic farming, controlling pest population to prevent both pre-harvesting and post-harvesting crop damages, and using crop varieties which are resistant to the pests (Devi et al., 2017, Devi, 2010).

Pests are living creatures like weeds, bugs, bacteria, fungi, viruses, and animals that hurt crop production and make our lives harder. Pests hurt the amount and quality of crops by reducing their production and destroying crops that have been stored. But they can also harm other animals, compete with people for food, harm people's health, and cause a lot of damage to the land. In conclusion, pests make farming much more expensive as a whole. Physical (pulling weeds by hand, mulching, giggling, filling) and biological methods can be used to control the number of pests (cultivar choice, crop rotation, antagonists, predators, etc). methods that use chemicals (pesticides) (Parra- Arroyo et al., 2022, Morin-Crini et al., 2022). The seeds and the soil are treated

with pesticides that have been diluted to the appropriate concentrations. Every year, there are reports of irrigating water and crops to reduce the risk of damage. The most recent illustration of this is the widespread insect infestation that occurred in the Bt cotton crop that was grown in northern India. As a result of this, the amount of land used for cotton production in Punjab and Haryana has decreased by 27% (during the fiscal year 17 harvests year), as farmers have moved their attention to other crops after suffering enormous financial losses as a result of the whitefly pest infestation (The Hindu,2016). It is estimated that over 25 percent of the crop the world is lost due to diseases, weeds, and pests. This is not a good sign for farming given the serious difficulties that lie ahead, and as a result, agrochemicals are playing an increasingly important role.

There is a significant risk to global food security as a result of increased crop damage caused by pests and the losses that result, which has led to the enormous relevance of agrochemicals (Abhilash and Singh, 2009). In the process of cultivating crops, pesticides play the role of a plant production agent to increase the amount of food that is produced. Pesticides are chemical poisons purposely used in agricultural fields to control the proliferation of pests' populations. Due to increased demand for agricultural products consistent and intentional use of chemical pesticides has now become an integral component of modern agriculture. The increased production of a diverse range of crops as a result of the application of pesticides has resulted in significant economic benefits for the world as a whole. In addition, the application of pesticides is an extremely important factor in the fight against the transmission of a wide range of infectious diseases (Kadhiru et al., 2022).

Unquestionably, pesticides have originated as a sensation and have greatly improved crop production rates in the last years. Detection of pesticide residues in ecosystems and their ingestion via various routes negatively influences human health and emerges as an alarming issue to mankind. despite their role in enhancing agricultural productivity, maltreatment of chemical pesticides during various stages like production, processing, storage, and transport led to contamination of the ecosystem in various ways. It has been documented that the major part of the pesticides applied in fields reaches healthy ecosystems and gets accumulated into other organisms. Pesticides impose hazardous effects on biotic communities specifically on humans when exposed via contamination of ground and surface water and through the food chain (Verma and Bhardwaj, 2015).

2.2 Pesticide Consumption and Production- Indian Scenario

Insects, weeds, and diseases cause the loss of a significant proportion of the world's crop production every year, which poses a risk to the world's farming community. On the other hand use of agrochemicals in agriculture has gained importance. India has 16% of the global human population but only accounts for 2% of the world's total land area. Indian farmers have been compelled to use a substantial number of chemicals as a result of the rapid development of the country's population as well as the obligation to meet the nation's food requirements. The primary source of income for close to 58 percent of rural families is derived from agricultural activities (Abhilash and Singh, 2009). Agriculture has always been the most important sector of the Indian economy, and it currently contributes 15% of the total gross domestic product of the country (Arora et al., 2013). It has also been claimed that in India, approximately 15–25 percent of the potential crop yield is lost due to the presence of pests, weeds, and diseases. Country of India is the continent's second-largest producer of pesticides. It is the nation that produces the fourth most pesticides in the entire globe, following the United States of America, Japan, and China (Agnihotri, 2000; Kumar et al., 2012).

First, ever endeavor of the utilization of synthetic pesticides took place in 1948-49 when DDT(Dichlorodiphenyltrichloroethane) and BHC (Benzene Hexachloride) were used for malaria and locust control respectively (Shetty, 2008). Since then pesticide consumption has improved many folds from 154 MT in 1954 to 41,822 MT in 2009-2010. The scenario of the usage of pesticides within India and worldwide is quite different (as shown in Figure 2.1). In India, 76% of pesticides used is an insecticide, and in global usage 44%. (Devi et al 2017; Rathore and Nollet, 2012).

The government of India has made measures to guarantee that pesticides are used in a manner that is both safe and responsible, and these measures have been implemented by the government. The Insecticides Act was enacted in 1968 and went into force in India on August 1, 1971. This law places restrictions on the importing, manufacturing, selling, transiting, distributing, and using of pesticides. The goal of these restrictions is to protect both humans and animals from potential harm, as well as to address concerns that are related to the act itself.

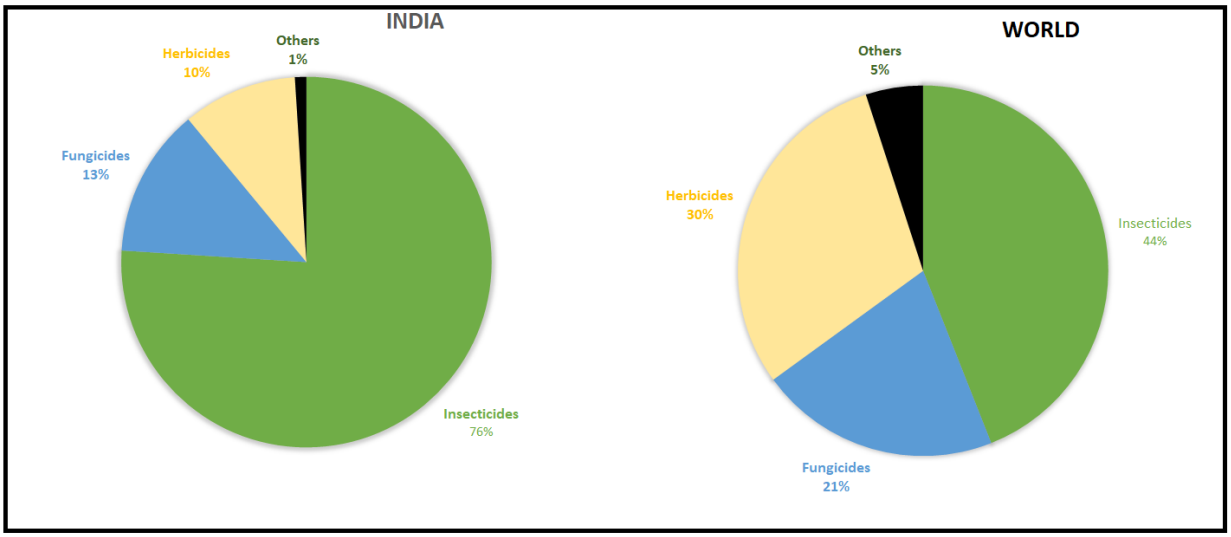

Figure 2.1 Pesticides consumption pattern in India and the world

(Image recreated: Source Akhtar et al., 2009)

The Act was promulgated in 1968, and it went into effect on August 1, 1971. The Insecticides Act was written into law to reduce the likelihood of harm coming to animals or people, as well as for issues related to this goal. On August 1, 1971, this act began its full implementation. (Kumar et al., 2016). Manufacturing has also been responsible for managing the state and district levels of authority, both for the safe application of pesticides and to ensure their correct use.

In India, the use of pesticides is not limited to the agricultural sector; in fact, they are also utilized in a wide variety of other areas, such as industrial, household, and domestic. Insecticides make up the largest portion of India's overall pesticide consumption, accounting for sixty percent of the country's total. In comparison, fungicides account for eighteen percent, herbicides for sixteen percent, and other pesticides for six percent. Taking into consideration the rest of the world, where herbicide uses accounts for thirty percent and fungicide use accounts for twenty-one percent, this scenario stands in stark contrast. The higher consumption of insecticides in India may be due to the higher hatching rate of insects in warm humid and tropical climates which provides favorable breeding climate conditions (Aktar et al., 2009). Chlorpyrifos is one of the insecticides that have the greatest consumption rates in India (Bhushan et al., 2013).

Conventional pesticides make up the majority of the product catalog for the country's various distributors. They are utilized most frequently in the form of dusting powder at a rate of 85%, followed by water-soluble dispersible powder at a rate of 12%, and emulsification concentrates at a rate of 2%. Granules are still being utilized, even though their use offers numerous benefits, including less drift, simpler administration, and increased safety during operation.

Due to a lack of adequate education and awareness regarding health issues, Indian agricultural products were found to contain significant quantities of pesticide residues, as was revealed in a report titled "Pesticide Residues in Indian Food and Agricultural Products." This was the case because of the lack of education. Incorrect advice given to farmers by those who sell pesticides is another primary contributor to the widespread use of indiscriminate amounts of pesticides (Mittal et al., 2014).

Farmers in most advanced nations, like the United States, Japan, Korea, and China, have access to more information, and the application of pesticides is carried out with an extremely methodical approach (Sarkar et al., 2008).

In comparison to the other Asian continents, India has the second highest rate of pesticide use (0.29 kg/ha) (Sharma et al., 2020). After India gained its independence, the country's crop production was not sufficient to meet the need of the country (Sebby, 2010). As a direct consequence of India's participation in the green revolution, the country's traditional method of cultivating edible crops was transformed into a capital-intensive, technologically advanced, and surplus-producing form of agriculture. As a direct consequence of this transformation, India's overall food grain production increased by a factor of ten between the years 1960 and 2000. (Davies, 2003; Kannuri and Jadhav, 2018).

As part of the green revolution, high-yielding varieties were used. These HYVs needed huge amounts of nitrogenous fertilizers to produce enough crops to feed India's constantly growing population (Kannuri and Jadhav, 2018; Sharma et al., 2019). Still, the continued use of pesticides led to the development of pests that can survive the chemicals. Due to the narrow heritable traits of high-yielding rice and wheat varieties, monocropping, and India's tropical climate, the plants became more vulnerable to pests and diseases. This made farmers rely too much on pesticides to keep their crops from dying. This, in turn, led to a huge rise in the number of pesticides used in India, from 154 metric tonnes in 1954 to 88,000 metric tonnes in 2000, or a 570 percent increase

in less than 50 years. In other words, the number of pesticides used in India went up from 154 metric tonnes in 1954 to 88,000 metric tonnes in 2000. (Kumar et al., 2016; Bonvoisin et al., 2020). Even so, the Indian government took strong steps that led to pesticide use dropping from 88,000 metric tonnes in 2000 to about 58,634 metric tonnes in 2015–16. This was done by putting limits on how many pesticides could be sold in India. Still, this amount has reached about 62,193 metric tonnes in 2020–21, and it keeps going up (as shown in Figure 2.2) (Directorate of Plant Protection, Quarantine, and Storage | GOI, 2021).

Punjab is the hub of agriculture and is ranked among the top five states of pesticide consumption. Farmers in Punjab mainly grow cotton, rice, and wheat crops on a large scale and agriculture is the back of the state. Punjab is geographically divided into three main regions i.e., Majha, Malwa, and Doaba. Out of total pesticide utilization in the Punjab, Malwa region solely consumes more than 70%. The cotton belt of Punjab is located in the Malwa region, which is also known as India's "Cancer Capital" because to the abnormally high number of pesticide-related cancer cases that have increased threefold in the preceding ten years. Malwa region is also known as India's "Cancer Capital" (Mittal et al., 2014). Each year, a certain number of cases of pesticide poisoning are reported. The Punjab Agricultural University in Ludhiana, Punjab, India, reports that farmers in this region sprayed their crops a total of 32 times over the course of a period of six months, which is about five times more than the recommended amount (Mathur et al., 2005).

Pesticide use is also linked to a rise in several diseases in the Malwa region, such as mental retardation and problems with reproduction. People who work in places where they are directly exposed to pesticides are the most at risk. Pesticides are used a lot in this area, which is one reason why the amount of residues in the food chain is going up. Pesticide residues from close to 17 different kinds have been found in the area (Mittal et al., 2014). The Central Insecticides Board and Registration Committee of India is the government agency in India that is in charge of registering pesticides (CIBRC). In comparison to the norms of the European Union, India use significantly higher quantities of organic pesticides that are persistent (Yadav et al., 2015).

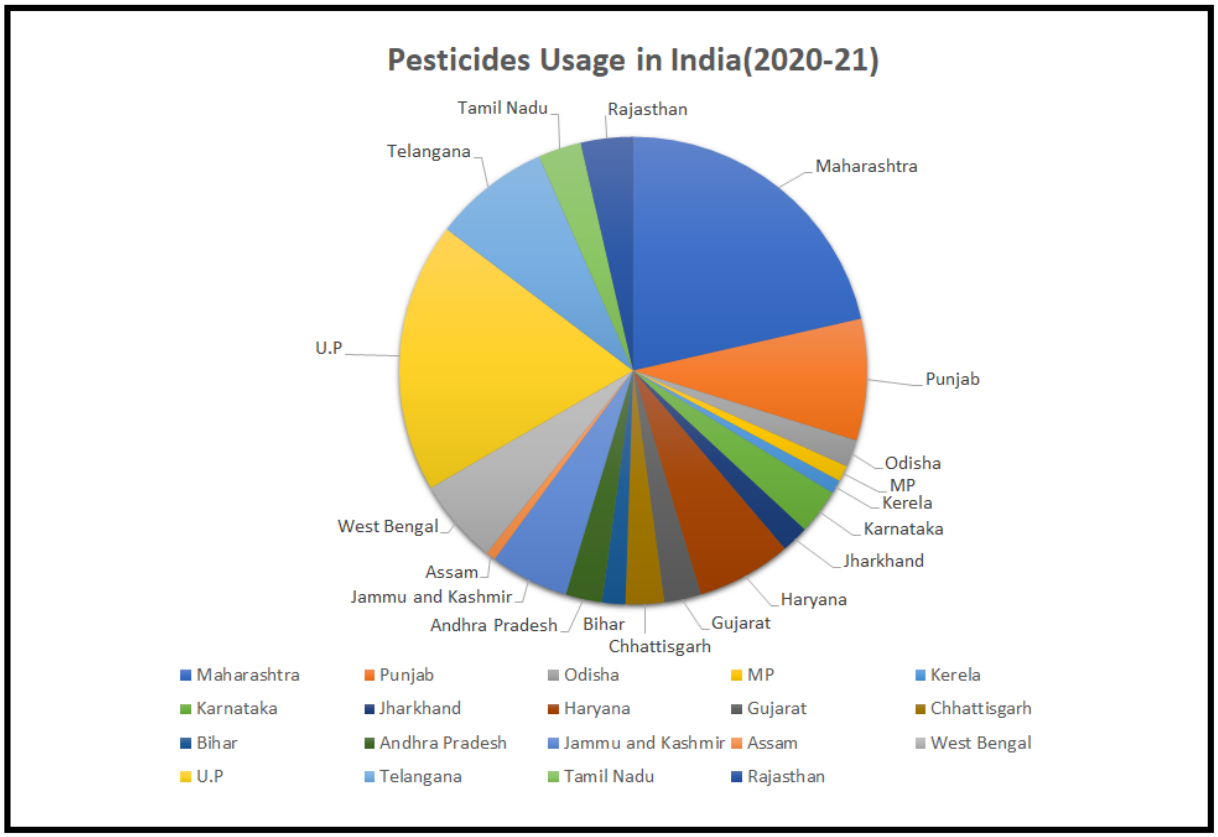

Figure 2.2 Pesticide usage in India. With an average of 13,243 M.T., Maharashtra has the highest use among the States. Data were taken from the statistical database of the GOI directorate of plant protection, quarantine, and storage (2021).

Pesticides are the second most common source of contamination in drinking water and are known to pose a significant danger to both human and animal health. Several different elements contribute to the pollution of groundwater by pesticides. Some of these factors include the chemical composition of the soil and pesticides, the pH level of the soil, hydraulic loading, and crop management methods. The use of pesticides in agriculture generally results in the soil becoming tainted and engrossed by the chemicals, and the use of certain persistent pesticides in conjunction with environmental factors can cause groundwater to become contaminated through leaching (Syafrudin et al., 2021). This increases the likelihood that water will be contaminated. Leaching, surface runoff, equipment washings, irresponsible disposal of empty containers, and other practices from agricultural fields are all contributing to the contamination of the water sources

caused by excessive and unacceptable consumption of pesticides in agricultural production (Zhang et al., 2011). The poisoning of surface and ground waters by pesticides and the residues left behind by such pesticides is a major cause for concern in today's world. Both leaching and volatilization are ways in which pesticides can be harmful to the environment. Leaching is a process in which pesticides can contaminate groundwater. Volatilization is another way. Due to the importance of groundwater in human life (Fenoll et al., 2011) as the supply of drinking water, the issue of pesticides seeping into water bodies is garnering considerable attention. The physicochemical qualities of pesticides, as well as their solubility, are what affect their ability to be carried away in surface runoff and leached into groundwater; the higher the solubility, the greater the leaching and carrying. It is common knowledge that the widespread use of OP pesticides contributes to the contamination of both groundwater and surface water. Herbicides, organophosphorus compounds, and organochlorines, which are now banned because of their persistence in aquatic environments, are the pesticide classes that are found in the water the most frequently (Kamrin, 1997).

The administration of the pesticide, whether it be through spray drift or foliar wash-off, causes Chlorpyrifos to infiltrate the soil ecosystem directly. The water solubility of the adsorbents and the nature of those adsorbents have a significant impact on the adsorptions-desorption, soil mobility, and water mobility of Chlorpyrifos. In soil, the behavior of pesticides is further impacted by a factor known as the partition coefficient. Adsorption tends to restrict the mobility of Chlorpyrifos, which in turn improves its persistence in the soil (Hua et al., 2009). The soil adsorption coefficient for Chlorpyrifos is larger than 5000, which indicates that it can be absorbed by the soil. The half-life of 41 CP in the soil can range anywhere from days to four years, depending not only on the concentration but also on the pace of application, the soil microorganisms, the kind of ecosystem, and the meteorological circumstances (Wang et al., 2013, Wan et al., 2021). Adsorbed Chlorpyrifos in the ground is susceptible to primary breakdown by the sun's rays (direct photodegradation), chemical hydrolysis, and the microorganisms in the ground (Racke et al., 1996). The degradation of agricultural pesticides in soil and water is of the utmost importance because these two mediums are key sinks for the chemicals in question. Because of this, it is essential to research what happens to pesticides in the environment and investigate methods for removing them from various parts of the ecosystem in a way that is economically feasible, commercially viable, technologically advanced, and kind to the natural world.

2.3 Present Technology for the treatment of Pesticides

Pesticides, in contrast to dyes, heavy metals, and other types of pollutants, are harmful to both human health and the environment even at extremely low concentrations. The soil and water ecosystems have been severely harmed as a result of the excessive and frequent use of pesticides, as well as a lack of information. Even though there is a wide range of remediation technology that may be used for cleaning up pesticide contamination in soil and water, choosing the method that will be most effective can be a challenging challenge. Additionally, if a single technique was shown to be wrong, then several technologies had to be blended to achieve satisfactory outcomes.

The removal of hazardous organic contaminants from wastewater has been the subject of a lot of research and development over the years, and several different procedures are currently in use. Conventional techniques for the elimination of these contaminants, such as surface adsorption (Andreau and Pico, 2004); membrane filtration (Islam et al., 2010); biological degradation (Ündeger and Basaran, 2005), are utilized in the treatment of pesticides. According to Rileanu et al., (2013), the ineffectiveness of currently available treatment procedures for the removal of pesticides has greatly raised the level of concern for the development of more advanced treatment technologies. The majority of recalcitrant contaminants are resistant to being broken down by traditional chemical and biological treatment procedures (Parra et al., 2002).

Chemical oxidation is another method that can be utilized in the process of removing pesticides from water (El-Temsah et al., 2012), though, this method is prohibitively costly and results in the contamination of the water with additional hazardous by-products. (Burrows et al., 2002). Biological therapy is thought of as a method that is kind to the environment, yet it is very time-consuming, inefficient, and has a restricted range of applications (Di-shun et al., 2009). In addition, these methods do not result in the entire transformation of pollutants into non-hazardous waste; rather, they merely move the pollutants from one phase to another (Echavia et al., 2009). There are currently numerous different methods that are employed for the removal of pesticides, all of which are detailed in Table 2.1 and Figure 2.3.

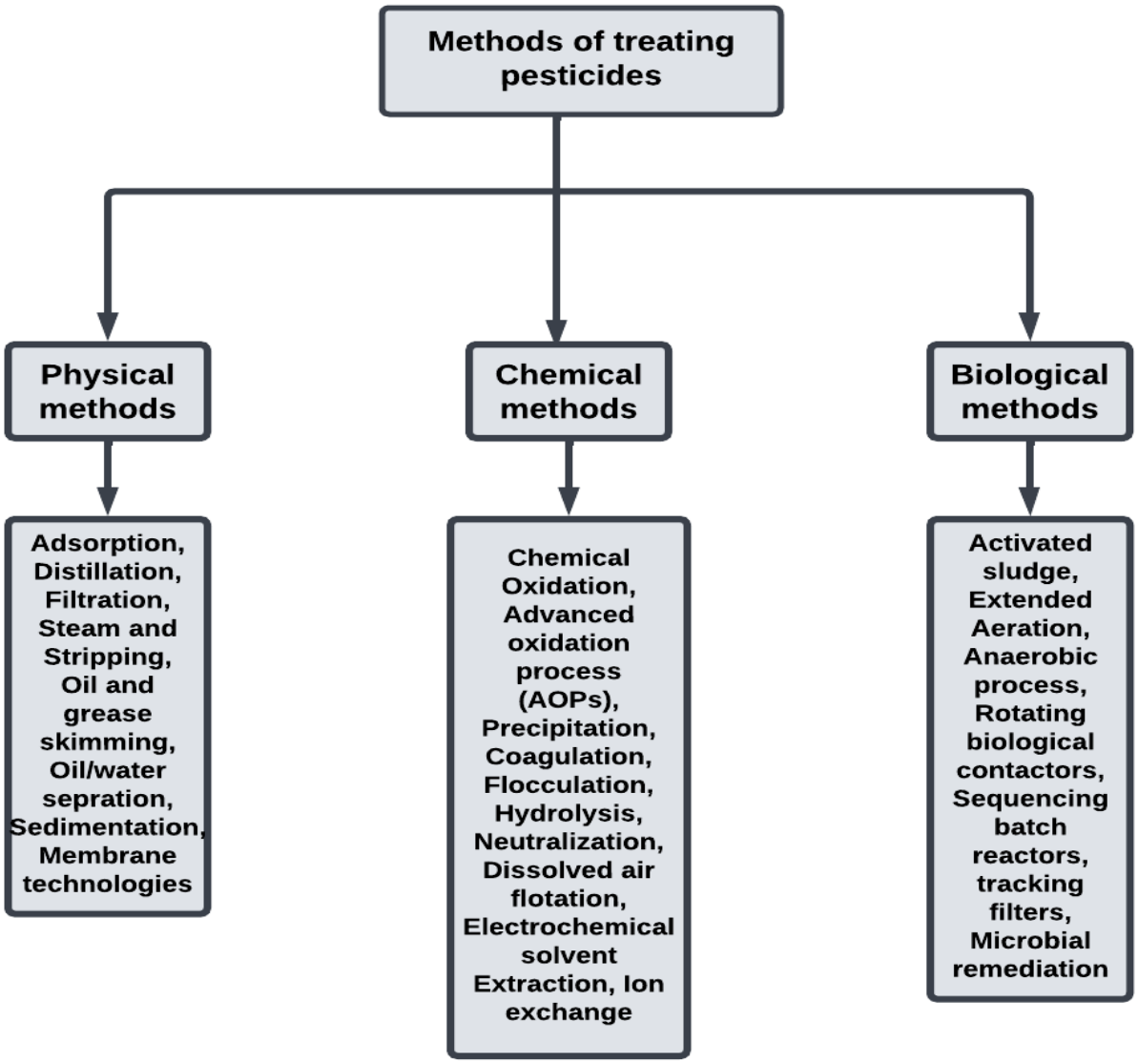

Figure 2.3 Different Treatment technology for Pesticide degradation

The strategies that have been discussed up until now are effective, but they have certain restrictions when it comes to their applicability, time commitment, and financial investment. In addition, the most common technique for getting rid of pesticides is incineration, which is a very costly process that most developing countries do not have access to (Evgenidou et al., 2005, Robert et al., 2002). One such process is known as chemical oxidation; however, not only is it prohibitively expensive, but it also results in the contamination of water with additional harmful chemicals. Therefore,

TABLE 2.1 Advantages and Disadvantages of different methods of pesticides degradations

scientists have no choice but to look forward to the development of alternative technology, such as enhanced oxidation processes, for the complete mineralization and degradation of pesticides

Method	**Technique**	**Advantages**	**Disadvantages**
Physical	Adsorption Settling Membrane filtration Air stripping	Rapid	No destruction of pesticides, By-product formation
Chemical	Oxidation Reduction Catalysis Hydrolysis Photo-Fenton Coagulation Ozonation Fluid extraction Solid phase extraction	Rapid Destructive Effective	High cost, Complex process, Toxic end products and by-products
Biological	Microbial degradation	Destructive	High cost, Comparatively slow Less effective, Toxic end product
Thermal	Combustion	Rapid and Destructive, No by-product	High cost Complex process

into molecules that are safe for the environment. The removal of organophosphate chemicals from water has been accomplished using a variety of techniques up until this point, including chemical and biological methods, among others. The approaches that have been discussed so far come with some downsides, the most notable of which are their toxicity, high cost, sluggish and drawn-out

procedure, and the production of harmful byproducts. As a result, photocatalysis appears to be the optimal approach that can overcome the limitations of the other methods that can be used to get rid of the persistent pesticide. During the photocatalytic process, potentially harmful organic contaminants are converted into carbon dioxide, water, and several other simple acids and salts. One of the benefits of using photocatalysis is that it eliminates the need for a secondary way of waste disposal. This is because there is no secondary technique required. The sole limiting element that is currently linked with photocatalysis is the post-recovery of the nano-catalyst from the solution after the treatment, which is a problem that can be handled by adopting a hybrid technique (Bhatkhande et al., 2002; Diban et al., 2013; Koe et al., 2020)

2.4 Nano-technological Approaches for Pesticide Remediation:

The scientific community's attention has been attracted by the ever-increasing pollution and the harmful repercussions it produces to the critical demand for the cleanup of wastewater that has been poisoned with pesticides. The most effective advanced oxidation method for removing pesticides and other forms of contaminants is nanotechnology, which makes use of nanoparticles as the photocatalyst. This technology is based on nanotechnology. This technology is based on using nanoparticles as the photocatalyst's active ingredient (Liqiang et al., 2003). The elimination of toxicants from trash, in addition to their mineralization, can be accomplished through the use of a technology called nano-photocatalysis. This can contribute to the sustainable development and cleaning up of the environment. It makes it possible for the resistant substances to be broken down into intermediates and non-toxic end products, and in some situations, complete mineralization can even be achieved as a result of this process.

In recent years, nano-based photocatalysis has shown a lot of promise as a green, low-cost, and long-lasting treatment method that uses chemicals. This potential has been demonstrated in several different ways. Recent research has pointed to this possibility as a positive outcome. Because it is simple to extract energy from either natural sunlight or artificial light, as well as because there is a great deal of it available everywhere, nano-photocatalysis has emerged as one of the technologies with the greatest potential. This is one of the reasons why it has become one of the most promising technologies (Oskoei et al., 2016). The removal of a wide variety of pollutants from wastewater has been accomplished by the application of photocatalytic degradation methods, which have proven successful in doing so. Photocatalysis has already demonstrated its capability of degrading

a wide variety of substances, including phenols, dyes, medicines, and compounds that disturb the endocrine system, as well as pesticides, in wastewater. One of the most significant benefits of the photocatalytic process in comparison to other technologies that are now in use is that there is no longer a requirement for alternative methods to get rid of trash. Because air itself serves as the oxidant, this method does not require the use of pricey oxidizing chemicals like those that are required by other more advanced oxidation technologies, such as those that utilize hydrogen peroxide and ozone as oxidants. This is different from other advanced oxidation technologies, like those that use hydrogen peroxide and ozone as oxidants (Vora et al., 2009). The majority of the time, heterogeneous catalysts consisting of semiconductors are the ones that are utilized (Fenoll et al., 2011). In the recent past, nano-based photocatalyst has demonstrated a great deal of promise as a low-cost, green chemistry-based, and ecologically friendly approach to the treatment of wastewater. This potential was shown by the fact that it was able to show a lot of promise (Ahmed et al., 2011). Several different kinds of nanomaterials have been used to break down and get rid of pesticides in the environment. These include metal and metal oxide nanoparticles, doped nanoparticles, nanotubes, nanocomposites, and bimetallic nanoparticles (Garcia and Takashima, 2003). Despite the significant amount of research that has been conducted in this field, it is still a problem to create an effective semiconductor-based photocatalyst that is capable of operating in solar, visible, and ultraviolet light.

The distinctive photophysical and photocatalytic capabilities of these tiny semiconductor particles are at the root of the widespread interest in them. Semiconductors are important as photocatalysts because of how their electronic structures, ability to absorb light, ability to move charges, and ability to stay excited for a long time (Mills et al.,1997). One of the study fields that has seen the most rapid expansion over the past decade focuses on the photochemistry of nano-based semiconducting materials. Semiconducting nanoparticles are one type of nanomaterial that has been the subject of a lot of research because they can be used in so many different ways (Quiroz et al., 2007). Other nanomaterials that have been the subject of extensive research include carbon nanotubes (Quiroz et al., (Sobczyski, 2001). The following is a list of benefits that come from using semiconductors: (i) they are affordable, (ii) they are nontoxic, iii they have a high surface area, and (iv) they exhibit adjustable features that can be adjusted by the application of doping and sensitizers. (v) being able to facilitate the process of multiple electron transfers, and (vi) being

capable of being used for longer periods without suffering a significant decrease in photocatalytic activity.

2.4.1 Photocatalytic Advanced Oxidation Processes

The term "advanced oxidation processes" (AOPs) refers to a group of chemical treatment treatments that are aimed to remove pollutants from water and wastewater through the process of oxidation via reactions with hydroxyl radicals (OH). These highly reactive OH are capable of oxidizing and mineralizing a variety of organic molecules, which results in the production of carbon dioxide and various inorganic ions (Glaze et al., 1987, Han et al., 2004). Advanced oxidation processes include the Fenton process, ozonation, the photo-Fenton process, ozone with a catalyst (O_3/CAT), ozone with /H_2O_2), ozone with ultraviolet light and AOPs. Large-scale applications are limited by the complexity of these technologies (AOPs), the large number of chemicals they use, and the high cost of treatment. This is in addition to the fact that it is hard to get rid of refractory organic contaminants.

Among these several methods (shown in Figure 2.4), photocatalysis has gained attention in environmental clean-up. This is mostly attributable to the efficiency of the g-C_3N_4 catalyst in the production of hydroxyl radicals, as well as the ecologically friendly features it possesses. The ability of semiconductor photocatalysis to produce oxidizing radicals in the environment without the addition of any additional chemicals is the most significant advantage of this AOP application. While other photochemical AOPs need to use costly photons and chemical oxidants (H_2O_2, O_3, persulfate) as precursors to form reactive oxygen species, persulfate is the most common of these oxidants. Under the influence of natural or artificial UV light, a process known as photocatalysis can indirectly activate ambient H_2O and O_2 to produce reactive oxygen species (ROS). In the following sections, we will focus on providing a comprehensive introduction to the idea of photocatalysis as well as its application in the process of removing contaminants from wastewater.

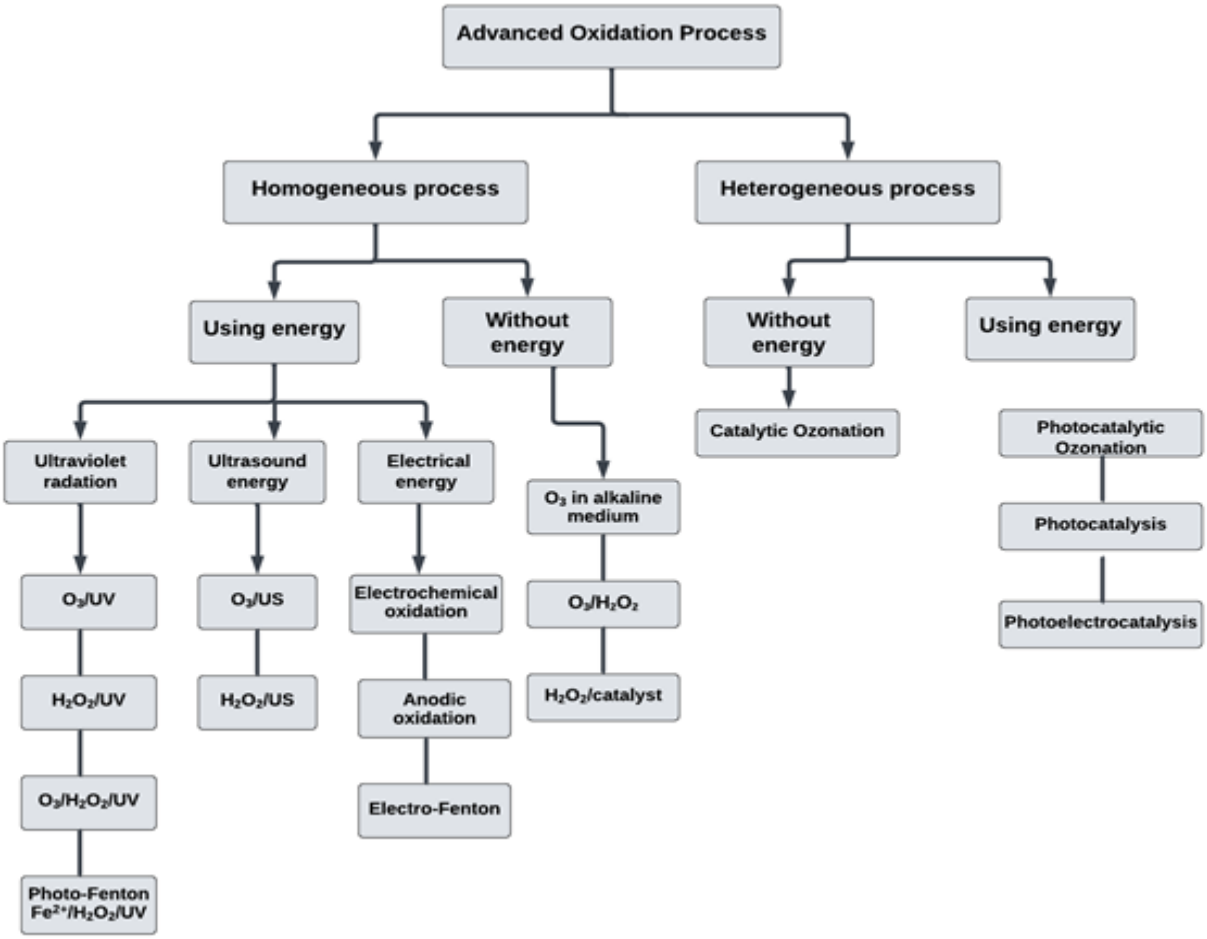

Figure 2.4 Classification of Advanced Oxidation Processes

(Image recreated: Source Han et al., 2004)

In the process of photocatalytic advanced oxidation, light is used to turn on a substance called a photocatalyst. The photocatalyst changes the speed of a chemical reaction without actually taking part in the change. Photocatalysis is the name for this process. Another way to describe photocatalysis is as a process in which a catalyst makes a photoreaction happen faster (Hoffmann et al., 1995, Kutal, 1985). Since Fujishima and Honda, 1972, first demonstrated that water may be electrochemically photolyzed on a TiO_2 electrode, there has been a substantial growth in interest in the topic of photocatalysis. In recent years, researchers' interest in employing semiconductors as photocatalysts to remove ambient quantities of pollutants. This can be used to clean up the environment, treat drinking water, make products for industry, or help people with health

problems. This shift in interest is because semiconductor materials can be used to remove pollutants. The two most significant applications of photocatalysis that have been discovered to date are the solar splitting of water and the purification of air and water pollutants. Both of these applications have shown considerable potential. Before wastewater from industrial or household sources is allowed to be discharged into the environment, any chemical contaminants that have been detected in the wastewater must either be eliminated or destroyed. These contaminants are also able to be detected in ground and surface water, both of which need to be treated in order to obtain an acceptable level of quality for drinking water. Within the realm of the destruction of pollutants, photocatalysis is garnering a significant amount of attention (Zhang et al., 2019). By using photocatalysis, the dangerous organic compounds can be turned into CO_2, H_2O (Ahmed and Ollis., 1984). The main benefit of this process over other technologies that are currently in use is that it doesn't require any extra steps for getting rid of waste. Since ambient oxygen is used as the oxidant in this process, no expensive oxidizing chemicals are needed, which is different from other advanced oxidation technologies, especially those that use hydrogen peroxide and ozone as the oxidant. Since the oxygen in the air is the oxidant in this process, there is no need for oxidizing chemicals. The fact that this method can be contrasted with other cutting-edge oxidation technologies is yet another advantage of utilizing it. Photocatalysts are reusable and recyclable materials that also have the ability to regenerate themselves. Homogeneous photocatalysis, which includes ozone and photo-Fenton systems, has its own set of restrictions, including the inability to immobilize or recycle the catalyst, as well as the removal of the catalyst. The heterogeneous photocatalysis that makes use of semiconductors is a more effective way than both other forms of advanced oxidation and more traditional approaches. Because this procedure breaks down the contaminated molecules molecule by molecule, there is no trace of the original substance left over, and as a result, there is no need for sludge disposal. The catalyst itself is not altered in any way during the operation, and there is no need to use any consumable chemicals. These factors lead to significant cost reductions as well as simplified procedures for operating the relevant machinery. In addition, the procedure will continue to be successful in the presence of very low concentrations of the pollutant as the pollutant is highly adsorbed on the catalyst surface. Therefore, as a result of the process, significant cost reductions in the production of water are achieved, as well as an improvement in the quality of the surrounding environment.

2.4.2 Mechanism of photocatalysis

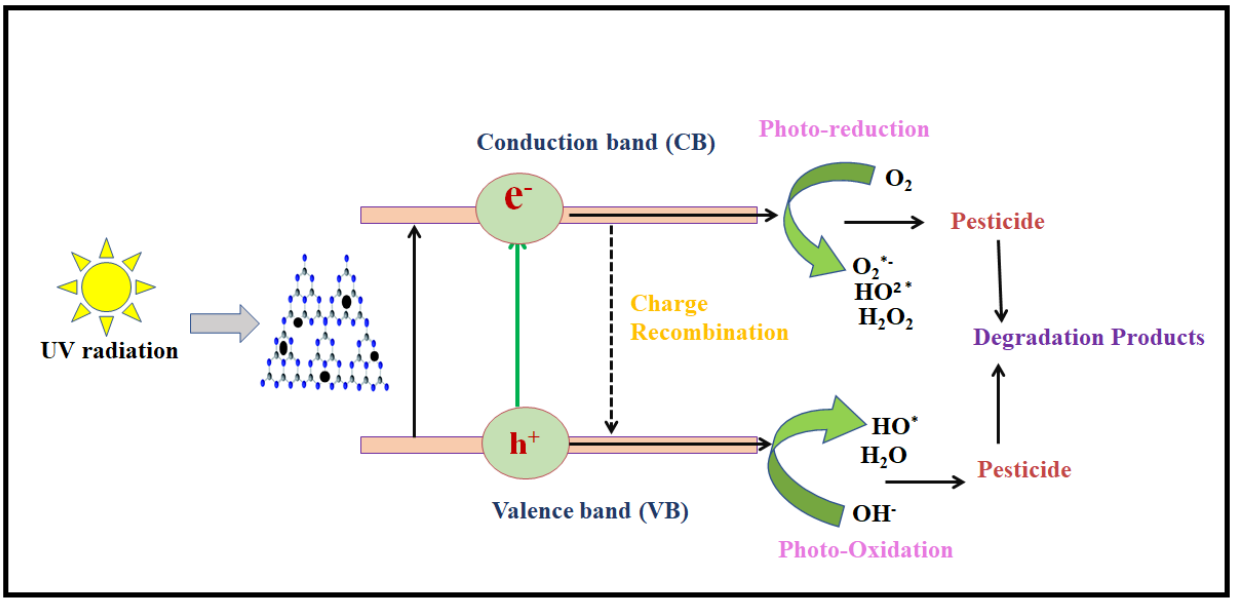

Figure 2.5: General Mechanism of Photocatalysis

During the photocatalytic process, ultraviolet (UV) and visible light radiation are employed to turn on a photocatalyst and produce a redox reaction. This is accomplished through the employment of the photocatalyst. This can be accomplished by exposing the photocatalyst to light of both wavelengths simultaneously. Due to the fact that their electrical structure consists of a full VB and an empty CB, semiconductors may possess both filled VB and empty CB. This enables them to function as photocatalysts for light-induced redox reactions (Hoffman et al., 1995). Bandgap energy refers to the difference in energy between the valence and conduction bands. This discrepancy exists because the VB is higher than the CB. In contrast to metals, semiconductors do not have a continuous network of interbond states, which makes it more difficult for electron-hole pairs to recombine. This makes sure that a pair of electrons and holes will live long enough to take part in the charge transfer that happens across interfaces. When electrons move from one atom to another across the contact, this charge transfer takes place. Even though the energy of the band gap keeps the bands apart, the fast recombination of electrons and holes is the biggest problem that semiconductor catalysts have to deal with. The photogenerated electron-hole pair can recombine either without giving off heat or by giving off heat. Either way, the energy that was put in is lost as heat. To use these charge carriers in redox reactions involving species that have been adsorbed,

the recombination of these charge carriers must be stopped. The charge carriers are able to take a variety of various routes since they are able to become stuck in either shallow traps or deep traps. They could have an interaction with electron donors or acceptors that have been adsorbed on the surface of the photocatalyst, which would be the last but not the least possibility. In point of fact, Serpone et al., 1996 demonstrated that the electrons and holes that are trapped on the surface of the photocatalyst are the cause of each and every photo-redox process that takes place there. Figure 2.6 shows some of the features that should be taken into account when choosing a photocatalytic material.

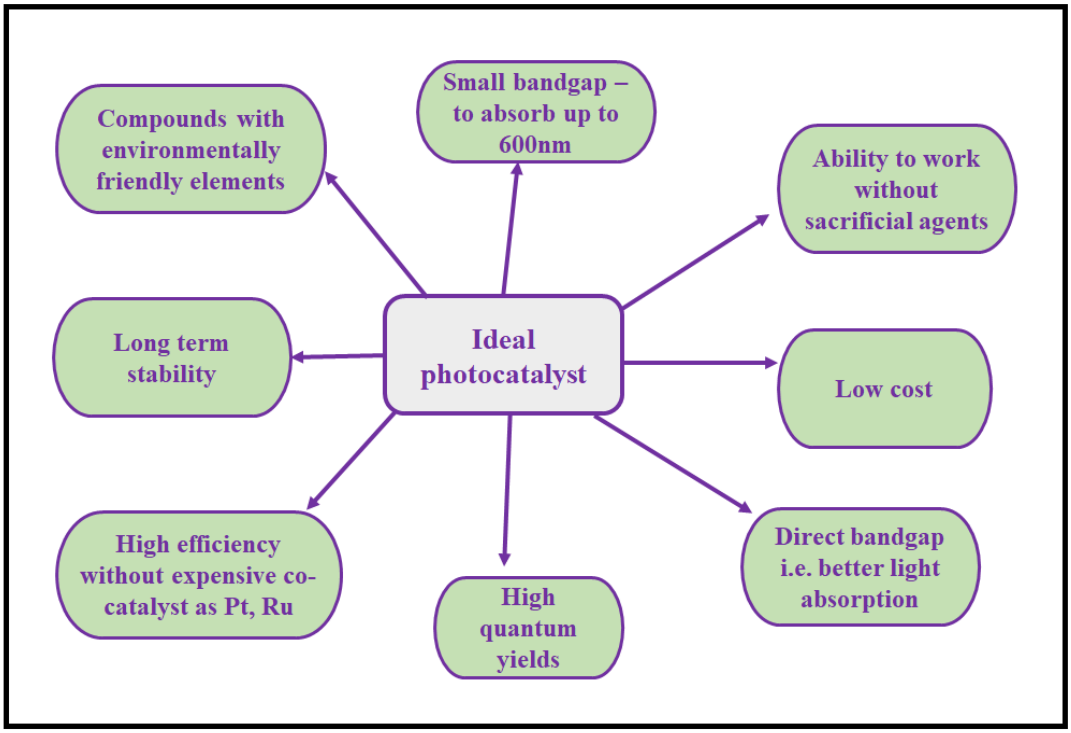

Figure 2.6 Some qualities of ideal photocatalyst

Semiconductor photocatalysis has the ability to eliminate a wide variety of organic contaminants by making use of the light of the sun and not requiring the inclusion of any additional chemical reagents or additional external energy (Lops et al., 2016).

Table 2.2 shows the list of different semiconductors widely used for photocatalytic application.

TABLE 2.2 Energy bandgap value of commonly used Photocatalysts Semiconductor

Semiconductors	Bandgap (eV)	References
g-C_3N_4	2.7	Cao et al 2015
ZnO	3.2	Chauhan and Kumar, 2012
WO_3	2.7	Lua et al 2017
Fe_2O_3	2.2	Guler et al, 2016
CuO	1.7	Wang et al, 2014
Cu_2O	2.2	Wang et al, 2014
Cds	2.4	Biswal et al, 2011
ZnS	3.7	Pouretedal and Hasanali, 2013
Agl	2.7	Beydoun et al, 2000
$BiPO_4$	3.8	Xu et al, 2012
SnO_2	2.1	Sun et al, 2015
In_2O_3	3.0	Mu et al, 2012

The use of visible and solar-powered photocatalysis has the potential to enable the fabrication of next-generation materials and systems for the environmentally friendly treatment of water and generation of electricity. However, there hasn't been much of a breakthrough in the development of solar activity and highly visible-light response personal computers that are also biocompatible and have a long shelf life. In recent years, research has been conducted on metal-free photocatalytic materials for the purpose of removing organic pollutants and splitting water utilizing solar and visible light as the light source. Heterogeneous photocatalysis is defined as a process in which UV-Visible light suitable for the optical bandgap energy of semiconductor particulate (TiO_2, ZnO, Fe_2O_3, Cu_2O, SnO_2, Ag_2O, Cds, MoS_2, and WO_3, etc.) (Chowdhury et al., 2014) is used to produce CB electrons and VB holes, which ultimately results in their photo-excited charge separation and other productive photophysical and photochemical decay channels (Goodnick et al., 2010). The various PCs with their bandgap energies, as well as the positions of CB and VB, the potential solar fuels, are associated with typical reduction potentials, as shown in Figure 2.7. In general, under

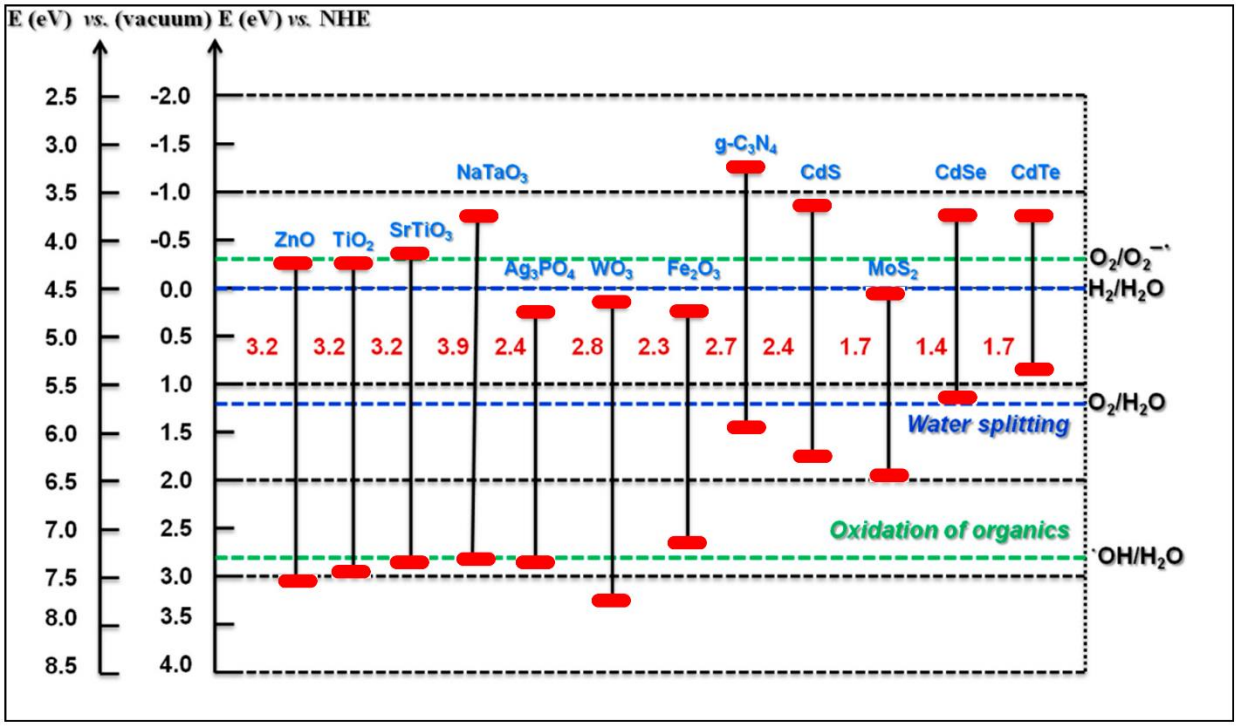

Figure 2.7 Bandgap position of some typical semiconductors

(Image recreated: Source Goodnick et al., 2010)

conditions of exposure to visible light, photon absorption will occur when the applied energy of photons becomes equal to or greater than the optical bandgap energy of presumed SCs. In the meantime, the photo-excited electrons (e^-) of the VB could be stimulated to the CB, leaving the VB with the same number of photo holes (h^+). The CB and VB edge potentials of g-C_3N_4 are measured to be around -1.13 and +1.57 eV, respectively (Tang et al., 2018). On the other hand, the photo-e^- could quickly travel from CB to VB. After that, the photo- e^- could lower the amount of adsorbed oxygen, which resulted in the rapid formation of the O_2^- species. Additionally, the photo -h^+ ions that are present in the VB of g-C_3N_4 react with OH to produce the species denoted by the symbol OH^-. The already-produced photo -e^- will then undergo a further reaction with the adsorbed oxygen on the surface of the catalyst to produce reactive O_2^- radicals, which will then prefer to interact with water to make OH^- radicals. As it has now been stated, such semiconductor NMs are being convinced to be applied in the photocatalysis process as a result of their inherently filled VB

potentials and empty CB potentials (Samsudin et al., 2015). Following the absorption of the active photons by these semiconducting substances, when hv is greater than Eg, photo-excited electrons (e^-) are stimulated between the VB and CB edges as shown in Figure 2.5. As a result, this can be explained in more depth in the subsequent reaction:

$$SC + hv \longrightarrow SC^* e^-_{CB} + h^+_{VB}$$

$$h^+_{VB} + H_2O \longrightarrow \cdot OH + H^+$$

$$O_2 + e^-_{CB} \longrightarrow O^{\cdot -}_2$$

$$O_2^- + H^+ \longrightarrow HO^{\cdot}_2$$

$$HO^{\cdot}_2 + HO^{\cdot}_2 \longrightarrow H_2O_2 + O_2$$

$$O^{\cdot -}_2 + HO^{\cdot}_2 \longrightarrow O_2 + HO^-_2$$

$$HO^-_2 + H^+ \longrightarrow H_2O_2$$

$$H_2O_2 + hv \longrightarrow 2 \cdot OH$$

$$H_2O_2 + O^{\cdot -}_2 \longrightarrow \cdot OH + OH^- + O_2$$

$$H_2O_2 + e^-_{CB} \longrightarrow \cdot OH + OH^-$$

$$\text{Organic Compound} + \cdot OH \longrightarrow \text{Degradation products}$$

$$\text{Organic Compound} + SC\ (h^+) \longrightarrow \text{Degradation products}$$

$$\text{Organic Compound} + SC\ (e^-) \longrightarrow \text{Degradation products}$$

$$\text{Organic Compound} + OH^{\cdot}/h^+ \longrightarrow \text{Degradation products} \longrightarrow H_2O + CO_2$$

2.4.3 Graphitic carbon nitride as a metal-free Catalyst material

Recently, a two-dimensional graphitic-like carbon nitride nanosheet with a layered structure has been gaining a lot of attention. This is due to the fact that it is easy to construct, has a controllable electronic structure, a 2D layered assembly (Zang et al., 2013), has a good visible-light response, and has a suitable optical bandgap. In addition to this, it is a material that is suitable and has enormous potential for applications such as visible-light-driven photo-degradation of microbial, organic, and inorganic pollutants, sensors, electrocatalysts, organic synthesis, supercapacitors, adsorption, water splitting, and lithium-ion batteries (Mamba et al., 2016).

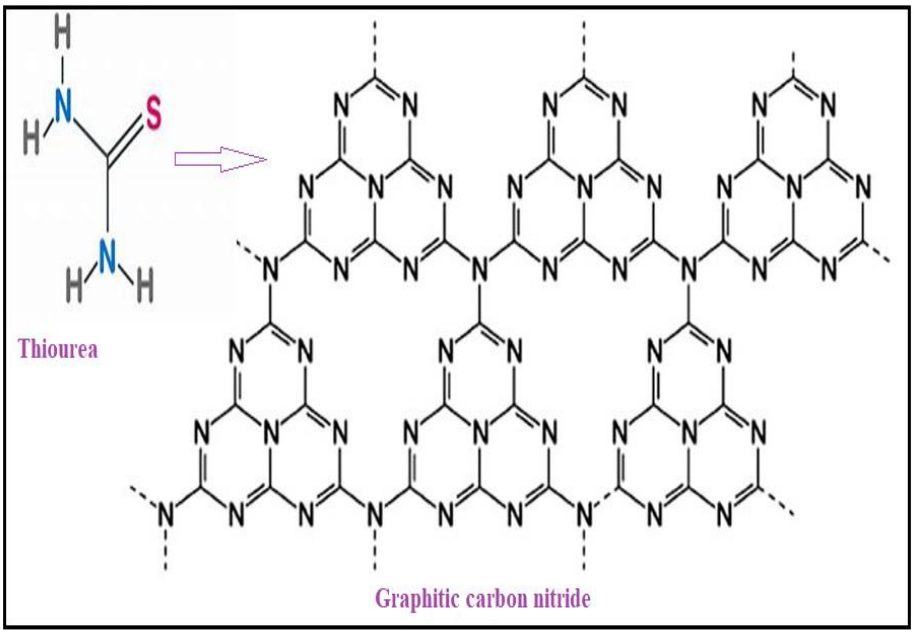

Figure 2.8 Structure of g-C_3N_4

In addition, g-C_3N_4 has a proper optical bandgap across all seven of its polymeric segments. This is because its sp^{2-}hybridized nitrogen (N) and carbon (C) atoms have conjugated electronic structures. These structures are also in agreement with the long-lasting covalent bonds that exist between the N and C atoms (as shown in Figure 2.8). In addition to this, the sp^2 hybridized conjugated electronic structure was responsible for the presence of unsaturated nitrogen (N) atoms within the tri-s-triazine linked amino-group layers. This was the case because of the fact that these layers contained amino groups. Because the VB edge location of the -C-N by normalized hydrogen energy is found to be 1.4 eV, and the CB edge position is found to be -1.3 eV (Liu et al., 2020). Figure 2.9 presents a few examples of how g-C_3N_4 can be put to use.

2.4.4 The g-C_3N_4 as a Photocatalyst

The development and description of a melon embryonic shape by Berzelius and Liebig in the year 1834 are considered to be the point at which the C_3N_4 materials were first conceived of and created. This is the first synthetic polymer to be introduced as a kind of interconnected tri-s-triazine through secondary nitrogen. It was done with this particular synthetic polymer. This specific polymer can be classified as a linear polymer. Research on this polymer was discontinued more than 150 years ago due to the fact that it does not dissolve in the majority of different solvents and is chemically inert.

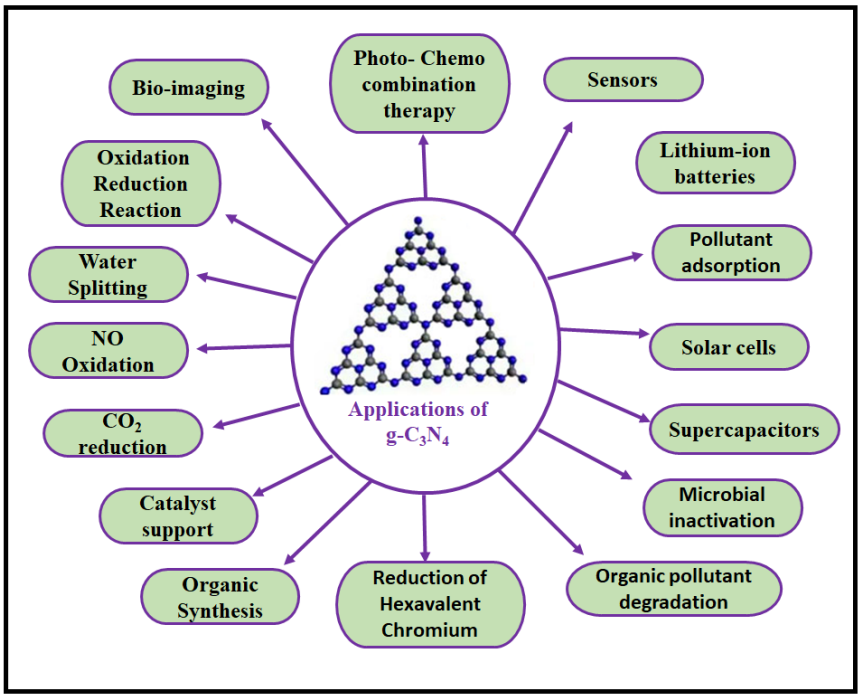

Figure 2.9 Illustration of several applications of g-C_3N_4 photocatalyst

Ultimately, in the 1990s, Liu and Cohen (Liu and Cohen, 1993) predicted that the creation of highly resistant carbon nitride would result in a diamond-like structure. Following that, b-C_3N_4 bulk hardness and modulus values were determined. This was subsequently shadowed by the discovery of numerous allotropes of C_3N_4 that each has their own unique set of properties, such as g-C_3N_4, a-C_3N_4, cubic C_3N_4, and pseudo-cubic C_3N_4. The carbon nitride (CxNy) known as g-C_3N_4 has a graphene-structured layer, which makes it resistant to all the carbon nitrides (CxNy) under the influence of the surrounding environment.

The fundamental structural units of the allotropes of g-C_3N_4 are the triazene C_3N_3 molecule, also known as "melam," and the heptazine / tri-s-triazane C_6N_7 molecule, also known as "melem." The latter is the one that has the phase that is the most resistant when it is in ambient circumstances.

A little over a decade ago, g-C_3N_4 was used for the first time in the context of heterogeneous photocatalysis. According to Wang and his fellow researchers, they were able to successfully use g-C_3N_4 as a conjugated stable to produce H_2 or O_2 from water splitting in an efficient manner (Wang et al., 2009). This was accomplished by utilizing lighting that is visible to the human eye as a result of its great optical properties, high stability in basic and acidic systems, good physical–

chemical stability, and nature that is beneficial to the environment. This was accomplished by utilizing lighting that was designed with the intention of minimizing its negative impact on the environment. Because of the superior optical qualities of visible light, that was the source of illumination that was utilized. In the following meeting, we went through in further depth the remarkable physicochemical properties of g-C_3N_4, which are a direct outcome of a large number of papers on the Web of Science that ensures the material's widespread use due to its widespread dissemination of information. Carbon and nitrogen are two elements that may be found in very high concentrations on earth (Huang et al., 2022; Wu et al 2022; Pham et al., 2022; Zhong et al., 2022; Che et al., 2022; Deng et al 2022). These elements make up the elemental composition of g-C_3N_4 as a semiconductor. To create this organic semiconductor, nitrogen-organic precursors are utilized throughout the majority of the manufacturing process. Melamine, urea, cyanamide, dicyanamide, and thiourea are a few examples of the nitrogen-organic precursors that can be found here. In spite of this fact, a range of different techniques to the synthesis of g-C_3N_4 have been published in a number of studies. A significant number of researches have also painstakingly documented the step-by-step processes for the production of g-C_3N_4, taking into account the circumstances of the reaction as well as the choice of the precursor. A wide variety of nitrogen-containing precursors are subjected to a process known as thermal polymerization in order to finish the construction of g-C_3N_4. The phrase "bottom-up method" is often used to refer to this approach. The purpose of the bottom-up technique, which is also known as the self-organization method, is the generation of substantially larger and more intricate systems from the self-assembly of any smaller components (such as atoms, molecules, and nanoparticles). This is accomplished through the use of the bottom-up methodology. In some circles, this method is also referred to as the bottom-up method. This is performed through the interactions that occur between the building units, which may make use of hydrogen bonding.

2.5 Limitations of g-C_3N_4 and remedy to the Obstacles

In a variety of photocatalytic processes during the past few years, g-C_3N_4 has emerged as the semiconductor of choice above other semiconductors. This is because of its superior features, which include its abundance, nontoxicity, inexpensiveness, high thermal and photochemical stability, biocompatibility, and moderation of activity in visible light (owing to low bandgap). Further advantages include biocompatibility and high thermal stability (Mao et al., 2022; Li et al.,

2022; Ye et al., 2022; Wang et al., 2022; Liu et al., 2022). In addition, the CB of g-C_3N_4 has a value that is a tremendous amount more negative than the potentials that are necessary for the creation of H_2 and O_2, processes that include CO_2 photoreduction. This value is a magnitude of a million times more negative (Swedha et al., 2022). In addition, because the photogenerated electrons have a high level of thermodynamic energy, the CB of g-C_3N_4 can reduce a variety of various molecules, including hydrogen and oxygen. But g-C_3N_4 has some flaws that make it less effective as a photocatalyst when exposed to visible light. Several modifications have been suggested in order to make g-C_3N_4 a better photocatalyst. It has been shown that the design of g-C_3N_4 with perfect activity depends mostly on its surface area, number of reactive sites, shape, and ability to absorb light for a long time. Everyone knows that g-C_3N_4 has both the properties of a two-dimensional (2D) polymer and a clear layered structure. Carbon and nitrogen that have gone through sp^2 hybridization make up the delocalized p-coupled system in g-C_3N_4. The quick recombination of charges is due to graphite's inherent p-conjugated structure, which is responsible for its chemical sluggishness. This is created by the fundamental structure of the plane and the random movement of charge carriers. The engineering method is selected from the many different surface modification techniques available to change and develop g-C_3N_4-based systems and flaws.

The photoactivity of g-C_3N_4 is negatively impacted as a result of the defect, which is typically caused when the episodic arrangement of the important unit in g-C_3N_4 is broken or otherwise disturbed. Because of surface imperfections designed onto g-C_3N_4 having C and N defects, the recombination of charges can be stopped by increasing the visible-light absorption area of the material. This makes the material opaquer. These imperfections, in general, affect the electrical structure as well as the characteristics of photocatalytic materials.

Numerous investigations have been carried out to advance the visible-light activity of g-C_3N_4 by engineering flaws. In most cases, the flaws have the potential to establish reaction sites inside the molecules of the reactants and to alter the characteristics of photocatalysis. Recent years have seen an increase in the number of proposals for enhancing the defect-induced photoactivity of g-C_3N_4. For example, Yu et al. (Yu et al., 2017) created the N-defected g-C_3Nx with a changeable band structure that is controlled via surface cyano groups and N vacancies. This allowed the band structure to be customized. Because of its capacity to segregate photoexcited charges, the N-defective form of g-C_3Nx can harvest visible light more efficiently than the pure g-C_3N_4. The

action of g-C_3N_4 can also be enlarged by the use of a different method, which involves the morphological and textural fabrication of regulated g-C_3N_4. As a consequence of this, structural engineering is an excellent technique for boosting the act of g-C_3N_4 (this includes managing the size, forms, and dimensions of the material) (Chen et al.,2017).

Two-dimensional structures, often known as building blocks, play an interesting role in the production of nanoscale structures. These structures are guided by a set of rules. Therefore, g-C_3N_4 with diverse morphologies has superior photocatalytic performance in comparison to a normal bulk structure. This is due to the fact that it is both efficient and simple, as well as having more reactive components and a greater specific surface area. Mesoporous structure with tabular nanostructures to impressively transport photo-induced charge along the 2D channel can be used to obtain excellent photocatalytic efficiency and enhanced optical features. This includes both electronic immigration which is quick and the direct route. The creation of nanocomposites or heterojunctions using a variety of semiconductors that have adequate band energies is the second technique to increase the performance of photocatalysis. This strategy is supported by a large body of well-established research literature. Because of this, the method is remarkable in that it slows down the rate of recombination of electron and hole pairs in an astonishing manner. Doping g-C_3N_4 with metal and non-metal components is the third tactic that can be utilized. Doping g-C_3N_4 with a variety of elements in recent times has proven to be an effective method for narrowing the energy gap of the material. As a consequence of these findings, the potentials of the redox bands may be tuned, the light-receiving ability can be modulated in a distinct manner, and g-luminescent C_3N_4's and electrical properties can be altered (Yu et al., 2022; Xia et al., 2022; Wang et al., 2022; Alejandra Quintana et al., 2022).In conclusion, coupling g-C_3N_4 with Vanadium and Lanthanum nanomaterials is the straightforward approach that was used to advance the performance of the material. Vanadium and Lanthanum compounds have exceptional qualities like great chemical stability, suitable electrical conductivity, and a large surface area are currently being used for a variety of applications.

2.6 Modification of g-C_3N_4 Photocatalyst

However, the practical usage of pure graphitic carbon nitride as a photocatalyst was impeded by (i) a good recombination rate of photoexcited electron-hole (e^- /h^+) pairs, (ii) a low quantum efficiency, and (iii) a relatively narrow visible-light responsive array. These three factors combined

make it difficult to employ g-C_3N_4 as a photocatalyst. Despite these drawbacks, the use of semiconductors is effective to some extent. As a consequence of this, ongoing hard work has been made to advance its photo-catalytic efficiency of it. These efforts include incorporating other active SCs with matching bandgap structures, metal/noble metal/non-metal deposition, and heterostructure coupling, all of which have fascinated great attention because of their capacity to generate dynamic PCs (Qi et al., 2019).

The quantum yield of the photocatalytic process can be increased by changing the surfaces of semiconductors with doping of different materials. This makes it feasible to improve the efficiency of the process. These surface modifications are beneficial because they reduce the rate at which electrons and holes recombine increasing the quantum yield. Doping is the method that has proven to be the most effective for modifying photocatalysts. Doping involves the addition of another metal oxide, which is then used to adjust the band gap and produce some major modifications in the material's original structure. In general, forming heterojunctions by combining g-C_3N_4 with other narrow optical bandgap SCs is viewed as a promising technique for increasing visible-light fascination, promoting photo-excited e^- /h^+ pair separation, and extending their lifetime. All of these factors contribute to improved photocatalytic performance.

2.6.1 Metal doping on g-C_3N_4 nanoparticles

Doping g-C_3N_4 with a variety of metallic species, including alkali metals, transition metals, and others has increased the material's photocatalytic efficiency for the photocatalytic detoxification of pollutants. This was accomplished with the goal of expanding the material's application. Many active transition metal oxides are capable of performing visible-light photocatalysis due to the low optical bandgap that characterizes these materials (Iqbal et al., 2021). Another method that has a lot of potential for enhancing the photocatalytic performance of graphitic carbon nitride is the deposition of transition metals or noble metals. In terms of photocatalytic activity, hybrid nanostructures that contained transition metals or other noble metal NPs such as Ag, Fe, Zn, Cu, Pt, Au, and Pd outperformed pure g-C_3N_4 when exposed to visible light (Ong et al., 2016). This was the case regardless of whether the illumination came from white light or ultraviolet light.

Under visible light, metal-ion-doped g-C_3N_4 nanomaterials have been the subject of a lot of research to see if they can improve the photocatalytic performance of breaking down a wide range of organic pollutants.

In the fields of catalysis, photocatalysis, and electrochemistry, metal-semiconductor composite systems show a great deal of potential. Since they can boost the surface reaction rate of a photocatalyst and facilitate charge separation in a Schottky junction with semiconductors, transition metals, such as noble metals, are widely utilized as co-catalyst. This is one of the reasons why noble metals are so valuable. This is the primary reason for the extensive use of transition metals, for example, noble metals. Because of their absolute band position, cocatalyst nanoparticles have the ability to function as electron sinkers. In order to place co-catalyst nanoparticles on the surface of the semiconductor, either the photo-deposition approach or the impregnation method can be utilized. These nanoparticles have a lower Fermi energy than the nanocomposite material itself does on its own. This is because the formation of these regions at the metal. One way to reach this goal is to act like a material that reacts to light. So, if you want to make the photocatalyst work faster, you can mix noble metals with g-C_3N_4. For example, Di et al. (2010) used three different methods to successfully prepare Au/g-C_3N_4 for making metal-semiconductor junctions for H_2O production with an electron donor when the solution was exposed to visible light. This made it possible for hydrogen to come out of the watery solution. This made it possible for hydrogen to evolve from a solution containing water.

Because it is non-toxic, inexpensive, and has a high activity level, Zinc oxide is also good photocatalyst. However, the fact that its energy can only be triggered under UV light poses a significant barrier to its practical application. This is because of the broad bandgap energy it possesses. Not only has it been demonstrated that the formation of nanocomposite with narrow bandgap semiconductors like g-C_3N_4 is a viable method for improving charge separation, but it has also been shown to be an effective method for increasing visible light absorption. For example, Meena et al., 2022, made a dye photooxidation g-C_3N_4/ZnO nanocomposite that works in visible light. Their investigation showed that the photo-degradation of the nanocomposites was much greater as compare to non-doped graphitic carbon nitride nanocomposite. They believed this was due to the increased charge transfer and separation generated by nanocomposites. WO_3, which has this characteristic, to bonded with graphitic carbon nitride (Mang et al., 2017) According to research, the bandgap of WO_3 is between 2.6 and 2.8 eV, which is very close to the bandgap of g-C_3N_4. For example, Nazarbad and Goharshadi (2020) showed that the Ag and graphitic carbon nitride has a good efficiency for Reactive Black 5 and hydrogen production.

A unique WO_3-g-C_3N_4 photocatalyst has been created for detoxification of rhodamine B under the irradiation of visible light, as was the subject of another investigation that was published by Aslam et al., 2014. It was discovered that superior optical absorption and accurate band locations of WO_3-g-C_3N_4 nanocomposite were accountable for the enlarged photocatalytic activity. In a separate piece of research, Li et al. used a simple method of impregnation and calcination to generate g-C_3N_4 nanosheets that were connected with MoS_2 nanosheets as a 2D material. This material was then used to degrade Rhodamine B and methyl orange. In a similar way, Peng and Li (2014) used a low-temperature hydrothermal method to make a nanosheet-g-C_3N_4-MoS_2 composite photocatalyst that breaks down MO when exposed to sunlight. In a separate but related study, Cheng et al. (2015) used an easy one-pot calcination method to make $CuFe_2O_4$/graphitic carbon nitride for H_2O production. This led to a big improvement in how well the composite material worked. Measurements of photocurrent and electrochemical impedance showed that the charge separation got better, which can explain this amazing improvement. Those measurements showed that there was a greater difference between positive and negative charges.

2.6.2 Non-metal doped g-C_3N_4 nanoparticles

Doping with non-metal ions is a common technique that is used to convert photocatalysts that are active in UV light into ones that are driven by visible light. Doping non-metals into g-C_3N_4 lattices, such as nitrogen, carbon, sulfur, boron, and fluorine, is an effective method for controlling photoelectrochemical and optical properties. Nitrogen doping of g-C_3N_4 has garnered a significant amount of attention recently. According to the recent findings by Zhu et al., 2021 nitrogen-doped g-C_3N_4 demonstrated improved photocatalytic activity and enhanced absorption of visible light. The N_2p level could overlap with the O_2p level, which would result in a reduction in the band gap and an increase in the photocatalytic activity. It is possible that the nitrogen species introduced into the g-C_3N_4 matrix as a result of the doping process will take the form of either a substitutional or an interstitial N atom. When exposed to visible light, a greater number of electrons and holes are produced, which helps to promote photocatalytic redox reactions (Zhu et al. 2021).

Hu et al. (2014) used $(NH_4)_2HPO_4$ as the source of the phosphorus and dicyandiamide as the starting material to make g-C_3N_4. They found that adding phosphorus makes it easier to separate charge carriers, narrows the bandgap, and slows the growth of crystals in g-C_3N_4. Also, the results

of their research showed that the P-N bond was made by putting P atoms between the spaces in the g-C_3N_4 lattice.

It was found that the photocatalytic efficacy of the S-doped g-C_3N_4 system increased with both the in situ and the ex-situ sulphur doping. This was the case despite the fact that just a minuscule portion of the dopant (less than 1.0 weight%) was utilized. Recent research has shown that using thiourea as an effective material for the production of an S-doped g-C_3N_4 is possible and can be done efficiently. In the initial step of their process, Hong and his coworkers produced in situ S-doped g-C_3N_4 by employing a TU unit. Analysis using XPS showed that there is a potential for the dopant to replace C, which would result in a likely energy decrease of 0.25 eV in the CB. For whatever reason, the S-doped g-C_3N_4 system performed astonishingly better than the unmodified system when it came to the synthesis of hydrogen (Hong et al.,2012). The longer and stronger light absorption brought about by S-doping, as well as the improved charge and mass transfer in the mesoporous structure, were thought to be responsible for the excellent photo reactivity (Cao et al., 2015).

O-doped g-C_3N_4 was initially produced by Li and colleagues via a straightforward H_2O_2 hydrothermal method (Li et al., 2012). XPS studies indicated that oxygen atoms bonded with Sp^2 hybridized carbon. This was evidenced by the fact that oxygen was transferred directly into the lattice during the formation of N-C-O. It is interesting to note that the oxygen doping did not have any effect on the maximum of the VB, but that the minimum of the CB did shift downward by 0.21 eV. Because of this, the introduction of oxygen into g-C_3N_4 could result in changes to the band and electronic structures, which would then result in an increased capacity for the separation of photogenerated carriers, an extension of the visible light response .

2.6.3 Co-doping of g-C_3N_4 nano-materials

Another fascinating strategy that has attracted a lot of attention over the course of the past ten years is the coupling of different semiconductors that have a range of different energy levels. In photocatalytic systems, connecting g-C_3N_4 to other semiconductors was meant to increase the range of wavelengths that could be absorbed into the visible light region and limit the recombination of charge carriers in each photoelectrode. These two objectives were accomplished with flying colors. An electron can be injected into g-C_3N_4 from the tiny band gap of the nanocomposite material, which acts as a "sensitizer," when it is combined with a small band gap

nanocomposite that has a more negative CB level. This occurs when g-C_3N_4 is combined with a semiconductor that has a minor band gap. When there is a larger negative CB level, this is one of the possible outcomes. It was essential for there to be a difference in the energy levels of adjacent band levels in order to facilitate the movement of charge carriers from one particle to its neighbor and to ensure that electrons and holes were kept separate from one another. This was done to ensure that charge carriers could move freely from one particle to its neighbor. In order to have an effective transfer of photogenerated electrons and holes from g-C_3N_4 to the sensitizer, it is necessary for there to be a difference in potential between the conduction bands and the valence bands of the two semiconductors. This is because the conduction bands and the valence bands are at different potentials. When this condition is met, the transfer will be successful.

Under the influence of visible light, the photocatalytic action of g-C_3N_4, when combined with metal such as CDs, V_2O_5, La_2O_3, SnO_2, WO_3, and FeO_2, has been utilized to a significant extent for the purpose of optimizing the process. Lee et al., 2015 used graphene-decorated V_2O_5 for energy storage and Hong et al 2016 use g-C_3N_4 decorated with V_2O_5 for the degradation of pollutants. Vignesh et al., 2022 used a-Fe_2O_3/V_2O_5 and g-C_3N_4 ternary nanocomposite for the detoxification of pollutants. La_2O_3/Cobalt oxide/g-C_3N_4 used for water splitting for hydrogen production(Iqbal,2021).

2.7 Types of Doping

Doping can be broken down into two categories: n-type and p-type. Both categories refer to the use of chemical to enhance performance. For n-type doping. Dopants, which are also known as donors, have the ability to give extra electrons as negative free charge carriers which is referred to as n-type doping, or they have the ability to accept extra electrons from nearby atoms to complete covalent chemical bonds, which is referred to as p-type doping. Both of these behaviors are referred to as "doping." Doping of either the n-type or the p-type variety occurs during either of these two procedures (referred to as p-type doping). This is based on how many valence electrons the dopants have (Park, 2002). The impurities in p-type and n-type doped semiconductors move the Fermi level blue- or red-shifted. This is shown by the band gaps of the different types of doped semiconductors (Reynolds et al., 2014; Righetto et al., 2020). It is possible for the electron and hole to quickly recombine, a process that is referred to as charge-recombination. This process is undesired for the photocatalyst because it results in the release of energy from the electron in the

form of heat, which ultimately causes the reaction to cease. Doping stops the electron from recombining with hole, is recommended as a method for separating the charge from the recombination that occurs in semiconductors. The lifetime of the + is on the order of femtoseconds, yet it is long enough to stimulate the redox process on the surface of the catalyst. Nonmetal dopants provide a number of advantages over metal dopants, including more photo-degradation action, greater constancy, and non-toxicity of dopant ions. Numerous materials, including the influence of impurity levels in the dopant on photocatalytic effectiveness, have been researched up to this point.

2.8 Method for Preparation of g-C_3N_4 Nanocomposites

2.8.1 Sol-gel method

The Sol-gel is a simple process for the production of nanoparticles at ambient temperature and normal air pressure; additionally, it does not need the use of complex equipment. This approach has some advantages like simplicity of processing, composition control, and the capacity to add dopants at high concentrations. This method was developed because other methods are difficult to implement. These benefits are in addition to the fact that it is superior to other preparation techniques. The precursors undergo hydrolysis and polymerization processes, which ultimately result in the formation of a colloidal suspension known as sol. In most cases, the predecessors of the metals are either inorganic metal salts or metal-containing organic molecules, such as metal alkoxides. The liquid sol phase changed into the solid gel phase as a result of the complete polymerization as well as the loss of the solvent.

The sol-gel technique is a highly chemical procedure, sometimes known as a wet chemical method, that is used for the synthesis of nano-structures, most notably nano-composite of metal oxide. The molecular precursor, which is often a metal oxide, is first dissolved in water or alcohol, then heated by hydrolysis or alcoholization, and finally transformed into a gel. Because the gel that is produced as a byproduct of the hydrolysis and alcoholization process is wet or damp, it is necessary to dry it using ways that are appropriate for the qualities that are sought. One such method is to burn the alcohol. The generated gels are first allowed to dry, then ground into powder, and finally calcined. Due to the low reaction temperature, the sol-gel method is not only an inexpensive technology, but it also provides excellent control over the chemical composition of the end product. In general, this method can be used in the process of producing pottery as a modeling material and as an

intermediary between thin films of metal oxides in a variety of applications. In addition, this method can be utilized in the process of forming pottery. Materials produced by the sol-gel process find applications in numerous subfields of technology, including those dealing with optics, electronics, energy, surface engineering, biosensors, pharmaceuticals, and separation. The construction of nanoparticles with a variety of chemical compositions can be accomplished using this tried-and-true commercial method. Producing a homogenous sol from the precursor and then converting it into a gel are the fundamental steps involved in the sol-gel process. The leftover gel was dried after a solvent that was present in the gel was removed from the gel system. The attributes of the dried gel primarily depend on the procedure that was used to dry the gel. To put it another way, the technique of solvent removal is chosen in accordance with the application in which the gel is applied. It is important to note that nanoparticles can be produced from the dry gel by grinding it using appropriate mills in order to reach the desired consistency. The dry gel is used in a range of industries, including surface coating, building insulation, and especially garment production. Figure 2.10 shows a schematic illustration of the production of nanoparticles using the sol-gel technique.

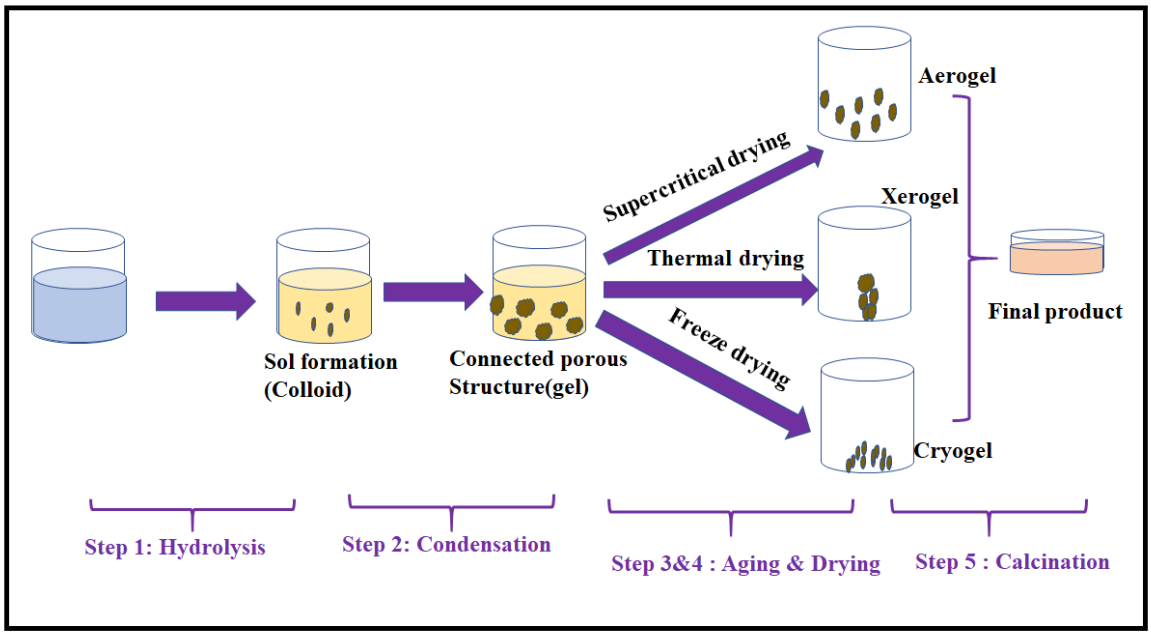

Figure 2.10 Synthesis of nanocomposite using Sol-gel method

2.8.2 Hydrothermal method

One of the significant processes that can be used to prepare g-C_3N_4 particles with the chosen silent feature like size, form, homogeneity in composition, and a high of crystallinity is the hydrothermal method. This method is one of the important techniques that can be used. One of the many reasons why the hydrothermal method is considered to be one of the most significant processes is because of this procedure. This methodology is just one of the many reasons why the hydrothermal method is considered to be one of the most significant processes. Some of the primary qualities that encourage a decrease in the agglomeration of particles with one another include narrow particle size distributions, phase homogeneity, and regulated particle morphology. This favors a decrease in the agglomeration of particles with one another. Favorable shape and form of the nanocomposite may also be exerted using this technology, in addition to ensuring a product with a consistent composition and excellent purity (Wei et al 2016; Colbeau Justin et al., 2004). The hydrothermal synthesis process is typically carried out in steel pressure containers (autoclaves) that may or may not be lined with Teflon. The reaction takes place in an aqueous solution and is carried out under temperature and/or pressure control. It is possible to raise the temperature above the point at which water begins to boil in order to attain the pressure at which vapor saturation occurs. The volume of solution and reaction temperature that is introduced to the autoclave both play a significant role in determining internal pressure. The temperature was kept at around 200 degrees Celsius throughout the hydrothermal procedures. A comprehensive comprehension of the hydrothermal chemistry of the media was necessary in order to produce g-C_3N_4 particles that possessed a high degree of crystallinity. These particles came in a variety of sizes and shapes, including nanoparticles, nanotubes, nanosheets, and nanofibers. The hydrothermal approach has been utilized by a number of researchers in order to produce g-C_3N_4 nanoparticles. Hydrothermal treatment was used by Colbeau-Justin et al. (2004) to produce nanocrystalline g-C_3N_4 with particle sizes ranging from 20-50 nm and specific surface areas ranging from 20-80 m^2 /g.

The term "hydrothermal synthesis" was coined by Wang et al., and it refers to a variety of processes that include crystallizing substances in an enclosed container while the substances are in an aqueous solution at their temperature (0.3 - 4 MPa). Under hydrothermal circumstances, the system consists of a solid linoleum metal, a liquid phase composed of ethanol and linoleic acid, and a solution that is either water or ethanol. The temperatures at which the reactions take place are varied. The crystalline metal oxide nanoparticles (MNPs)

produced by this process are of a higher quality than those acquired using any other method. Solvothermal method is quite similar to hydrothermal. The primary distinction lies in the fact that an aqueous solution is utilized during the hydrothermal process, whilst a non-aqueous solution is utilized during the solvothermal procedure. The NPs that are created using either method have a very crystalline structure.

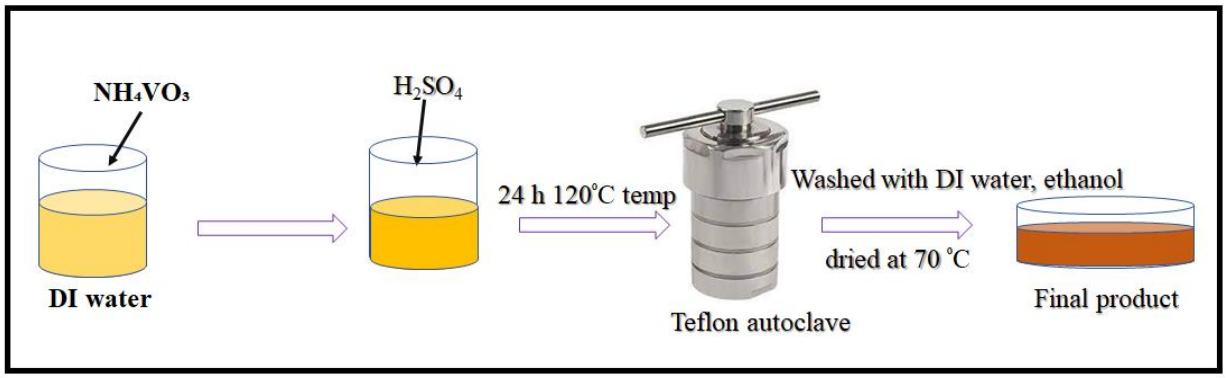

Figure 2.11: Synthesis of nanocomposite with hydrothermal method

2.8.3 Solvothermal method

The process of generating chemical compounds known as solvothermal synthesis involves placing a solvent that already contains reagents inside of an autoclave and subjecting it to high pressure and temperature. Under these conditions, many chemicals dissolve more completely in the same solvent than they do under standard conditions. This opens the door to reactions that would not normally take place and can result in the formation of novel compounds or polymorphs. The hydrothermal method and the solvothermal synthesis are relatively similar; both processes are commonly carried out in an autoclave made of stainless steel. The sole distinction between the hydrothermal method and the solvothermal strategy is that the latter makes use of a solvent that is not water. However, in order to get the desired results, the temperature needs to be greatly increased in comparison to the others method (Li et al., 2016). This method has been successful in producing g-C_3N_4/TiO_2 nanocomposite (Imbar et al., 2023). Recently, high-quality anatase TiO_2 single-crystal nanosheets and nanowires have also been synthesized utilizing a solvothermal synthetic approach Hu et al 2017).

2.8.4 Sonochemical method

The use of ultrasound has proven to be quite helpful in the production of a wide variety of nano-composite, such as transition metals with a huge surface area, oxides, and colloids. There is no evidence that direct interaction with molecular species is responsible for the chemical effects of

ultrasound. The process of cavitation, which involves the development, growth, and eventual collapse of bubbles in a liquid medium, is responsible for ultrasound's tremendous capacity to influence chemical transformations. A direct method for producing TiO_2 nanoparticles was disclosed in Elshikh et al., (2020) 's study. This method involved applying ultrasonic irradiation at a low temperature for a brief amount of time. During the course of a normal synthesis, deionized water and ethanol are combined in a sonication cell before being disseminated. The reaction temperature of mixture increases to around 37-90 degrees Celsius as it goes through the sonication process. The reaction will proceed for another three hours in order to finish the crystallization of g-C_3N_4.

2.9 Applications of g-C_3N_4 Nanocomposite

2.9.1 Photocatalytic water splitting

By the year 2080, it is anticipated that hydrogen will have established itself as the predominant form of energy generation (90%). This is due to the fact that H_2O possesses a higher energy content than other types of hydrocarbon fuels (120-142 MJ kg1). This prediction is based on the fact that hydrogen has a larger energy content than other types of hydrocarbon fuels. In addition, more than 44.5 million tonnes of hydrogen are created every year all over the world. As a result, advances in technology ought to offer up effective avenues for the process of producing hydrogen, as well as its delivery, storage, conversion, and use. At the moment, strategies for the production of hydrogen that are both economical and kind to the natural world make for an intriguing and alluring area of investigation. Nonetheless, at this point in time, the steam methane reforming process is the one that is responsible for the production of 95% of the world's hydrogen. The photocatalytic water splitting technology, which is based on semiconductors and has the potential to be used for the creation of H_2O using sun energy, is regarded as greatest essential answers to the current worldwide energy crisis. Another answer that is considered to be one of the most essential is the utilization of nuclear power.

Since the revolutionary work done by Fujishima and Honda in 1972, there has been a significant amount of progress made; however, there are still a significant number of obstacles to be overcome in the design of photo-catalysts with increased productivities for the synthesis of H_2O from water using sun light. To be more specific, practically all of the common oxide-based photocatalysts that are capable of splitting water have large bandgap energy and can only become excited when

exposed to ultraviolet light. This is because ultraviolet light is the only type of light that can excite these photocatalysts. In contrast to the visible solar spectrum, which is responsible for roughly 46% of the total solar energy, the contribution of ultraviolet (UV) irradiation to the total incoming solar energy is just a relatively small fraction (around 4%).

To begin, the photocatalyst must be able to effectively absorb sunlight or other visible light in order to form electron-hole pairs that are necessary for water-splitting reactions. Second, either the surface charge recombination or the bulk charge recombination, as well as the reverse process, needs to be stopped. Thirdly, it is imperative that any photo corrosion or deterioration of the photocatalyst that occurs during the process of photocatalysis, in addition to any harmful products, be strictly forbidden. In addition, the bandgap energy of the nanocomposite must be more than 1.23 eV for water splitting to be achieved. Yet, in order to make advantage of visible light, it must be lesser than 3.0 eV. For thermodynamic reasons, it is essential to carefully regulate the position of the CB (which is more negative than H/H_2 (0 V)) and the VB (which is more positive than O_2/H_2O (1.23 V)) in order to attain the water splitting reaction. This is because the CB is more negatively charged than H/H_2, and the VB is more positively charged. These conditions have been addressed by metal-free g-C_3N_4, a potential photocatalytic material that has been thoroughly investigated for the purpose of determining H_2O evolution activity. In spite of this, the performance of its photocatalytic hydrogen production is restricted because of the recombination of its fast charge carriers. It is possible to capture the photogenerated VB holes by including a sacrificial reagent, such as alcohol, in the photocatalytic reaction. This will allow for greater efficiency. In addition, an inhibition of the surface backward reaction can be achieved through the photo deposition of cocatalyst on the surface of the g-C_3N_4. Both of these methods are utilized on a large scale to improve charge separation and restrict charge recombination, which ultimately results in an increase in the photoactivity of the material. In addition, many photocatalysts, including Cds and Ag_2CrO_4, are susceptible to photo-corrosion in aqueous solutions as a result of oxidation caused by the photogenerated holes that take place during the photocatalytic reaction. This oxidation takes place as a direct result of the photocatalytic reaction. This is indeed the situation. g-C_3N_4 was further add to these photo-catalytic nanocomposites in order to prevent photo-corrosion and put a cap on charge recombination.

In addition, GO, a 2-dimensional macromolecular structure made of carbon atoms with a honeycomb structure, extraordinarily huge surface area, and thermal conductivity, has shown remarkable photocatalytic efficacy for the creation of hydrogen or oxygen. Graphene possesses these characteristics because it has a honeycomb structure. The year 2004 saw the discovery of graphene. In order to make multilayer composites, graphene sheets will first need to be included into the mix, and then g-C_3N_4 will need to be immobilized. The performance of the catalytic reaction will significantly enhance as a result of this approach. In this specific configuration, graphene sheets serve the purpose of conducting channels. This not only makes it possible to more effectively separate the photogenerated charge carriers, but it also boosts the system's capability to create hydrogen when it is illuminated by visible light. It was discovered that a graphene concentration of 1.0 weight percent yielded the best results, and the H_2 generation rate that corresponded to this value was 451 mol h^{-1} g^{-1}. Its rate was significantly higher than that of pure g-C_3N_4, which it exceeded by a factor of more than 3.07 times. This rate was noticeably higher than that of pure g-C_3N_4, which was the comparison being made. When graphitic carbon nitride is immobilized on the surface of GO sheets, this creates conditions that are more favorable for the hole-electron separation. This is the result of the immobilization of g-C_3N_4 on the surface of graphene sheets, which leads to the formation of layered composites. This is a natural occurrence that takes place when g-C_3N_4 is immobilized on the surface of graphene sheets in order to build layered composites. Yu et al., who synthesized mesoporous g-C_3N_4 /TiO_2 nanocomposites and integrated them into PSF substrate, employed a method that was quite similar to the one described above in order to degrade SMX. In comparison to the PSF membranes that were originally used, the nanocomposites demonstrated increased removal efficiency (ranging from 14% to 69%) while simultaneously reducing water fluidity (from 628.6 to 551.2 LMH/bar). Because there was no photocatalyst found, the percentage of photo-detoxification continued almost the same during the entire 30-hour test. It's probable that the tensile strength was diminished in some way as a result of hydroxyl radicals and UV irradiation breaking down the chemical bonds that held the material together. Combining g-C_3N_4 with other substances, such as carbon nanotubes (CNT) and graphene oxide (GO), has proven to be an effective strategy for combating the problem of recombination caused by g-C_3N_4 (Qu et al., 2018; Huang et al 2019).

2.9.2 Photocatalytic mineralization of organic pollutants

A problem that is becoming more and more of a global concern is the presence of poisonous organic compounds that don't break down naturally in water sources and industrial waste. There are a variety of agricultural practices and commercial wastewater discharges that are contributing to the introduction of high concentrations of these compounds into the water system at the present time. These activities and discharges include the production of dyes, plastics, textiles, pharmaceuticals, paper mills, oil processing, and coal gasification. Other examples include the production of herbicides and fungicides. Evidence is also available for the fact that wild animals' reproductive systems experience endocrine disruption as a result of being exposed to environmental contaminants. Commonly employed endocrine disruptive substances include phenols, substituted phenols, pesticides (insecticides, herbicides, and fungicides), polychlorinated biphenyls, polybrominated biphenyls, phthalates, bisphenol-A, and surfactants (nonyl phenol and its ethoxylates). As a component of water remediation, applications that involve the efficient treatment of resistant contaminants have been necessary. The AOP, which seems to be the greatest evolving technology, has received a significant amount of interest for the complete oxidation of organic molecules to innocuous into CO_2 and H_2O. This has been the main focus of concentration throughout the process. Due to the fact that it is a stable and cost-effective photosensitized material, the g-C_3N_4 semiconductor has been shown to be the most effective and commonly used technology for photo- detoxification of pollutants. This is because of the fact that it has been shown to be the most effective. This has contributed to the widespread adoption of this technique.

2.9.3 Dyes:

One of the most significant categories of organic compounds that are becoming an increasing concern for the environment is that which is produced through the use of textile dyes and other industrial dyestuffs. Humans are also exposed to a potential health danger from dyes. In recent years, an alternative to traditional methods that are based on the generation of especially reactive species such as hydroxyl radicals has been offered as a technique to oxidize quickly and non-selectively a wide variety of organic pollutants, including a number of different color. This is in contrast to traditional methods, which are based on the formation of very reactive species. It is the purpose of these AOPs to oxidize a wide variety of organic contaminants, which includes a few different colors. These advanced oxidation processes (AOPs) are designed to oxidize a broad range of organic pollutants. Researchers Mongal et al., (2019) investigated the efficiency of g-

C_3N_4/titanium dioxide in an aqueous solution for the photodegradation of Rhodamine B pigments when the solution was exposed to irradiation at a power level of 400 watts. Rhodamine B was broken down with the help of g-C_3N_4 according to Yang et al. (2021). Research on the photocatalytic destruction of colored organic substances, such as rhodamine B and methyl orange, was carried out by Chen et al., (2021), making use of g-C_3N_4 as the catalyst.

Prakash et al., 2019 also synthesized graphene oxide/ g-C_3N_4 /CDs in order to examine the efficiency of this combination using the hydrothermal method on the photodegradation of crystal violet (CV) and RhB. The GO/g-C_3N_4/CDs nanocomposite showed the maximum potential amount of photoactivity when subjected to illumination from visible light.

Constructing a photocatalyst using a Z-scheme, for instance, is an excellent method for achieving effective photo-excited e^-/h^+ separation while yet maintaining the PC's noteworthy redox capacity. In this study, a novel ternary $BiVO_4$/p- g-C_3N_4/AgI photocatalyst with a two-fold Z-scheme mechanism was effectively created using an electrostatic self-assembly technique to load $BiVO_4$ onto protonated g-C_3N_4 generated by an in-situ precipitation pathway (Xu et al., 2021). The increased photocatalytic activity of $BiVO_4$/ g-C_3N_4 /AgI is evidenced by the elimination of 94.67% of RhB after 60 minutes of exposure to visible light. RhB was employed as the target of exclusion in this study. The rate at which RhB photodegraded was 0.04963 min^{-1}, which was faster as compare to others. An increase in photo-catalytic activity is associated with a number of factors, including an improved capacity for absorbing visible light, a speedier capacity for charge carrier separation and transportation, and a more influential redox ability as a consequence of the creation of a double Z-scheme heterostructure.

In order to increase the photocatalytic efficiency while maintaining a well-matched band alignment, novel g-C_3N_4/CdS/MoS_2 hybrids have been designed. Because of the strategic preparation of g-C_3N_4/CdS/MoS_2, it was possible to achieve step-by-step separation of electrons and holes in pairs. During this time, the conductive layer MoS_2 made it possible to easily transmit electrons across the surface that leads to a more active photoreduction of electron/hole pairs recombination relative to earlier research due to the fact that it compares well to that research. In contrast to pure g-C_3N_4, the RhB photodegradation rate constant of hybrid PCs is found to be 0.0533 min^{-1} higher, having grown from 0.0309 min^{-1}. The loading separation cocatalyst method

can be utilized on a extensive diversity of extra PCs in order to upsurge the efficiency with which they utilize sunlight (Zhang et al 2019).

It was recently revealed that in situ thermal polycondensation can be used as a straightforward one-step method for the manufacture of MoS_2/ g-C_3N_4 nanocomposites (NCs). The mesoporous MoS_2/ g-C_3N_4 PCs showed characteristics of being looser, thinner, and bimodal. It was necessary for the MoS_2 species to be homogenous of the g-C_3N_4 in order to realize a reliable heterojunction. Because of its advantageous structural makeup, the MoS_2/ g-C_3N_4 exhibited a stronger visible light action and good recycling stability during the RhB dye photodegradation process. The much-increased activity can be attributed to both the rise in visible-light absorption and the fall in photogenerated carrier recombination. Both of these factors contributed equally (Xue, 2018).

Under the influence of solar radiation, photocatalytic degradation of Rhodamine B and Crystal violet dyes with the use of GO/ g-C_3N_4/Cds as the catalyst was examined. In-depth research was conducted on a number of aspects (Prakash et al., 2019).

2.9.4 Phenols

The Phenols are recognized as potentially dangerous pollutants due to the fact that they have the ability to negatively impact human health. Heterogeneous photocatalysis with g-C_3N_4 as the photocatalyst looks to be the most promising new method for the degradation of phenol, among the alternative organic processes. A different approach was utilized in the production of a TiO_2/ g-C_3N_4 thin film electrode. This composite film did an excellent job of carrying out the photoelectric degradation of the phenol, which also involved wastewater. (Wei et al 2017; Wang et al 2020) synthesized S-SnO_2/ g-C_3N_4 heterostructure composite for the detoxification of phenol and trichlorophenol. The composite was able to photodegrade phenol at a bias voltage of 1.5 V in less than 1.5 hours when it was exposed to solar irradiation that was simulated.

In addition to that, composites based on g-C_3N_4 were taken into consideration as a potentially useful component in photocatalytic disinfection. According to Wang et al. in 2013 reduced GO and g-C_3N_4 sheets were wrapped around crystals of cyclooctasulfur to make a new type of metal-free ternary heterojunction photocatalysts (-S8). Sheets of reduced graphene oxide (RGO) and carbon nanotubes (CN) were wrapped around one another in a variety of different orders, which ultimately led to the construction of two distinct structures. The RGO sheets sandwiched in the

CN sheets in the opposite orientation (i.e., RGOCNS870). When exposed to visible light, both structures, whether in an aerobic or anaerobic environment, showed exceptionally high levels of antimicrobial activity. For the purpose of evaluating the photocatalytic water disinfection performances, Coli bacillus was chosen as a representative microbe. This effort not only allowed the opportunity to create adequate procedures for photocatalytic water treatment under a variety of conditions, but it also provided fresh breakthroughs into the investigation and understanding the mechanism of bacterial inactivation.

For instance, Huang et al. discovered that metal-free robust g-C_3N_4 photocatalysts show antibacterial action for the inactivation of E. coli under the irradiation of visible light (Huang et al 2014). Wrapping the RGO and g-C_3N_4 sheets around the sulphur (-S8) atoms allowed Wang and his colleagues to successfully create a unique heterojunction that was related to g-C_3N_4. According to the findings, the amount of visible light required to kill bacteria was significantly raised. When the shell layout changes in RGO and g-C_3N_4, this enhancement will also be affected.

The increased activity could be caused by the movement of electrons or holes inside the system (Wang et al., 2013). In addition, Li and colleagues made the discovery that an atomic single layer of g-C_3N_4 with a thickness of 0.5 nm proved the efficacy of photocatalytic decontamination for inactivating E. coli (Li et al 2015). This was determined to be a result of the material's reduced charge transfer resistance as well as its effective charge separation capabilities. This was done by demonstrating that the photocatalytic action of the doped photocatalytic material was significantly higher. This was accomplished by showing that the photocatalytic activity of the hybrid photocatalyst was noticeably higher than that of the standard photocatalyst. It was established that the enhancement in photocatalytic action was the result of enhanced light absorption as well as effective charge separation.

2.9.5 Pharmaceuticals

Antibiotics and other toxins have been found in water, putting human health and the ecosystem at danger. Surface water has also been shown to contain antibiotics. This is due to the fact that they are not biodegradable and have the capacity to persist in the environment. As a consequence of this, a number of research works pertaining to the elimination of antibiotics have been published, resulting in an increasing body of scholarly work in this area. The elimination of antibiotics was analyzed (Wang et al., 2017), who used a g-C_3N_4/CDs-based nanocomposite to conduct their

research. Making an N-doped CDS (NCDs)/g-C_3N_4 allowed us to accomplish this goal. To improve the capacity of indomethacin (IDM) to degrade when exposed to visible light, a trace amount of non-carbohydrate degradation products (1.0 weight percent) was added. The effect that NCDs have, which has been exceptionally proved by UV–vis DRS, causes an increase in the photocatalyst's capacity to react to visible light. This is the outcome of an increase in the photocatalyst's capacity to respond to visible light. This improvement can be ascribed to the fact that UV–vis DRS. When contrasted with g-C_3N_4, the NCDs/g-C_3N_4 compound impressively demonstrated a narrowing of the energy gap that occurred as a result of the incorporation of NCDs. This nanocomposite has been formed as a result of the formation of the material. (Wang et al 2019, 2020). According to the process that was explained, there was a significant increase in the photocatalytic activity, and the probability of charge carriers recombining was significantly reduced. This resulted in IDM degradation.

The use of pharmaceuticals is essential to maintaining a healthy existence. The rise in the prevalence of uncommon and contagious diseases has led to an increase in the number of patients who require pharmaceutical treatment. As a result of hospitals and farms discharging pharmaceutical waste without first undergoing an adequate treatment process, there is a potential threat to the health of both humans and aquatic life (Khan et al., 2020, Wang et al., 2020). Antibiotics are found in high concentrations in pharmaceutical wastewater, making their removal potentially challenging. Antibiotics including sulfamethoxazole (SMX) and tetracycline hydrochloride (TCH) are used extensively as antibacterial drugs in the food industry, animal husbandry, and aquaculture (Feng et al., 2020). Under visible light, it has been demonstrated that particulate matter (PM) that has been altered with nano-composite, such as g-C_3N_4 nanoparticles and g-C_3N_4 nanocomposites, exhibits photocatalytic activity for drugs. An investigation into the decomposition of tetracycline antibiotics was carried out by Wang et al., 2017 using TiO_2/g-C_3N_4.

2.9.6 Pesticides

The field of Nano-photocatalysis is becoming increasingly popular as a result of the significant potential it possesses to aid in the elimination of environmental issues. Over the course of the last few decades, there has been a lot of focus placed on the application of photocatalysts for the destruction of insecticides in water (Lhomme et al., 2008). The extremely durable organochlorine (OC) pesticide might be different from the rapidly deteriorating organophosphate (OP),

organohalogen (OH), carbamate group, and synthetic pyrethroids pesticides (Devi et al., 2005, Herrmann and Guillard, 2000). The scientific community that is working on photocatalysis research faces a significant obstacle, which is to expand the spectral sensitivity of nano-based semiconductor photocatalysts so that they are sensitive to visible light as well as ultraviolet light. Only then will photocatalysis research be practical for the scientific community. A significant amount of effort is currently being put into mitigating the negative effects that herbicides and pesticides have on plants and the soil. This is mostly accomplished through photocatalysis with nanoparticles of metal oxides like TiO_2 and ZnO. (Mengyue et al., 1995).

Under the influence of solar radiation, photocatalytic degradation of the pesticide Diuron was studied by employing g-C_3N_4/N- doped CeO_2 as the catalyst. Extensive research was carried out on a variety of different aspects, such as the starting concentration of the contaminant, the amount of catalyst that was utilized, the pH of the solution, and the effect that oxidizing agents had. Graphitic carbon nitride nanosheets were found to have an excellent dispersion of ceria nanocomposite with a size of approximately 3 nm, as determined by morphological analyses. The doping of nitrogen into cerium oxide caused a decrease in the bandgap of cerium oxide doped with g-C_3N_4. When compared to the action g-C_3N_4, photocatalytic capabilities that involve the degradation of diuron showed that the composite exhibited superior performance. This higher performance can be accredited to the increased separation efficiency of photo-induced electron-hole pair as a consequence of the construction of a heterojunction between ceria and g-C_3N_4.(Kasrala et al., 2019).

Isaac et al. produced g-C_3N_4 functionalized with ferrocene carboxaldehyde (Fc) in order to investigate its effectiveness in degradation of TBT herbicide by utilizing hydrogen peroxide (H_2O_2 – HP) or persulfate as an oxidant under the irradiation of white light. The optimal circumstances for the experiments were obtained in acidic solutions (pH 3); however, the complete elimination of TBT in a synergistic manner could only be accomplished by making use of H_2O_2. This is because of the in situ chemical activation of the H_2O_2 and persulfate oxidants using g-C_3N_4 /Fc to produce the HO• and SO_4 • . In spite of the formation of HO• (the principal functioning oxidant) and SO_4 • radicals, there was not a discernible degree of degradation of pollutants load detected for either of the oxidants, and this was demonstrated by the utilization of non-selective scavengers. (Sanchez, 2023).

Another intriguing study was conducted by Raizada, 2019, which involved the preparation of a Z-scheme silver-doped g-C_3N_4/Bi_2O_3 nanocomposite for the purpose of decomposing imidacloprid. This was accomplished by a hydrothermal procedure. Under the influence of visible light, the nanocomposite was applied to the organochlorine insecticides, and within only ten hours, the substances were totally mineralized. This degradation proceeded according to the kinetics of a pseudo-first order, and the nanocomposite material remained stable even after being recycled ten times. Li et al. successfully created a nanocomposite by combining graphitic carbon nitride and bismuth oxide, but they did it without adding any doping (Li et al., 2014). Under the influence of visible light, the nanocomposite proved to be an effective tool for the degradation of 4-chlorophenol. In a study conducted by Cui et al., it was found that these organochlorine compounds could also be broken down by mesoporous graphitic carbon nitride (Cui et al 2012).

Degradation of pesticides was achieved by Sharma et al., 2019, and Vigneshwaran et al, 2019 through the use of graphitic carbon nitride and also through the utilization of its nanocomposite with chitosan. This photocatalyst proved successful in degrading 85% of the harmful pesticide that it was exposed to. (Raizada, 2019) describes the fabrication of four distinct nanocomposites that are based on g-C_3N_4. One of the nanocomposites consisted of p-doped g-C_3N_4 combined with graphene oxide. Each of them was put to use in the process of degrading four distinct types of pesticides, including organochlorine insecticides. It was discovered that all of them are effective photocatalysts for getting rid of pesticides. The removal of pesticides from juice was accomplished by Guan et al. 2015 using a graphitic carbon nitride nano vessel. Pang, 2016 found that the use of graphitic carbon nitride nanosheet was successful in removing more than 80 percent of the pesticides.

Zheng and his colleagues were able to produce g-C_3N_4 that had been doped with carbon. (Zheng et al., 2016). It was discovered that this photocatalyst was significantly more effective in removing a pervasive organic contaminant from both wastewater and natural water when compared to the usage of pure g-C_3N_4 for the same task. Pang et al., 2019 found that fluazaindolizine may be broken down in an aqueous solution by using a nanosheet of graphitic carbon nitride and subjecting it to irradiation from visible light. When 5 mg of the catalyst was utilized, the half-life was able to be reduced to 2.7 hours, which was a significant improvement. In order to break down pesticides, a nanocomposite was created by combining graphitic carbon nitride, peroxymonosulfate, and

activated carbon. This nanocomposite was employed (atrazine). Dangwang, 2019 found that using the nanocomposite with peroxymonosulfate as a photocatalyst resulted in a better level of efficiency than using the nanocomposite without it.

Tang et al., 2020 developed a Z-scheme that was AgI/ g-C_3N_4 /Ag_3PO_4, and the catalyst obtained a greater degradation of pesticides. The Z-scheme was a Z-scheme. This was due to the catalyst's capacity to build a Z-structure, which led to this result. It was possible to extricate recalcitrant PCB from a sample of water by making use of a composite of g-C_3N_4 that had the appearance of velvet (Li, 2017). The nanocomposite had a high potential for reuse, which increased the material's already high level of interest. Nanocomposites that were created by co-doping oxygen and sulphur with g-C_3N_4 were able to breakdown seven different pesticides (Liu, 2020). Within thirty minutes, a degradation rate of more than ninety percent was reached for some of these pesticides. Zou et al., 2018 utilized a photocatalyst that was made up of vanadium pentoxide and graphitic carbon nitride to decompose ortho-dichlorobenzene. When only 2% of the nanocomposite was employed, the organochlorine was destroyed within 8 hours to the extent of approximately 62.4%. In addition, it was found that the efficiency of removal was 2.18 and 2.77 times higher than it was when the degradation was carried out using pure graphitic carbon nitride and pure vanadium pentoxide, respectively. Both of these compounds are considered to be pure forms of their respective substances. In addition, Jo et al., 2015 created TiO_2/ g-C_3N_4 nanotubes and nanopores; both of these components were utilized in the process of degrading pesticides one at a time. Within a response period of approximately four hours, it was observed that the nanocomposite containing nanotubes was successful in decomposing 90.8% of the pesticide. In some of the other studies that were described, the activation of peroxymonosulfate elaborate the usage of activated carbon reinforced by g-C_3N_4 (Wei, 2016). This was done in order to degrade pesticide pollutants.

Through the utilization of g-C_3N_4 as a photocatalyst and exposure to visible light, trihalomethane and halo acetonitrile were able to be broken down (Chang, 2019). Recently, g-C_3N_4 which has been modified with -cyclodextrin has been utilized for the degradation of contaminants (Zou, 2019). Zheng et al., 2016 utilized graphitic carbon nitride in their experiment to decompose persistent organic pollutants that were exposed to visible light irradiation. Under conditions of simulated irradiation, graphitic carbon nitride was also utilized in order to decompose fluazaindolizine. Pang, 2019 presents an in-depth discussion on the mechanism of action for

fluazaindolizine. Under the irradiation of visible light, a nanocomposite composed of Bi_2WO_6 and g-C_3N_4 has been employed to photo-catalytically break down the herbicide 2,4-dichlorophenol (Wang, 2019). For the degradation of various organic contaminants, it has been reported that a nanohybrid of NiO/WO_3 ornamented on graphitic carbon nitride can be effective (Devi, 2019). Under the irradiation of visible light, platinum nanoparticles that had been coated on carbon nanotubes of g-C_3N_4 were utilized for the purpose of eliminating p-chlorophenol (Li 2015). The decomposition of isoniazid has been accomplished by Jo et al., 2015 using both Z-scheme nanotubes and nanoparticles of g-C_3N_4 /TiO_2. The breakdown mechanism for isoniazid was also proposed during this process.

To facilitate the elimination of thiamethoxam, Barbosa Cruz et al., 2022 g-C_3N_4 was manufactured. Because of the partial negative charges that are located in the core of the molecule, the electrostatic potential indicates that this is the optimal location for the matrix to interact with the molecule. TMX has been shown to interact with the g-C_3N_4 matrix through the formation of H_2 bonds, and also bond dimensions of these connections varied from 2.61o to 3.538. The characteristics of the compound's structure provide evidence of this point. The QTAIM research was successful in locating the BCP of the H_2 bonds, determining that the hydrogen bond is fragile, and quantifying the EHB values, which ranged from 0.98 to 6.58 kilojoules per mole of the substance. Additionally, the hydrogen bond was characterized as weak. As a result of the computations of the energies involved in the processes, it was shown that there was an interaction between the g-C_3N_4 matrix and TMX. Additionally, it was shown that the procedure was impulsive and produced exothermic heat. As a result of this, one can reach the conclusion that the g-C_3N_4 matrix is also an effective material for the elimination of insecticides.

TABLE 2.3 Photocatalytic degradation of different pesticides by using g-C_3N_4-based semiconductor

Photocatalyst	**Pesticide**	**Efficiency**	**References**
P/ g-C_3N_4	Imidacloprid	91%	Sudhaik,2020
g-C_3N_4/Ag_3PO_4/AgI	Neonicotinoid	95%	Tang.2019
g-C_3N_4/Bi_2O_3	Imidacloprid.	96%	Raisada,2019
g-C_3N_4/SnO_2	Indomethacin	90.8%	Li, 2020
OMC/ g-C_3N_4	Imidacloprid	90	Liu,2014
Fe_3O_4-SnO_2-gC_3N_4	Carbofuran	89	Mohanta,2021
Graphene/ g-C_3N_4	Malathion	94	Sudhaik,2020
g-C_3N_4	Chlorpyrifos	85	Vigneshwaran,2019
GO/g-C_3N_4/Ag	paraoxon-ethyl	97.05	Zhao, 2020
V_2O_5/g-C_3N_4	ortho-dichlorobenzene	62.4	Zou et al., 2018

2.10 Graphene-supported g-C_3N_4 nanoparticle

As a result of graphene oxide's high surface area, its utilization in heterogeneous photocatalysis for the purpose of organochlorine insecticides degradation was given preference. Because it just consists of carbon, hydrogen, and oxygen, it may easily disperse in water (Bustos, 2015). Additionally, it does not contain any metals. Graphene oxide possesses advantageous features such as hydrophilicity, low conductivity, chemical stability. In addition, graphene oxide possesses functional groups. In point of reality, graphene oxide is utilized the majority of the time in the capacity of a co-catalyst due to the scarcity of information concerning its capacity to be initiated by sunlight (Kuang,2020). It has been stated, on the other hand, that their presence considerably boosted the efficiency of the photocatalytic elimination process. This is due to the part performed in absorbing the contaminant, functioning as an electron acceptor, functioning as a surfactant, and (Nguyen-Phan, 2011; Celaya 2020; Zhang, 2014; Gholami,2019; Panda, 2019). It is possible to reduce graphene oxide, which will then result in reduced graphene oxide. Unlike GO, which has a high oxygen-to-carbon ratio, reduced graphene oxide has a low oxygen-to-carbon ratio and

significant defects. In contrast, graphene oxide has a high O_2-to-CO_2 ratio. In a lot of ways, GO and rGO exhibit features that are similar. Graphene oxide, on the other hand, seems to be a brown powder, whereas decreased GO looks to be a black powder. Both of these forms of graphene oxide are known as graphite. When the procedure is carried out, either of these two could be combined with other types of semiconductors to boost the level of effectiveness with which organochlorine pesticides are degraded. It's possible that a variety of distinct reasons, such as improved light absorption, a narrower band gap, reduced recombination of charge carriers, and enhanced separation of charge carriers, are all responsible for the higher efficiency (Gaddam, 2019; Kalyani 2018).

For the purpose of degrading 4-chlorophenol in water, graphitic oxide and graphene oxide have been utilized. Bustos-Ramirez, 2015 reports that under optimal conditions, around 92 and 97% of the compound were successfully decomposed. El-Shafai, 2019 produced nanocomposite from both titanium oxide and GO, which was then used to breakdown two toxic pesticide. (El-Shafai, 2019) (imidacloprid and carbaryl). Compared to regular GO or pure titanium oxide, the nanocomposites that were created featured a band gap that was narrower, and their photodegradation of the insecticides was significantly more effective. In a study that was quite similar to this one, Sharma et al., 2019 used the microwave technique to make a nanocomposite of nickel, cobalt, and laurel that was supported on graphene oxide. Under the influence of the sun's rays, this catalyst was put to use in order to break down 2-chlorophenol. In a span of just 300 minutes, 71% of the organochlorine was rendered inert. On the other hand, the findings demonstrated a degradation of approximately 57% in the same amount of time, without the utilization of graphene oxide as a component. The introduction of graphene oxide into the nanocomposite reduced the capacity of holes and electrons to recombine, resulting in a considerable enhancement of the material's charge transfer efficiency. This was made possible by the material's much increased charge transfer efficiency.

Cruz et al., 2017 were successful in removing four different pesticides from water by utilizing a Nano-catalyst that was constructed from the mixture of titanium oxide and graphene oxide. Utilization of the Nano-catalyst allowed for the successful completion of this task. According to the results of their research, the photocatalytic performance of this nanocomposite was not influenced in any way by the various water materials that were examined. There was a marked

acceleration in the process of deterioration that occurred when the ultra-pure water and the natural water were used in separation from one another. Alterations in the water matrix, on the other hand, had an effect on the photocatalytic efficiency of a catalyst composed of pure titanium oxide. The subject of the experiment was subjected to continuous irradiation with visible light across its totality. In a fashion that is analogous, Mostafa et al., 2017 used mesoporous GO-Fe_3O_4/TiO_2 as a visible light active photocatalyst to break down fenitrothion, which is an insecticide that contains organochlorine. The fenitrothion was destroyed as a direct consequence of this event.

2.11 Scope and Objectives of the Present Thesis

Conventional treatment methods such as adsorption, incineration, biodegradation, and oxidation with peroxide or ozone all have their own limitations, which means that they are unable to remove hazardous chemicals from wastewater. This has been a complex problem that cannot be solved using these methods because they have their own restrictions. The advanced oxidation process, also known as AOP, has the ability to treat a wide variety of organic pollutants found in wastewater, such as pesticides and dyes, some of which are dangerous to human health due to their propensity to cause cancer and endocrine disruption. For the elimination of organic contaminants found in wastewater, photocatalytic degradation using semiconductors as photocatalysts is an approach that shows great promise and appeal as a potential solution. In-situ production of hydroxyl radicals is the fundamental principle behind the advanced oxidation process. The organic compounds that are present in wastewater will be oxidized by these hydroxyl radicals, which are highly reactive and non-selective oxidants. The end products of this process will be water and carbon dioxide. In the past several years, photocatalysis has been the subject of a significant amount of study for the removal of pesticides and other hazardous substances from wastewater. The photocatalytic purification of dirty wastewater by means of metal oxide semiconductor mediation is an exciting new approach to environmental remediation, particularly for dealing with low concentrations of organic pollutants. g-C_3N_4 has been shown to be the most suitable for widespread environmental applications among the many semiconductor photocatalysts. It is of the utmost importance to work toward increasing the sensitivity of g-C_3N_4 for use in photocatalytic applications. Because of the increased surface area and the modifications to the optical characteristics brought about by size quantization, the nano-scale g-C_3N_4 particles demonstrated improved photocatalytic efficiency for accomplishing this goal. At the mesoscale, the correct

spatial arrangement of layered inorganic materials can act as a mediator for the flow of electrons and energy (Hoertz & Mallouk 2005). In recent times, the fabrication of hierarchically structured materials has garnered a lot of attention as a result of the fundamental and practical uses that these materials have. In particular, the g-C_3N_4 nanoparticles are a highly effective photocatalyst for the breakdown of pollutants and the creation of hydrogen. Due to the huge band gap, however, its use is restricted to the near ultraviolet area of the electromagnetic spectrum. There have been a lot of attempts made to make g-C_3N_4 more sensitive so that it can absorb light in the visible spectrum. The primary purpose of this research is to find ways to improve the photocatalytic activity of g-C_3N_4 in the visible spectrum. In order to accomplish this goal, the techniques for synthesis will need to be optimized, and metal and non-metal doping will need to be applied to g-C_3N_4. Visible light active g-C_3N_4, and with and without graphene supported g-C_3N_4/V_2O_5 and g-C_3N_4/La_2O_3 catalysts have been produced, and the Physico-chemical characteristics of all of these catalysts have been examined in great detail. The effectiveness of these materials as photocatalysts in destroying cancer-causing and endocrine-disrupting compounds, such as Chlorpyrifos and Carbofuran was examined.

The g-C_3N_4 was synthesized using thiourea was selected for doping. The doped material g-C_3N_4/GO, g-C_3N_4/V_2O_5, g-C_3N_4/La_2O_3, g-C_3N_4 /GO/V_2O_5, g-C_3N_4/GO/La_2O_3 was further characterized using the advanced instrumentation like FT-IR, XRD, SEM, EDX, TGA and UV-VIS spectroscopy for the detailed study.

Insects that feed on plants and leaves, are controlled by Chlorpyrifos, which has a widespread of biological action. There have been claims of contamination as far as 24,000 metres from the first application site. Acute poisoning may cause a number of symptoms, including headache, nausea, muscular twitching, convulsions, and in the most severe instances, death.

An association between birth abnormalities in humans and exposure to chlorpyrifos and its derivatives has also been established. Moreover, it has an effect on the reproductive system of men. Beneficial arthropods such as bees, beetles, and parasitic wasps are among the arthropods that are killed by exposure to Chlorpyrifos. Even in quantities as little as a parts per trillion, it is lethal to fish. It is anticipated that metal ions that have unoccupied d and f orbitals will act in a Lewis acid-like manner. On the surface of the photocatalyst, the Lewis base chlorpyrifos has the potential to form an extremely stable complex.

The purpose of this study is to assess the semiconductor photolysis process as a potential strategy for removing pesticides from the environment. Using UV-visible spectroscopy, research into the process of pesticide degradation has focused on determining whether or not there has been a drop in the amount of Chlorpyrifos present. Tests were carried out under light under a variety of various circumstances. As a result, in the current work, a comprehensive investigation into the photodegradation of Chlorpyrifos and Carbofuran insecticides that have been sensitized by doped and undoped nanocrystals of g-C_3N_4 in aqueous solution has been carried out. This investigation was carried out with light.

At the moment, there have been no reports of in-depth studies on the intermediates produced by Chlorpyrifos photocatalysis. As a result, the main goals of this research are to identify the reaction intermediates and gain an understanding of the reaction pathways involved in the photodegradation of Chlorpyrifos (CP) and Carbofuran in g-C_3N_4/light processes. Both of these objectives are intended to serve as a foundation for the development of potential applications in the future. The following objectives have been taken into consideration for this study:

Objectives

1. Synthesis of lanthanum oxide and vanadium oxide doped g-C_3N_4 nanocomposites using hydrothermal process and their characterization

2. Fabrication of co-doped g-C_3N_4 immobilized with graphene oxide (GO) to improve the photo-metal oxide dispersion and enhance the bilateral process of removal using adsorption and photo-degradation.

3. To complete mineralization of Organophosphate and Carbamate from agricultural aquatic waste using synthesized novel photo-catalyst under solar irradiation.

4. To develop a Photo-catalytic continuous removal process under solar light irradiation.

5. Characteristic analysis of novel Photo-catalytic system for complete mineralization of agricultural aquatic pollutants.

CHAPTER-3

MATERIAL AND METHODS

Introduction

In recent years, there has been a rise in interest regarding the synthesis of a variety of metal oxide nanoparticles that are supported on g-C_3N_4. In this article, we described the thorough synthesis strategies for several metal-oxide based g-C_3N_4 nanocomposites. Additionally, we covered the various physio-chemical approaches that are employed for the characterization of as-synthesized catalysts. Various physio-chemical characterization techniques, such as XRD, FTIR, TGA, UV-Vis spectroscopy, FESEM, EDX, DRS, are utilized in order to investigate the phase, morphology, oxidation states, and textural features of all as-synthesized metal oxide g-C_3N_4 nanocomposites. This section provides a comprehensive breakdown of the catalytic process that underpins the photodegradation of pollutants.

3.1. Chemical and Solvents

Thiourea (99%), ethanol, sodium hydroxide, hydrogen peroxide, graphite flakes, sodium nitrate (98 percent), potassium permanganate (99 percent), ammonium metavanadate, hydrogen peroxide (40 percent wt), sulphuric acid (98 percent), $La(NO_3)_3.6H_2O$, KOH and hydrochloric acid were 33from Loba Chemie PVT.LTD, India. All reagents were analytical grade and were not purified further. Deionized water was used to prepare the stock solution. The insecticide known as Chlorpyrifos and Carbofuran was purchased from a local farmer's market in Punjab, India.

3.2 Physiochemical Characterization Technique

3.2.1 UV-VIS Spectroscopy

The UV-VIS spectroscopy is a major analytical technique that is frequently utilized for the specific purpose of determining the absorption characteristic of an analyte when the analyte is brought into contact with light. During the process of analysis, when photon hits the specimen, an electron there absorbs it and becomes excited, moving from its ground state to an excited state with a higher energy level. It is possible for various types of electronic transitions to take place, such as σ -σ *, n-σ *, π-π* transitions for organic molecules. After these transitions, charge transfer transitions may also take place. This is determined by the type of bonding that exists between the molecules or atoms that are present in the specimen. The resultant recorded absorbance spectrum showed the

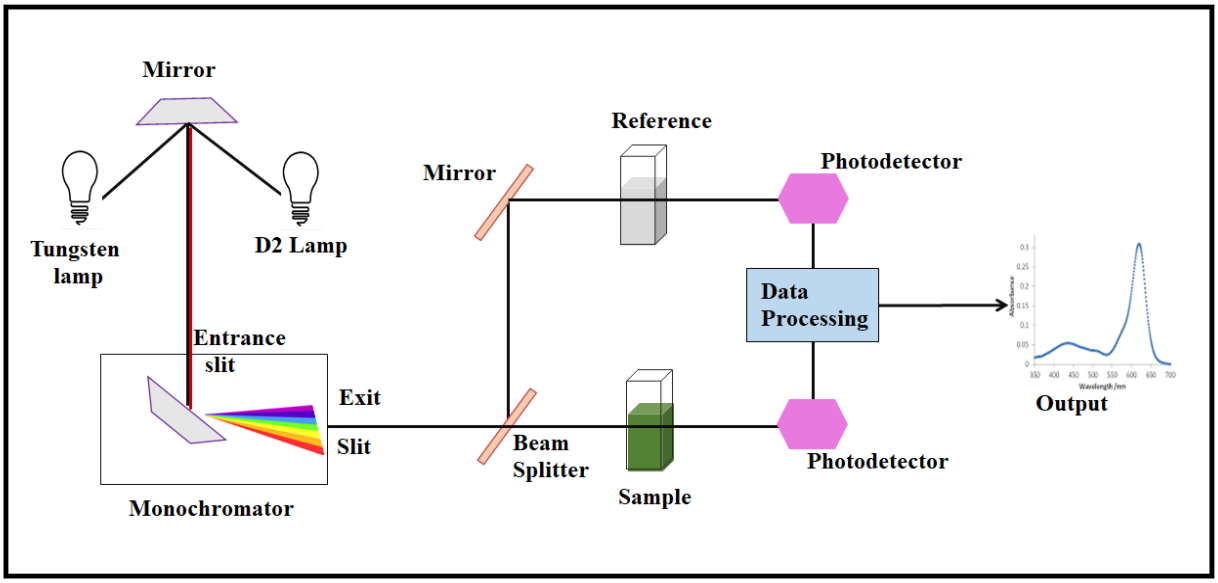

Figure 3.1 Schematic diagram of UV-Vis Spectroscopy

photons being absorbed by the specimen between the range of 200 and 800 nanometers, and the spectrum was profiled as absorbance against wavelength (nm). The diagram of a UV-Vis spectrophotometer is shown in Figure 3.1. We need to apply the Lambert-Beer law in order to comprehend the experimental applications of the experiments.

$$A = \varepsilon.c.l$$

Where A stands for the sample's absorbance, ε is the absorption coefficient, c is the concentration of the sample, and l represent the length of the cell. It is possible to determine the absorption coefficient using the recorded UV/Vis spectrum along with the mass of the specimen that is known. The equation shown above was utilized to create a value for the solution's concentration. Using Tauc's plot, we were able to determine the band gap of the material based on the absorbance range. The formula for this calculation is (hv)2 = A(h - Eg), where is the absorption coefficient, h is Planck's constant, is the light frequency, A is the proportionality constant, and Eg is the band gap energy of the material.

3.2.2 X-ray diffraction

The X-ray diffraction (XRD) technique is a non-destructive method that is extensively utilised for the characterization of a wide variety of macro-, micro-, and nano-crystalline materials. Some examples of these materials include inorganic and organic compounds, pharmaceuticals, minerals,

and catalysts. Crystalline polymers are also characterized using XRD. In addition to determining the catalyst's purity, degree of crystallinity, unit cell characteristics, and crystallite size, the primary objective of XRD patterns is to ascertain the crystallographic phase of the material being analyzed (catalysts). The X-ray powder diffraction (XRD) works on the fundamental idea that every single atom in a crystalline solid would scatter the incoming X-rays in every possible direction. The elements CuKα, CoKα, FeKα, and MoKα are the ones most frequently utilized as X-ray generators. The X-ray source is typically CuKα radiation, which has a wavelength of 0.154 nm and an energy of 8.04 keV. X-rays are scattered constructively in the directions provided by Bragg's law when they are scattered by atoms in an ordered lattice (Bragg & Bragg 1949).

$$n\lambda=2d\sin\theta$$

where n = 1, 2, 3, ... represents reflection, represents the wavelength of the X-ray, d represents the lattice planes distance, and ş represents Bragg's angle. This law establishes a connection between the wavelength of electromagnetic radiation and a crystalline sample's diffraction angle as well as the lattice spacing. Diffraction patterns are the names given to the spatial arrangements of the many thousand different reflections that can be formed by crystal formations. It is possible to assign a unique index, also known as a hkl value, to each reflection. This value will identify the reflection's position within the diffraction pattern. A symmetrical relationship can be seen throughout the structure. Using the Fourier technique, one is able to transform the relationship that exists between the crystalline lattice and the unit cell in the actual space.

The X-ray diffractogram provided insight into various significant and applicable details regarding the sample.

1. The nature of the solid, namely whether it is crystalline or amorphous.

2. The investigation of the deformation of crystal structures.

3. The rate of crystallization of a substance during its production, known as its kinetics.

4. Identification of the presence of an impurity phase using a fingerprint comparison of a known sample and the sample that was synthesized.

5. Alterations in the form and dimensions of the unit cell as a function of the place of the peaks.

6. Using the Scherrer Equation, determine the crystallite size, denoted by "D," in a solid sample based on the corrected line broadening "β".

$$D = K\lambda/\beta \cos\theta \qquad (1)$$

where D represents the crystal size, O represents the wavelength (1.54 microns), E represents the FWHM, K represents a constant value (equal to 0.89), and T represents Bragg's angle (as depicted in Figure 3.2).

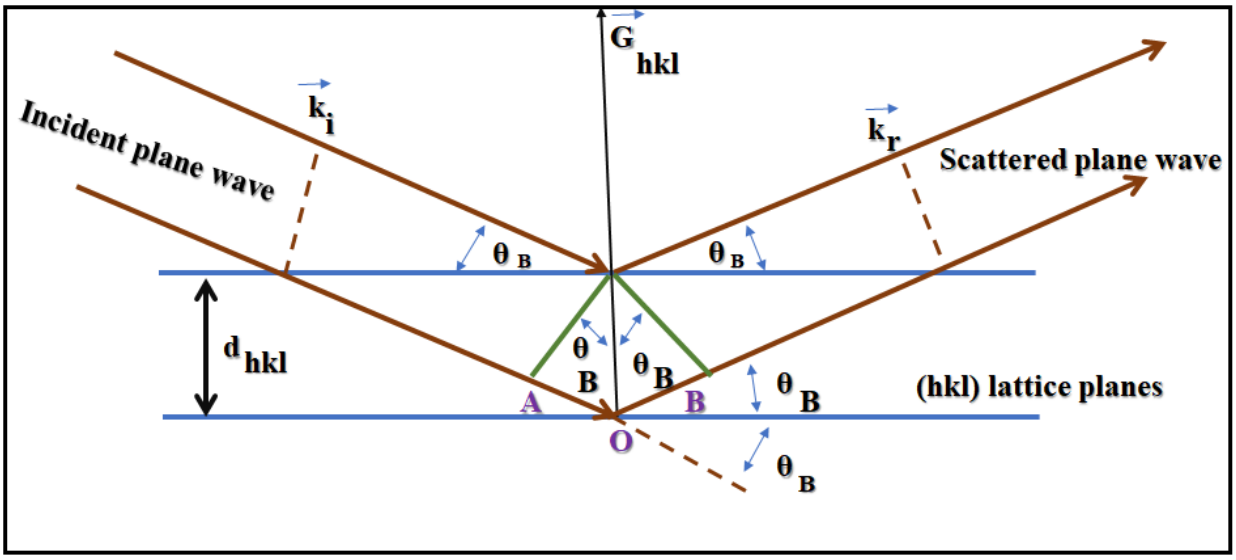

Figure 3.2 Geometrical drawing of crystal planes and Braggs law

3.2.3 Fourier Transform - Infrared Spectroscopy

Infrared vibrational spectroscopy is a typical method that is used for determining the functional groups of a sample by measuring structural features such as the vibrational frequencies of molecules and phonons. The measurement of the amount of IR light that is transmitted through a material is the foundation of IR spectroscopy. The vibrational modes of molecules are what the selection rule uses to define what the infrared spectrum of those molecules should look like. Changes in vibrational or phonon frequencies are typically caused when surface molecules or ions interact with nanoparticles. These interactions can be either positive or negative. As a result, the variations in frequencies that are recorded within an IR spectrum can provide information on the interaction that occurs between nanoparticles and surface molecules.

The infrared spectrum of a molecule is the result of the vibration and rotation of its atoms, which causes a change in the molecule's permanent dipole moment. This change is what gives the spectrum its characteristic pattern. Mid-infrared, which spans the range from 4000 cm^{-1} to 400 cm^{-1}, is the portion of the infrared spectrum that is utilized the vast majority of the time.

The FT-IR spectrum can reveal important details about the fundamental properties of the molecule, such as the composition of the atoms, and the chemical connection forces among the atoms. The numerous functional groups of the support and active component of the catalyst have been identified through the significant use of infrared spectroscopy, which has been employed extensively. It is also possible to detect the surface acidity of the catalysts by using FT-IR with a modification that is performed in the cell compartment. By employing the ATR sampling approach and the KBr pellet technique, the spectra of the samples were recorded on an FT-IR spectrometer manufactured by Perkin Elmer and titled Spectrum Two. In order for the catalyst, when it is in powder form, is often manufactured as a thin pellet so that it is visible through the infrared beam. In most cases, the KBr pellet is made by grinding together 2 milligrams of the catalyst and 200g of the KBr. The diagram of FTIR spectrophotometer is shown in Figure 3.3.

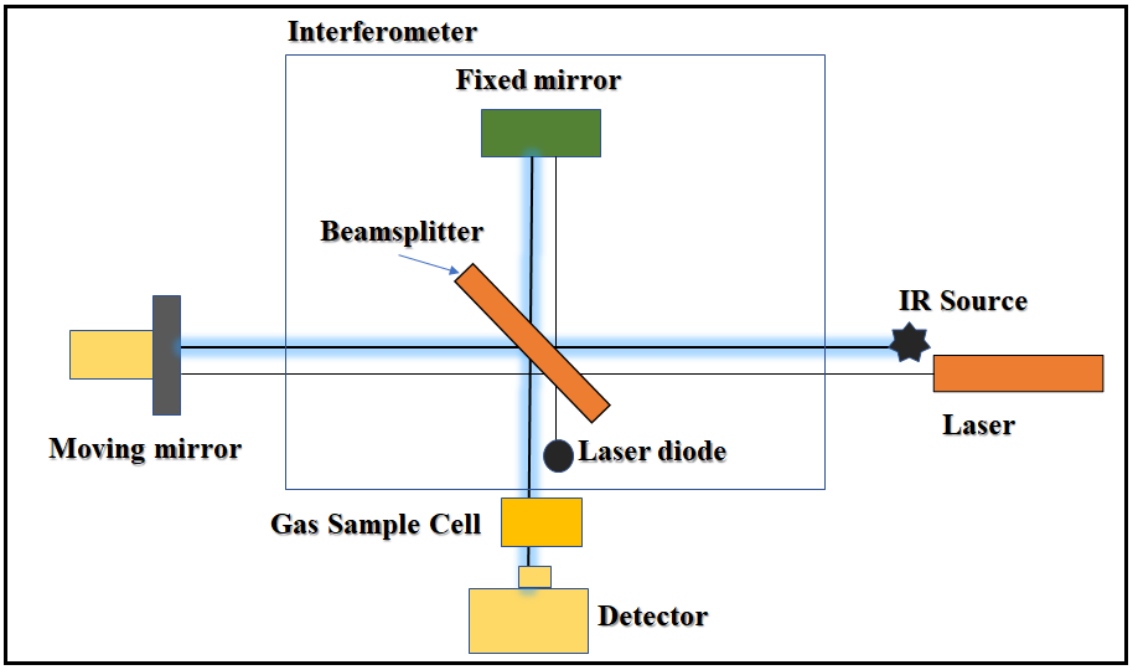

Figure 3.3 Schematic diagram of FTIR

3.2.4 Scanning electron microscopy-Energy dispersive X-ray Diffractometer

Using a scanning electron microscope with an energy-dispersive X-ray diffractometer attached, the shape and elemental makeup of the catalysts were studied (SEM-EDAX, Hitachi S 3400 N). The scanning electron microscope, also known as an SEM, is effectively a microscope that produces an electron beam and scans in both directions across a sample.

It provides information about the topography or roughness of the surface, as well as the size, shape, organization, and chemical composition of the particles that are adjacent to the surface. In addition, it shows the relationship between the particles and the surface. The SEM, is a type of microscope that magnifies descriptions using electrons rather than light. The majority of the catalysts that were utilized in the research are poor conducting materials; hence, the catalysts were sputtered with gold in order to provide them with a gold coating.

3.2.5 Energy Dispersive X-Ray Spectroscopy

The EDX spectroscopic description was carried out using the HR-SEM instrument that was attached to the SEM instrument in order to further describe the chemical composition of the as-synthesized nanocomposite as well as the element distribution. It is a method that can be employed for the purpose of determining the elemental configuration of the specimen, as a component of the attention paid to it.

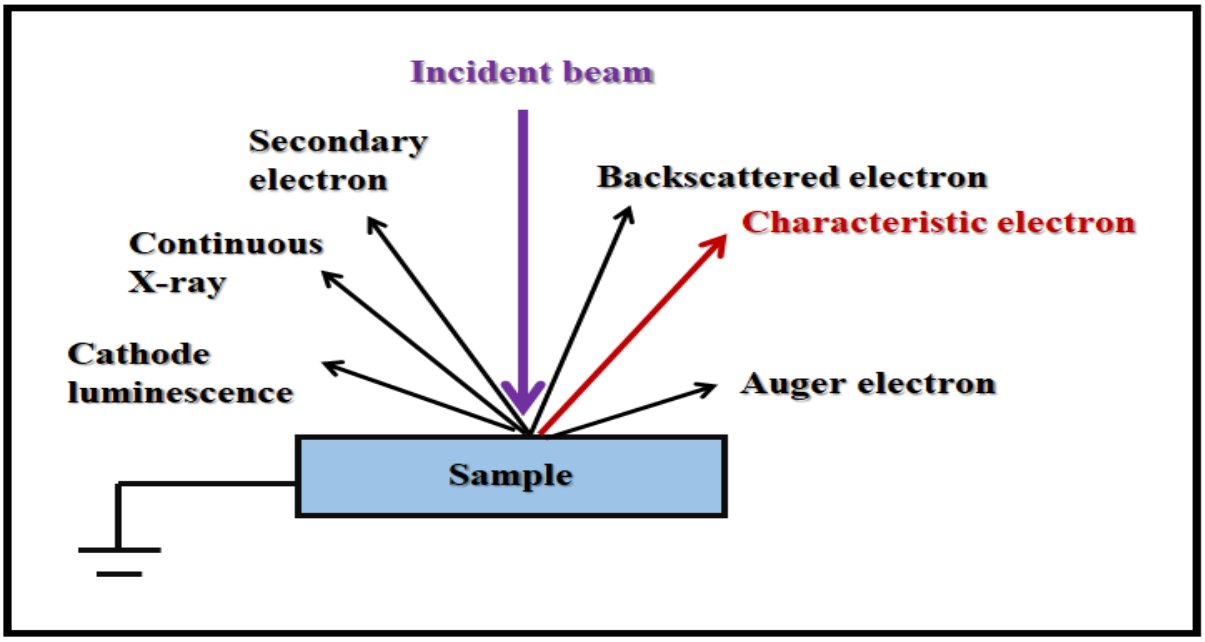

Figure 3.4 Principle of Scanning electron Microscopy

An EDX spectrum, which is a plot of the number of times an X-ray is captured, is the product of an EDX study. This spectrum is made for each different level of voltage. In an EDX spectrum, you can usually see peaks that are similar to the power degrees you get when you expose something to the most X-rays. Each peak is unique to a certain atom, which means that each one represents a different element. If a peak in a spectrum is more noticeable, it means that there are more of that element in the specimen. An EDX spectrum map not only shows what details each peak is similar to, but it also shows what kind of X-ray each peak is related to. For example, the K peak is a height that corresponds to the amount of energy that X-rays give off when an electron moves from the L-shell to the K-shell. The top that is emitted by electrons in the M-shell onto the K-shell, which corresponds to X-rays, is referred to as a K height, and it can be seen in Figure 3.5.

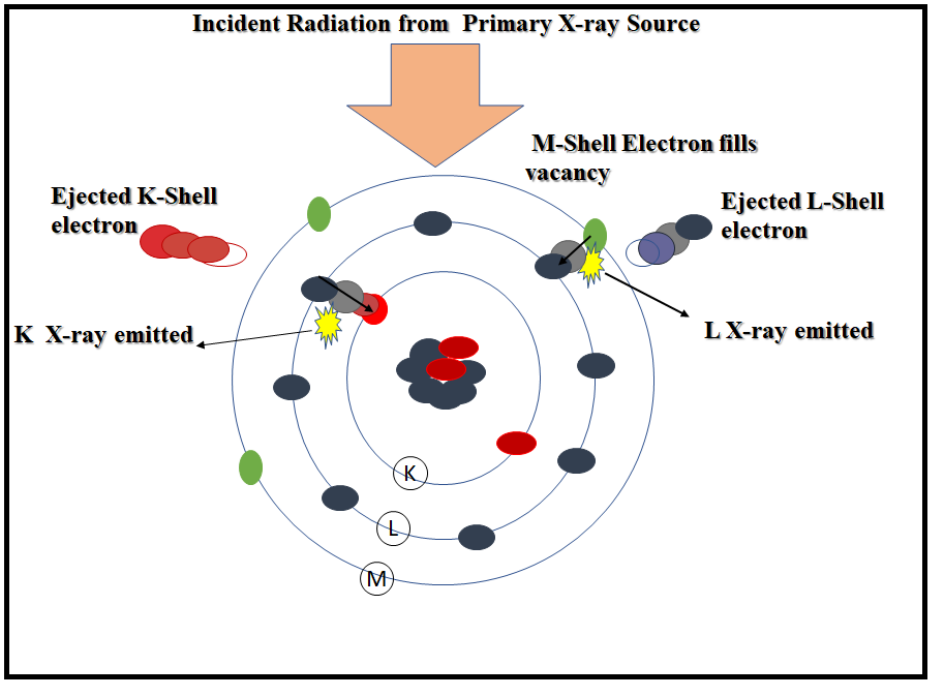

Figure 3.5 Emission of X-rays

3.2.6 Thermogravimetric Analysis

The TGA, is a kind of thermal investigation in which the sample's mass is measured over time as the temperature variations. This kind of analysis is known by its technical title, thermogravimetric analysis. This measurement provides us with information regarding a variety of different physical and chemical processes, including phase shifts. A piece of machinery known as a thermogravimetric analyzer is utilized in the process of carrying out the thermogravimetric

analysis (also known as TGA). The mass of a sample can be continuously measured using a thermogravimetric analyzer, even when the temperature of the sample gradually shifts over time. The most fundamental components of thermogravimetric analysis are the measurements of mass, temperature, and time. Having said that, you can derive a great many different measures from just these three measurements. A TGA analyzer usually has a precision scale, a sample pan, and a boiler that can be set to a certain temperature. This configuration is housed inside of a furnace. In order to initiate a thermal reaction, the temperature is often raised at a pace that is held constant (alternatively, for some purposes, the temperature is maintained so that there is a constant loss of mass). The thermal reaction could take place in a variety of distinct atmospheres and densities, including the surrounding air, a hoover, an inert gas, or even a "self-generated atmosphere." In addition, the reaction may take place under a variety of pressure conditions, such as a high hoover, a high pressure, a continuous pressure, or a controlled pressure.

3.3. Experimental Section

3.3.1. Synthesis of nanomaterials

Synthesis of g-C_3N_4:

Since its discovery in 2009, the typical synthetic polymer g-C_3N_4 has become an increasingly prominent subject of discussion in the world of material science, notably for photocatalysis, due to its cost effective, ease of manufacture, good stability, and unique physico-chemical features. This is especially true for photocatalysis due to the fact that it is inexpensive and simple to perform. Throughout the course of the past decade, this has been the circumstances (Wang et al ., 2009). Many people believe that the s-trizine rings, which have a chemical formula of C_3N_3, and the tri-s-triazine rings, which have a chemical formula of C_6N_7, are the two fundamental tectonic units that make up the specific architecture of the C_3N_4 molecule (Wang et al., 2012). Compounds with g-C_3N_4 can be readily produced by the use of thermal condensation in conjunction with very small organic molecules that serve as nitrogen-rich precursors. The types of tectonic units that can be identified are significantly influenced by the reaction processes in a major way (Reddy et al.,2019). The procedure of thermal condensation makes it possible to quickly and readily produce g-C_3N_4 containing materials in the vast majority of circumstances.

Graphitic carbon nitride may be created via the controlled thermal decomposition of several carbon- and nitrogen-rich precursors in a controlled environment (Hwang et al., 2017; Yu et al., 2013). This procedure may be performed as many as required. This approach is used extensively in the production of composite materials based on graphitic carbon nitride. Ismael and Wu constructed a $LaFeO_3/g\text{-}C_3N_4$ composite photocatalyst for the degradation of RhB and 4-CP when exposed to visible light. $FeO_3/g\text{-}C_3N_4$ Composite Photocatalyst for the Degradation of MO and 4-CP under Visible Light Irradiation Produced by a Simple Calcination Process (Ismeal et al., 2019). Another study that was similar to this one, used a straight forward calcination technique to produce $g\text{-}C_3N_4$ from three distinct precursors (melamine, thiourea, and urea) (Ismael et al., 2018).

The method of thermal breakdown was altered very slightly in order to facilitate the synthesis of $g\text{-}C_3N_4$ that was presented in work. $g\text{-}C_3N_4$ was produced through the use of thiourea. At the temperature of 550 degree Celsius, the synthesis was carried out. Figure 4.1 depicts a typical preparation in which 10 g of thiourea are deposited in a ceramic crucible before being put into a muffle furnace and calcinated at a temperature of 550 degree Celsius for two hours at thermal rate of 3 º /min. After cooling at room temperature obtained yellowish material was crushed into fine powder in an agate mortar.

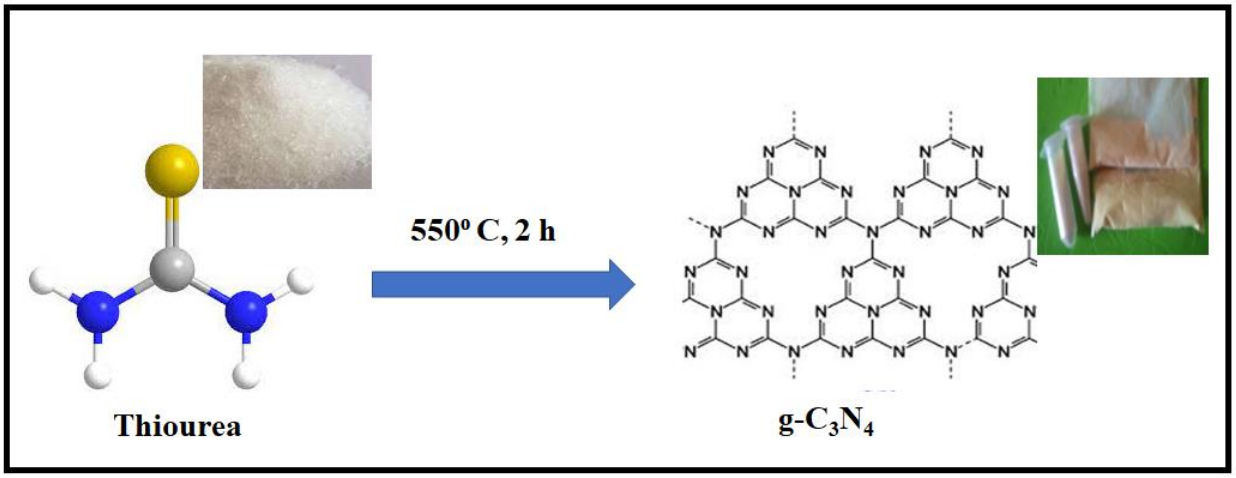

Figure. 3.6 Schematic Representation of $g\text{-}C_3N_4$ synthesis

Graphene Oxide Synthesis

A modified Hummers approach was used to make GO, which involved oxidizing extremely fine graphite powder (99%) with sulfuric acid, sodium nitrate, and potassium permanganate. An outline of the GO synthesis process is given below: A 0.5 gram of graphite powder and 23 ml of H_2SO_4

were poured into a 500 ml glass beaker put in an ice bath, and then stirred at 500 rpm for 30 minutes. In the solution, 0.5 gm of $NaNO_3$ was added and was continuously agitated at 600 rpm for 60 minutes. Then, while maintaining the solution's temperature at 15°C, 3 grams of $KMnO_4$ was progressively added. The resulting mixture was agitated at 600 rpm for 60 minutes.

The solution temperature was then elevated up to 35°C. 50 ml of DI water was gradually added throughout the stirring process. The temperatures were increased to 95 degrees Celsius and maintained for the next 30 minutes. The slurry cooled down and stirred overnight at room temperature at 600 rpm. Finally, 50 ml DI water and 1.5 ml H_2O_2 was used to stop the process (1.5 ml). The mixture had to be centrifuged at 3000 rpm for 7 minutes and cleaned with 4% hydrochloric acid and Deionized water to get rid of any remaining metal ions and acid residues. This procedure was constantly repeated until the pH of the solution reached neutral (as shown in Figure 3.7).

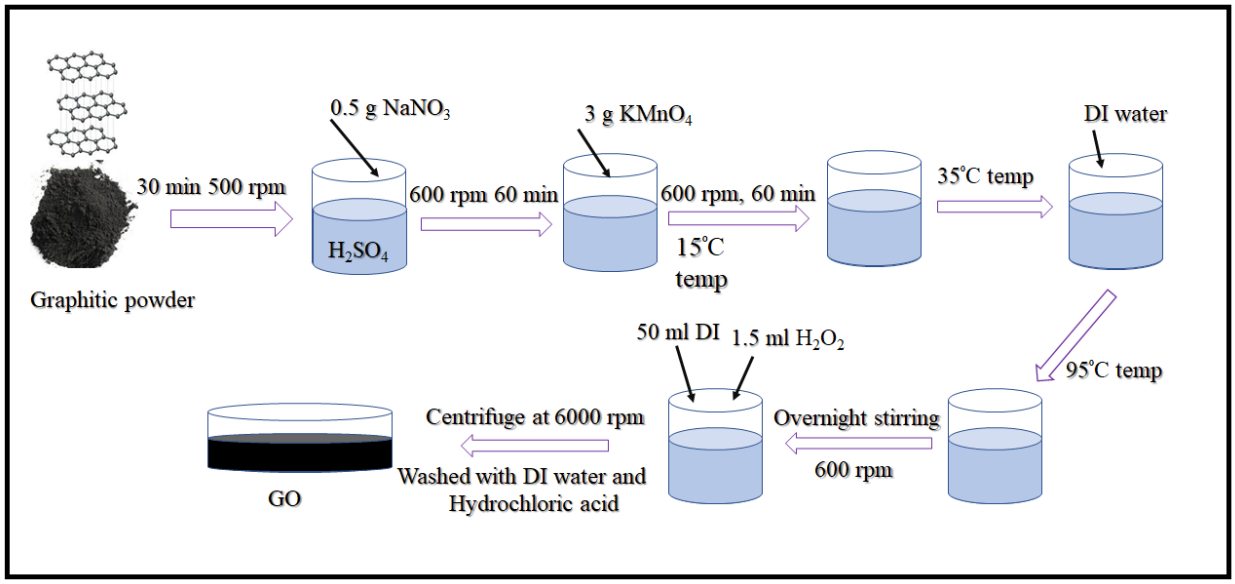

Figure 3.7 Schematic representation of the GO Synthesis process

V_2O_5 Synthesis

To synthesize V_2O_5, 0.1M ammonium metavanadate (NH_4VO_3) was dissolved in 80 mL of distilled water. Dilute sulfuric acid was added dropwise in the solution till the pH reached around 4. The orange-colored solution was moved into a autoclave that was lined with Teflon and kept there for 24 hours at 120°C. at room temperature, the solution was then cooled. After centrifugation, 100% alcohol and distilled water were used to repeatedly wash the precipitate. The powder obtained was dried at 70° C under a vacuum for 8 hours (as shown in Figure 3.8).

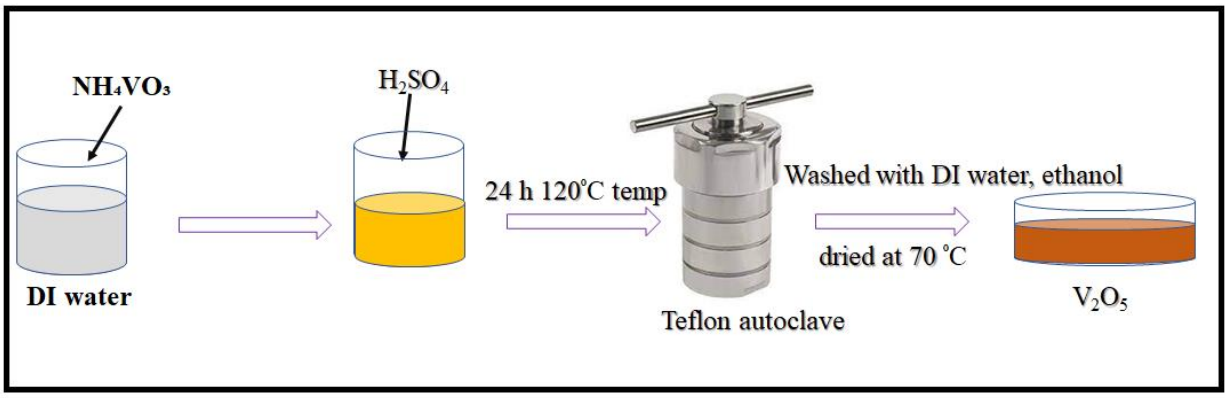

Figure 3.8 Schematic representation of V_2O_5 synthesis

Synthesis of g-C_3N_4 /GO/V_2O_5

To produce g-C_3N_4 doped with GO and V_2O_5, 1.0 g of g-C_3N_4 was dispersed in 85 ml of DI water with specific different amounts of GO and V_2O_5. The resulting solution was stirred and ultrasonicated for 30 minutes. The suspension (100 ml) was then placed into a autoclave and heated at 200°C for 8 hours. Following the reaction, the resulting suspension was centrifuged and washed several times with deionized water and ethanol before being vacuum dried at 80°C for 60 minutes. The reaction and the process flow for g-C_3N_4/GO/V_2O_5 composite synthesis are shown in Figure 3.9.

3.3.2. Photocatalytic activity tests

The degradation action of produced nanocomposites was determined by breaking down 0.1g/l Chlorpyrifos in the presence of visible light. Photocatalytic activities were carried out in a suitable batch reactor that was illuminated with visible light. For a particular photocatalytic test, 30 ml of Chlorpyrifos solution and 10 mg of the nanocomposite were both added and using 0.1 M HCL and NaOH pH was adjusted at 4. Before the reaction was initiated, the solution was exposed to visible light at room temperature. A predetermined amount of solution was centrifuged and filtered through Whatman (0.45 mm) paper at regular intervals during the exposure to light. At 290 nm, the filtrates were examined using a UV-Vis spectrometer. The effects of the pH, time of exposure/dose, and H_2O_2 on chlorpyrifos were investigated. The following equation (1) was used to compute the amount of photocatalytic pesticide degradation:

Percent Degradation $= \frac{AO-At}{AO} \times 100$ eq (1)

Where Ao is the absorbance of pesticides at the initial stage, and At, is the absorbance of pesticides at a time "t".

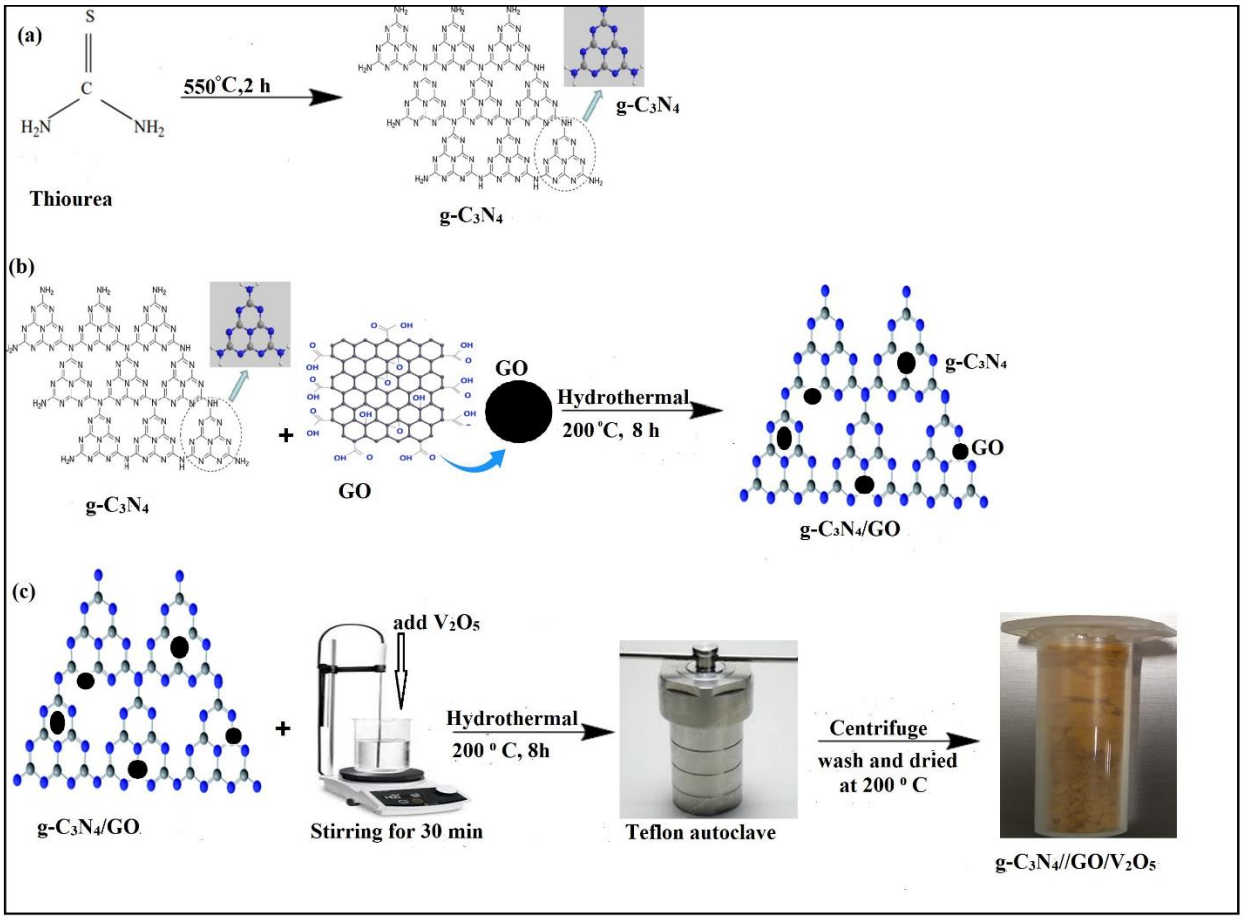

Figure 3.9 Schematic process flow chart of g-C_3N_4-GO/V_2O_5

Continuous study

Under the irradiation of visible light, the photoreactor was put into operation so that the effectiveness of the photocatalytic degradation process could be measured. A Xenon lamp is used as a source of visible light, and it has a water inlet on one side and a water outlet on the other side. The light source was maintained at a distance of at least 6 centimeters above the reaction mixture at all times. The column was then stuffed with g-C_3N_4/GO/La_2O_3 nanocomposite (the layer of nanocomposite was equal to 2 and 4 cm^3, and a steel net sheet with a diameter of 0.001 centimeters

was placed underneath it. For the purpose of enhancing and preserving the flow distribution, the column packing with g-C_3N_4/GO/La_2O_3 nanocomposite consisted of filter paper and glass wool of a volumetric equivalent of 0.5 cm^3.After 30 minutes, a small portion of the reaction solution was removed, centrifuged, and its optical absorbance was measured by UV-Visible absorption spectroscopy. The percentage of degradation was calculated using the following formula:

$$\% \text{ of degradation} = C_0\text{-}C_t / C_0 \times 100$$

where C_0 is the initial concentration of the pesticide and C_t is the concentration of dye at 't' min. The degradation of pesticide molecules was measured in terms of a reduction in the optical absorption intensity.

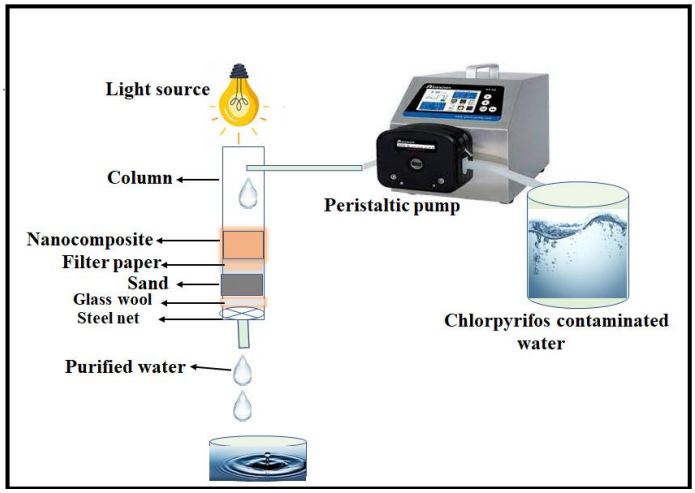

Figure 3.10: Diagram of column experiment

CHAPTER- 4

RESULTS AND DISCUSSION

This chapter discusses the synthesis, characterization, and degradation action of g-C_3N_4, La_2O_3, and V_2O_5, as well as the fabrication of these materials using GO nanostructured material using the hydrothermal technique. FE-SEM, XRD, EDX, FT-IR, UV-Vis-DRS, and TGA were used to describe the synthesized material; the results demonstrate the major role that the precursor ions play in determining various properties of g-C_3N_4. Pictures obtained using FE-SEM equipment demonstrated that anions play an important part in shaping both the interior and external surface shape of g-C_3N_4. As a result of the action of the precursor ions, a variety of structural morphologies were produced. The XRD analysis reveals that g-C_3N_4 has a crystal structure consisting of hexagons. The samples also had a high oxygen vacancy and massive crystallographic flaws. The synthesis of pure g-C_3N_4 has been confirmed by EDX analysis.

The photocatalysis method is a relatively new environmental application that has a significant amount of potential for the future. The mineralization of chlorpyrifos and carbofuran by as-synthesized pure and doped g-C_3N_4 in the integrated system is another topic that is covered in this chapter. In great detail, the mechanisms of degradation, irradiation time, pH effect, H_2O_2 effect, dosage effect, and the efficiency of the Continuous system, as well as the efficiency of the pure and doped photocatalyst, have been studied.

Introduction

Nanoparticles have emerged as a sustainable alternative to typical bulk materials, as catalyst support that is robust and has a high surface area. This is due to the fact that their physical, morphological, and optical properties are all unique and can be modified (Tiwari et al., 2008). The form and size-dependent optical and photocatalytic characteristics of g-C_3N_4 nanostructures have involved a great amount of attention in recent years. The g-C_3N_4 is essentially a two-dimensional structure that is layered, similar to graphene. Graphene has garnered a lot of attention because of the fact that it can transmit electrical charges and has a tight band gap of less than 2.7 eV. Mixing g-C_3N_4 with other semiconductor photocatalysts may be one of the most promising ways to produce a photocatalytic system with relatively superior properties and efficiency.

To raise the charge separation in photocatalysis by minimizing the electron and hole recombination a substantial amount of labor is necessary to connect g-C_3N_4 with other nanomaterial with an optimal band gap. This chapter presents a simple method for the synthesis of g-C_3N_4 using the calcination methodology as the central concept.

At the moment, a number of researches has been carried out in order to examine binary composites, however, comparatively few studies have been carried out on ternary nanostructures. Relatively recently, the binary g-C_3N_4/TiO_2 (Desore et al., 2018), g-C_3N_4-ZnO (Bhatia, 2017), and g-C_3N_4/Cu_2O (Mia et al 2019). PCs displayed remarkable photocatalytic efficacy; nevertheless, there are still some limitations on their practical use due to their high recombination rate and restricted UV and visible light consumption. The doped material (such as Bi_2WO_6/RGO/g-C_3N_4, g-C_3N_4/Ag-ZnO, g-C_3N_4 /CeO_2/ZnO, and g-C_3N_4/Fe_3O_4/TiO_2) have enhanced photo-electron (e^-) trapping and prevents the recombination of photo-excited h+/ e^- pairs, enhancing the charge separation(Pearce et al., 2003; Wang et al., 2016; Ohgaki, 2015).

V_2O_5 has been extensively explored for the construction of heterostructures by g-C_3N_4 because it is an efficient cocatalyst that can be paired with effective band-structure SCs. This occurs as a result of V_2O_5's optimum bandgap (2.3 eV), abundance, strong visible-light responses, excellent stability, and inexpensive cost (Pandey, et al., Lops 2019).

V_2O_5 is another component of the photocatalyst because it is a layered semiconductor with various benefits, including a low bandgap (2.3 eV), a wide response spectrum to light, relative chemical stability, and a strong oxidation ability. (Preeyanghaa et al.,2022, Zhang et al.,2022). Specifically, we have chosen V_2O_5 because of its broad response spectrum to light. In addition, V_2O_5 possesses suitable band edges, which, when combined with g-C_3N_4, have the potential to combine effectively to generate an S-scheme heterostructure (Preeyanghaa et al.,2022).

Recent research has shown that a heterostructure composed of V_2O_5 and g-C_3N_4 can advance the degradation activity of a material. According to Preeyanghaa et al.,2022 the S-scheme rod-like g-C_3N_4/ V_2O_5 heterostructure improves the performance of tetracycline antibiotic degradation. In addition to this, Le et al. showed that the V_2O_5/ g-C_3N_4 S-scheme nanocomposite displayed good removal effectiveness for amoxicillin when it was exposed to sunlight.

By subjecting pure V_2O_5 and P- g-C_3N_4 to heat treatment, Zhang et al. created a V_2O_5/P- g-C_3N_4 composite material and discovered that it displayed better methyl orange elimination effectiveness than the pure materials (Zhang et al.,). Oliveros et al. exhibited photocatalytic diclofenac elimination using a V_2O_5/B- g-C_3N_4 composite, with an efficiency that reached close to one hundred percent (Hassan et al., 2022)

According to the findings of Dadigala et al., V_2O_5 nanorods/ g-C_3N_4 displayed a good photoreduction efficiency for Cr (VI) and photodegradation for Congo red dye. All of the reports show that heterojunction, which helps to separate charges during the photocatalytic process, is superior to the usage of pure V_2O_5 and g-C_3N_4 when it comes to increasing the efficiency of the photocatalytic reaction. Degradation of the contaminants has been the exclusive focus of study on the V_2O_5/ g-C_3N_4 heterostructure so far. On the other hand, it was just recently revealed that the existence of nitrogen defects in g-C_3N_4 can be beneficial in photocatalytic reactions. The ternary nano-catalyst demonstrates a persistent oxidation/reduction activity for MB and Cr+6. Many spectroscopic approaches were utilized in order to determine the properties of the ternary catalyst Ag/ g-C_3N_4/V_2O_5. In addition, the ternary catalyst's ability to post-illuminate improved the oxidation and reduction of MB and Cr+6 in proportion. This study demonstrates that the nano-catalyst Ag/ g-C_3N_4/V_2O_5 has the capability to remove pollutants. This could be an additional benefit for the treatment of water in a variety of settings (El-Sheshtawy et al 2019). Hence, it

displays the photo reaction over a wide range because it boosts the ability to absorb UV and visible light, which was demonstrated to be the most ideal material for photocatalytic application.

On the basis of the aforementioned circumstances, we have successfully prepared and examined the combination of energetic visible-light sensitive GO/V_2O_5 and La_2O_3 for surface coupling via g-C_3N_4 NMs.

Section-I

4.1 Efficient photocatalytic degradation of Chlorpyrifos pesticide from aquatic agricultural waste using g-C_3N_4 decorated graphene oxide/V_2O_5 nanocomposite

Abstract

Herein, we synthesized graphitic carbon nitride/GO/V_2O_5 nanocomposite and utilized this photocatalyst for the degradation of the pesticide Chlorpyrifos. The nanocomposite was prepared using the hydrothermal method at a temperature of 200°C for 8 hours. The crystal structure was determined using powder X-ray diffraction of ternary nanocomposite material crystallite size, phase, and defects. Surface morphologies and functional groups were evaluated by scanning electron microscopy (SEM) and FT-IR. Chlorpyrifos, a target pollutant, was photodegraded under the visible light to determine the effectiveness of the photocatalysts. The photocatalytic studies indicated that the graphitic carbon nitride/GO/V_2O_5 composites significantly outperformed the pure versions of g-C_3N_4 in photocatalytic degradation of Chlorpyrifos. The excellent photocatalytic removal efficiency of more than 88% obtained using a graphitic carbon nitride/GO/V_2O_5 catalyst pointed toward a great alternative catalyst for the treatment of Chlorpyrifos and other hazardous pesticides from wastewater.

4.1.1 Introduction:

Pesticides are synthetic compounds or mixtures that are intended to prevent, eliminate, or manage pests such as disease vectors, unwanted plant and animal species, and animals that cause damage during the manufacturing, storage, distribution, transportation, or sale of food or agricultural farming produce (Rasmussen et al., 2019).

Pesticides containing organophosphorus are widely used across the world. These insecticides are commonly used in agriculture to boost yields and satisfy nutritional requirements. Carbon, nitrogen, oxygen, and Sulphur are also bonded to a central phosphorus atom in organophosphorus insecticides. Organophosphorus insecticides have also attracted attention because of their great efficacy and limited stability (Gao et al., 2009). Besides their increasing worldwide utilization,

water pollution arising from these agro-pesticides is one of the most pressing environmental concerns due to their potential toxicity and bioaccumulation (Kumar et al., 2014). Pesticide residue is ubiquitous in stream, river, and groundwater sources, and their presence corresponds to the region's geographic and seasonal insecticide consumption trends (Zhang et al., 2011).

They get into water supplies through a variety of routes, including industrial effluent, agricultural runoff, and chemical usage. Pesticide concentrations in drinking water are capped at 0.1 g/l by the European Economic Community. It has been observed that pesticide concentrations in water in several nations surpassed US Environmental Protection Agency (EPA) regulations (WHO, 2011). Most organophosphate pesticides are poisonous and persistently stable, endangering human health and substantially harming the ecosystem when they infiltrate into water. The human neurological, cardiovascular, and respiratory systems are severely harmed by prolonged exposure to Chlorpyrifos, an organophosphate (Dehghani et al., 2017).

Photocatalysis (Shan et al., 2017; Palmisano et al., 2015), electro-degradation (Foroughi et al 2017; Brinzila et al., 2019), adsorption (Guo et al., 2015; Guo et al., 2015), ozonation (Li et al., 2008; Sousa et al., 2017), and direct anodic oxidation (Ammar et al; Yahiaoui t al., 2013) have been investigated as innovative strategies for removing pesticide pollutants from wastewater. Photo-catalysis technology has sparked a lot of interest in solar-energy-driven semiconductors during the last 40 years due to its exceptional characteristics of being environmentally friendly, strong stability, highly efficient, and direct use visible light (Gong et al, 2018; El-Sheikh et al., 2016; Vellaichamy et al., 2017). Environmental photocatalysis (organic pollutants removal) (Wang et al., 2017; Wei et al., 2019), photocatalysis for energy production (water splitting) (Wang et al., 2016; Wang et al., 2017), photocatalytic sterilization (Staphylococcus aureus, Escherichia coli, and other bacteria) (Long et al., 2017; Magdalane et al., 2018; Li et al., 2019), and photocatalytic synthesis (photocatalytic reduction of dinitrogen to ammonia, and other bacteria) are all applications of photocatalysis technology (Liu et al., 2019; Wang et al., 2018, Zhang et al., 2018). g-C_3N_4 is an excellent photocatalyst due to its features such as correct band locations, high stability, and non-toxicity (Zaiwang et al., 2014). The highly reactive catalyst graphite carbon nitride may be synthesized via a simple thermal polycondensation technique. Because the band gap of g-C_3N_4 is extremely small (2.7 e V) (Zhang et al., 2018).

Despite these benefits, g-C_3N_4 falls short of meeting practical expectations due to quick charge carrier recombination, limited surface area, and low harvesting capacity of visible light (less than 460 nm) (Chen et al., 2009; Su et al., 2017). There have been several attempts to increase the degradation efficiency of g-C_3N_4, including heterojunction fabrication (increasing photo-generated electron and hole separation efficiency) (Zhang et al., 2017; Min et al., 2017) porous structure optimization (Xinchen et al., 2009), doping of ion (turning off the optical band gap) (Yu et al., 2018; Zhang et al., 2017; Li et al., 2018) and so on.

Because of low cost and non-toxic, V_2O_5 is frequently employed as a powerful environmental catalyst among many semiconductors. V_2O_5 exhibits a variety of features, including a narrower band gap, chemical stability, and toxicity. It's been employed in a variety of applications, including antifungal and antimicrobial textile additives and wastewater treatment (Rauf et al., 2007; Teramura et al., 2004).

Graphene oxide (GO), on the other hand, is a honeycomb-shaped two-dimensional conjugated sheet of carbon atoms that has attracted significant attention due to its remarkable properties (Chen et al., 2014; Li et al., 2015; Zhang et al., 2004). Nevertheless, it has been used to make inorganic nanocomposites material, and it has been used for a variety of applications including drug delivery (Balapanuru et al., 2010), biochemical sensors (Zhu et al., 2011), electrochemical (Wang et al., 2010), optoelectronics (Zhuang et al., 2010), and catalysis (Chen et al., 2010), among others.

Graphitic carbon nitride electronic integration with a variety of carbonaceous materials having conjugated electrons, such as nanotubes of carbon, black carbon, graphene, and carbon nanodots, may greatly increase delocalization, slow charge recombination, and maintain charge separation, resulting in enhanced degradation activity (Xu et al., 2015). Nonetheless, no data on the synthesis of graphitic carbon nitride/GO/V_2O_5 ternary nanocomposite material and their use for photocatalytic of Chlorpyrifos is known to our knowledge.

The research that was proposed resulted in the effective creation of the g-C_3N_4/GO/V_2O_5 nanocomposite, which was afterward used to remove chlorpyrifos insecticide from the aqueous solution. SEM, EDX, XRD, and FT-IR are some of the techniques that were used for characterization the photocatalyst that was utilized. This photocatalyst was produced by utilizing a straightforward hydrothermal approach. In addition to this, the g-C_3N_4/GO/V_2O_5 nanocomposite in its as-prepared state showed improved degradation action towards the destruction of

Chlorpyrifos. It is probable that the enhanced photocatalytic activity and stability of the g-C_3N_4/GO/V_2O_5 nanocomposite are the consequence of the electron reservoir function provided by GO and V_2O_5, which transfers photogenerated electrons and holes in a substantial manner. According to the findings of the experiment involving radical capture, the most significant reactive species in the photocatalytic process are ˙OH, radicals. In addition to that, both the reusability and any potential mechanisms that could be involved were investigated.

4.1.2 Result and Discussion

4.1.2.1 Characterization part of nanomaterials

i. X-Ray Diffraction analysis

Using X-ray diffraction, the crystallinity of all photocatalyst materials was measured. Figure 4.1 depicts the crystalline phase of derived materials as determined by X-ray Diffraction methods. [JCPDS FILE NO. 87-1526]. Characterization peaks for graphitic carbon nitride are seen at 13.0 and 27.8 which correspond to crystallographic planes (100) and (002), respectively. Peaks at 13.0 and 27.8 nm indicate the formation of the hexagonal phase of graphitic carbon nitride, and the computed distance is 0.67 nm. Second peak relates to interlayer stacking of aromatic segments 0.32 nm apart (Wang et al., 2016; Wang et al 2017).

The main peak in the GO pattern results from the (001) reflection at 10.8 degrees and a distance of 0.89nm. This exhibits the oxidation and exfoliation of the flake Graphite precursor, as well as the loss of reflection from significant graphitic planes like (002) and (004), which are indicative of graphite crystal structure. Graphene oxide is characterized by the presence of a hexagonal lattice structure.

The graphene oxide shows a wide diffraction that is at $2\theta = 10.8^{o}$. When oxygen-functional groups and water molecules are incorporated into the carbon layer structure, the graphene oxide has a greater distance between its fields. This is owing to the fact that graphene oxide contains water molecules. The fact that the minor peaks may still be seen at $2\theta = 20.1°$, and 26.4° suggests that graphene oxide is not completely associated with oxygen atoms (Ameer et al., 2016).

A set of different peaks for V_2O_5 observe at 2θ values of 20.3^{o}, 26.1^{o}, 31.07^{o}, and 34.30^{o} which correspond to the characteristic diffraction of (001), (110), (301), (310) lattice planes of

orthorhombic V_2O_5. The Sharp and strong peaks of V_2O_5 reveal a high degree of Crystallinity (Jing et al., 2020).

The XRD of g-C_3N_4/GO contributed to the peaks corresponding to g-C_3N_4 and GO that verify the successful synthesis of hybrid nano-composite material (Long et al.,2017). The distinctive peaks of g-C_3N_4 gradually grow weaker in the g-C_3N_4/V_2O_5 composited samples, while the peak intensities of V_2O_5 also become noticeable. As seen in Figure 4.5, the development of GO, V_2O_5, and g-C_3N_4 associated diffraction peaks in the g-C_3N_4/GO/V_2O_5 nanocomposites suggests that nanocomposites suggest that nanocomposites were successfully formed.

Debye-formula Scherr's was employed to determine the average particle size.

$$d = 0.9\lambda/\beta \cos \theta$$

Where d is crystalline size, λ is X-ray wavelength, β is FWHM of the diffraction peak, and θ is diffraction angle. The crystalline size of g-C_3N_4, g-C_3N_4/GO, g-C_3N_4/V_2O_5, and g-C_3N_4/GO/V_2O_5 were 44, 44.05, 44.35, and 44.43 nm for all nanocomposite material.

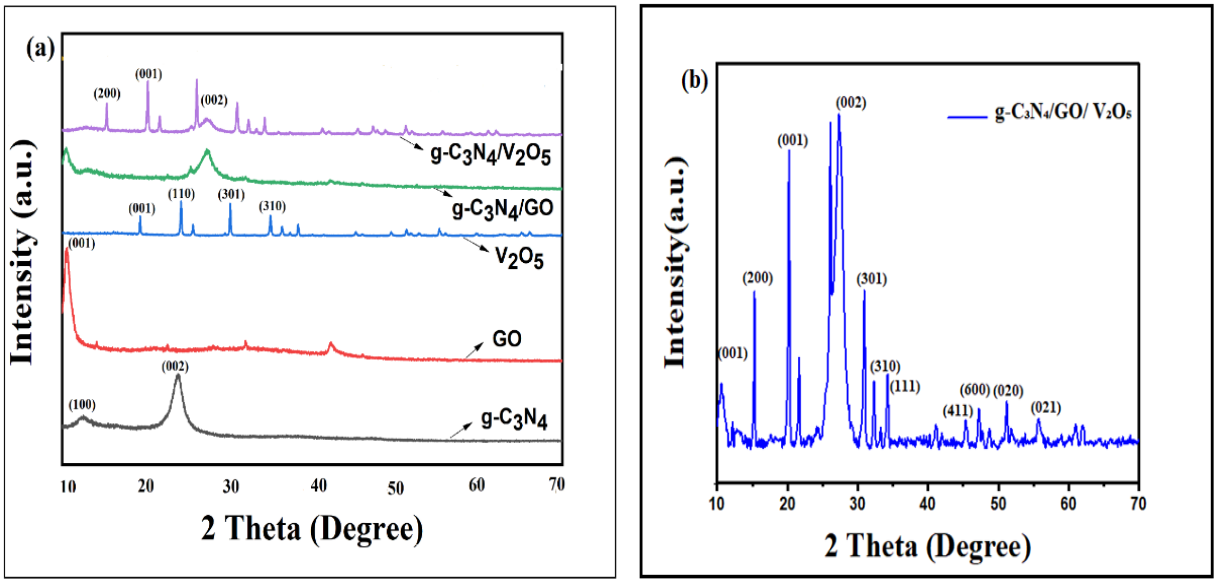

Figure: 4.1 XRD pattern of (a) g-C_3N_4, GO, g-C_3N_4/GO, V_2O_5, g-C_3N_4/V_2O_5, and (b) g-C_3N_4/GO/ V_2O_5 nanocomposite

ii) FT-IR analysis

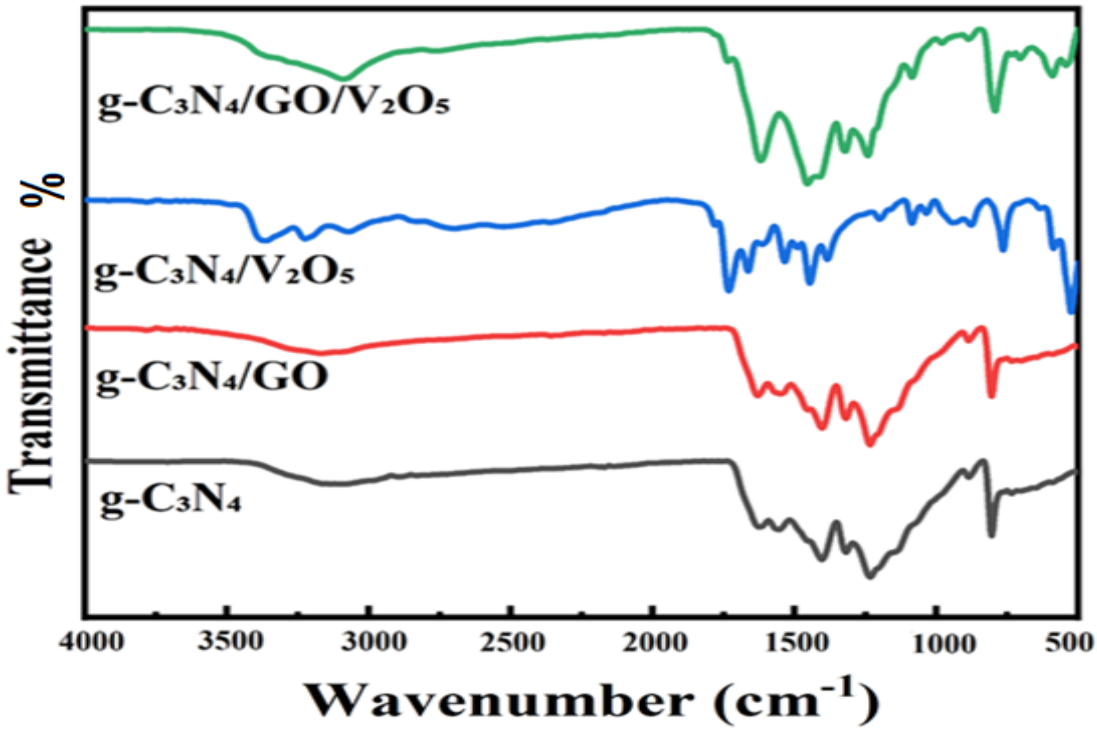

Figure 4.2 FTIR pattern of g-C_3N_4, g-C_3N_4/GO, g-C_3N_4/V_2O_5, and g-C_3N_4/GO/ V_2O_5 nanocomposite.

The FT-IR spectra further established the chemical composition and structural interactions between these components. Figure 4.2 shows the FT-IR spectra of all photocatalyst compounds.

Peaks at 1200-1650 cm^{-1} in pure graphitic carbon nitride might be attributed to heterocycle C-N and C=N stretching modes (Wang et al., 2016; Long., 2017). Furthermore, the sharp and dominant peak at 804 $^{-1}$ is attributable to the tri-s-triazine unit breathing mode, showing that triazine units exist in the backbone of g-C_3N_4. Whereas, the peak at 3430 cm^{-1} is due to N-H stretching vibration (amino group).

The FT-IR spectra of GO reveal peaks 1060, 1403, and 1728 cm^{-1}, representing stretching vibration of (C-O), bending vibration of (C-OH), and carbonyl (C=O) functional groups. V_2O_5 sample has two distinctive absorption bands at 824 am^{-1} and 1014 cm^{-1}. The V-O-V bonds asymmetric stretching modes are responsible for the bands at 586 cm^{-1} and 824 cm^{-1}, whereas the V=O bonds stretching vibration is responsible for the peak at 1014 cm^{-1}.

Table 4.1 FT-IR Frequency Assignments of Nanocomposite

Type	**Vibration mode**	**Frequency in cm^{-1}**	
		Observed	**Reported**
	C-N, C=N stretching modes	1200-1650 cm^{-1}	1240-1640 cm^{-1}
	Bending vibration tri-s-triazine unit	804^{-1}	815cm^{-1}
Amino group	N-H stretching vibration	3430 cm^{-1}	3000-3500cm^{-1}
	-OH bending and Stretching	3200-3500 cm^{-1}	3000-3500cm^{-1}
	Stretching vibration of C-O	1060cm^{-1}	1039-1060 cm^{-1}
	Bending vibration of C-OH	1403cm^{-1}	1220-1420 cm^{-1}
Carbonyl	Carbonyl (C=O) functional groups	1728 cm^{-1},	1500-1800 cm^{-1}
	V–O stretching vibration	1014 cm^{-1}	1008-1022 cm^{-1}
	Stretching modes of the oxygen shared by three vanadium atoms	586 cm^{-1}	504-590 cm^{-1}
	V=O bonds stretching	824 cm^{-1}	825 cm^{-1}

iii) Scanning Electron Microscopy

The morphologies of the g-C_3N_4, g-C_3N_4/GO, g-C_3N_4/V_2O_5, and g-C_3N_4/GO/V_2O_5 nanomaterials were studied using scanning electron microscopy. Figure 4.3, illustrates a typical picture of g-C_3N_4, g-C_3N_4/GO, g-C_3N_4/V_2O_5, and g-C_3N_4/GO/V_2O_5 nano material. As shown in the Figure. 4.7 (a), g-C_3N_4 has an irregular plane structure (Wang et al 2017). The SEM image of GO nanomaterial was depicted in the Figure. 4.3 (b), which displayed a monolayer wrinkled 2-D sheet-like morphology due to exfoliation whereas g-C_3N_4 has an irregular structure (Long et al 2017). After introducing the V_2O_5, the g-C_3N_4/V_2O_5 composites samples showed some agglomeration of nanocomposite on the surface of g-C_3N_4. Furthermore, the elemental mapping study is in the Figure 4.4, reveals that the C, N, and V elements are distributed uniformly in g-C_3N_4/GO/V_2O_5.

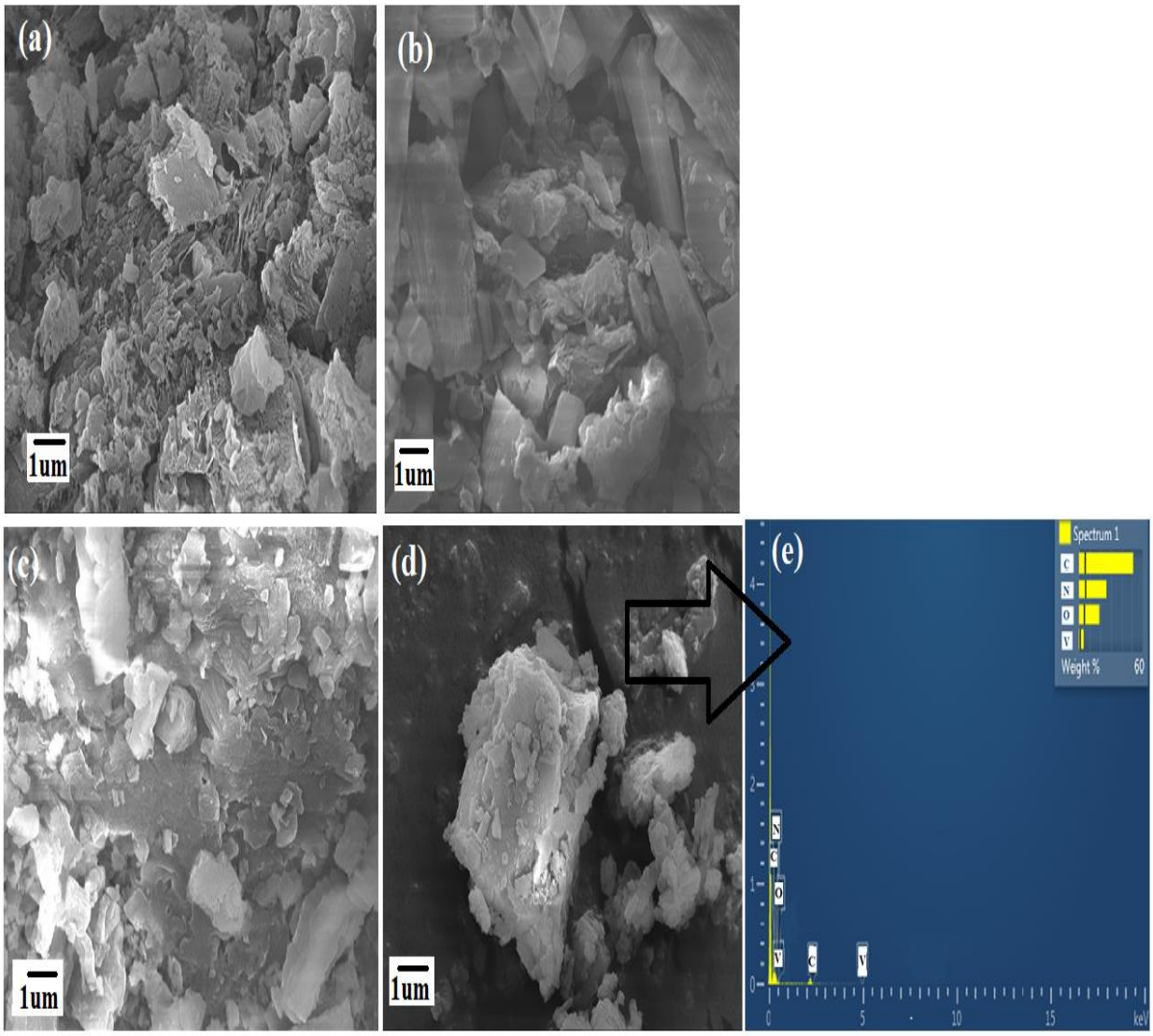

Figure.4.3 FESEM (a) g-C_3N_4 (b) g-C_3N_4/GO (c) g-C_3N_4/V_2O_5 (d) g-C_3N_4/GO/ V_2O_5 (e) EDS spectrum of the g-C_3N_4/GO/V_2O_5 nanocomposite

iv) Thermogravimetric Analysis

The Thermogravimetric Analysis was determined for the nanomaterials that were synthesized using the combustion process. In thermogravimetric analysis, the mass of a specific material was measured as a temperature function by heating the sample at a constant rate. In order to carry out this study, the sample was heated at a rate of 10 degrees Celsius per minute. Figure 4.5 depicts the variance in the sample's loss of weight as a function of temperature over the course of the

experiment. The image depicts a weight reduction transition that occurs in two stages for g-C_3N_4, g-C_3N_4/GO, g-C_3N_4/V_2O_5, and for g-C_3N_4/GO/V_2O_5 major degradation occurs at the temperature

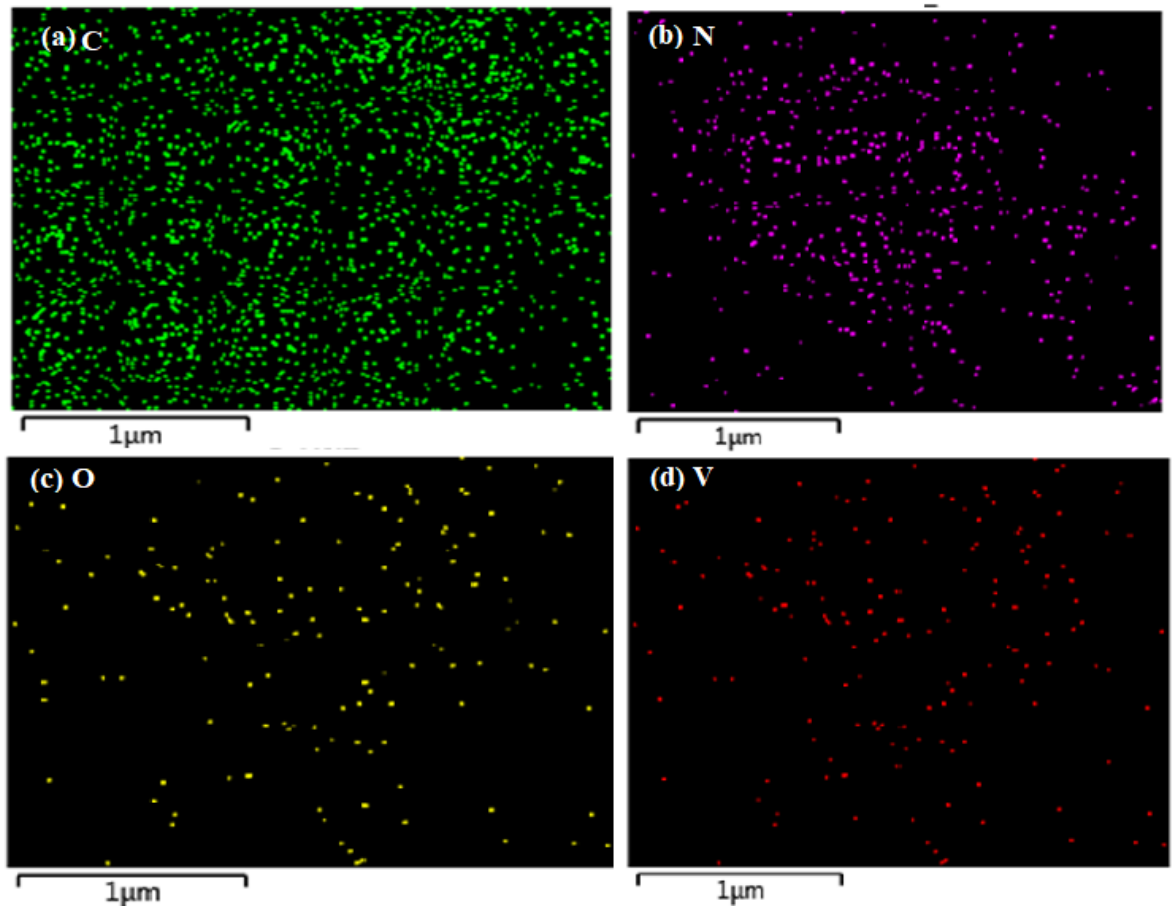

Figure.4.4. Elemental mapping images of g-C_3N_4/GO/ V_2O_5 nanocomposite (a) carbon (b) nitrogen (c) oxygen (d) vanadium

range 300-580 ºC. According to the Thermogravimetric Analysis curve, the initial weight loss was between 6 and 9 % and occurred at temperatures lower than 500 degrees Celsius. This was caused by the evaporation of water molecules contained inside the crystal lattice of the particles. Around 500 degrees Celsius, pure g-C_3N_4 is relatively stable, but above that temperature, it begins to decompose completely. When VO is loaded onto g-C_3N_4, the thermal stability of the compound experiences a considerable drop. The V_2O_5 molecule acts as a catalyst that can absorb and activate O_2 in the air, which subsequently oxidizes the g-C_3N_4 compound at a relatively low temperature (Long et al 2017). The bulk of the weight loss in graphitic carbon nitride-based materials is due to the thermal breakdown of g-C_3N_4, while the remaining residue is due to the concentration of V_2O_5.

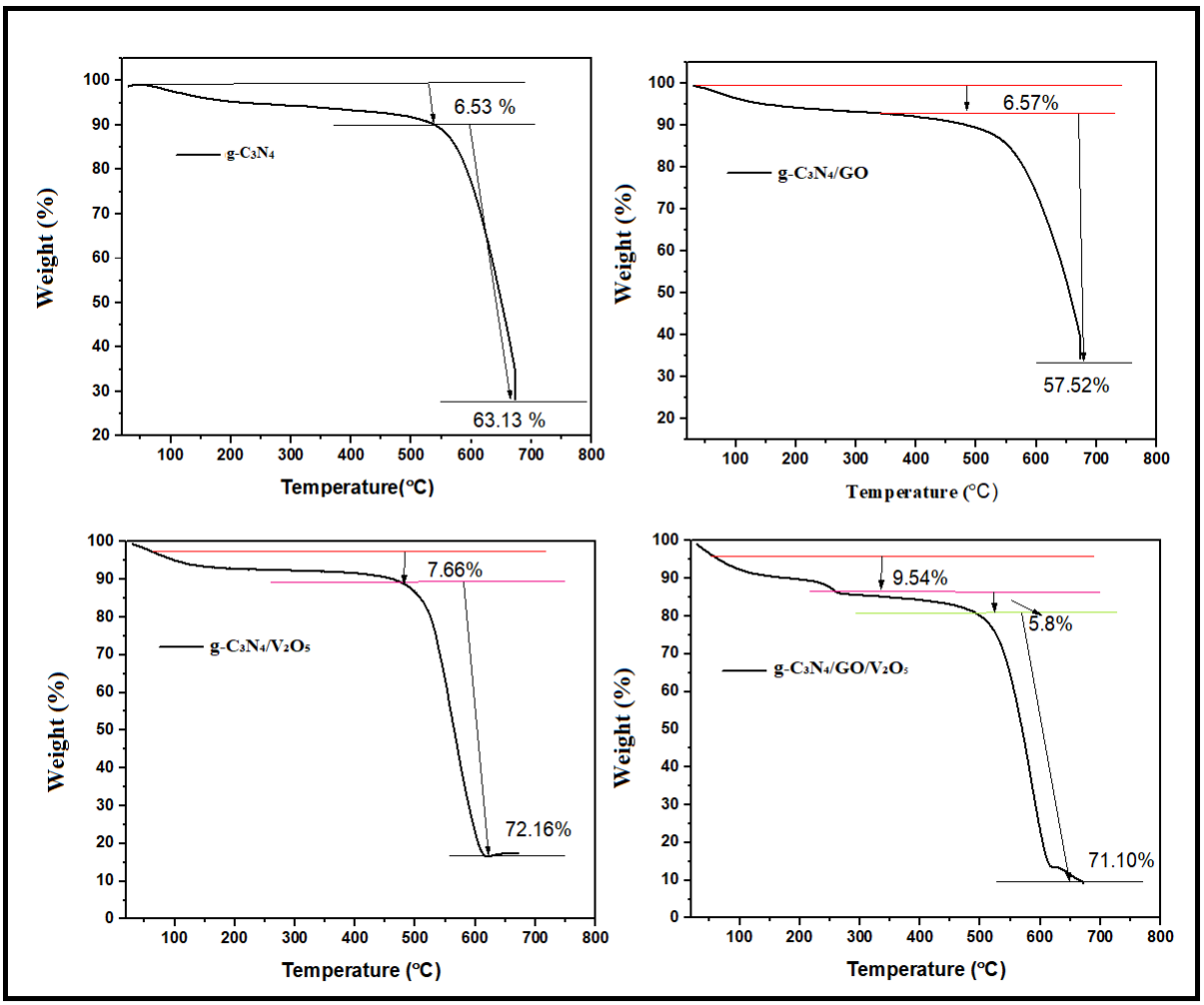

Figure 4.5 Thermogravimetric Analysis curves of g-C_3N_4, g-C_3N_4/GO, g-C_3N_4/V_2O_5, g-C_3N_4/GO/ V_2O_5

v) UV-Visible spectroscopic analysis

The results of investigations using UV-DRS spectroscopy to examine the optical properties of the as-obtained materials are presented in Figure 4.6. The photoexcitation of an electron causes it to move from the VB of the N^2p orbital to the CB of the C^2p orbital, which can be seen as photo-absorption around 440 nm in the visible-light region at the absorption edge of graphitic carbon nitride. This is due to the fact that photoexcitation occurs in the visible-light region. In contrast, the photo-absorption band edge of g-C_3N_4/GO may be observed in the visible-light region at a wavelength of around 448 nm. This is because the appropriate electron transition occurs during n-π^*. Whereas the adsorption edge for g-C_3N_4/GO/V_2O_5 nanocomposite was observed to be shifted

toward the higher wavelength side, even pure graphitic Carbon has an absorption edge at 440 nm. Because of these repercussions, it is possible to deduce that the g-C_3N_4/GO/V_2O_5 has advanced visible-light activity than as-synthesized pure g-C_3N_4, g-C_3N_4/GO, g-C_3N_4/V_2O_5 respectively.

The resultant optical bandgap of g-C_3N_4, g-C_3N_4/GO, g-C_3N_4/V_2O_5, and the g-C_3N_4/GO/V_2O_5 nanocomposite was estimated by means of a Tauc plot using Kubelka-Munk function; the founded value is 2.7, 2.59, and 2,2 eV respectively. This is illustrated in Figure 4.7. the g-C_3N_4/GO/V_2O_5 composite has a computed bandgap value that is smaller than that of g-C_3N_4, g-C_3N_4/GO, and g-C_3N_4/V_2O_5 nanocomposite. These findings indicate that the addition of GO/V_2O_5 to the g-C_3N_4 composite altered the electronic band structure of the graphitic material, allowing it to absorb visible light. It further specifies that the enhancement of photoexcited e-/h+ charge carriers increases light utilization efficiency, resulting in a high level of responsive photocatalytic activity when exposed to visible light. This was achieved as a result of the upgrading of photoexcited e^- /h^+ charge carriers. In addition, the capability of GO and V_2O_5 to intercept light because of their low band gap energy is a critical component of greater photo-absorption process.

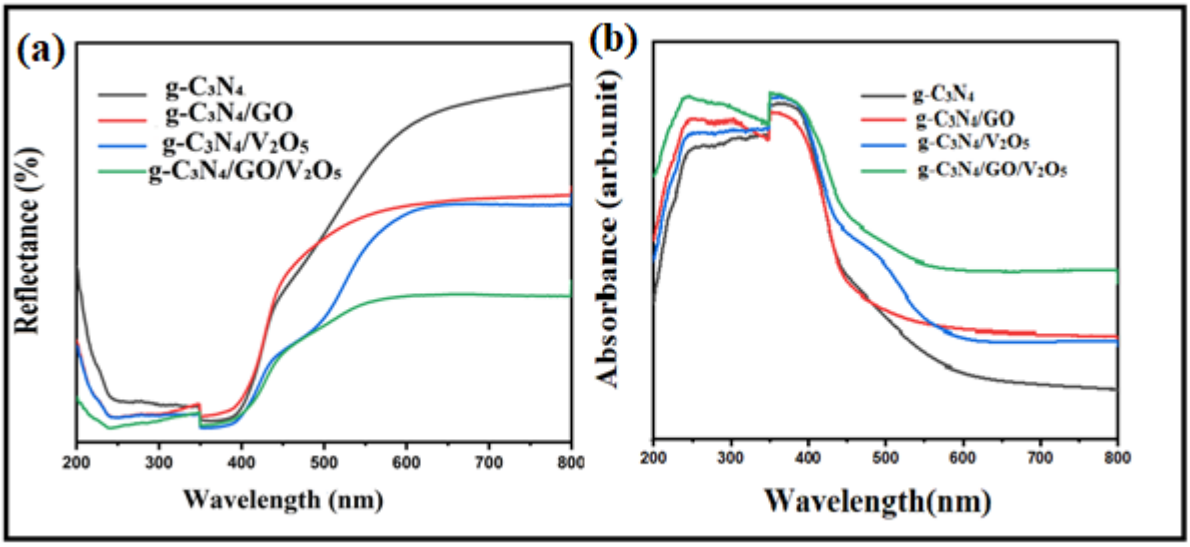

Figure 4.6 UV-DRS absorption and reflectance spectra of g-C_3N_4, g-C_3N_4/GO, g-C_3N_4/V_2O_5, g-C_3N_4/GO/V_5

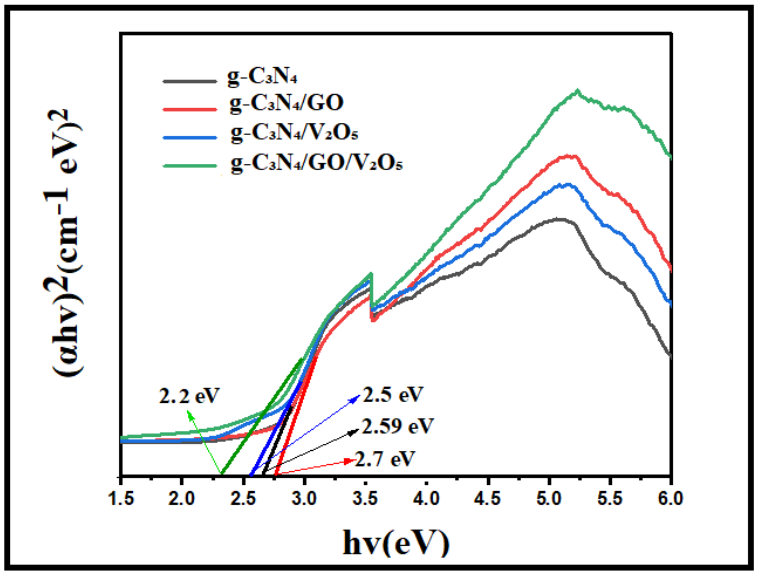

Figure 4.7 Calculated band gap of nanocomposites

4.1.3.2 Photocatalytic activity towards photodegradation of Chlorpyrifos

i) Effect of pH

The effects of pH on the photocatalysis of chlorpyrifos by all nanocomposite materials when exposed to visible light are shown in Figure.4.8(a). For all photocatalysts, the efficacy of Chlorpyrifos removal increased with increasing pH in the acidic pH range of 2 to 4 but declined as pH increased from 4 to 10. The optimal pH was determined to be 4.0, which is somewhat acidic, with highest Chlorpyrifos removal efficiencies of 67.47, 80.21, 70.45, and 88.97% with g-C_3N_4, g-C_3N_4/GO, and g-C_3N_4/GO/V_2O_5, respectively, in the visible area. The elimination of Chlorpyrifos is largely accomplished by the photocatalyst's surface charge. All photocatalyst surfaces become mostly positively charged at an acidic pH (pH 4), which causes them to repel cationic moiety electrostatically. All photocatalyst surfaces become negatively charged at alkaline pH (pH > 7.5) where electrostatic repulsion toward anionic substances is dominant (Wang et al., 2017; Long et al., 2017). The Chlorpyrifos removal was maximized with the g-C_3N_4/GO/V_2O_5 nanocomposite. It's also likely that OH^-/H_2O and localized holes engaged in an electron transfer reaction, producing a large number of hydroxyl radicals that accelerated the breakdown of Chlorpyrifos in the presence of visible light.

ii) Effect of contact time

Figure 4.8(b), depicts the effect of contact (irradiation) time, the elimination efficiency increased with irradiation time. Figure 4.8 (b), shows that increasing the irradiation time interval from 20 to 120 minutes increased the percentage of degradation from 24.52 to 88.97 % for as-synthesized nanocomposite. This may be ascribed to the fact that as the irradiation period rises, the Chlorpyrifos molecules have more time to react with the catalyst's surface and create hydroxyl radicals, which speeds up the photocatalytic process and so raises the percentage of degradation.

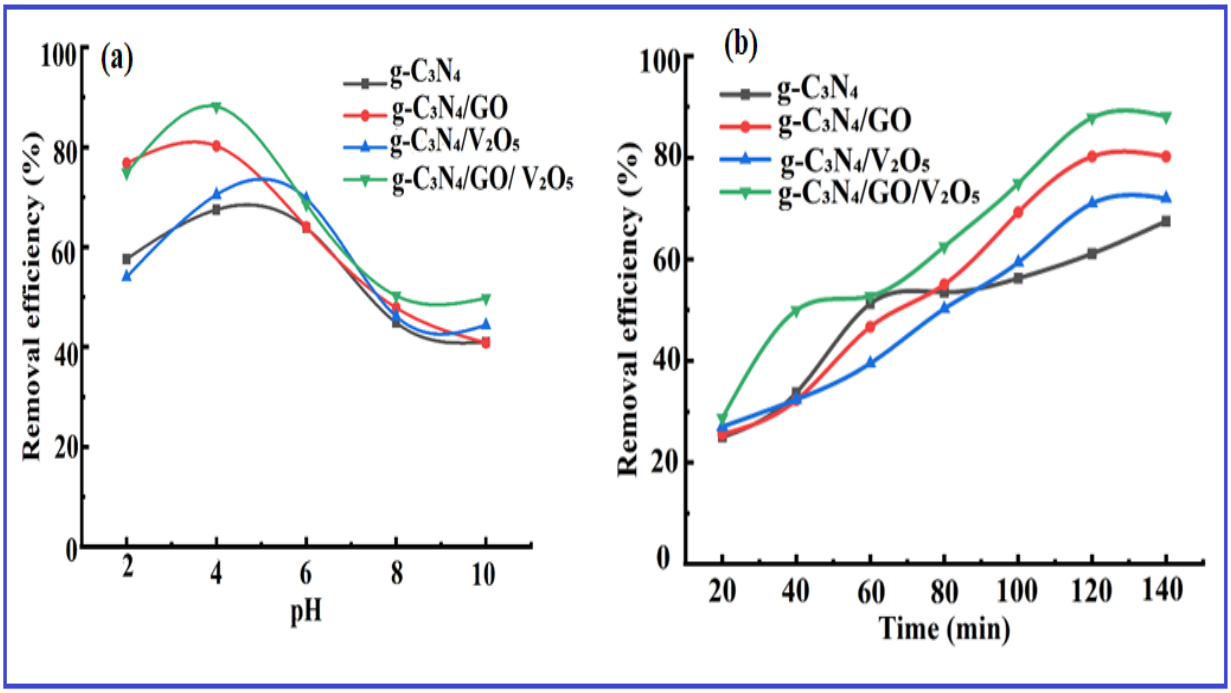

Figure 4.8 Photocatalytic degradation of Chlorpyrifos pesticide (a) at different pH (b) effect of time on degradation

iii) H_2O_2 effect

H_2O_2 can produce more OH^- radicals, improving photocatalytic removal and producing colorful intermediates. The effect of H_2O_2 on the photocatalytic elimination of Chlorpyrifos by g-C_3N_4 is seen in Figure 4.9 (a), where H_2O_2 was raised from 0.01 to 1 %. In the absence of H_2O_2 photodegradation, the efficiency was 88%. Nonetheless, increasing the H_2O_2 concentration from 0.01 to 0.1% enhanced the photocatalytic elimination of Chlorpyrifos from 88 to 90.5 %. However, as the H_2O_2 concentration was raised even higher to 1%, the removal rate fell to 76.1%. This

decrease in removal efficiency was considered to be caused by an increase in H_2O_2 acting as an inhibitor when combined with hydroxyl radicals. The coupled e/h^+ can be stabilized by trapping photoinduced e^- in H_2O_2. The reaction between H_2O_2 and e^- or O_2 can produce the $^{\bullet}OH$, radicals. Therefore, it was anticipated that adding H_2O_2 to the photocatalytic reaction system would improve the elimination of Chlorpyrifos.

iv) Effect of photo-catalyst dose

The effect of photocatalyst dose on nanocomposite's photocatalytic activities is represented in Figure 4.9(b). The quantities of the g-C_3N_4, g-C_3N_4/GO, g-C_3N_4/V_2O_5, and g-C_3N_4/GO/V_2O_5 nanocomposites ranged from 0.1 to 0.5 g/l in 100 ml of Chlorpyrifos solution with 0.1% H_2O_2 and 100 w intensity at pH 4.0 for up to 2 hours to identify the best photocatalytic dosage. The photocatalytic elimination efficiency of Chlorpyrifos rose from 27.1 to 90.5% as the photocatalyst dose was raised from 0.1 to 0.3 g/l Figure 4.9 (b). However, the elimination efficiency was not affected by an increased dose beyond 0.3 g/l. This finding indicates that the addition of a huge quantity of photocatalytic nanocomposite reduced light penetration due to the increased suspension of photocatalysts (Zhang et al., 2017; Yu et al., 2018).

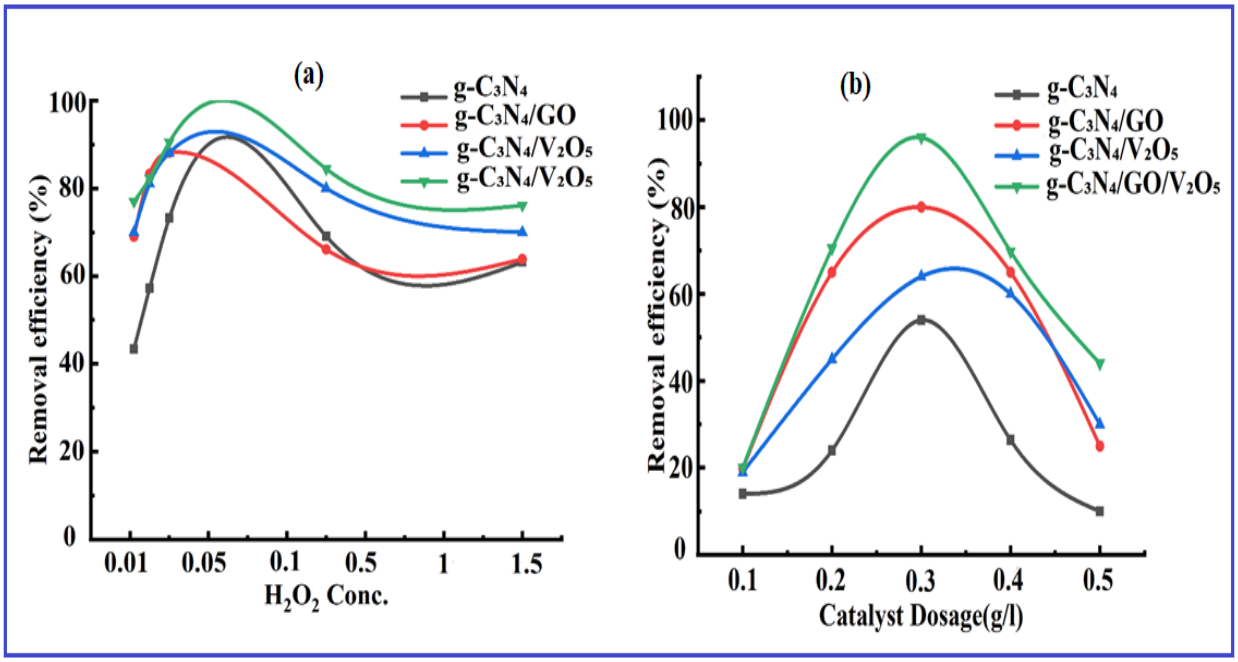

Figure.4.9. Photocatalytic degradation of Chlorpyrifos pesticide (a) at the addition of various H_2O_2 concentrations on photocatalytic degradation (b) effect of photocatalyst dose on degradation

v) Photocatalyst regeneration

The synthesized nanocomposite material must be recycled for 'n' cycles to boost the catalyst's viability from an economic standpoint. The utilized photocatalyst was treated with 0.1 g/10 ml of a H_2O_2 solution for regeneration with stirring for one hour. The efficiency of Chlorpyrifos removal peaked at 49.5% in the fifth cycle and then gradually decreased as regeneration cycles increased until the fifth cycle. The H_2O_2 treatment, which also serves as a novel photocatalyst, can liberate the molecules, by oxidizing surface-trapped molecules to H_2O_2 and CO_2 while providing free active sites and a negatively charged surface.

vi) Degradation mechanism:

When exposed to light, O, O-ethyl O-3,5,6-trihydroxypyridin-2-yl phosphonothioate can be generated by the oxidation of Chlorpyrifos by OH attack. The product is then dealkylated, which involves the release of $-C_2H_5$ and $-OC_2H_5$, followed by the oxidation of the P=S to P=O group to yield ethyl O-3,5,6-trihydroxyridin-2-yl O-hydrogen phosphonothioate and 3,5,6-trihydroxypridin-2-yl hydrogen phosphate. By cleaving the C-O bond, this compound can degrade into pyridine-2,3,5-triol (Zhang et al., 2015; Sivakumar et al., 2019). Following ring oxidation, two minor products, 3,4,4-trihydroxybut-3-en-2-one and (z)-3-amino-2,3-dihydroxyacylaldehyde, will be generated (Fadaei et al., 2013). These substances could eventually mineralize into H_2O and CO_2. The other possibility is that when diethythiophosphate is lost, Chlorpyrifos will transform into (z)-3-amino-2,3-dichloroacrylaldehyde via an intermediate called 4,5,6-trichloropyridin-2-ol (Sivakumar et al., 2019; Fadaei et al., 2013) as shown in Figure 4.10.

Vii) **Adsorption study**

The degradation of Chlorpyrifos and Carbofuran pesticide was carried out in the dark in order to evaluate the adsorption capacity of pure g-C_3N_4 and other doped nanomaterials. When compared to the pure g-C_3N_4 nanocomposite, the level of Chlorpyrifos and Carbofuran degradation achieved by the ternary nanocomposite i.e. g-C_3N_4/GO/V_2O_5 Catalyst was much higher. This is because ternary nanocomposite has a large surface area, which correlates to a great adsorption ability. The explanation for this may be found in the word "adsorption." In addition, the increased capacity for adsorption can be linked to the amounts of doped material present in the ternary nanocomposite.

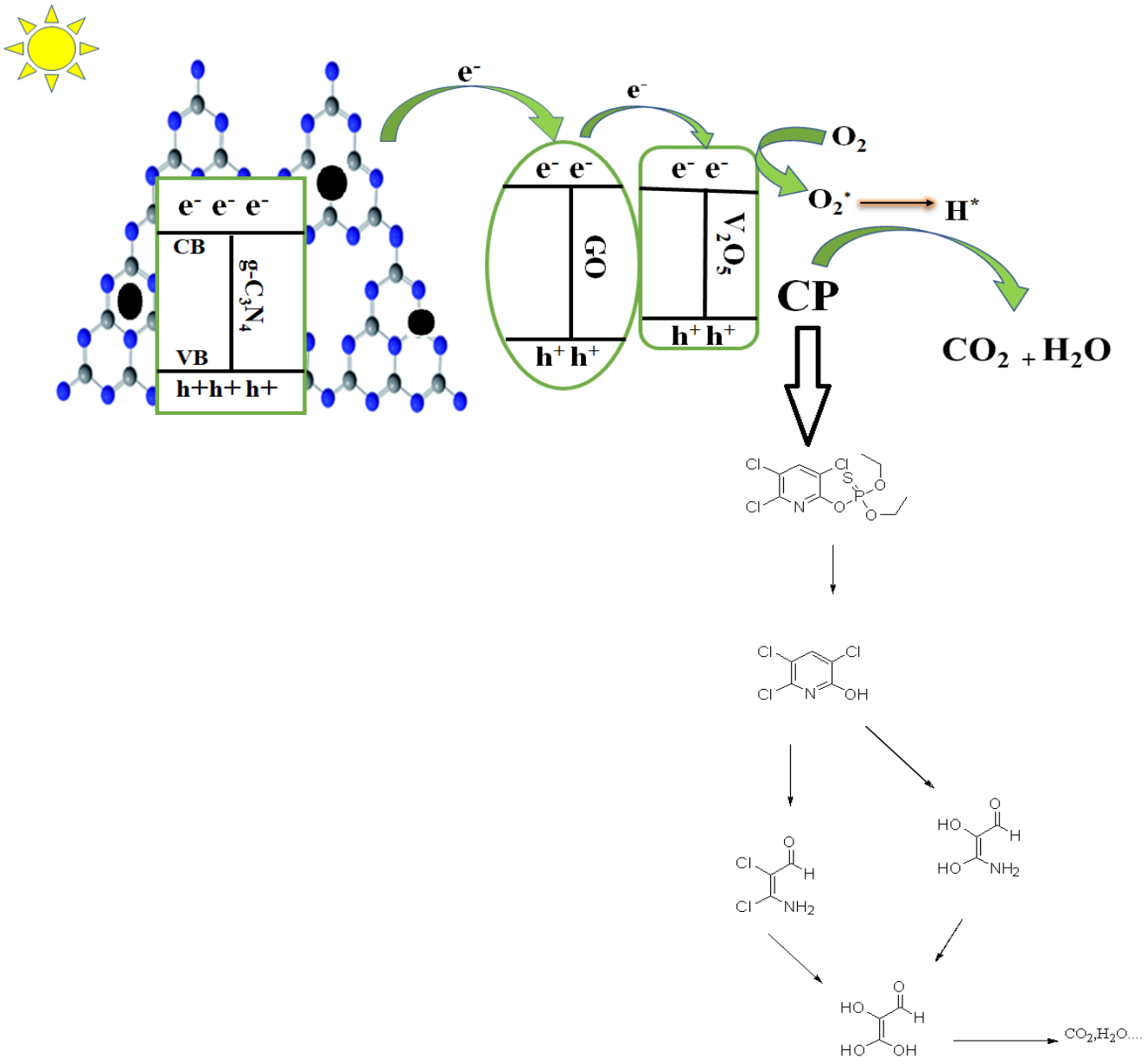

Figure 4.10 Proposed degradation pathway of Chlorpyrifos using g-C_3N_4/GO/V_2O_5 nanocomposite

4.1.3.3 Photocatalysis Study of the Carbofuran

i) Effect of pH

The findings of a research study are depicted in Figure 4.11(a), which shows the influence of pH on the photodegradation of Carbofuran by all photocatalyst materials when the substances were exposed to visible light. The efficiency of Carbofuran removal increased with an increasing pH range of 6.0 to 7.0 but reduced as the pH was elevated further from 7.0 to 9.0. This phenomenon was observed across all photocatalysts. The ideal pH value, which was found to be 7.0, was found to have maximum Carbofuran removal efficiencies of 57.62, 71.12, 70.12, and 83.75% with g-C_3N_4, g-C_3N_4/GO, g-C_3N_4/V_2O_5, and g-C_3N_4/GO/V_2O_5 photocatalytic material, respectively. The surface charge contributes significantly to the removal of Carbofuran from the environment. When exposed to a pH 7, the surfaces of all photocatalysts become predominantly positively charged, which leads them to electrostatically rebuff cationic moiety. When the pH of the environment is alkaline (more than 7.5), the electrostatic repulsion towards anionic compounds is predominant. This causes all photocatalyst surfaces to become negatively charged. Using the g-C_3N_4/GO/V_2O_5 nanocomposite resulted in the greatest amount of Carbofuran being removed. It is also possible that OH^-/H_2O and holes participated in an electron transfer reaction, which resulted in the production of a high number of hydroxyl radicals that speed up the decomposition of Carbofuran when it was exposed to visible light.

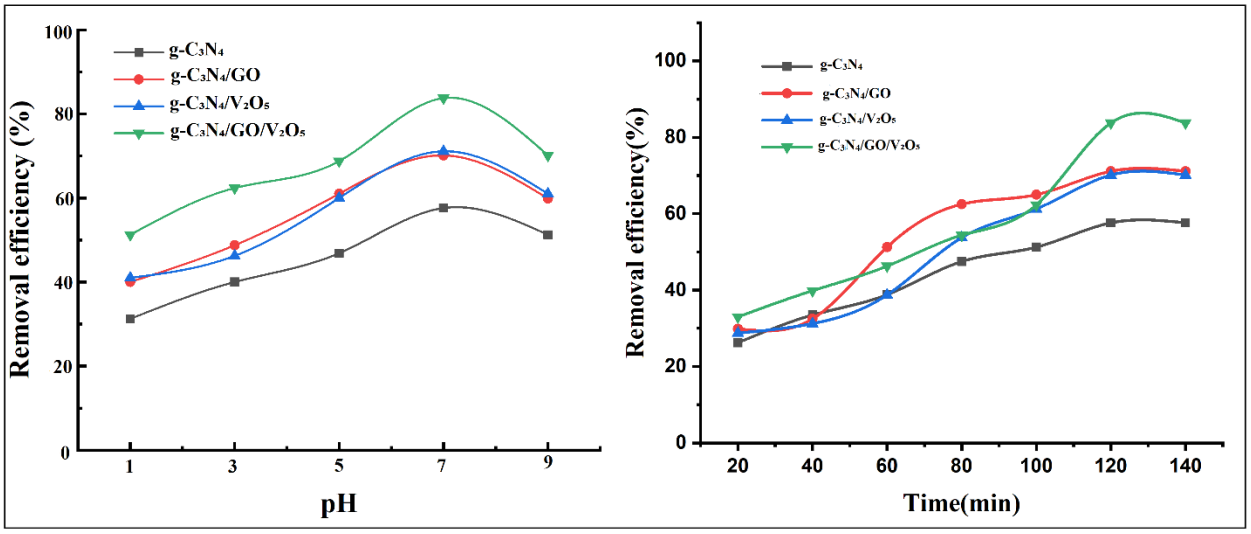

Figure 4.11 Photocatalytic degradation of Carbofuran pesticide (a) at different pH (b) effect of time on degradation

ii) Irradiation time

The effect of contact (irradiation) time is shown in Figure 4.11(b), elimination efficiency rose as the irradiation time increased. As can be seen in Figure 4.11(b), extending the irradiation time interval from 20 minutes to 120 minutes resulted in an increase in the percentage of degradation from 26.25 to 83.75% for the nanocomposite that had just been manufactured. This may be attributed to the fact that as the irradiation period increases, the Carbofuran molecules have more time to react with the catalyst and create hydroxyl radicals. This speed up the photocatalytic process, which in turn raises the percentage of Carbofuran that has been degraded.

iii) H_2O_2 effect

The formation of additional OH radicals by H_2O_2 can enhance photocatalytic elimination and result in the formation of intermediates. Figure 4.12(a) depicts the effect of increasing the concentration of H_2O_2 on the photocatalytic removal of Carbofuran by g-C_3N_4. The amount of H_2O_2 was increased from 0.01% to 1%. The effectiveness was 83.75% when there was no photodegradation of H_2O_2 present. The photocatalytic elimination of Carbofuran was improved from 83.75% to 92.6% when the concentration of H_2O_2 was raised from 0.01% to 0.1%. However, when the concentration of H_2O_2 was increased even further, all the way up to 1%, the clearance rate dropped to 73.8%. It was hypothesized that a rise in the proportion of H_2O_2 that acted as an inhibitor when paired with hydroxyl radicals was the root cause of this decline in removal efficiency. It is possible to maintain the stability of the linked e/h^+ by entrapping the photoinduced e^- in H_2O_2. The production of $^{\cdot}OH$, radicals are possible by the interaction of H_2O_2 with e^- or O_2. As a result, it was hypothesized that by including H_2O_2 in the photocatalytic reaction, the system would result in an increase in the amount of Carbofuran that was removed.

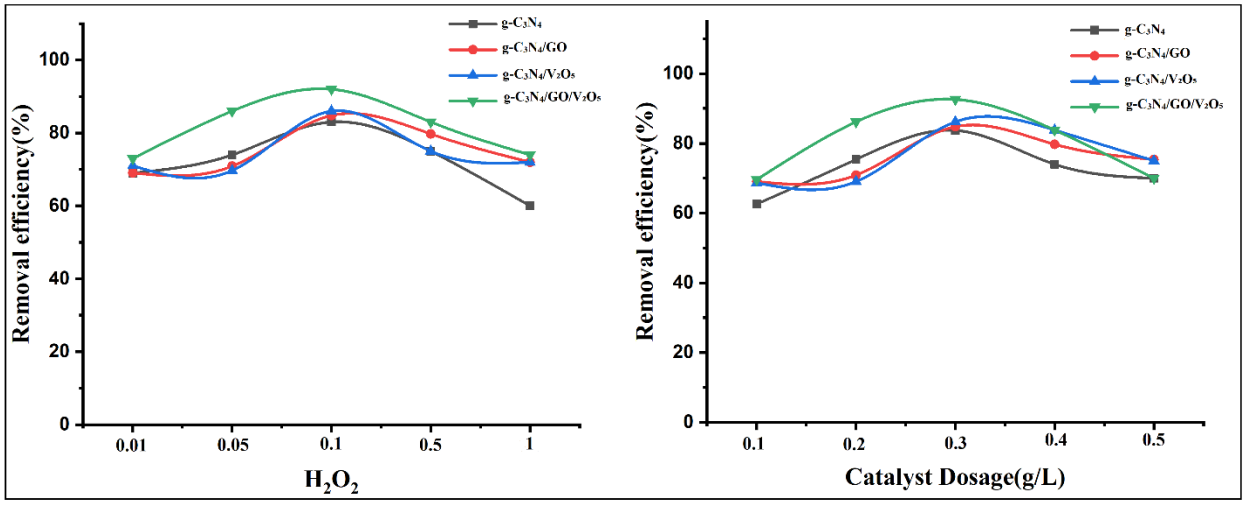

Figure 4.12 Photocatalytic degradation of Carbofuran pesticide (a) effect of H_2O_2 (b) effect of photocatalytic dose on degradation

iv) Catalytic Dose

In order to identify the best photocatalytic dose, 0.1 to 0.5 g/l of g-C_3N_4, g-C_3N_4/GO, g-C_3N_4/V_2O_5, and g-C_3N_4/GO/V_2O_5 nanocomposites were added to 100 ml of Carbofuran solution with 0.1% H_2O_2 and 100 w intensity at pH 7.0 for up to 2 hours. The Carbofuran photocatalytic removal effectiveness rose from 69% to 92.6% when the photocatalyst dosage was raised from 0.1 to 0.3 g/l. Nevertheless, exceeding 0.3 g/l had no influence on the efficacy of the elimination process. This data suggests that the inclusion of a large quantity of photocatalytic nanocomposite reduced the amount of light penetration as a result of the higher suspension of photocatalysts (as shown in Figure 4.12).

v) **Desorption/regeneration studies**

Experiments on desorption were carried out in order to ascertain whether or not photocatalyst regeneration is even possible. As a desorbing agent, 0.1 M HCL was utilized for the purpose of conducting research on the desorption of contaminants from the surface of the nanocomposite. In a nutshell, 0.1 g of used nanocomposite material was added to each separate pollutant solution while the pH was maintained at 4, and the mixture was agitated for a total of 2 hours.

After that, the pollutant-loaded adsorbent was centrifuged to separate it from the pollutants, and the residual concentration was measured.

Following the adsorption being carefully cleaned with DI water to remove any adsorbed molecules that may have been present on the surface of the adsorbent, it was then air dried so that it could be used in subsequent cycles. The equation allowed for the determination of desorption efficiency.

$$D\% = \left(\frac{q1,desorption}{q2,adsorption}\right) \times 100$$

Vi) Conclusions

A simple and affordable hydrothermal approach was strategically followed to synthesize a g-C_3N_4/GO/V_2O_5 nanocomposite. Because of improved charge separation and transport mechanism, the ternary g-C_3N_4/GO/V_2O_5 photocatalyst outperformed the g-C_3N_4, binary g-C_3N_4/GO, and g-C_3N_4/V_2O_5 photocatalysts. The chlorpyrifos removal efficiency was 67.47, 80.21, and 88.97% using g-C_3N_4, g-C_3N_4/GO, g-C_3N_4/V_2O_5, and g-C_3N_4/GO/V_2O_5. By using H_2O_2 concentration the elimination efficiency reached 90.5% with g-C_3N_4/GO/V_2O_5. According to the finding, alkaline pH removal effectiveness was lower than acidic pH removal efficiency. Increasing the catalyst dosage to 0.3g/l resulted in the highest improvement in Chlorpyrifos degradation. Moreover, due to the right quantity of H_2O_2, the g-C_3N_4/GO/V_2O_5 photocatalyst maintained its degrading efficacy at five regeneration cycles. And the photocatalytic removal efficiency of Carbofuran increased from 69% to 92.6% by using 0.1% H_2O_2.

Section-II

4.2 Prolific Fabrication of Lanthanum Oxide with Graphitic Carbon/Graphene Oxide for Enhancing Photocatalysis Degradation of Carbofuran from Aqueous Solution

Abstract

Due to its small cost and effective performance in regulatory pests in farming fields and gardens, Carbofuran insecticide is one of the most widely used Carbamate pesticides. Pesticides in the aquatic environment cause a wide range of issues for both humans and ecosystems. The purpose of this research is to investigate the photocatalytic detoxification of carbamate in wastewater using g-C_3N_4/GO/La_2O_3 nanoparticles. The g-C_3N_4/GO/La_2O_3 nanocomposite was effectively manufactured using calcination and a hydrothermal method. In addition, the photocatalytic detoxification of carbofuran was studied by adjusting a variety of parameters such as catalyst concentrations, irradiation time, and pH. According to the finding of this study, the photo detoxification efficiency of Carbofuran pesticides increases with increasing illumination time and the photo-catalyzed about 80% of carbofuran and by adding H_2O_2 degradation was 85.6%, respectively. According to this study, Graphitic carbon nitride/GO/La_2O_3 nanocomposite outperformed pure forms of g-C_3N_4, g-C_3N_4/GO, and g-C_3N_4/La_2O_3 in photo catalytically degrading Carbofuran making it a great alternative for wastewater treatment.

4.2.1 Introduction

Concern over environmental pollution, water shortages, and climate change have grown due to rapid industrial activity (Breffle et al., 2013; Pink et al., 2016). Pesticides are widely used to increase agricultural output and eliminate harmful organisms. However, it has been stated that only 15% of pesticides used achieve their intended results, with the remaining harming the environment (Cahill et al 2011). In addition, these chemicals are persistent organic pollutants, which tend to accumulate in biota and/or sediments and remain in aquatic systems for lengthy periods. They have the potential to spread over large areas and, even at low concentrations, they are hazardous to the environment, as well as to people and other kinds of life (Katsikantami et al., 2019; Yeganeh et al., 2021). The probable causes of pesticide pollution include their discharge from mining, urban and industrial activity, and water runoff in agricultural fields (Cahill et al., 2011; Varma et al.,

2005). As of the year 2020, approximately more than 50 countries used around 3.5 million tonnes of pesticides to encourage agricultural productivity. Humans are exposed to pesticides in a variety of ways, and because these exposures vary in degree, so do the consequences they have (Wiklund et al., 1987)

These pesticide exposures are responsible for numerous illnesses, including Parkinson's disease, non-Hodgkin lymphoma, and Hodgkin's disease (Luo et al., 2016; Brouwer et al., 2014; Wang et al 2017). Furthermore, the presence of pesticides in drinking and surface water has the potential to cause endocrine disruption and is extremely toxic (Rehana et al., 1995; Salazar-Arredondo et al., 2008).

One of the broad-range pesticides carbofuran (2,3-dihydro-2,2-dimethylbenzofuran-7-yl methylcarbamate, or CBF) is a carbamate and, has been used against foliar pests found in fruits, vegetables, and forest crops (Lu et al., 2018).

Inhibiting acetylcholinesterase, an enzyme that is essential to the health and function of the regulated neurological system, makes carbofuran a candidate for the category of substance known as an endocrine disruptor. In addition to this, carbofuran has a very high mobility in soils and a very high solubility in water (700 mg/l). Carbofuran was found in open water as well as groundwater, according to a number of investigations (Lu et al., 2011).

Therefore, it is of the utmost importance to develop a treatment method that is both successful and reasonably priced in order to remove carbofuran from the aqueous system. It appears that hydrolysis and the breakdown of carbofuran by microbes are the two processes that are most successful in removing carbofuran from aqueous systems. Carbofuran is degraded through these activities, however the process takes a very long period (Lopez-Alvarez et al., 2011).

In comparison to more traditional treatment methods, photocatalytic degradation of hazardous compounds in aqueous media offers a number of distinct benefits (Katsumata et al., 2005; Ollis et al., 1991). It differs from typical oxidation procedures in aqueous media. It differs from typical oxidation procedures in a number of ways, including the full mineralization of the pollutant, the use of near-UV radiation, and the absence of chemical addition. This method has been the subject of a significant amount of research over the past twenty years. According to the findings of these investigations (Legrini et al., 1993; Hoffmann et al., 1995; Augugliaro, 1991), the photocatalytic

degradation of a number of water-soluble chemicals originating from a variety of industries is possible. Despite this, there are no data available on the synthesis of the ternary nanocomposite material g-C_3N_4/GO/La_2O_3 or their photocatalytic degradation of carbofuran.

4.2.2 Synthesis of nanocomposite

In order to produce bulk g-C_3N_4, thiourea was placed in a ceramic crucible, heated to 550 degrees Celsius, and then placed in a muffle furnace. The thermal heating rate was 30 degrees Celsius per minute. After being taken from the muffle furnace and allowed to cool to room temperature, it is then put through a grinding process in an agate mortar to produce a powder.

A modified version of Hummers' approach was used in the synthesis of the GO. After filling a glass beaker with 500 ml of liquid and placing it in an ice bath, the next step was to add 0.5 grams of graphite powder, 23 milliliters of hydrochloric acid, and 30 minutes of agitation at 500 revolutions per minute. After adding (0.5 gm) of $NaNO_3$, the solution was mixed continuously for 60 minutes at a speed of 600 revolutions per minute (rpm). After that, three grams of $KMnO_4$ were gradually added to the mixture while maintaining the temperature of the solution at 150 degrees Celsius. The resulting mixture was stirred for 60 minutes at 600 rpm. The temperature of the solution was gradually raised to 35 $^{\circ}$ C. 50 ml DI water was added to the solution. After that, the temperature was increased to 95 degrees Celsius for a period of thirty minutes, and the mixture was stirred overnight while it was kept at room temperature. In the end, the procedure was terminated by adding 1.5 milliliters of H_2O_2 to 50 milliliters of DI water. This mixture was added to the reaction vessel. After centrifuging the mixture (at 3000 rpm for 7 minutes), it was washed down with 4% weight hydrochloric acid and deionized water in order to remove any metal ions and acid residues. The washing process was repeated multiple times till the solution reached neutral. Repeating this process allowed the pH of the proceeding solution to reach neutral.

In order to synthesize g-C_3N_4/GO, it was dissolved in 100 milliliters of deionized water and the mixture was agitated for one hour. The slurry was transferred into an autoclave, which was then securely sealed before being heated to a temperature of 200 degrees Celsius for a period of twelve hours. Following the heating process, the temperature of the autoclave was lowered to room temperature. The product was gathered by centrifuging it, then cleaned three times with deionized water, and then oven-dried at a temperature of 800 degrees Celsius. For g-C_3N_4 doped La_2O_3 precursor powder ($La(NO_3)_3.6H_2O$ and graphitic carbon nitride with KOH. The solution was

stirred and transferred in Teflon autoclave at 200 º C for 10 h and obtained material calculated at 900 º C for 2 hours.

Graphite carbon nitrite and other doping ingredients were dissolved in DI water with strong stirring and combined for one hour with steady stirring; 0.5 M NaOH was added dropwise until the pH reached 10; and the mixture was cooled to room temperature. Using a digital pH meter, the pH value of the solution was measured. The solution was placed in an autoclave and heated at 200 degrees Celsius for ten hours. The resultant colored material was filtered, washed with double-distilled water and ethyl alcohol, and then dried at 800 degrees Celsius (as shown in Figure 4. 13.

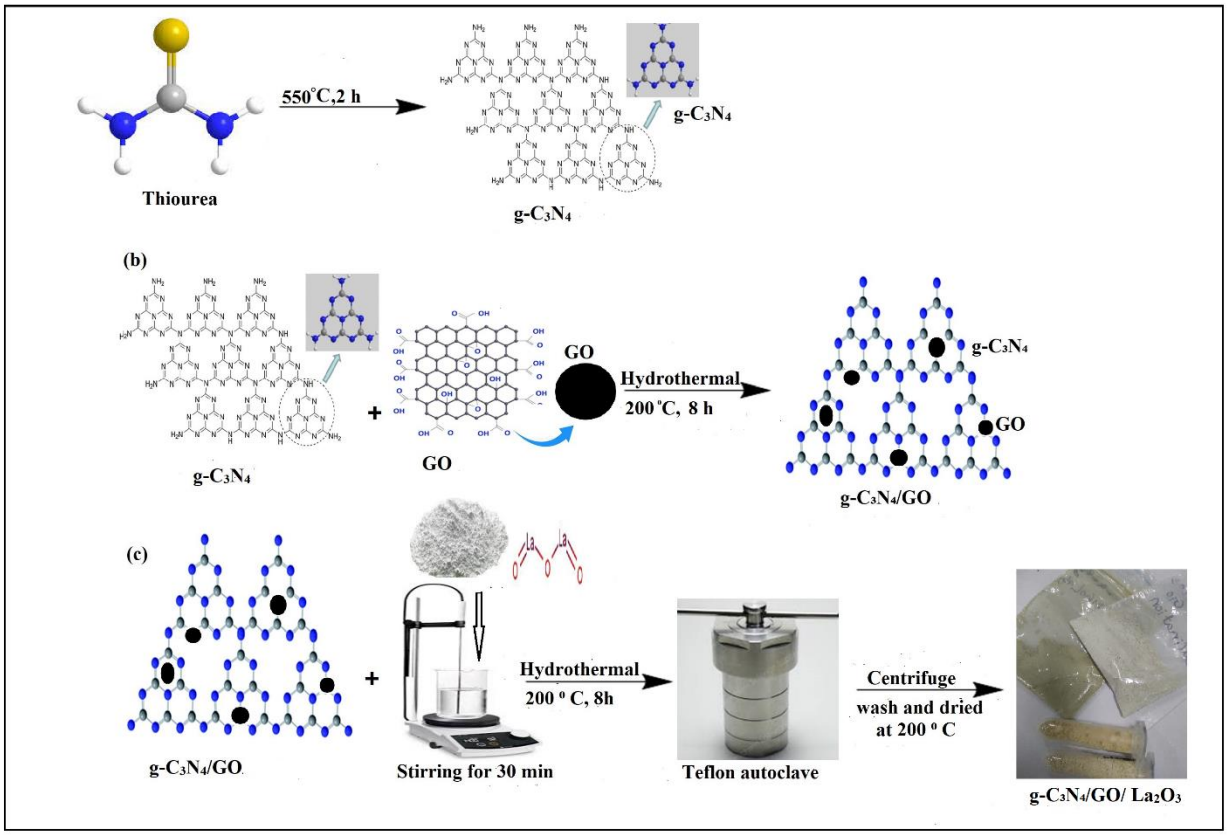

Figure 4.13 Schematic representation of ternary nano-composite

4.2.3 Characterization of nanomaterials

i) X-Ray Diffraction analysis

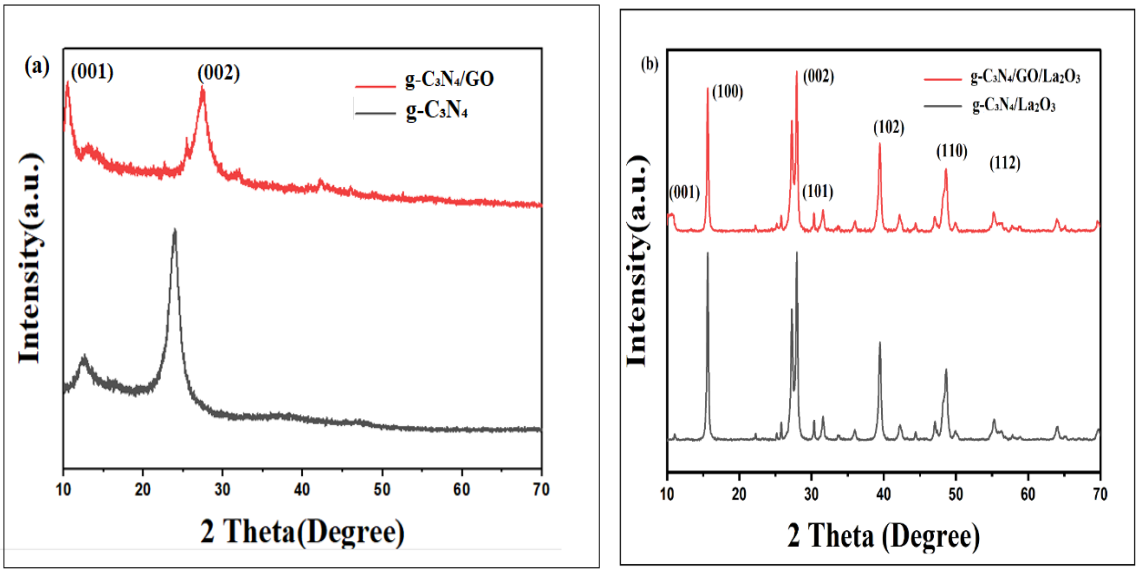

Figure 4.14. XRD pattern of (a) g-C_3N_4, g-C_3N_4/GO, (b) g-C_3N_4/La_2O_3, g-C_3N_4/GO/La_2O_3 nanocomposite

The presence of amorphous carbon in GO is denoted by the presence of a broader diffraction peak located at 2θ= 11.40. The reflection plane of graphitic carbon was thought to be responsible for the broad and weak characteristics peak at 2θ=26.4°. Figure 4.14 shows that GO and g-C_3N_4-related diffraction peaks emerge in the GO/g-C_3N_4 nanocomposite, suggesting that nanocomposites were successfully formed. It is also apparent that in g-C_3N_4/La_2O_3, the 2 peaks of g-C_3N_4 found at 13 disappeared slightly, whilst the 2 peaks at 27 joined with characteristic peaks of La_2O_3 oxide. This was the case when the two compounds were analyzed together. As a consequence of this, it was determined that the hydrothermal process was responsible for the production of nanocomposite materials by impregnating La with the triazine structures of g-C_3N_4. Moreover, despite variations in the peak's strength in g-C_3N_4, g-C_3N_4/GO, and g-C_3N_4/GO/La_2O_3 nanomaterials, no new diffraction peaks were discovered (Pathan et al., 2017; Iqbal et al., 2021; Han et al., 2014). This confirms that the hydrothermal approach of adding metal precursors effectively produced nanocomposite materials.

ii) FT-IR analysis

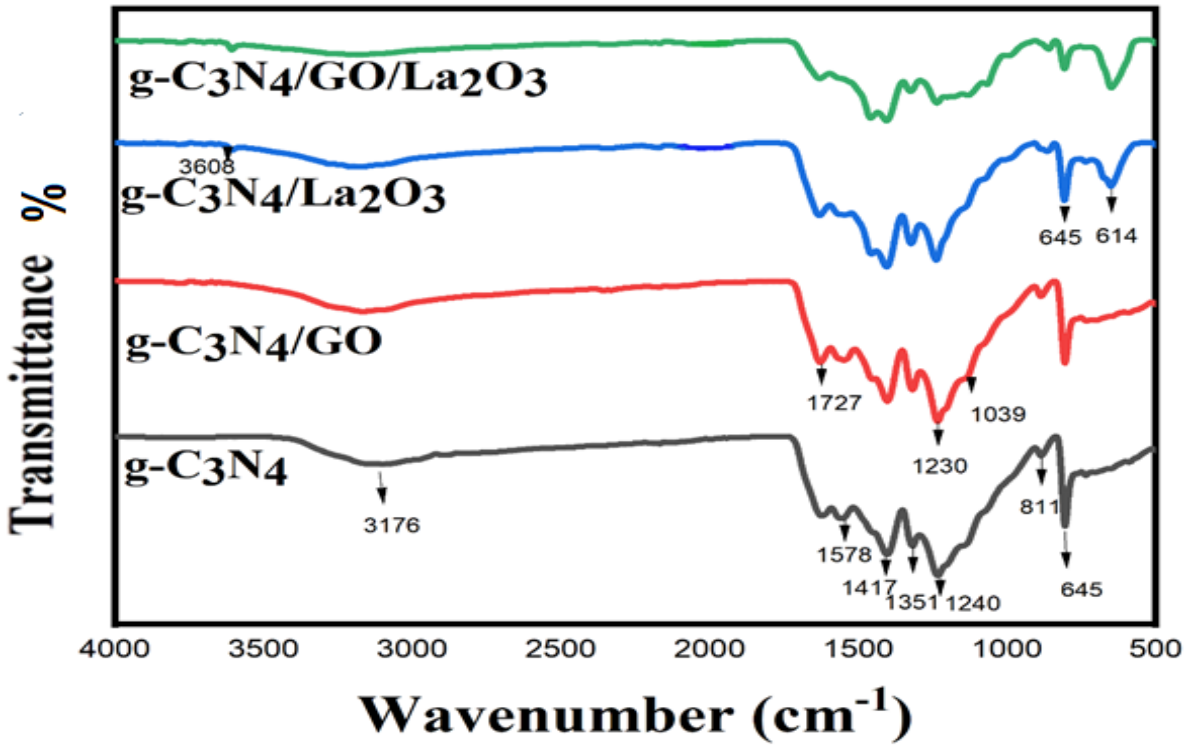

Figure 4.15 FT-IR pattern of g-C_3N_4, g-C_3N_4/GO, g-C_3N_4/La_2O_3, g-C_3N_4/GO/La_2O_3 nanocomposite.

The wavelength range of 500–4000 cm^{-1} was used for the FT-IR analysis that was carried out. The FT-IR spectra of the g-C_3N_4, g-C_3N_4/GO, g-C_3N_4/La_2O_3 and g-C_3N_4/GO/La_2O_3 nanocomposites are depicted in Figure 4.19. These spectra were obtained after the nanocomposites were manufactured. The typical C-N stretching mode of heterocycles was found to be responsible for the peaks that appeared in the 1200-1650 cm^{-1} area of the pure g-C_3N_4 FT-IR spectra (curve a) (Iqbal et al., 2021). The CN stretching vibration mode is responsible for the absorption band located at 645 cm^{-1}. This mode was developed for the sp^2 hybridized network that was present in the g-C_3N_4 network. According to Iqbal et al., 2021, the peaks that can be found at 1240, 1351, 1417, and 1578 cm-^{1} are the result of aromatic C-N stretching. Therefore, the band at 804 cm-^{1} exhibits the distinctive stretching vibration that is characteristic of s-triazine rings.

The stretching vibrations of the g-C_3N_4 were responsible for the peaks that appeared at 1060, 1402, and 1728 cm^{-1} on the FTIR spectrum of GO (curve b). Figure 4.15 displays the FTIR spectra of the nanocomposite, and those spectra have all of the characteristic peaks that are associated with a g-C_3N_4 and La_2O_3 nanocomposite. Significant differences were discovered between the FTIR

spectra of g-C_3N_4 nanoflakes and g-C_3N_4 /GO/La_2O_3 nanocomposite. Because of the stretching of the La-O molecule, the absorption bands at 614 cm^{-1} ranged from moderate to strong. Therefore, the bands discussed above provide evidence that g-C_3N_4/GO/La_2O_3 is a nanocomposite containing both La_2O_3 and GO.

iii) Scanning Electron Microscopy

The morphologies of the g-C_3N_4, g-C_3N_4/GO, g-C_3N_4/La_2O_3, and g-C_3N_4/GO/La_2O_3 nanocomposite were clarified with the use of scanning electron microscopy (SEM). The uneven platelets-like plane structure of g-C_3N_4 and the monolayer wrinkled 2-D sheet-like morphology that results from exfoliation are both depicted in Figure 4.16(a). The photographs taken with the SEM make it abundantly evident that the nanocomposite is composed of g-C_3N_4 nanoflakes that have La_2O_3 and GO nanoparticles encapsulated inside of them. Also seen were agglomerations that resembled sponges and had a variety of holes and gaps throughout their surfaces. The EDX spectrum showed that GO/La_2O_3 had been successfully injected into the g-C_3N_4 nanocomposites, which are essential parts of the nanocomposite material. Furthermore, La, C, N, and O elements are present in good atomic ratios at their characteristic energy peaks and intensities as shown in elemental mapping Figure 4.17.

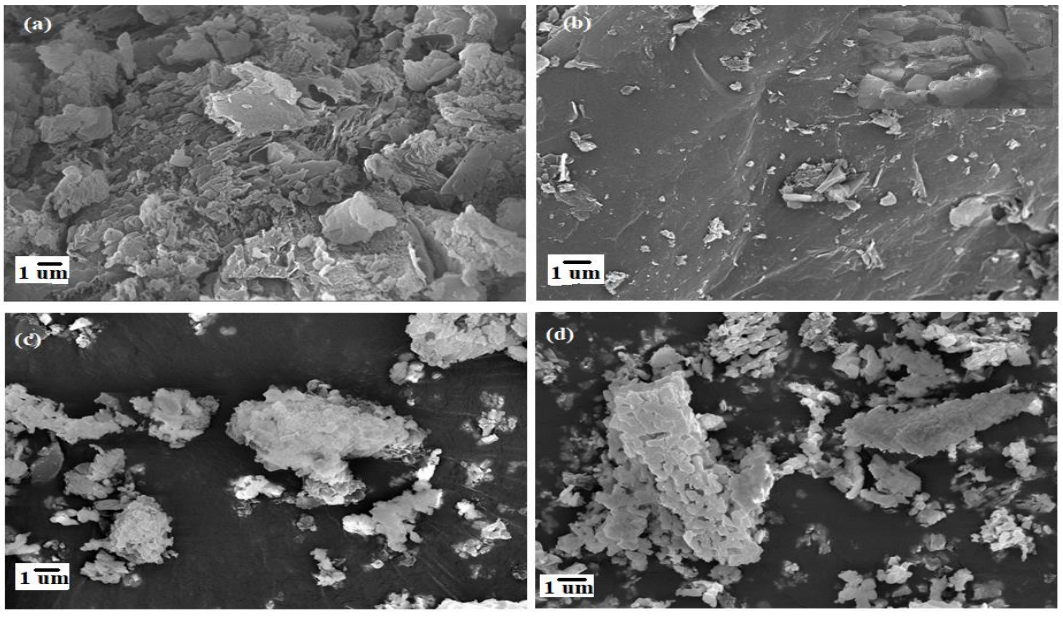

Figure 4.16 FESEM: Morphological image of (a) g-C_3N_4(b) g-C_3N_4/GO (c) g-C_3N_4/La_2O_3 (d) g-C_3N_4/GO/La_2O_3

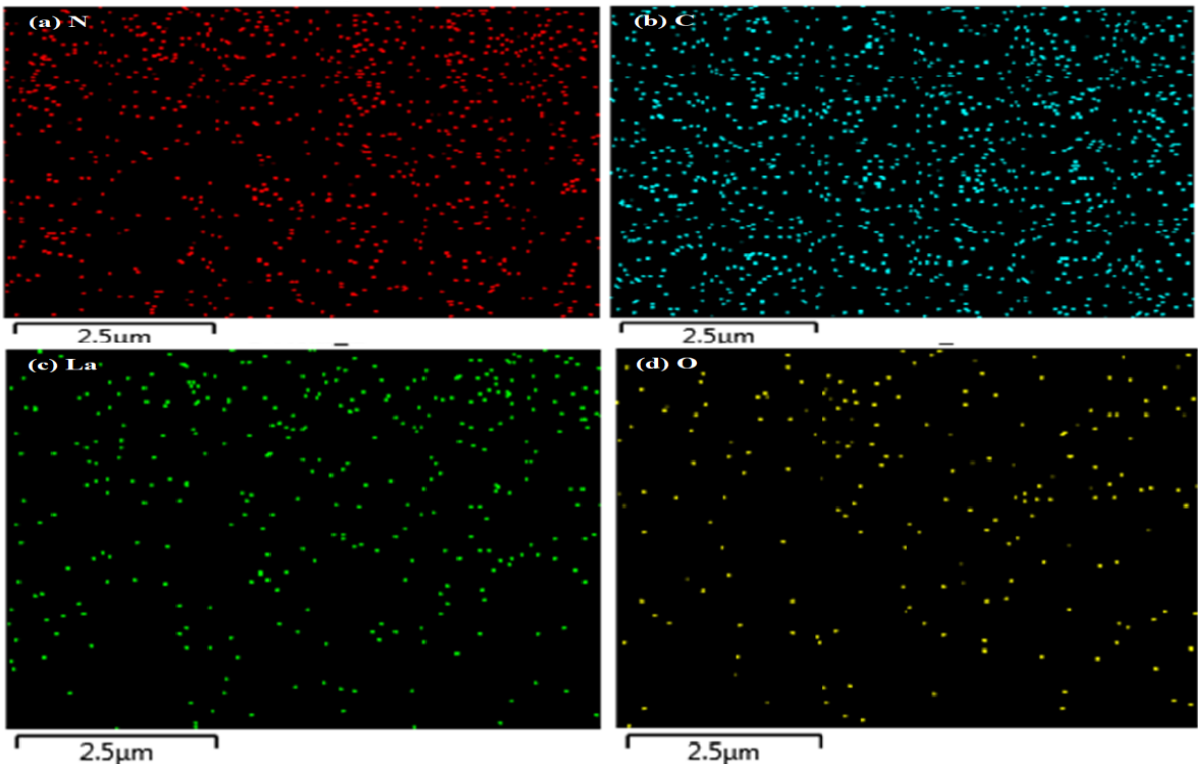

Fig. 4. 17 Elemental mapping images of g-C_3N_4/GO/ La_2O_3 nanocomposite (a) carbon (b) Nitrogen (c) Oxygen (d) lanthanum

iv)Thermogravimetric Analysis

The thermogravimetric analysis (TGA) was performed on the nanomaterials. During a thermogravimetric study, the sample was heated at a consistent pace in order to obtain a temperature function that could be used to regulate mass of a specific material. The illustration was subjected to heating at a rate of 10 degrees Celsius per minute so that this investigation could be carried out. Throughout the course of the experiment, the sample experienced a variable amount of weight loss as a function of the temperature, which is depicted in Figure 4.18. This graphic illustrates a process of gradual weight loss that takes place over the course of two stages. The first weight loss, as indicated by the TGA curve, ranged from 6 to 11% and took place at temperatures lower than 500 degrees Celsius. The vaporization of water molecules that were embedded within the crystalline lattice of the particles was the root cause of this phenomenon. Pure g-C_3N_4 is rather stable at temperatures up to around 500 degrees Celsius, but if the temperature rises above that point, it starts to break down totally. With additional heating to 800.1 degrees Celsius, a significant amount of degradation (63.18%) takes place, which suggests that it possesses an inherent thermal instability in this temperature range.

In addition, the g-C_3N_4/GO/La_2O_3 TGA curve showed stronger thermal stability upon heating than the g-C_3N_4 and g-C_3N_4/GO TGA curves. The reason for this is the powerful interaction that exists between the La nanoparticles and the interlayer stacking patterns of the g-C_3N_4/GO. Only g-C_3N_4/GO/La_2O_3 exhibits greater stability with reduced mass loss (34.02%) after heating to 800 °C, indicating that this material is more stable than its single and binary equivalents, g-C_3N_4, g-C_3N_4/GO, and g-C_3N_4/La_2O_3 (as shown in Figure 4.18).

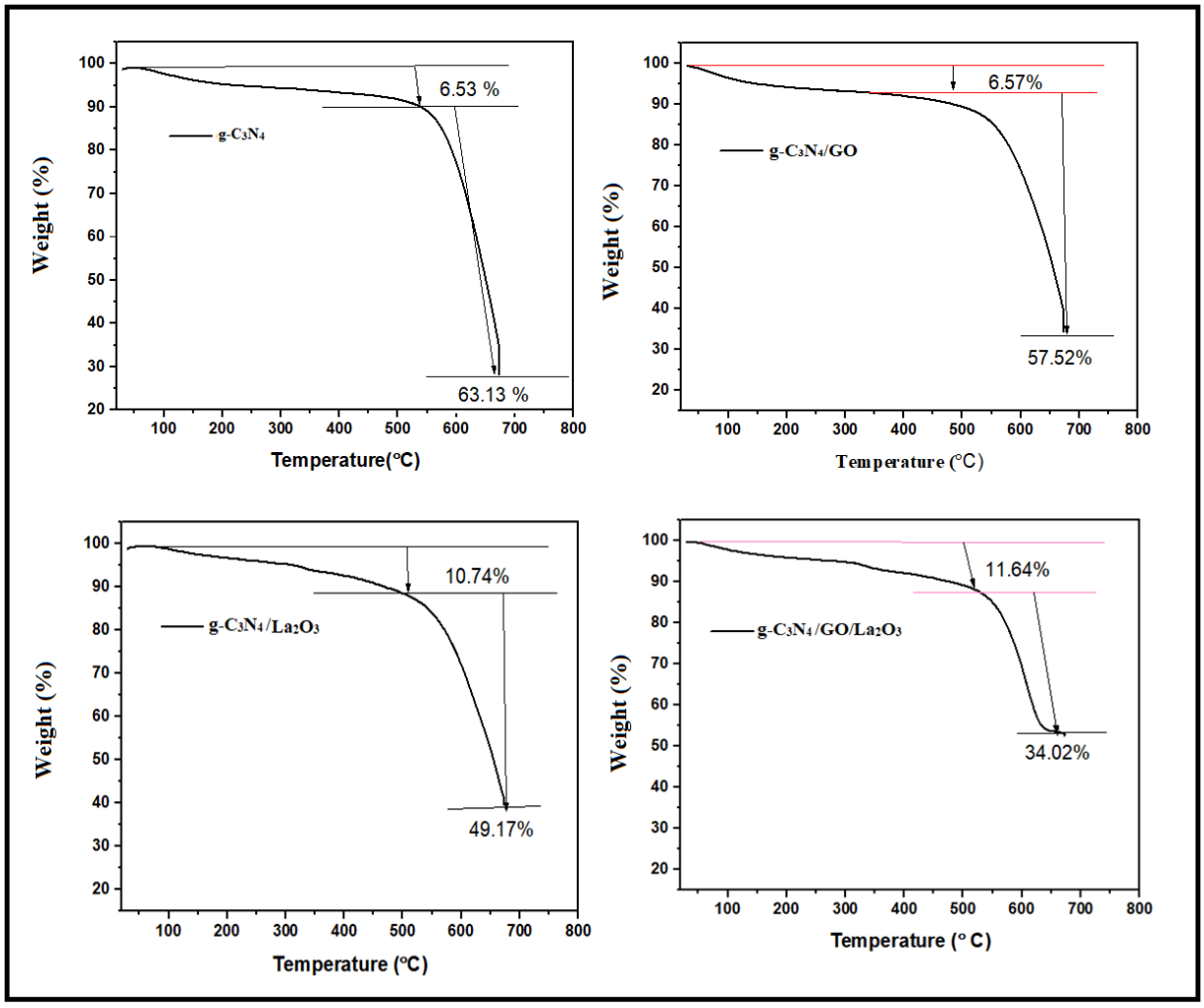

Figure 4. 18 TGA curves of g-C_3N_4, g-C_3N_4/GO, g-C_3N_4/La_2O_3, and g-C_3N_4/GO/La_2O_3

v) UV-Visible spectroscopic analysis

The light utilization capacity of samples was studied through UV-Diffused reflectance spectroscopy. UV-DRS spectra of pure g-C_3N_4 and doped material are presented in Figure 4.19.

The g-C_3N_4 displays photo absorption of visible light at a wavelength of 440 nm. This is because the photoexcitation of one electron causes it to move from the valence band (VB) of the N^2p orbital to the conduction band (CB) of the C^2p orbital appropriately. The doped nanomaterial has exhibited redshift and increased visible light absorption. The wavelength of g-C_3N_4 in doped composites has shifted significantly towards the wavelength region. g-C_3N_4 coupled with La_2O_3 and GO had a stronger visible light adsorption capacity. Because of the high-efficiency optical absorption capacity and the narrow band gap, more active electrons were able to make the transition from the valence band (VB) to the conduction band (CB). To put it another way, the photocatalytic performance of these samples was extremely high. It was determined that the band gap of the g-C_3N_4, in addition to that of the other doped material, was 2.7 eV. The band gap of the other doped material was determined to be 2.5 eV, 2.3 eV, and 2.2 eV, respectively, as is demonstrated in Figure 4.20. The g-C_3N_4 and La_2O_3 were driven to form a heterojunction as a result of their almost identical valence and conduction band potentials. In addition, several notches that were produced on the surface worked to reduce the amount of recombination that occurred between photogenerated electrons and holes, which helped to further increase the photocatalytic performance.

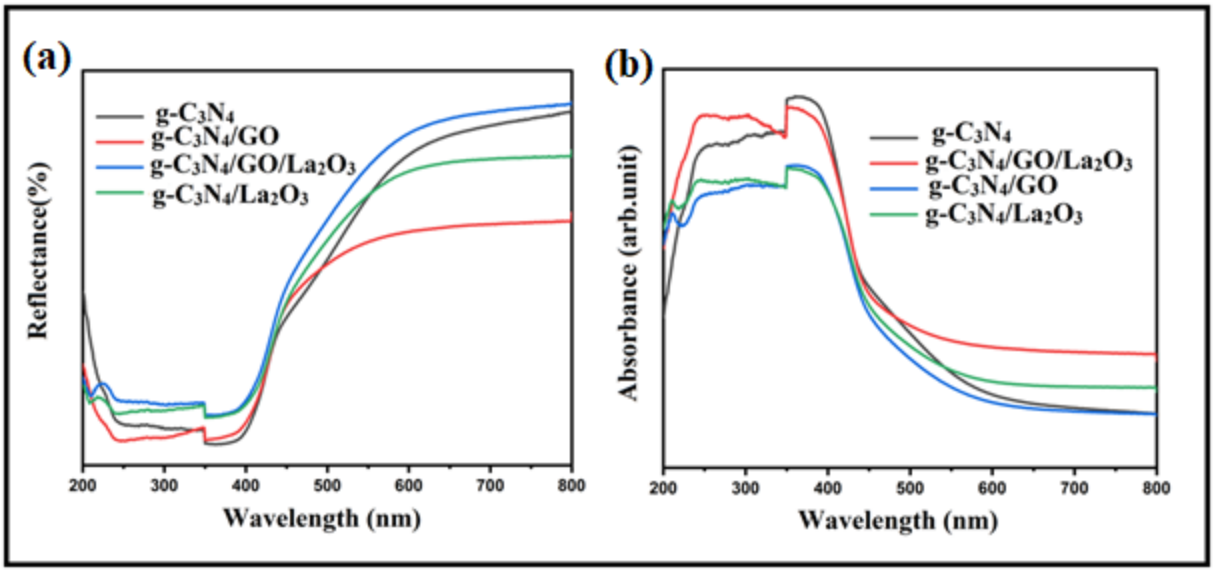

Figure 4.19 UV-VIS DRS absorption and reflectance spectra for g-C_3N_4, g-C_3N_4/GO, g-C_3N_4/La_2O_3 and g-C_3N_4/GO/La_2O_3

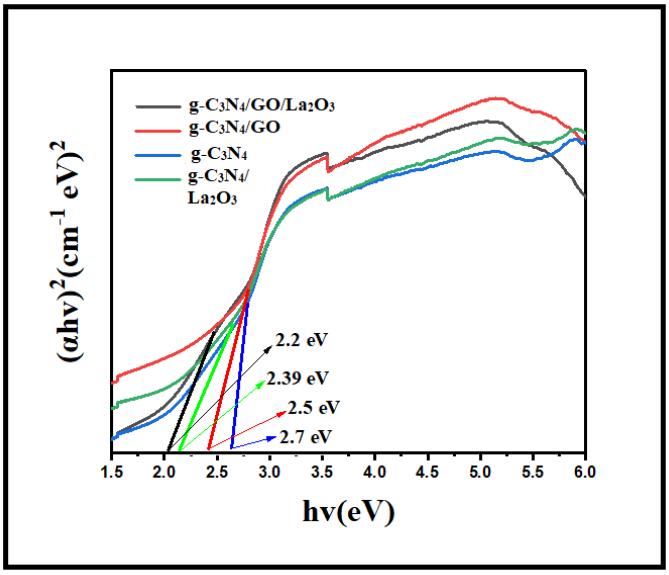

Figure 4.20 Calculated band gap of nanocomposite materials

4.2.2.2 Photocatalytic activity towards photodegradation of Carbofuran

i) pH effect

In assessing aqueous phase photocatalytic processes, the pH of the solution is an essential variable. The influence of pH on the rate of photocatalytic degradation was investigated by adjusting the pH value of the pesticide solution while maintaining all of the other experimental parameters in their original states. In the pH range of 1 to 7, an increase in carbofuran's elimination efficiency was observed with increasing pH; however, its effectiveness was observed to decline as the pH increased beyond 7 to 9.

The best pH value was determined to be 7.0, with the maximum Carbofuran elimination efficiencies of 53.75, 62.5, 67.5, and 80% in the visible region with g-C_3N_4, g-C_3N_4/GO, g-C_3N_4/La_2O_3, and g-C_3N_4/GO/La_2O_3 photocatalytic nanocomposite, respectively. At a pH of 7, it is possible to protonate Carbofuran at the carbonyl oxygen. Because of this protonation, there is the potential for electrostatic repulsion. The catalyst and Carbofuran decrease the rate of deterioration. The negative charge of Carbofuran, which is attached to the negative charge of the catalyst surface, is the cause of the increased rate of degradation at 7 pH (as shown in Figure 4. 21).

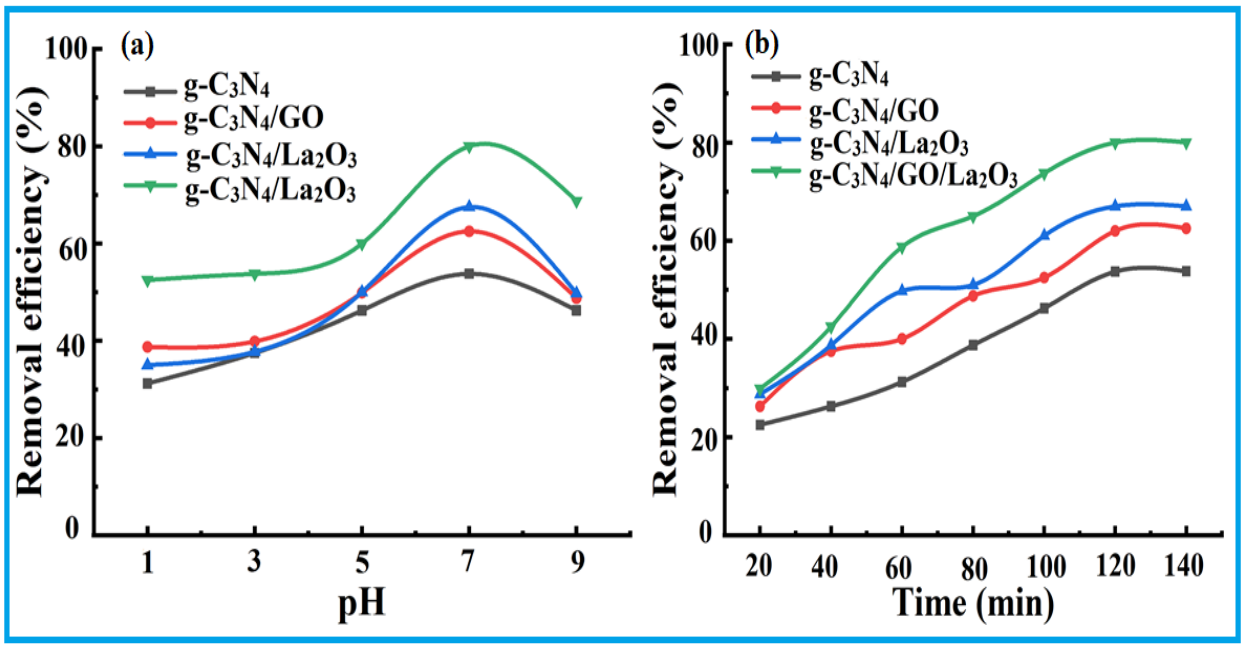

Figure 4. 21 Photocatalytic degradation of Carbofuran pesticide as a function of (a) pH and (b) time

ii) Irradiation study

The influence of contact time is shown in Figure 4.21(b). It has been established that the effectiveness of removal improves as the amount of time that it is exposed to the substance. When the irradiation time interval was increased from 20 to 120 minutes, as shown in Figure 4.21 (b), the percentage of degradation for the as-produced nanocomposite climbed from 24.52 to 80%. This is very obvious from the data presented in the figure. This could be related to the fact that as the duration of the irradiation increases, the carbofuran molecules have a greater opportunity to interact with the surface of the catalyst and form hydroxyl radicals.This speeds up the photocatalytic reaction, which in turn increases the percentage of degradation.

iii) H_2O_2 effect

The capacity of H_2O_2 to produce more OH radicals will boost photocatalytic removal and produce vivid intermediates. Figure 4.22 (a) illustrates the influence of H_2O_2 on the photocatalytic elimination of Carbofuran by g-C_3N_4/GO/La_2O_3 when the concentration of H_2O_2 is varied from 0.01 to 1%. Without H_2O_2, the photodegradation efficiency was 80%. When the concentration of

H_2O_2 was raised from 0.01% to 0.1%, there was a corresponding increase in the removal of carbofuran by photocatalysis from 80% to 85.6%. Nevertheless, when the concentration of H_2O_2 was raised to 1%, the clearance rate dropped to 73%. It was hypothesized that an increase in the amount of H_2O_2 acting as an inhibitor when paired with hydroxyl radicals was the reason of this drop. It is possible to stabilize the linked e/h+ by enclosing photoinduced e in hydrogen peroxide. The OH radicals are the outcome of the process that takes place when H_2O_2 reacts with e or O_2. After that, many thoughts that incorporating H_2O_2 into the photocatalytic reaction system would make the process of removing carbofuran from the environment more effective. Because this quantity of H_2O_2 was administered, the number of OH radicals that were able to destroy carbofuran was reduced.

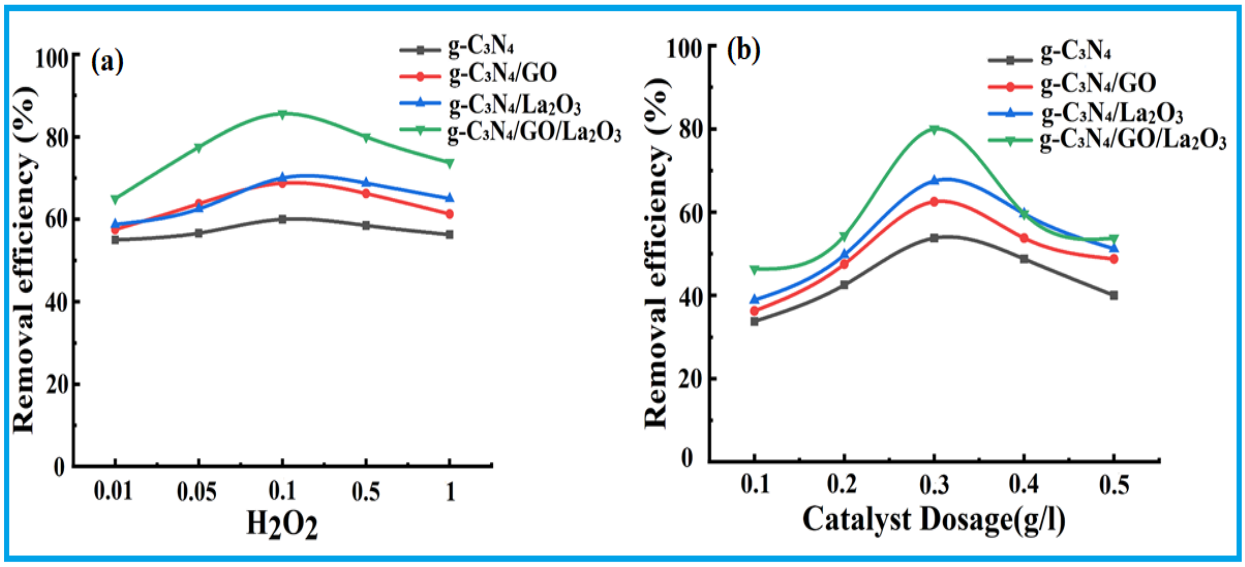

Figure 4.22 Photocatalytic degradation of Carbofuran pesticide (a) effect of H_2O_2 (b) effect of photocatalytic dose on degradation

iv) Effect of photo-catalyst dose

Carbofuran is metabolized in a manner that is more effective when the photocatalyst is readily accessible and present in adequate quantities. Figure 4.22(b) depicts how the quantity of photocatalyst added to the nanocomposites has an effect on the photocatalytic activity of the nanocomposites. The concentration of the g-C_3N_4, g-C_3N_4/GO, g-C_3N_4/La_2O_3, and g-C_3N_4/GO/La_2O_3 nanocomposite was changed from 0.1 to 0.5 g/L in 100 ml of Carbofuran solution with the addition of 0.1% H_2O_2 so that the optimal photocatalyst dosage could be determined.

Carbofuran photocatalytic removal efficiency increased from 46.37 to 85.6% when the dosage of the photocatalyst was raised from 0.1 to 0.5 g/L, as shown in Figure 4.22(b). Increasing the dosage, on the other hand, had no extra influence on the efficiency of the elimination process. This result suggested that the greater photocatalyst suspension caused a reduction in light penetration in the presence of a large amount of photocatalyst. This was demonstrated by the fact that the reduction in light penetration occurred.

v) Photocatalyst regeneration

From an economic point of view, the synthesized photocatalyst should be reused 'n' times to make the catalyst more useful. For renewal, the used photocatalyst was mixed for an hour with 0.1 g/10 ml of a 30% H_2O_2 solution. Carbofuran removal was most effective at 48% in the fifth cycle. After that, it got less and less effective with each cycle of renewal until the fifth cycle. By providing free active sites and a negatively charged surface, the H_2O_2 treatment, which also serves as a novel photocatalyst, can liberate the molecules bound on the surface.

vii) Degradation Mechanism

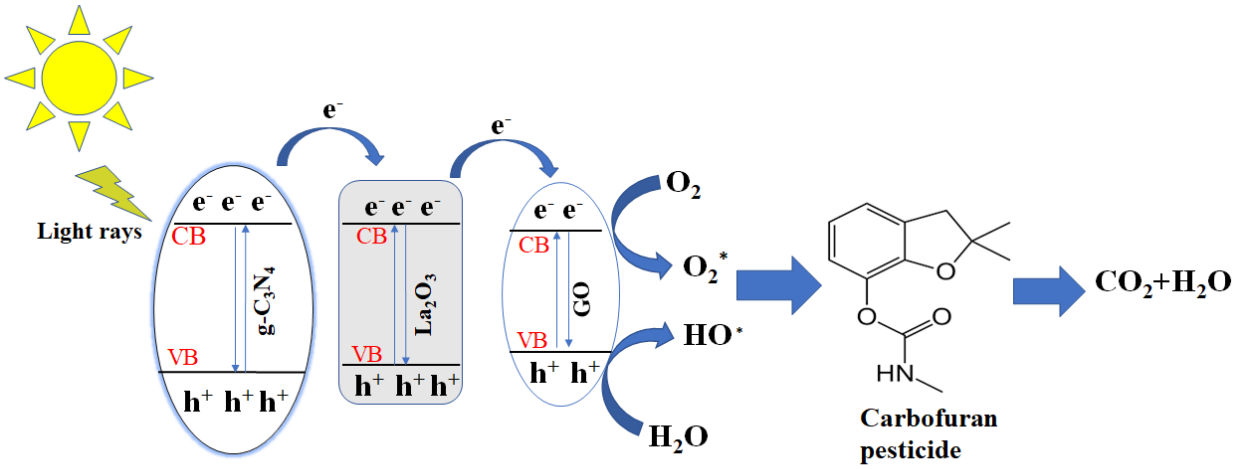

Figure 4.23. The proposed mechanism for the removal of Carbofuran using g-C_3N_4/GO/La_2O_3 nanocomposite

The conversion of Carbofuran during detoxification was accompanied by the simultaneous appearance of 2,3,-dihydro-2,2-dimethyl benzofuran-7-oland 2,3-dihydro benzofuran-7-ylmethyl carbamate. The first intermediate is produced when the carbofuran group is removed from the

parent molecule of carbofuran (Katsumata et al., 2001). The second molecule results from the demethylation of the original carbofuran molecule. Upon the addition of hydroxyl radical to 2,3,-dihydro-2,2-dimethyl benzofuran-7-ol, the furan ring was oxidized to create 7-hydroxy-2,2 dimethylbenzofuran-3(2H)-one. Similarly, photo-transformation of molecular bonds, such as the opening of ring structures, happened in 2,3-dihydro benzofuran-7-ylmethyl carbamate and 7-hydroxy2, 2dimethylbenzofuran-3(2H)-one to generate 1,4-benzene-dicarboxaldehyde and other simple chemical byproducts (Lu et al., 2001). Figures 4.23 and 4.24 depict the eventual creation of the mineralized by-products CO_2, H_2O, and H_2 as a result of the continuing sequential oxidation of the generated two intermediates.

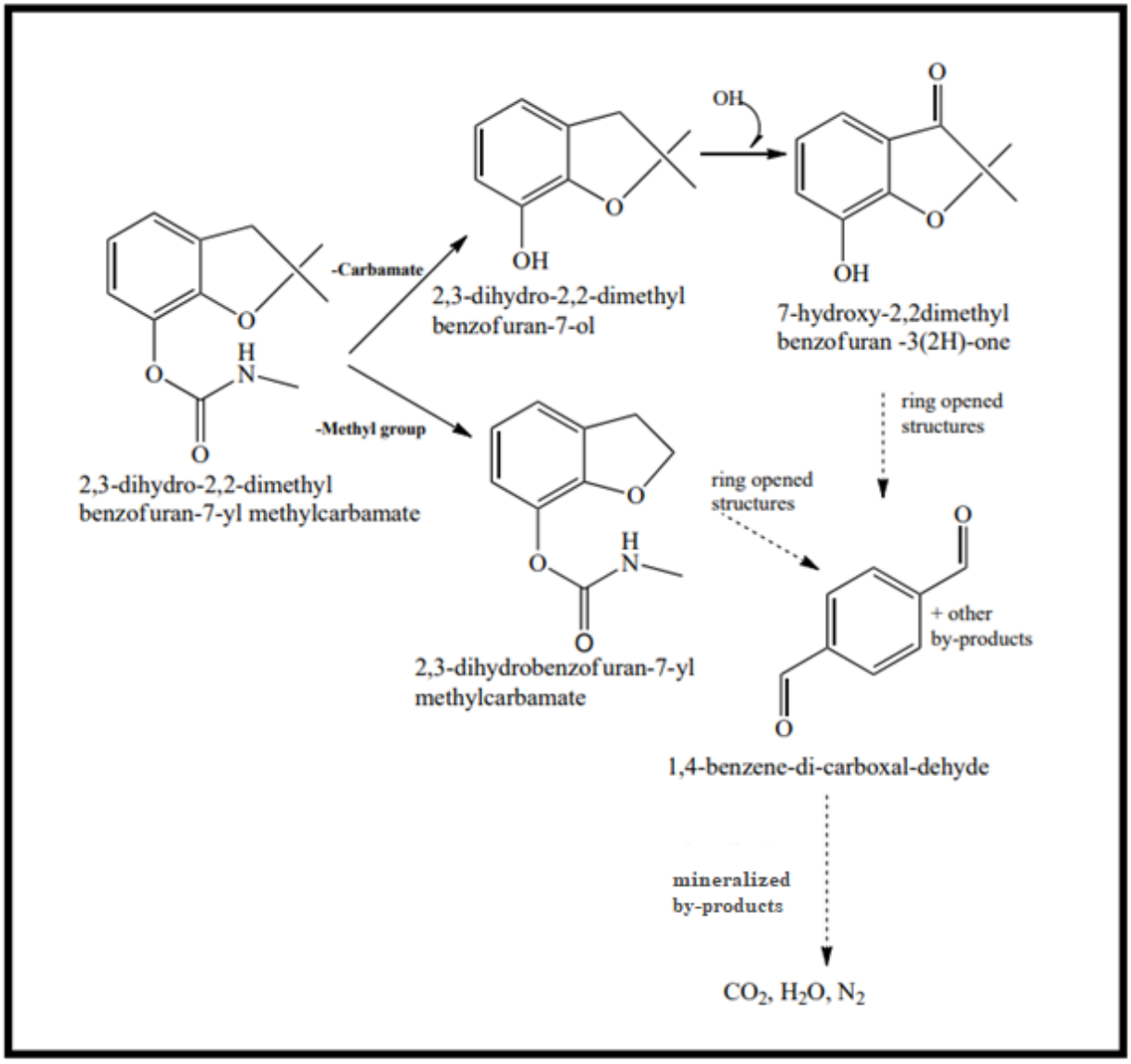

Figure 4.24 Proposed degradation pathway of Carbofuran using g-C_3N_4/GO/La_2O_3 nanocomposite

4.2.3.3 Photocatalytic degradation of Chlorpyrifos

i) Continuous Column study

The g-C_3N_4/GO/La_2O_3 nanocomposite was applied as a photo-catalyst to the particular column that was created to eliminate Chlorpyrifos in a continuous flow process using the column. The visible light was used to irradiate the photo-catalyst. The g-C_3N_4/GO/La_2O_3 nanocomposite was created by hydrothermal doping procedures in instruction to solve the problem of column feeding that was caused by the variable sizes of packing sorbent particles. This was done in order to regulate the problem. A cylindrical tube with an actual capacity was part of the continuous-flow system along with an electrode assembly, a feed pump, and a direct current power supply unit.

For the purpose of conducting a column breakthrough analysis of Chlorpyrifos detoxification in the existence of visible light, a specially built column through an inside diameter of 0.7 cm and a length of 17 cm was developed specifically for this purpose. The column was then stuffed with g-C_3N_4/GO/La_2O_3 nanocomposite (the layer of nanocomposite was equal to 2 and 4 cm^3, and a steel net sheet with a diameter of 0.001 centimeters was placed underneath it. For the purpose of enhancing and preserving the flow distribution, the column packing with g-C_3N_4/GO/La_2O_3 nanocomposite consisted of filter paper and glass wool of a volumetric equivalent of 0.5 cm^3. Five, ten, and twenty ppm of Chlorpyrifos were the initial concentrations of Chlorpyrifos in the column test run for the photocatalytic removal of Chlorpyrifos. The Chlorpyrifos solution had a pH of 4, and the required flow rate with the down-flow mode was set to 0.004-0.008 L/min. For the purpose of analyzing the breakthrough kinetics, the solutions of Chlorpyrifos that made it through a particular column were compiled at a variety of time intervals following its exit. To determine the maximal Chlorpyrifos removal effectiveness, the mass of the Chlorpyrifos that was removed was divided by the mass of the g-C_3N_4/GO/La_2O_3 nanocomposite employed in the experiment.

Optimization of the breakthrough analysis of Chlorpyrifos removal was accomplished by varying the flow rate, the amount of g-C_3N_4/GO/La_2O_3 nanocomposite used as a bed height, and the concentration of Chlorpyrifos. After five minutes of continuous operation, when the Chlorpyrifos concentration at the reactor exhaust had attained a consistent value and the operation had become steady, Chlorpyrifos samples were taken for analysis. The absorbance of the solution was

measured at a wavelength of max = 290 nm after the samples were evaluated using UV–vis spectroscopy (1700 UV–vis Shimadzu). Using a calibration curve, the absorbance of the solution was transformed into a measurement of the Chlorpyrifos concentration.

RTD measurement

Examining the flow pattern in non-ideal reactors using the Residence Time Distribution (RTD) technique is one of the most effective ways available. The step approach was utilized in this investigation in order to get cumulative RTD curves. The cumulative RTD function, F(t), can be determined using the following Equation:

$$F(t)= \frac{Ct}{CO}$$

Where C_t and C_O are the concentrations of the tracer measured at the time t and at the inlet of the reactor, respectively.

ii) pH effect

Figure.4.25(a) shows the effects of pH on visible light-induced photodegradation of chlorpyrifos by all photocatalyst materials. All photocatalysts removed Chlorpyrifos better in the acidic pH range of 2 to 4.0 than from 4.0 to 10.0. The optimal pH value was 4.0, which is somewhat acidic, and the photocatalytic nanocomposite g-C_3N_4/GO/La_2O_3 had maximum Chlorpyrifos removal efficiencies of 67.47, 80.21, 77.85, and 87.62% in the visible area. Photocatalyst surface charge eliminates chlorpyrifos. Photocatalyst surfaces reject cationic moiety electrostatically at pH 4. At alkaline pH (pH > 7.5), electrostatic repulsion towards anionic compounds dominates, negatively charging all photocatalyst surfaces (Wang et al., 2017; Long et al., 2017). g-C_3N_4/GO/La_2O_3 nanocomposite increased Chlorpyrifos elimination. OH^-/H_2O and localized holes presumably produced several hydroxyl radicals that increased Chlorpyrifos breakdown in visible light.

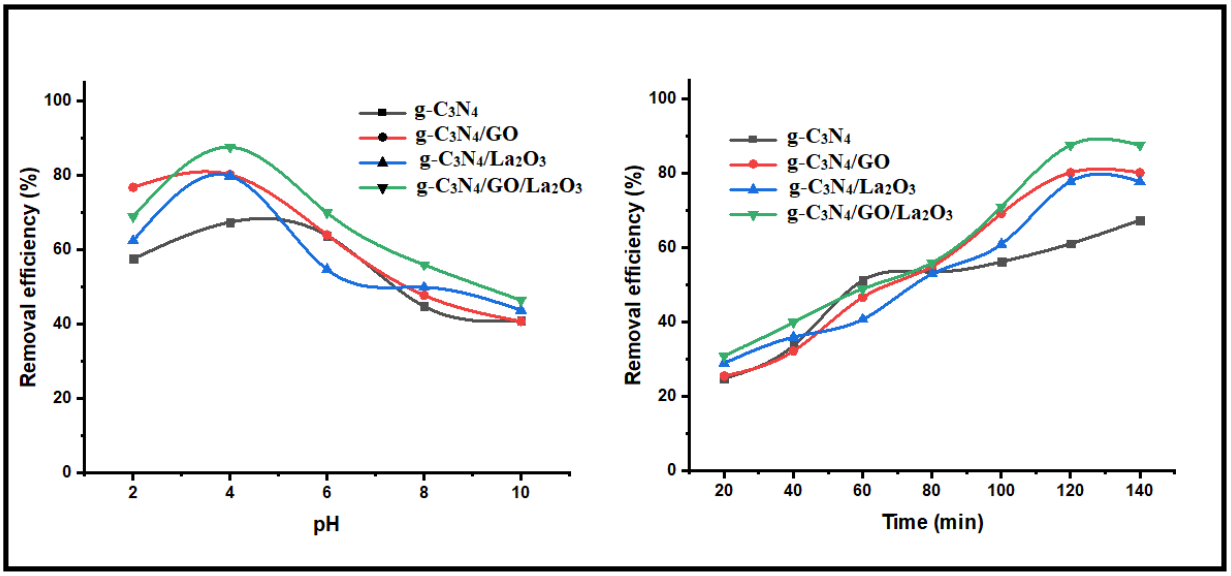

Figure 4. 25 Photocatalytic degradations of Chlorpyrifos pesticide as a function of (a) pH and (b) time

iii) Irradiation time

As shown in Figure 4.25(b), increasing the irradiation time interval from 20 minutes to 120 minutes resulted in an increase in the amount of degradation from 31 to 87.62% for the nanocomposite that had just been synthesized. Chlorpyrifos molecules have a greater chance of reacting with the surface of the catalyst and producing hydroxyl radicals as the length of time that they are exposed to the irradiation rises. This results in a quicker photocatalytic process and an increased rate of degradation.

iv) H_2O_2 effect

The Experiments were carried out to examine the effect of H_2O_2 concentration on its rate of formation/decomposition by adding H_2O_2 externally to the system at the beginning.H_2O_2 increases OH- radicals, enhancing photocatalytic elimination and creating intermediates. Figure 4.26 (a) shows the photocatalytic removal of Chlorpyrifos by g-C_3N_4 with H_2O_2 from 0.01 to 1%. Increasing H_2O_2 from 0.01 to 0.1% increased Chlorpyrifos photocatalytic elimination from 87% to 94.5 %. Trapping photo-induced e^- in H_2O_2 stabilizes coupled e/h^+. H_2O_2 with e^- or O_2 can produce $^{\cdot}OH$, radicals. Hence, adding H_2O_2 to the photocatalytic reaction system was expected to increase Chlorpyrifos removal (as shown in Figure 4.26).

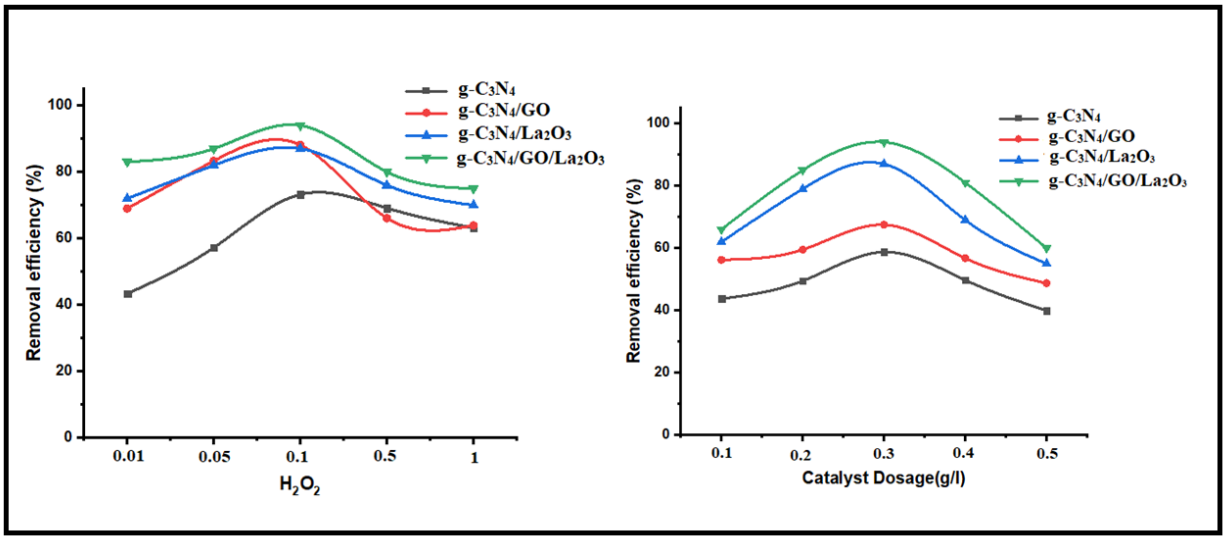

Figure 4.26 Photocatalytic degradation of Chlorpyrifos pesticide (a) effect of H_2O_2 (b) effect of photocatalytic dose on degradation

v) Effect of Photocatalytic dose

Figure 4.26(b) Shows how photocatalyst dose affects nanocomposite photocatalytic activity. The optimal photocatalytic dose was determined by adding 0.1 to 0.5 g/l of the g-C_3N_4 nanocomposites to 100 ml of Chlorpyrifos solution with 0.1% H_2O_2 and 100 w intensity at pH 4.0 for 2 hours. This was done in order to identify the optimal photocatalytic dosage. When the quantity of photocatalyst was increased from 0.1 to 0.3 g/l, the amount of chlorpyrifos that could be removed rose from 66.5% to 94.5% (Zhang et al., 2017; Yu et al., 2018).

vi) Continuous study:

In the presence of visible light and at pH 4, the column that was packed with the g-C_3N_4/GO/La_2O_3 nanocomposite had a particle size of around 100 millimeters. The time at which the concentration of Chlorpyrifos in the effluent is comparable to the concentration of Chlorpyrifos that was introduced into the system is known as the breakthrough time.

There were three different column flow rates that were tested: 0.004, 0.006, and 0.008, 0.01 L/min. As the flow rate was increased, the Chlorpyrifos removal efficiency declined, which resulted in shorter breakpoint times. The conclusion that can be drawn from this performance is that the amount of Chlorpyrifos that is removed is reduced because there was insufficient contact time.

Both the bonding capacity and the contact duration for the photocatalytic removal of Chlorpyrifos in the light phase were shortened as a result of a lack of time. This was caused by the presence of Chlorpyrifos.

The best removal was achieved with a flow rate of 0.004 L/min, despite the fact that a higher flow rate shortened the mass transfer zone more than the lower flow rate did. In the course of analyzing the data about the Chlorpyrifos removal efficiency, it was found that the total removal capabilities were consistent with the batch process. Because of the saturation of the g-C_3N_4/GO/La_2O_3, the amount of time it takes for Chlorpyrifos to break through the barrier decreases as the concentration of Chlorpyrifos at the inlet increases.

vii) Adsorption study

In order to test the adsorption capability of pure g-C_3N_4, g-C_3N_4/GO, g-C_3N_4/La_2O_3, g-C_3N_4 /GO/La_2O_3 nanomaterials, the degradation of the pesticide Chlorpyrifos was carried out in the dark. The level of Chlorpyrifos degradation that was accomplished by the g-C_3N_4 /GO/La_2O_3 ternary nanocomposite was much higher when contrasted with that which was achieved by the pure g-C_3N_4 nanocomposite. This is due to the fact that ternary nanocomposite possesses a large surface area, which directly translates to an excellent capacity for adsorption. The concept of "adsorption" might be the key to understanding why this is the case. In addition, one can make a connection between the levels of doped material present in the ternary nanocomposite and the improved capacity for adsorption that it possesses.

Conclusions

Carbofuran and Chlorpyrifos pesticides were degraded with the help of a photocatalyst that was synthesized out of g-C_3N_4/GO/La_2O_3. This photocatalyst was robust and reusable, and it was made. In order to characterize the nanomaterial that was synthesized, XRD, FT-IR, and SEM were used. The prepared nanocomposite exhibits a wonderful activity for the removal of Carbofuran pesticide under sunlight irradiance. Carbofuran was degraded photo catalytically to the extent of 80% after being exposed to light for a period of 120 minutes. Degradation of chlorpyrifos was accomplished to the extent of 94.5% while utilizing hydrogen peroxide. As a point of comparison, the photocatalytic degradation employing g-C_3N_4, g-C_3N_4/GO, and g-C_3N_4/La_2O_3 were only 53.75, 62.5, and 67.5% respectively. In addition to having the ability to take in more visible light, this

ternary nanocomposite has the capability to efficiently restrict the recombination of photo-induced electron-hole pairs. In addition, ternary photocatalysts show excellent sustainability and recyclability in the photocatalytic degradation of carbofuran after five cycles, achieving an efficiency of 48% in the process.

CHAPTER- 5

Conclusion of work

Conclusion of work

The contamination of the natural environment by byproducts of industrial processes is a significant challenge. These new ecologically friendly catalysts will flourish as restrictions on environmentally damaging technologies grow increasingly tight. According to the findings of our investigation, the commercial viability of photocatalysis of a number of different pesticides carried out in a batch and continuous progression has been attired. The current research aims to investigate the photocatalytic characteristics of nanocomposites in order to decompose harmful substances that are found in degraded wastewater. Inert support is required for the nanocomposites in order to improve their effectiveness of the nanocomposites. Although many different supports have been investigated for pollutant degradation investigations, The g-C_3N_4-based ternary photocatalyst have been demonstrated to be superior to those of the other supports. In addition to that, this thesis presents the g-C_3N_4-based ternary nanocomposite photocatalysts as a solution to the competition that requires a catalyst with high photocatalytic efficiency.

The as-obtained ternary nanocomposites demonstrated improved photocatalytic performance of Chlorpyrifos and Carbofuran in comparison to the pure g-C_3N_4 and the corresponding g-C_3N_4 binary samples. The as-prepared g-C_3N_4/GO/V_2O_5 and g-C_3N_4/GO/La_2O_3 nanocomposites demonstrate a higher photocatalytic efficacy than g-C_3N_4, g-C_3N_4/GO, g-C_3N_4/V_2O_5, and g-C_3N_4 /La_2O_3, respectively.

The g-C_3N_4/GO/V_2O_5 nanocomposite that was subjected to 120 minutes of irradiation was found to be the most effective high-efficiency photocatalyst. Graphene, Vanadium, and Lanthanum including g-C_3N_4/GO/V_2O_5 and g-C_3N_4/GO/La_2O_3 nanocomposite would look to be capable candidates for excessive practical attention. This is because suitable metal nanoparticles might stimulate various catalytic things. The main results of all these chapters are summarized as follows and given in Table 5.1.

- The X-ray diffraction peak characterization peaks for graphitic carbon nitride are seen at 13.0 and 27.50, which correspond to crystallographic planes (100) and (002), respectively. Peaks at 13.0 and 27.50 nm indicate the formation of the hexagonal phase of graphitic carbon nitride, and the computed distance is 0.67 nm.

- Graphene oxide exhibits a broad diffraction that occurs at the value of 2θ = 10.80. A set of different peaks for V_2O_5 observe at 2θ values of 20.3º, 26.1º, 31.07º, and 34.30º which correspond to the characteristic diffraction of (001), (110), (301), (310) lattice planes of orthorhombic V_2O_5. XRD of g-C_3N_4/GO/V_2O_5 contributed to the peaks corresponding to g-C_3N_4, GO and V_2O_5 that verify the successful synthesis of ternary nanocomposite.
- The FT-IR peaks at 1200-1650 cm^{-1} in pure graphitic carbon nitride might be attributed to heterocycle C-N and C=N stretching modes. The tri-s-triazine unit breathing mode is responsible for the sharp and dominating peak at 804 $^{-1}$, which demonstrates the presence of triazine units in the backbone of g-C_3N_4. Peaks at 1060, 1403, and 1728 cm^{-1} are seen in the FT-IR spectra of GO. These peaks reflect the stretching vibration of (C-O), the bending vibration of (C-OH), and the carbonyl (C=O) functional groups, respectively. V_2O_5 sample has two distinctive absorption bands at 824 am^{-1} and 1014 cm^{-1}.

Enhanced photo-degradation performance of nanocomposites

- The elimination efficiency of chlorpyrifos improved with increasing pH in the acidic pH range of 2 to 4, but it declined as the pH increased from 4 to 10. The optimal pH was determined to be 4.0, which is somewhat acidic, with the highest Chlorpyrifos removal efficiencies of 67.47, 80.21, 70.45, and 88.97% with g-C_3N_4, g-C_3N_4/GO, and g-C_3N_4/GO/V_2O_5, respectively, in the visible area.
- Increasing the H_2O_2 concentration from 0.01 to 0.1% enhanced the photocatalytic elimination of Chlorpyrifos from 88 to 90.5 % and Carbofuran from 83.72% to 92.6%.
- Besides, the photocatalyst displayed good recycling ability on the degradation of Chlorpyrifos degradation reaching 49.5% Carbofuran at 44 % after five consecutive cycles, indicating its stability and durability.
- The removal of carbofuran was more effective at increasing the pH from 6.0 to 7.0, but it became less effective as the pH went further from 7.0 to 9.0. The ideal pH value, which was found to be 7.0, was found to have maximum Carbofuran removal efficiencies of 57.62, 71.12, 70.12, and 83.75% with g-C_3N_4, g-C_3N_4/GO, g-C_3N_4/V_2O_5, and g-C_3N_4/GO/V_2O_5 photocatalytic material.
- At optimum photocatalytic test conditions, the Carbofuran and Chlorpyrifos were degraded 80% and 87 % within 120 minutes of irradiation time using g-C_3N_4/GO/La_2O_3.

- The elimination of Carbofuran by g-C_3N_4/GO/La_2O_3 rose from 80 to 85.6 % and Chlorpyrifos from 87% to 94.5% when the H_2O_2 concentration was increased from 0.01 to 0.1 %.

Table. 5.1. The key results of synthesized photocatalysts like degradation efficiency, band gap, and irradiation time

S. No.	Photocatalyst	Band gap(eV)	Irradiation Time(min)	Degradation efficiency	
				Chlorpyrifos	Carbofuran
1	g-C_3N_4	2.7	120	67.47%	57.62%
2	g-C_3N_4/ La_2O_3	2.39	120	78.5	67.5
3	g-C_3N_4/V_2O_5	2.59	120	70.45	70.12
4	g-C_3N_4/GO	2.5	120	80.21	71.12
5	g-C_3N_4/GO/ La_2O_3	2.2	120	87	80
6	g-C_3N_4/GO/ V_2O_5	2.21	120	88.97	83.75

In addition, the ternary nanocomposites were able to ensure superior visible-light absorption capacity, smaller crystalline size, a smaller bandgap, effective interfacial charge charrier s (e-/h+) separation/transfer, and their recombination rate was dominated by a quick transference of organic pollutants to the surface of the photocatalyst. Prior to this, we had placed a strong emphasis on the reaction mechanism that can be backed up by spectroscopic evidence. It is omnipotent in the environment with a great biological reactant, which may be a reason for its enhanced photocatalytic action. Typically, all ternary nanocomposites have OH-reactive species, which play an important role in the photodegradation process and consequently the oxidative destruction of organic pollutants. These ternary photocatalyst nanocomposites would appear to be prospective aspirants for great practical attention to be examined for large-scale applications with reusability, which would ultimately result in the exploitation of freely available solar energy. Furthermore, the reusability of ternary nanocomposites can demonstrate a good recyclability capacity and greater steadiness for a few consecutive cycles without any structural alteration; as a result, the nanocomposites that have been obtained must save both energy and money. The ternary

nanocomposite that was discussed in the thesis might be regarded as advantageous in terms of wastewater treatment and potential applications linked with g-C_3N_4 that are centered on ternary nanocomposites.

Scope for Future Work

Increasing the spectral sensitivity of semiconductor photocatalysts to visible light is one of the primary issues facing the scientific and industrial community interested in photocatalytic research. More dopants, a different way of dopant integration into the semiconductor structure, and novel applications in environmental technology would be the primary focus of future study.

- Using high-tech analysis methods like mass spectrometry, investigate the products and intermediates formed during the degradation of dyes over mesoporous g-C_3N_4-based photocatalyst with and without the presence of externally visible light illumination.
- To use electrochemical techniques to directly see the charge migration, separation, and recombination on g-C_3N_4-based nanocomposites under visible light irradiation, therefore monitoring the electron-transfer process.
- To apply an in-situ characterization approach, such as solid-state NMR on the irradiated sample, to learn how photo-induced charge carriers affect the reactivity of bonds on the surface of mesoporous nanocomposites.
- To employ numerous surface hybrids and potential site selectivity in mesoporous g-C_3N_4-based nanocomposites for the photoreduction of carbon dioxide, organic molecules (like phenol), metal ions, and so on.
- Further research into the composite structure of graphitic carbon nitride nanosheets and the interfacial interaction between these two phases is needed to inform the design of future structures.
- To develop multifunctional catalysts by fabricating innovative structured porous carbon nitride composites (core-shell, single crystal).
- For the purpose of cleaning up industrial wastewater containing several pollutants from different industries such as the printing, textile dyeing, and pesticide industries, among others.

REFERENCES

Abhilash, P. C., & Singh, N. (2009). Pesticide use and application: an Indian scenario. *Journal of hazardous materials*, *165*(1-3), 1-12.

Agarwal, A., Prajapati, R., Singh, O. P., Raza, S. K., & Thakur, L. K. (2015). Pesticide residue in water—a challenging task in India. *Environmental monitoring and assessment*, *187*, 1-21.

Agnihotri, D. N. (2000). Pesticide consumption in agriculture in India-an update. *Pesticide Research Journal*, *12*(1), 150-155.

Agoramoorthy, G., Chen, F. A., & Hsu, M. J. (2008). Threat of heavy metal pollution in halophytic and mangrove plants of Tamil Nadu, India. *Environmental pollution*, *155*(2), 320-326.

Ahmed, S., Rasul, M. G., Martens, W. N., Brown, R., & Hashib, M. A. (2011). Advances in heterogeneous photocatalytic degradation of phenols and dyes in wastewater: a review. *Water, Air, & Soil Pollution*, *215*, 3-29.

Ahmed, S., Rasul, M. G., Brown, R., & Hashib, M. A. (2011). Influence of parameters on the heterogeneous photocatalytic degradation of pesticides and phenolic contaminants in wastewater: a short review. *Journal of environmental management*, *92*(3), 311-330.

Ahmed, S., & Ollis, D. F. (1984). Solar photo-assisted catalytic decomposition of the chlorinated hydrocarbons trichloroethylene and trichloromethane. *Solar energy*, *32*(5), 597-601.

Akhtar, W., Sengupta, D., & Chowdhury, A. (2009). Impact of pesticides use in agriculture: their benefits and hazards. *Interdisciplinary toxicology*, *2*(1), 1.

Alavanja, M. C., Samanic, C., Dosemeci, M., Lubin, J., Tarone, R., Lynch, C. F., ... & Blair, A. (2003). Use of agricultural pesticides and prostate cancer risk in the Agricultural Health Study cohort. *American Journal of Epidemiology*, *157*(9), 800-814.

Allen, G. T., Veatch, J. K., Stroud, R. K., Vendel, C. G., Poppenga, R. H., Thompson, L., ... & Braselton, W. E. (1996). Winter poisoning of coyotes and raptors with Furadan-laced carcass baits. *Journal of Wildlife Diseases*, *32*(2), 385-389.

Altan, O., & Kalay, E. (2022). The influence of band bending phenomenon on photocatalytic Suzuki-Miyaura coupling reaction: The case of AgPd alloy nanoparticles supported on graphitic carbon nitride. *Applied Surface Science*, *580*, 152287.

Ameer, S., & Gul, I. H. (2016). Influence of reduced graphene oxide on effective absorption bandwidth shift of hybrid absorbers. *PLoS One*, *11*(6), e0153544.

Ammar, H. B., Brahim, M. B., Abdelhédi, R., & Samet, Y. (2016). Green electrochemical process for metronidazole degradation at BDD anode in aqueous solutions via direct and indirect oxidation. *Separation and Purification Technology*, *157*, 9-16.

Anand, N., Chakraborty, P., & Ray, S. (2021). Human exposure to organochlorine, pyrethroid, and neonicotinoid pesticides: Comparison between urban and semi-urban regions of India. *Environmental Pollution*, *270*, 116156

Anderson, S. W. and Yerraguntla, K. M. 2002. Remedial Alternatives for Agricultural Contamination. Proceedings-Waste Research Technology. No. 312.

Andreu, V. and Picó, Y. 2004. Determination of pesticides and their degradation products in soil: critical review and comparison of methods. TrAC Trends in Analytical Chemistry. 23(10-11), 772-789.

Anju, A., Ravi S, P., & Bechan, S. (2010). Water pollution with special reference to pesticide contamination in India. *Journal of Water Resource and Protection*, *2010*.

Arora, S. K., Batra, P., Sharma, T., Banerjee, B. D., & Gupta, S. (2013). Role of organochlorine pesticides in children with idiopathic seizures. *International Scholarly Research Notices*, *2013*.

Asadi, F., Goharshadi, E. K., & Sadeghinia, M. (2020). Highly Efficient Solar-Catalytic Degradation of Reactive Black 5 Dye Using Mesoporous Plasmonic Ag/g-C_3N_4 Nanocomposites. *Chemistry Select*, *5*(9), 2735-2745.

Ashesh, A., Singh, S., Devi, N. L., & Yadav, I. C. (2022). Organochlorine pesticides in multi-environmental matrices of India: A comprehensive review on characteristics, occurrence, and analytical methods. *Microchemical Journal*, 107306.

Aslam, I., Cao, C., Tanveer, M., Khan, W. S., Tahir, M., Abid, M., ... & Mahmood, N. (2014). The synergistic effect between WO_3 and gC_3N_4 towards efficient visible-light-driven photocatalytic performance. *New Journal of Chemistry*, *38*(11), 5462-5469.

Augugliaro, V., Palmisano, L., Schiavello, M., Sclafani, A., Marchese, L., Martra, G., & Miano, F. (1991). Photocatalytic degradation of nitrophenols in aqueous titanium dioxide dispersion. *Applied Catalysis*, *69*(1), 323-340.

Bai, J. G., Creehan, K. D., & Kuhn, H. A. (2007). Inkjet printable nanosilver suspensions for enhanced sintering quality in rapid manufacturing. *Nanotechnology*, *18*(18), 185701.

Balapanuru, J., Yang, J. X., Xiao, S., Bao, Q., Jahan, M., Polavarapu, L., ... & Loh, K. P. (2010). A graphene oxide–organic dye ionic complex with DNA-sensing and optical-limiting properties. *Angewandte Chemie International Edition*, *49*(37), 6549-6553.

Banday, M. U. D. D. A. S. I. R., Dhar, J. K., Aslam, S. H. A. F. I. Q. A., Qureshi, S. A. B. I. A., Jan, T. A. R. I. Q., & Gupta, B. H. A. V. N. A. (2012). Determination of pesticide residues in blood serum samples from inhabitants of "Dal Lake" hamlets in J&K, India (2008–2010). *Int. J. Pharm. Pharm. Sci*, *4*(5), 389-395.

Beydoun, D., Amal, R., Low, G., & McEvoy, S. (1999). Role of nanoparticles in photocatalysis. *Journal of Nanoparticle Research*, *1*, 439-458.

Bhanti, M., & Taneja, A. (2007). Contamination of vegetables of different seasons with organophosphorus pesticides and related health risk assessment in northern India. *Chemosphere*, *69*(1), 63-68.

Bhatia, S. C. (2017). *Pollution control in the textile industry*. CRC Press.

Bhatkhande, D. S., Pangarkar, V. G., & Beenackers, A. A. C. M. (2002). Photocatalytic degradation for environmental applications–a review. *Journal of Chemical Technology & Biotechnology: International Research in Process, Environmental & Clean Technology*, *77*(1), 102-116.

Bhushan, B., Saxena, P. N., & Saxena, N. (2013). Biochemical and histological changes in rat liver caused by cypermethrin and beta-cyfluthrin. *Archives of industrial hygiene and Toxicology*, *64*(1), 57-67.

Bishnu, A., Chakrabarti, K., Chakraborty, A., & Saha, T. (2009). Pesticide residue level in tea ecosystems of Hill and Dooars regions of West Bengal, India. *Environmental monitoring and assessment*, *149*, 457-464.

Biswal, N. 2011. Efficient Hydrogen Production by Composite Photocatalyst CdSZnS/Zirconium-Titanium Phosphate (ZTP) under Visible Light Illumination. Int. J. Hydrogen Energy. 36 (21), 13452–13460.

Blankson, G.K., Osei-Fosu, P., Adeendze, E.A., Ashie, D., (2016). Contamination levels of organophosphorus and synthetic pyrethroid pesticides in vegetables marketed in Accra, Ghana. Food Control 68, 174–180.

Boedeker, W., Watts, M., Clausing, P., & Marquez, E. (2020). The global distribution of acute unintentional pesticide poisoning: estimations based on a systematic review. *BMC public health*, *20*(1), 1-19.

Bolognesi, C., Merlo, F.D., (2011). Pesticides: Human Health Effects. National Cancer Research Institute, Genoa, Italy.

Bolognesi, C., Peluso, M., Degan, P., Rabboni, R., Munnia, A., & Abbondandolo, A. (1994). Genotoxic effects of the carbamate insecticide, methomyl. II. In vivo, studies with pure compound and the technical formulation, "lannate 25". *Environmental and molecular mutagenesis*, *24*(3), 235-242.

Bondarenko, S., Gan, J., Haver, D. L., & Kabashima, J. N. (2004). Persistence of selected organophosphate and carbamate insecticides in waters from a coastal watershed. *Environmental Toxicology and Chemistry: an International Journal*, *23*(11), 2649-2654.

Bonvoisin, T., Utyasheva, L., Knipe, D., Gunnell, D., & Eddleston, M. (2020). Suicide by pesticide poisoning in India: a review of pesticide regulations and their impact on suicide trends. *BMC public health*, *20*(1), 1-16.

Breffle, W. S., Muralidharan, D., Donovan, R. P., Liu, F., Mukherjee, A., & Jin, Y. (2013). Socioeconomic evaluation of the impact of natural resource stressors on human-use services

in the Great Lakes environment: a Lake Michigan case study. *Resources Policy*, *38*(2), 152-161.

Brinzila, C. I., Pacheco, M. J., Ciríaco, L., Ciobanu, R. C., & Lopes, A. (2012). Electrodegradation of tetracycline on BDD anode. *Chemical Engineering Journal*, *209*, 54-61.

Brown, P., Charlton, A., Cuthbert, M., Barnett, L., Ross, L., Green, M., ... & Fletcher, M. (1996). Identification of pesticide poisoning in wildlife. *Journal of Chromatography A*, *754*(1-2), 463-478.

Burrows, H. D. 2002. Reaction pathways and mechanisms of photodegradation of pesticides. J. Photochem. Photobiol. B, 67, 71–108.

Bustos-Ramirez, K.; Barrera-Diaz, C.E.; Icaza-Herrera, M.D.; Martinez-Hernandez, A.L.; Natividad-Rangel, R.; Velasco-Santos, C. 4-chlorophenol removal from water using graphite and graphene oxides as photocatalysts. *J. Environ. Health Sci. Eng.* **2015**, *13*, 33.

Cahill, M. G., Caprioli, G., Stack, M., Vittori, S., & James, K. J. (2011). Semi-automated liquid chromatography–mass spectrometry (LC–MS/MS) method for basic pesticides in wastewater effluents. *Analytical and bioanalytical chemistry*, *400*, 587-594.

Cao, K., Jiang, Z., Zhang, X., Zhang, Y., Zhao, J., Xing, R., ... & Pan, F. (2015). Highly water-selective hybrid membrane by incorporating g-C_3N_4 nanosheets into the polymer matrix. *Journal of Membrane Science*, *490*, 72-83.

Cao, W., Liu, L., Yuan, R., & Wang, H. (2022). High-efficiency electrochemiluminescence of 3D porous g-C_3N_4 with dissolved O_2 as co-reactant and its sensing application for ultrasensitive detection of microRNA in tumor cells. *Biosensors and Bioelectronics*, *214*, 114506.

Carbamate pesticides: a general introduction (EHC 64, 1986) WHO ISBN 92 4 154264 0

Carvalho, F. P. (2006). Agriculture, pesticides, food security, and food safety. *Environmental science & policy*, *9*(7-8), 685-692.

Celaya, C.A.; Delesma, C.; Valades-Pelayo, P.J.; Jaramillo-Quintero, O.A.; Castillo-Araiza, C.O.; Ramos, L.; Sebastian, P.J.; Muniz, J. Exploring the potential of graphene oxide as a functional material to produce hydrocarbons via photocatalysis: Theory meets experiment. *Fuel* **2020**, *271*, 117616.

Chai, L. K., Wong, M. H., & Hansen, H. C. B. (2013). Degradation of chlorpyrifos in humid tropical soils. *Journal of environmental management*, *125*, 28-32.

Chandra, S., Kumar, M., Mahindrakar, A. N., & Shinde, L. P. (2014). Effect of washing on residues of chlorpyrifos and Monocrotophos in vegetables. *Int J Adv Res*, *2*, 744-750.

Chang, X.; Yao, X.; Ding, N.; Yin, X.; Zheng, Q.; Lu, S.; Shuai, D.; Sun, Y. Photocatalytic degradation of trihalomethanes and haloacetonitriles on graphitic carbon nitride under visible light irradiation. *Sci. Total Environ.* **2019**, *682*, 200–207.

Chauhan, R, and Kumar, A. 2012. Photocatalytic Studies of Silver Doped ZnO Nanoparticles Synthesized by Chemical Precipitation Method. J Sol-Gel Sci Technol. 546–53. doi:10.1007/s10971-012-2818-3.

Che, H., Xiao, L., Zhou, W., Zhou, Q., Li, H., Hu, P., ... & Wang, H. (2022). Decorating tungsten oxide on g-C3N4 nanosheet as Z-scheme heterogeneous photocatalyst for efficient hydrogen evolution. *Journal of Alloys and Compounds*, *896*, 162931.

Chen, C., Cai, W., Long, M., Zhou, B., Wu, Y., Wu, D., & Feng, Y. (2010). Synthesis of visible-light responsive graphene oxide/TiO2 composites with p/n heterojunction. *ACS nano*, *4*(11), 6425-6432.

Chen, F., Yan, F., Chen, Q., Wang, Y., Han, L., Chen, Z., & Fang, S. (2014). Fabrication of Fe_3O_4@ SiO_2@ TiO_2 nanoparticles supported by graphene oxide sheets for the repeated adsorption and photocatalytic degradation of rhodamine B under UV irradiation. *Dalton Transactions*, *43*(36), 13537-13544.

Chen, F., Yang, H., Luo, W., Wang, P., & Yu, H. (2017). Selective adsorption of thiocyanate anions on Ag-modified g-C_3N_4 for enhanced photocatalytic hydrogen evolution. *Chinese Journal of Catalysis*, *38*(12), 1990-1998.

Chen, J., Zhao, D., Diao, Z., Wang, M., Guo, L., & Shen, S. (2015). Bifunctional modification of graphitic carbon nitride with $MgFe_2O_4$ for enhanced photocatalytic hydrogen generation. *ACS Applied Materials & Interfaces*, *7*(33), 18843-18848.

Chen, X., Jun, Y. S., Takanabe, K., Maeda, K., Domen, K., Fu, X., ... & Wang, X. (2009). Ordered mesoporous SBA-15 type graphitic carbon nitride: a semiconductor host structure for

photocatalytic hydrogen evolution with visible light. *Chemistry of Materials*, *21*(18), 4093-4095.

Chen, Z., Chen, W., Liao, G., Li, X., Wang, J., Tang, Y., & Li, L. (2022). The flexible construct of N vacancies and hydrophobic sites on g-C_3N_4 by F doping and their contribution to PFOA degradation in photocatalytic ozonation. *Journal of Hazardous Materials*, *428*, 128222.

Chowdhury, S., & Balasubramanian, R. (2014). Graphene/semiconductor nanocomposites (GSNs) for heterogeneous photocatalytic decolorization of wastewaters contaminated with synthetic dyes: a review. *Applied Catalysis B: Environmental*, *160*, 307-324.

Christensen, K., Harper, B., Luukinen, B., Buhl, K., & Stone, D. (2009). Chlorpyrifos technical fact sheet. *National Pesticide Information Center, Oregon State University Extension Services*.

Chu, Y., Fan, J., Wang, R., Liu, C., & Zheng, X. (2022). Preparation and immobilization of Bi2WO6/BiOI/g-C3N4 nanoparticles for the photocatalytic degradation of tetracycline and municipal waste transfer station leachate. *Separation and Purification Technology*, *300*, 121867.

Cruz, M.; Gomez, C.; Duran-Valle, C.J.; Pastrana-Martinez, L.M.; Faria, J.L.; Silva, A.M.T.; Faraldos, M.; Bahamonde, A. Bare TiO_2 and graphene oxide TiO_2 photocatalysts on the degradation of selected pesticides and influence of the water matrix. *Appl. Surf. Sci.* **2017**, *416*, 1013–1021.

Cui, Y., Guo, J., Xu, B., & Chen, Z. (2011). Genotoxicity of chlorpyrifos and cypermethrin to ICR mouse hepatocytes. *Toxicology Mechanisms and Methods*, *21*(1), 70-74.

Cui, Y.; Huang, J.; Fu, X.; Wang, X. Metal-free photocatalytic degradation of 4-chlorophenol in water by mesoporous carbon nitride semiconductors. *Catal. Sci. Technol.* **2012**, *2*, 1396–1402.

Curtis, C., & Olsen, C. P. (2004). The Africa Stockpiles Programme: cleaning up obsolete pesticides; contributing to a healthier future. *Industry and Environment*, *27*(2), 37-38.

Cycoń, M., Żmijowska, A., Wójcik, M., & Piotrowska-Seget, Z. (2013). Biodegradation and bioremediation potential of diazinon-degrading Serratia marcescens to remove other organophosphorus pesticides from soils. *Journal of Environmental Management*, *117*, 7-16.

Dadigala R, Bandi R, Gangapuram BR, Dasari A, Belay HH, Guttena V. Fabrication of novel 1D/2D V_2O_5/g-C_3N_4 composites as Z-scheme photocatalysts for CR degradation and Cr (VI) reduction under sunlight irradiation. J Environ Chem Eng 2019;7:102822.

Dalvie, M. A., Africa, A., & London, L. (2006). Disposal of unwanted pesticides in Stellenbosch, South Africa. *Science of the total environment*, *361*(1-3), 8-17.

Dangwang Dikdim, J.M.; Gong, Y.; Noumi, G.B.; Sieliechi, J.M.; Zhao, X.; Ma, N.; Yang, M.; Tchatchueng, J.B. Peroxymonosulfate improved photocatalytic degradation of atrazine by activated carbon/graphitic carbon nitride composite under visible light irradiation. *Chemosphere* **2019**, *217*, 833–842.

Dar, M. A., Hamid, B., & Kaushik, G. (2023). Temporal trends in the use and concentration of organophosphorus pesticides in Indian riverine water, toxicity, and their risk assessment. *Regional Studies in Marine Science*, 102814.

Davies, J. E. D., & Jabeen, N. (2003). The adsorption of herbicides and pesticides on clay minerals and soils. Part 2. Atrazine. *Journal of inclusion phenomena and macrocyclic chemistry*, *46*, 57-64.

De Angelis, M., Piccolo, M., Vannini, L., Siragusa, S., De Giacomo, A., Serrazzanetti, D. I., ... & Francavilla, R. (2013). Fecal microbiota and metabolome of children with autism and pervasive developmental disorder not otherwise specified. *PloS one*, *8*(10), e76993.

De Angelis, S., Tassinari, R., Maranghi, F., Eusepi, A., Di Virgilio, A., Chiarotti, F., ... & Mantovani, A. (2009). Developmental exposure to chlorpyrifos induces alterations in thyroid and thyroid hormone levels without other toxicity signs in Cd1 mice. *Toxicological Sciences*, *108*(2), 311-319.

Dehghani, M. H. and Fadaei, A. M. 2012. Photocatalytic Degradation of Organophosphorus Pesticide using Zinc Oxide. Research Journal of Chemistry and Environment. 16 (3).

Dehghani, M. H., Niasar, Z. S., Mehrnia, M. R., Shayeghi, M., Al-Ghouti, M. A., Heibati, B., ... & Yetilmezsoy, K. (2017). Optimizing the removal of organophosphorus pesticide malathion from water using multi-walled carbon nanotubes. *Chemical Engineering Journal*, *310*, 22-32.

Deng, X., Wang, D., Li, H., Jiang, W., Zhou, T., Wen, Y., ... & Wang, L. (2022). Boosting interfacial charge separation and photocatalytic activity of 2D/2D g-C_3N_4/$ZnIn_2S_4$ S-scheme heterojunction under visible light irradiation. *Journal of Alloys and Compounds*, *894*, 162209.

Desore, A., & Narula, S. A. (2018). An overview of the corporate response towards sustainability issues in the textile industry. *Environment, Development and Sustainability*, *20*, 1439-1459.

Devi, M.; Das, B.; Barbhuiya, M.H.; Bhuyan, B.; Dhar, S.S.; Vadivel, S. Fabrication of nanostructured NiO/WO_3 with graphitic carbon nitride for visible light-driven photocatalytic hydroxylation of benzene and metronidazole degradation. *New J. Chem.* **2019**, *43*, 14616–14624.

Devi, P. I. 2009. Health risk perceptions, awareness and handling behavior of pesticides by farm workers. Agricultural Economics Research Journal. 22(9): 263- 268.

Devi, P. I. 2010. Pesticide in agriculture—A boon or a curse? A case study of Kerala. Economic and Political Weekly. 45: 26-27.

Devi, P. I.; Thomas, J.; Raju, R. K. 2017. Pesticide Consumption in India: A Spatiotemporal Analysis. Agricultural Economics Research Review. 30 (1), 163– 172.

Di, Y., Wang, X., Thomas, A., & Antonietti, M. (2010). Making Metal Carbon Nitride Heterojunctions for Improved Photocatalytic Hydrogen Evolution with Visible Light. *ChemCatChem*, *2*(7), 834-838.

Diban, N., Aguayo, A. T., Bilbao, J., Urtiaga, A., & Ortiz, I. (2013). Membrane reactors for in situ water removal: a review of applications. *Industrial & Engineering Chemistry Research*, *52*(31), 10342-10354.

Directorate of Plant Protection, Quarantine, and Storage report | GOI, 2021.

Di-shun, Z., Jia-lei, W., Xue-heng, Z., & Juan, Z. (2009). TiO2/NaY composite as photocatalyst for degradation of omethoate. *Chemical Research in Chinese Universities*, *25*(4), 543-549.

Duirk, S. E and Collette, T.W. 2005. National Exposure, and U S Environmental Protection Agency. Organophosphate Pesticide Degradation under Drinking Water Treatment Conditions. EPA/600/R-05/103.

Echavia, G. R. M., Matzusawa, F., and Negishi, N. 2009. Photocatalytic degradation of organophosphate and phosphonoglycine pesticides using TiO2 immobilized on silica gel, Chemosphere. 76, 595–600.

Ecobichon, D. (2019). CarbamicAcidEsterInsecticides. In Pesticides and Neurological Diseases (pp. 263–302). CRC Press

Ecobichon, D. J. (2001). Pesticide use in developing countries. *Toxicology*, *160*(1-3), 27-33.

Elliott, J. E., Wilson, L. K., Langelier, K. M., Mineau, P., & Sinclair, P. H. (1997). Secondary poisoning of birds of prey by the organophosphorus insecticide, phorate. *Ecotoxicology*, *6*, 219-231.

Elliott, M. (1980). Established pyrethroid insecticides. *Pesticide Science*, *11*(2), 119-128.

El-Shafai, N.M.; El-Khouly, M.E.; El-Kemary, M.; Ramadan, M.S.; Derbalah, A.S.; Masoud, M.S. Fabrication and characterization of graphene oxide–titanium dioxide nanocomposite for degradation of some toxic insecticides. *J. Ind. Eng. Chem.* **2019**, *69*, 315–323.

El-Sheikh, S. M., Khedr, T. M., Zhang, G., Vogiazi, V., Ismail, A. A., O'Shea, K., & Dionysiou, D. D. (2017). Tailored synthesis of anatase–brookite heterojunction photocatalysts for degradation of cylindrospermopsin under UV–Vis light. *Chemical Engineering Journal*, *310*, 428-436.

El-Sheshtawy, H. S., El-Hosainy, H. M., Shoueir, K. R., El-Mehasseb, I. M., & El-Kemary, M. (2019). Facile immobilization of Ag nanoparticles on g-C_3N_4/V_2O_5 surface for enhancement of post-illumination, catalytic, and photocatalytic activity removal of organic and inorganic pollutants. *Applied Surface Science*, *467*, 268-276.

Elshikh, M. S., Al-Hemaid, F. M., Chen, T. W., Chinnapaiyan, S., Ali, M. A., & Chen, S. M. (2020). Sonochemical synthesis of graphitic carbon nitrides-wrapped bimetal oxide nanoparticles hybrid materials and their electrocatalytic activity for xanthine electro-oxidation. *Ultrasonics Sonochemistry*, *64*, 105006.

El-Temsah Y. S. and Joner E. J. 2012. Impact of Fe and Ag nanoparticles on seed germination and differences in bioavailability during exposure in aqueous suspension and soil. Environ Toxicol. 27:42–49.

Engel, L. S., Hill, D. A., Hoppin, J. A., Lubin, J. H., Lynch, C. F., Pierce, J., ... & Alavanja, M. C. (2005). Pesticide use and breast cancer risk among farmers' wives in the agricultural health study. *American Journal of Epidemiology*, *161*(2), 121-135.

Evgenidou, E., Fytianos, K., & Poulios, I. (2005). Photocatalytic oxidation of dimethoate in aqueous solutions. *Journal of Photochemistry and Photobiology A: Chemistry*, *175*(1), 29-38.

Fadaei, A., & Kargar, M. (2013). Photocatalytic degradation of chlorpyrifos in water using titanium dioxide and zinc oxide. *Fresenius Environ Bull*, *22*(8A), 2442-2447.

Feng, L., Cheng, Y., Zhang, Y., Li, Z., Yu, Y., Feng, L., ... & Xu, L. (2020). Distribution and human health risk assessment of antibiotic residues in large-scale drinking water sources in the Chongqing area of the Yangtze River. *Environmental Research*, *185*, 109386.

Fenoll, J. et al. 2011. Heterogeneous Photocatalytic Oxidation of Cyprodinil and Fludioxonil in Leaching Water under Solar Irradiation. Chemosphere. 85 (8): 1262–68. doi:10.1016/j.chemosphere.2011.07.022.

Fenoll, J. et al. 2013. Degradation Intermediates and Reaction Pathway of Carbofuran in Leaching Water Using TiO2 and ZnO as Photocatalysts under Natural Sunlight.‖ Journal of Photochemistry and Photobiology A: Chemistry. 251. 2013. 33–40. doi:10.1016/j.jphotochem.2012.10.012.

Fikes, J. D. (1990). Organophosphorus and carbamate insecticides. *Veterinary Clinics of North America: Small Animal Practice*, *20*(2), 353-367.

Foroughi, M., Arezoomand, H. R. S., Rahmani, A. R., Asgari, G., Nematollahi, D., Yetilmezsoy, K., & Samarghandi, M. R. (2017). Electrodegradation of tetracycline using stainless steel net electrodes: screening of main effective parameters and interactions using a two-level factorial design. *Korean Journal of Chemical Engineering*, *34*, 2999-3008.

Fox, Marye Anne, and Maria T. Dulay. "Heterogeneous photocatalysis." *Chemical Reviews* 93.1 (1993): 341-357.

FSSAI, 2011. Food Safety and Standards (Contaminants, Toxins, and Residues) Regulations, 2011. https://www.fssai.gov.in/upload/uploadfiles/files/Compendium_Contaminants_Regulations_20_08_2020.pdf.

Fukuto, T. R. (1990). Mechanism of action of organophosphorus and carbamate insecticides. *Environmental health perspectives*, *87*, 245-254.

Furlong, C. E., Holland, N., Richter, R. J., Bradman, A., Ho, A., & Eskenazi, B. (2006). PON1 status of farmworker mothers and children as a predictor of organophosphate sensitivity. *Pharmacogenetics and genomics*, *16*(3), 183-190.

Gaddam, S.K.; Pothu, R.; Boddula, R. Graphitic carbon nitride (g-C3N4) reinforced polymer nanocomposite systems—A review. *Polym. Compos.* **2019**, *41*, 430–442.

Gao, J., Liu, L., Liu, X., Zhou, H., Lu, J., Huang, S., & Wang, Z. (2009). The occurrence and spatial distribution of organophosphorus pesticides in Chinese surface water. *Bulletin of environmental contamination and Toxicology*, *82*, 223-229.

Gao, R. H., Ge, Q., Jiang, N., Cong, H., Liu, M., & Zhang, Y. Q. (2022). Graphitic carbon nitride (g-C_3N_4)-based photocatalytic materials for hydrogen evolution. *Frontiers in Chemistry*, *10*.

Garcia J. C. and Takashima K. (2003). Photocatalytic degradation of imazaquin in an aqueous suspension of titanium dioxide J. Photochem. Photobio. A: Chem. 155, 215-222.

Gaya, U. I. and Abdullah, A. H. (2008). Heterogeneous Photocatalytic Degradation of Organic Contaminants over Titanium Dioxide: A Review of Fundamentals, Progress, and Problems. J. Photochem. Photobiol. C Photochem. Rev. 9 (1), 1–12.

Gebremariam, S. Y., Beutel, M. W., Yonge, D. R., Flury, M., & Harsh, J. B. (2012). Adsorption and desorption of chlorpyrifos to soils and sediments. *Reviews of environmental contamination and toxicology*, 123-175.

Gholami, P., Khataee, A., Soltani, R. D. C., & Bhatnagar, A. (2019). A review on carbon-based materials for heterogeneous sonocatalysis: fundamentals, properties and applications. *Ultrasonics Sonochemistry*, *58*, 104681.

Gholipour, B., Zonouzi, A., Shokouhimehr, M., & Rostamnia, S. (2022). Integration of plasmonic AgPd alloy nanoparticles with single-layer graphitic carbon nitride as Mott-Schottky junction toward photo-promoted H2 evolution. *Scientific Reports*, *12*(1), 13583.

Ghosh, P. G., Sawant, N. A., Patil, S. N., & Aglave, B. A. (2010). Microbial biodegradation of organophosphate pesticides. *International Journal of Biotechnology & Biochemistry*, *6*(6), 871-877.

Ghosh, S., Tiwari, S. S., Srivastava, S., Sharma, A. K., Kumar, S., Ray, D. D., & Rawat, A. K. S. (2013). Acaricidal properties of Ricinus communis leaf extracts against organophosphate and pyrethroids resistant Rhipicephalus (Boophilus) microplus. *Veterinary Parasitology*, *192*(1-3), 259-267.

Glaze, W. H., Kang, J. W., & Chapin, D. H. (1987). The chemistry of water treatment processes involves ozone, hydrogen peroxide,and ultraviolet radiation.

Goddard, J. Bed Bugs (Cimex lectularius L.) in Mississippi: Survey of the Scope, Extent, and Control of the Problem.

Goodall, J. B., Kellici, S., Illsley, D., Lines, R., Knowles, J. C., & Darr, J. A. (2014). Optical and photocatalytic behaviours of nanoparticles in the Ti–Zn–O binary system. *Rsc Advances*, *4*(60), 31799-31809.

Grube, A., Donaldson, D., Kiely, T., & Wu, L. (2011). Pesticides industry sales and usage. *US EPA, Washington, DC*.

Guan, W., Long, Z., Liu, J., Hua,Y., Ma, Y., & Zhang, H. (2015). Unique graphitic carbon nitride snanovessels as recyclable adsorbent for solid phase extraction of benzoylurea pesticides in juices samples. *Food analytical methods*, *8*, 2202-2210.

Guidelines for Drinking Water Quality. 4th ed., World Health Organization (WHO) " Geneva, Switzerland, (2011).

Güler, S. H., Güler, Ö., Evin, E., & Islak, S. (2016). Electrical and optical properties of ZnO-milled Fe2O3 nanocomposites produced by powder metallurgy route. *Optik*, *127*(6), 3187-3191.

Guo, X., Ge, J., Yang, C., Wu, R., Dang, Z., & Liu, S. (2015). Sorption behavior of tylosin and sulfamethazine on humic acid: kinetic and thermodynamic studies. *RSC advances 5*(72), 58865-58872.

Guo, X., Zhang, J., Ge, J., Yang, C., Dang, Z., Liu, S., & Gao, L. (2015). Sorption and photodegradation of tylosin and sulfamethazine by humic acid-coated goethite. *RSC advances*, *5*(122), 100464-100471.

Gupta, R. C. (1994). Carbofuran toxicity. *Journal of Toxicology and Environmental Health, Part A Current Issues*, *43*(4), 383-418.

Han, C.; Ge, L.; Chen, C.; Li, Y.; Xiao, X.; Zhang, Y.; Guo, L. Novel visible light-induced Co_3O_4 -g-C_3N_4 heterojunction photocatalysts for efficient degradation of methyl orange. Appl. Catal. B Environ. 2014, 147, 546–553.

Han, W., Zhu, W., Zhang, P., Zhang, Y., & Li, L. (2004). Photocatalytic degradation of phenols in aqueous solution under irradiation of 254 and 185 nm UV light. *Catalysis Today*, *90*(3-4), 319-324.

Harris, T. D., & Smith, V. H. (2016). Do persistent organic pollutants stimulate cyanobacterial blooms? *Inland Waters*, *6*(2), 124-130.

Hashmi, T. A., Qureshi, R., Tipre, D., & Menon, S. (2020). Investigation of pesticide residues in water, sediments and fish samples from Tapi River, India as a case study and its forensic significance. *Environmental Forensics*, *21*(1), 1-10.

Hassan, A. E., Elsayed, M. H., Hussien, M. S., Mohamed, M. G., Kuo, S. W., Chou, H. H., ... & Wen, Z. (2022). V_2O_5 nanoribbons/N-deficient g-C_3N_4 heterostructure for enhanced visible-light photocatalytic performance. *International Journal of Hydrogen Energy*.

Hassan, M. M., & Carr, C. M. (2018). A critical review of recent advancements in the removal of reactive dyes from dyehouse effluent by ion-exchange adsorbents. *Chemosphere*, *209*, 201-219.

Haviland, J. A., Butz, D. E., & Porter, W. P. (2010). Long-term sex-selective hormonal and behavioral alterations in mice exposed to low doses of chlorpyrifos in utero. *Reproductive Toxicology*, *29*(1), 74-79.

Hayes W (2001) Principles and methods of toxicology, 4th ed. Taylor and Francis, London, pp 587–591

Helfrich, L. A., Weigmann, D. L., Hipkins, P. A., & Stinson, E. R. (2009). Pesticides and aquatic animals: a guide to reducing impacts on aquatic systems.

Herrmann, J. M., & Guillard, C. (2000). Photocatalytic degradation of pesticides in agricultural used waters. *Comptes Rendus de l'Académie des Sciences-Series IIC-Chemistry*, *3*(6), 417-422.

Hill EF (1989) Brain divergent effects of post-mortem ambient temperature on organophosphorus and carbamate-inhibited brain cholinesterase activity in birds. Pestic Biochem Physiol 33:264–275

Hill EF, Fleming WJ (1982) Anticholinesterase poisoning in birds. Field monitoring and diagnosis of acute poisoning. Environ Toxicol Chem 1:27–38

Hodgson E, Roe RM, Motoyama N (1991) Pesticides and the future: toxicological studies of risks and benefits. Rev Pestic Toxicol 1:3–12

Hoertz, P. G., & Mallouk, T. E. (2005). Light-to-chemical energy conversion in lamellar solids and thin films. *Inorganic chemistry*, *44*(20), 6828-6840.

Hoffmann, M. R., Martin, S. T., Choi, W., & Bahnemann, D. W. (1995). Environmental applications of semiconductor photocatalysis. *Chemical Reviews*, *95*(1), 69-96.

Hogan, M., Patmore, L., Latshaw, G., & Seidman, H. (1973). Computer Modeling of Pesticide Transport in Soil for Five Instrumented Water sheds, Prepared for the UA Environmental Protection Agency Southeast Water Laboratory, Arthens, CA by ESL Inc. *Sunny Vale, California*.

Hong, J., Xia, X., Wang, Y., & Xu, R. (2012). Mesoporous carbon nitride with in situ sulfur doping for enhanced photocatalytic hydrogen evolution from water under visible light. *Journal of Materials Chemistry*, *22*(30), 15006-15012.

Hong, Y., Jiang, Y., Li, C., Fan, W., Yan, X., Yan, M., & Shi, W. (2016). In-situ synthesis of direct solid-state Z-scheme V_2O_5/g-C_3N_4 heterojunctions with enhanced visible light

efficiency in photocatalytic degradation of pollutants. *Applied Catalysis B: Environmental*, *180*, 663-673.

Hopkins AW, Scholz LN (2006) Ecotoxicology of anticholinesterase pesticides: data gaps and research challenges. Environ Toxicol Chem 25(5):1185–1186

Howard, J. (2018). Toxic 17 Disorders. *Myasthenia Gravis and Related Disorders*, *275*.

Hu, S., Ma, L., You, J., Li, F., Fan, Z., Lu, G., ... & Gui, J. (2014). The enhanced visible light photocatalytic performance of g-C_3N_4 photocatalysts co-doped with iron and phosphorus. *Applied surface science*, *311*, 164-171.

Hua, F., Yunlong, Y. U., Xiaoqiang, C. H. U., Xiuguo, W. A. N. G., Xiaoe, Y. A. N. G., & Jingquan, Y. U. (2009). Degradation of chlorpyrifos in laboratory soil and its impact on soil microbial functional diversity. *Journal of Environmental Sciences*, *21*(3), 380-386.

Huang, J., Hu, J., Shi, Y., Zeng, G., Cheng, W., Yu, H., ... & Yi, K. (2019). Evaluation of self-cleaning and photocatalytic properties of modified g-C_3N_4 based PVDF membranes driven by visible light. *Journal of colloid and interface science*, *541*, 356-366.

Huang, W., Ruan, S., Zhao, M., Xu, R., Chen, Z., Zhihong, G., & Song, H. (2021). Visible-light-driven photocatalytic inactivation of Escherichia coli by 0D/$_2$D CeO_2/g-C_3N_4 heterojunction: bactericidal performance and mechanism. *Journal of Environmental Chemical Engineering*, *9*(6), 106759.

Huang, Y., Mei, F., Zhang, J., Dai, K., & Dawson, G. (2022). Construction of 1D/2D W18O49/porous g-C_3N_4 S-scheme heterojunction with enhanced photocatalytic H_2 evolution. *Acta Phys. Chim. Sin.*, *38*(7), 2108028.

Hwang, S., Lee, S., & Yu, J. S. (2007). Template-directed synthesis of highly ordered nanoporous graphitic carbon nitride through polymerization of cyanamide. *Applied surface science*, *253*(13), 5656-5659.

Imbar, A., Vadivel, V. K., & Mamane, H. (2023). Solvothermal Synthesis of g-C3N4/TiO2 Hybrid Photocatalyst with a Broaden Activation Spectrum. *Catalysts*, *13*(1), 46.

Iqbal, N. (2021). Tailoring g-C_3N_4 with lanthanum and cobalt oxides for enhanced photoelectrochemical and photocatalytic activity. *Catalysts*, *12*(1), 15.

Iqbal, N., Afzal, A., Khan, I., Khan, M. S., & Qurashi, A. (2021). Molybdenum-impregnated g-C_3N_4 nanotubes as potentially active photocatalysts for renewable energy applications. *Scientific Reports*, *11*(1), 16886.

Iqbal, N., Khan, I., Ali, A., & Qurashi, A. (2022). A sustainable molybdenum oxysulphide-cobalt phosphate photocatalyst for effectual solar-driven water splitting. *Journal of Advanced Research*, *36*, 15-26.

Iqbal, S., Ahmad, N., Javed, M., Qamar, M. A., Bahadur, A., Ali, S., ... & Qayyum, M. A. (2021). Designing highly potential photocatalytic comprising silver deposited ZnO NPs with sulfurized graphitic carbon nitride (Ag/ZnO/Sg-C_3N_4) ternary composite. *Journal of Environmental Chemical Engineering*, *9*(1), 104919.

Islam, N. M., Chatterjee, M., Ikushima, Y., Yokoyama, T., & Kawanami, H. (2010). Development of a novel catalytic membrane reactor for heterogeneous catalysis in supercritical CO_2. *International Journal of Molecular Sciences*, *11*(1), 164-172.

Ismael, M., & Wu, Y. (2019). A facile synthesis method for fabrication of LaFeO $_3$/gC_3N_4 nanocomposite as efficient visible-light-driven photocatalyst for photodegradation of RhB and 4-CP. *New Journal of Chemistry*, *43*(35), 13783-13793.

Ismael, M., Elhaddad, E., Taffa, D. H., & Wark, M. (2018). Solid state route for the synthesis of $YFeO_3$/g-C_3N_4 composites and its visible light activity for degradation of organic pollutants. *Catalysis Today*, *313*, 47-54.

Ismael, M., Wu, Y., Taffa, D. H., Bottke, P., & Wark, M. (2019). Graphitic carbon nitride synthesized by simple pyrolysis: role of precursor in photocatalytic hydrogen production. *New Journal of Chemistry*, *43*(18), 6909-6920.

Jacob, J., & Buckle, A. (2018). Use of anticoagulant rodenticides in different applications around the world. *Anticoagulant rodenticides and wildlife*, 11-43.

Jacobs, A. (2015). Timeline-history of pesticides. *Pesticides & University of Oregon. Available from http://blogs. uoregon. edu/ajacobssu13gateway/timeline/. Accessed Jan*, *14*, 2015.

Janotti, A., Jalan, B., & Stemmer, S. (2009). C. G V. d. Walle. *Rep. Prog. Phys*, *72*, 126501.

Jayaraj, R., Megha, P., & Sreedev, P. (2016). Organochlorine pesticides, their toxic effects on living organisms, and their fate in the environment. *Interdisciplinary toxicology*, *9*(3-4), 90-100.

Jeffrey F B., Ellen M. C., Courtney G., Emina H., P. Lee F., Claudia K. G., Mark R. W, "Chlorpyrifos degradation via photoreactive TiO_2 nanoparticles: Assessing the impact of a multi-component degradation scenario" J Hazard Mater. **372**: 61–68 (2019).

Jing, P., Wei, W., Luo, W., Li, X., Xu, F., Li, H., ... & Liu, G. (2020). In-situ XRD study of the structure and electrochemical performance of V_2O_5 nanosheets in aqueous zinc ion batteries. *Inorganic Chemistry Communications*, *117*, 107953.

Jo, W.-K.; Natarajan, T.S. Influence of TiO_2 morphology on the photocatalytic efficiency of direct Z-scheme g-C_3N_4/TiO_2 photocatalysts for isoniazid degradation. *Chem. Eng. J.* **2015**, *281*, 549–565.

John, E. M., & Shaike, J. M. (2015). Chlorpyrifos: pollution and remediation. *Environmental Chemistry Letters*, *13*, 269-291.

Johnson, A. M., Ou, Z. Y. A., Gordon, R., & Saminathan, H. (2022). Environmental neurotoxicants and inflammasome activation in Parkinson's disease–a focus on the gut-brain axis. *The International Journal of Biochemistry & Cell Biology*, *142*, 106113.

Kadhiru, S., Patil, S., & D'Souza, R. (2022). Effect of pesticide toxicity in aquatic environments: A recent review. *Int. J. Fish Aquat. Stud*, *10*(3), 113-118.

Kalyani, R., & Gurunathan, K. (2018). Effective harvesting of UV induced production of excitons from Fe_3O_4 with proficient rGO-PTh acting as BI-functional redox photocatalyst. *Renewable Energy*, *115*, 1035-1042.

Kamrin, M. A. (1997). *Pesticide profiles: toxicity, environmental impact, and fate*. CRC press.

Kannuri, N. K., & Jadhav, S. (2018). Generating toxic landscapes: impathe ct on well-being of cotton farmers in Telangana, India. *Anthropology & Medicine*, *25*(2), 121-140.

Karalliedde, L., & Senanayake, N. (1989). Organophosphorus insecticide poisoning. *British Journal of Anaesthesia*, *63*(6), 736-750.

Katsikantami, I., Colosio, C., Alegakis, A., Tzatzarakis, M. N., Vakonaki, E., Rizos, A. K., ... & Tsatsakis, A. M. (2019). Estimation of daily intake and risk assessment of organophosphorus pesticides based on biomonitoring data–the internal exposure approach. *Food and chemical toxicology*, *123*, 57-71.

Katsumata, H., Matsuba, K., Kaneco, S., Suzuki, T., Ohta, K., & Yobiko, Y. (2005). Degradation of carbofuran in aqueous solution by Fe (III) aquacomplexes as effective photocatalysts. *Journal of Photochemistry and Photobiology A: Chemistry*, *170*(3), 239-245.

Kaur, R., Mavi, G. K., Raghav, S., & Khan, I. (2019). Pesticides classification and its impact on the environment. *Int. J. Curr. Microbiol. Appl. Sci*, *8*(3), 1889-1897.

Kenko, D. B. N., Ngameni, N. T., Awo, M. E., Njikam, N. A., & Dzemo, W. D. (2023). Does pesticide use in agriculture present a risk to the terrestrial biota? *Science of The Total Environment*, *861*, 160715.

Kesarla, M. K., Fuentez-Torres, M. O., Alcudia-Ramos, M. A., Ortiz-Chi, F., Espinosa-González, C. G., Aleman, M., ... & Godavarthi, S. (2019). Synthesis of g-C_3N_4/N-doped CeO_2 composite for photocatalytic degradation of an herbicide. *Journal of Materials Research and Technology*, *8*(2), 1628-1635.

Khan, W., Nam, J. Y., Byun, S., Kim, S., Han, C., & Kim, H. C. (2020). Emerging investigator series: quaternary treatment with algae-assisted oxidation for antibiotics removal and refractory organics degradation in livestock wastewater effluent. *Environmental Science: Water Research & Technology*, *6*(12), 3262-3275.

Koe, W. S., Lee, J. W., Chong, W. C., Pang, Y. L., & Sim, L. C. (2020). An overview of photocatalytic degradation: photocatalysts, mechanisms, and development of photocatalytic membrane. *Environmental Science and Pollution Research*, *27*, 2522-2565.

Kuang, Y., Shang, J., & Zhu, T. (2019). Photoactivated graphene oxide to enhance photocatalytic reduction of CO2. *ACS applied materials & interfaces*, *12*(3), 3580-3591.

Kuhr, R. J., & Dorough, H. W. (1976). *Carbamate insecticides: chemistry, biochemistry, and toxicology*. CRC Press, Inc.

Kumar, N., Pathera, A. K., Saini, P., & Kumar, M. (2012). Harmful effects of pesticides on human health. *Annals of Agri-Bio Research*, *17*(2), 125-127.

Kumar, P., Singh, H., Kapur, M., & Mondal, M. K. (2014). Comparative study of malathion removal from aqueous solution by agricultural and commercial adsorbents. *Journal of Water Process Engineering*, *3*, 67-73.

Kumar, S., Kaushik, G., & Villarreal-Chiu, J. F. (2016). The scenario of organophosphate pollution and toxicity in India: A review. *Environmental Science and Pollution Research*, *23*, 9480-9491.

Kumar, S., Kaushik, G., Dar, M. A., Nimesh, S., Lopez-Chuken, U. J., & Villarreal-Chiu, J. F. (2018). Microbial degradation of organophosphate pesticides: a review. *Pedosphere*, *28*(2), 190-208.

Kumar, V., & Kumar, P. (2019). Pesticides in agriculture and environment: Impacts on human health. *Contaminants in agriculture and environment: health risks and remediation*, *1*, 76.

Kumari, B., Madan, V. K., & Kathpal, T. S. (2008). Status of insecticide contamination of soil and water in Haryana, India. *Environmental monitoring and assessment*, *136*, 239-244.

Kumari, B., Madan, V. K., Singh, J., Singh, S., & Kathpal, T. S. (2004). Monitoring of pesticidal contamination of farmgate vegetables from Hisar. *Environmental Monitoring and Assessment*, *90*, 65-71.

Kutal, C., Weber, M. A., Ferraudi, G., & Geiger, D. (1985). A mechanistic investigation of the photoinduced reduction of carbon dioxide mediated by tricarbonylbromo (2, 2'-bipyridine) rhenium (I). *Organometallics*, *4*(12), 2161-2166.

L. Zhang, L. Du, X. Yu, S. Tan, X. Cai, P. Yang, Y. Gu, W. Mai, Significantly enhanced photocatalytic activities and charge separation mechanism of Pd-decorated ZnO graphene oxide nanocomposites, ACS Appl. Mater. Interfaces 6 (2014) 3623–3629.

Lari, S. Z., Khan, N. A., Gandhi, K. N., Meshram, T. S., & Thacker, N. P. (2014). Comparison of pesticide residues in surface water and groundwater of aagriculture-intensiveareas. *Journal of Environmental Health Science and Engineering*, *12*, 1-7.

Lau, T. K., Chu, W., & Graham, N. (2007). Degradation of the endocrine disruptor carbofuran by UV, O_3, and O_3/UV. *Water Science and Technology*, *55*(12), 275-280.

Le, S., Zhu, C., Cao, Y., Wang, P., Liu, Q., Zhou, H., ... & Duan, X. (2022). V_2O_5 nanodot-decorated laminar C_3N_4 for sustainable photodegradation of amoxicillin under solar light. *Applied Catalysis B: Environmental*, *303*, 120903.

Lee, M., Balasingam, S. K., Jeong, H. Y., Hong, W. G., Lee, H. B. R., Kim, B. H., & Jun, Y. (2015). One-step hydrothermal synthesis of graphene-decorated V_2O_5 nanobelts for enhanced electrochemical energy storage. *Scientific reports*, *5*(1), 8151.

Lee, W. J., Sandler, D. P., Blair, A., Samanic, C., Cross, A. J., & Alavanja, M. C. (2007). Pesticide use and colorectal cancer risk in the Agricultural Health Study. *International Journal of Cancer*, *121*(2), 339-346.

Legrini, Oliveros, E. Oliveros, and A. M. Braun. "Photochemical processes for water treatment." *Chemical Reviews* 93.2 (1993): 671-698.

Lellis, B, Fávaro-Polonio, C.Z, Pamphile, J.A Polonio, J.C (2019) Effects of textile dyes on health and the environment and bioremediation potential of living organisms, Biotechnology Research and Innovation. 3 (2019) 275–290. doi:10.1016/j.biori.2019.09.001.

Lhomme, L., Brosillon, S. T. E. P. H. A. N., & Wolbert, D. (2008). Photocatalytic degradation of pesticides in pure water and a commercial agricultural solution on TiO_2 coated media. *Chemosphere*, *70*(3), 381-386.

Li, D., Zhu, J., Wang, M., Bi, W., Huang, X., & Chen, D. D. Y. (2017). Extraction of trace polychlorinated biphenyls in environmental waters by well-dispersed velvet-like magnetic carbon nitride nanocomposites. *Journal of Chromatography A*, *1491*, 27-35.

Li, F., Jiang, X., Zhao, J., & Zhang, S. (2015). Graphene oxide: A promising nanomaterial for energy and environmental applications. *Nano Energy*, *16*, 488-515.

Li, G., Nie, X., Chen, J., Jiang, Q., An, T., Wong, P. K., ... & Yamashita, H. (2015). Enhanced visible-light-driven photocatalytic inactivation of Escherichia coli using g-C_3N_4/TiO_2 hybrid photocatalyst synthesized using a hydrothermal-calcination approach. *Water research*, *86*, 17-24.

Li, G., Wang, B., Zhang, J., Wang, R., & Liu, H. (2020). Er-doped g-C_3N_4 for photodegradation of tetracycline and tylosin: High photocatalytic activity and low leaching toxicity. *Chemical Engineering Journal*, *391*, 123500.

Li, H., Shan, C., & Pan, B. (2018). Fe (III)-doped g-C_3N_4 mediated peroxymonosulfate activation for selective degradation of phenolic compounds via high-valent iron-oxo species. *Environmental science & technology*, *52*(4), 2197-2205.

Li, J., Shen, B., Hong, Z., Lin, B., Gao, B., & Chen, Y. (2012). A facile approach to synthesize novel oxygen-doped g-C_3N_4 with superior visible-light photoreactivity. *Chemical communications*, *48*(98), 12017-12019.

Li, J., Wu, Q., & Wu, J. (2016). Synthesis of nanoparticles via solvothermal and hydrothermal methods. In *Handbook of nanoparticles* (pp. 295-328). Springer, Cham.

Li, K., Yediler, A., Yang, M., Schulte-Hostede, S., & Wong, M. H. (2008). Ozonation of oxytetracycline and toxicological assessment of its oxidation by-products. *Chemosphere*, *72*(3), 473-478.

Li, K., Zeng, Z., Yan, L., Luo, S., Luo, X., Huo, M., & Guo, Y. (2015). Fabrication of platinum-deposited carbon nitride nanotubes by a one-step solvothermal treatment strategy and their efficient visible-light photocatalytic activity. *Applied Catalysis B: Environmental*, *165*, 428-437.

Li, L., Ma, D., Xu, Q., & Huang, S. (2022). Constructing hierarchical $ZnIn_2S_4$/ g-C_3N_4 S-scheme heterojunction for boosted CO_2 photoreduction performance. *Chemical Engineering Journal*, *437*, 135153.

Li, M., Liu, F., Ma, Z., Liu, W., Liang, J., & Tong, M. (2019). Different mechanisms for E. coli disinfection and BPA degradation by CeO_2-AgI under visible light irradiation. *Chemical Engineering Journal*, *371*, 750-758.

Li, X., Zhang, X., Ma, H., Wu, D., Zhang, Y., Du, B., & Wei, Q. (2014). Cathodic electrochemiluminescence immunosensor based on nanocomposites of semiconductor carboxylated g-C_3N_4 and graphene for the ultrasensitive detection of squamous cell carcinoma antigen. *Biosensors and Bioelectronics*, *55*, 330-336.

Li, Y., Zhang, C., Shuai, D., Naraginti, S., Wang, D., & Zhang, W. (2016). Visible-light-driven photocatalytic inactivation of MS_2 by metal-free g-C_3N_4: virucidal performance and mechanism. *Water Research*, *106*, 249-258.

Li, Y.; Wu, S.; Huang, L.; Xu, H.; Zhang, R.; Qu, M.; Gao, Q.; Li, H. g-C_3N_4 modified Bi_2O_3 composites with enhanced visible-light photocatalytic activity. *J. Phys. Chem. Solids* **2014**, *76*, 112–119.

Liqiang, J., Xiaojun, S., Jing, S., Weimin, C., Zili, X., Yaoguo, D., & Honggang, F. (2003). Review of surface photovoltage spectra of nano-sized semiconductor and its applications in heterogeneous photocatalysis. *Solar Energy Materials and Solar Cells*, *79*(2), 133-151.

Liqiang, J., Yichum, Q., Baiqi, W., Shudan, L., & Baojiang, J. (2006). L. Y, F. Wei, F. Honggang and S. Jiazhng," Review of photoluminescence performance of nano-sized semiconductor materials and its relationships with photocatalytic activity,". *Solar Energy Materials & Solar Cells*, (90), 1773-1787.

Liu, A. Y., & Cohen, M. L. (1989). Prediction of new low compressibility solids. *Science*, *245*(4920), 841-842.

Liu, S. H., Tang, W. T., & Chou, P. H. (2020). Microwave-assisted synthesis of triple 2D g-C_3N_4/Bi2WO6/rGO composites for ibuprofen photodegradation: kinetics, mechanism and toxicity evaluation of degradation products. *Chemical Engineering Journal*, *387*, 124098.

Liu, S. Y., Zada, A., Yu, X., Liu, F., & Jin, G. (2022). $NiFe_2O_4$/ g-C_3N_4 heterostructure with an enhanced ability for photocatalytic degradation of tetracycline hydrochloride and antibacterial performance. *Chemosphere*, *307*, 135717.

Liu, S., Wang, S., Jiang, Y., Zhao, Z., Jiang, G., & Sun, Z. (2019). Synthesis of Fe_2O_3 loaded porous g-C_3N_4 photocatalyst for photocatalytic reduction of dinitrogen to ammonia. *Chemical Engineering Journal*, *373*, 572-579.

Liu, X.; Li, C.; Zhang, B.; Yuan, M.; Ma, Y.; Kong, F. A facile strategy for photocatalytic degradation of seven neonicotinoids over sulfur and oxygen co-doped carbon nitride. *Chemosphere* **2020**, *253*, 126672.

Liu, Y., Liu, F., Pan, X., & Li, J. (2012). Protecting the environment and public health from pesticides.

Lopez-Alvarez, B., Torres-Palma, R.A., Penuela, G., 2011. Solar photocatalytic treatment of carbofuran at lab and pilot scale: effect of classical parameters, evaluation of the toxicity and analysis of organic by-products. J. Hazard. Mater 191, 196e203.

Lops, C., Ancona, A., Di Cesare, K., Dumontel, B., Garino, N., Canavese, G., ... & Cauda, V. (2019). Sonophotocatalytic degradation mechanisms of Rhodamine B dye via radicals generation by micro-and nano-particles of ZnO. *Applied Catalysis B: Environmental*, *243*, 629-640..

Lops, C., Ancona, A., Di Cesare, K., Dumontel, B., Garino, N., Canavese, G., ... & Cauda, V. (2019). Sonophotocatalytic degradation mechanisms of Rhodamine B dye via radicals generation by micro-and nano-particles of ZnO. *Applied Catalysis B: Environmental*, *243*, 629-640.

Lu, L.A., Ma, Y.S., Kumar, M., Lin, J.G., 2011. Photochemical degradation of carbofuran and elucidation of removal mechanism. Chem. Eng. J. 166, 150e156.

Lua, J. et al. 2017. Fabrication of a direct Z-scheme type WO_3/Ag_3PO_4 composite photocatalyst with enhanced visible-light photocatalytic performances, Appl. Surf. Sci. 393 180-190. https://doi.org/10.1016/j.apsusc.2016.10.003

Luo, D., Zhou, T., Tao, Y., Feng, Y., Shen, X., & Mei, S. (2016). Exposure to organochlorine pesticides and non-Hodgkin lymphoma: a meta-analysis of observational studies. *Scientific reports*, *6*(1), 1-11.

Lyman, W. J., Reehl, W. F., & Rosenblatt, D. H. (1990). Handbook of chemical property estimation methods.

Magdalane, C. M., Kaviyarasu, K., Raja, A., Arularasu, M. V., Mola, G. T., Isaev, A. B., ... & Maaza, M. (2018). Photocatalytic decomposition effect of erbium doped cerium oxide nanostructures driven by visible light irradiation: investigation of cytotoxicity, antibacterial growth inhibition using catalyst. *Journal of Photochemistry and Photobiology B: Biology*, *185*, 275-282.

Mamba, G., & Mishra, A. K. (2016). Graphitic carbon nitride ($g\text{-}C_3N_4$) nanocomposites: a new and exciting generation of visible light driven photocatalysts for environmental pollution remediation. *Applied Catalysis B: Environmental*, *198*, 347-377.

Mandal, K., & Singh, B. (2010). Magnitude and frequency of pesticide residues in farmgate samples of cauliflower in Punjab, India. *Bulletin of environmental contamination and toxicology*, *85*, 423-426.

Mao, S., Liu, C., Wu, Y., Xia, M., & Wang, F. (2022). Porous P, Fe-doped $g\text{-}C_3N_4$ nanostructure with enhanced photo-Fenton activity for removal of tetracycline hydrochloride: Mechanism insight, DFT calculation and degradation pathways. *Chemosphere*, *291*, 133039.

Marrs, T. C. (1993). Organophosphate poisoning. *Pharmacology & therapeutics*, *58*(1), 51-66.

Mathur, H. B., Agarwal, H. C., Johnson, S., & Saikia, N. (2005). Analysis of pesticide residues in blood samples from villages of Punjab. *CSE Report, India*, 1-15.

Matsuo, N. (2019). Discovery and development of pyrethroid insecticides. *Proceedings of the Japan Academy, Series B*, *95*(7), 378-400.

McRae IC (1989) Microbial metabolism of pesticides and structurally related compounds. Rev Environ Contam Toxicol 109:1–34

Mdeni, N. L., Adeniji, A. O., Okoh, A. I., & Okoh, O. O. (2022). Analytical evaluation of carbamate and organophosphate pesticides in human and environmental matrices: a review. *Molecules*, *27*(3), 618.s

MEENA, P. L., Poswal, K., Surela, A. K., & Saini, J. K. (2022). Fabrication of g-C_3N_4/ZnO Nanoheterostructures for Effective Degradation of Methylene Blue Dye under Visible Light Irradiation.

Meng, J., Pei, J., He, Z., Wu, S., Lin, Q., Wei, X., ... & Zhang, Z. (2017). Facile synthesis of g-C_3N_4 nanosheets loaded with WO_3 nanoparticles with enhanced photocatalytic performance under visible light irradiation. *Rsc Advances*, *7*(39), 24097-24104.

Mengyue, Z., Shifu, C., & Yaowu, T. (1995). Photocatalytic degradation of organophosphorus pesticides using thin films of TiO_2. *Journal of Chemical Technology & Biotechnology*, *64*(4), 339-344.

Menon, P., Gopal, M., & Prasad, R. (2004). Influence of two insecticides, chlorpyrifos and quinalphos, on arginine ammonification and mineralizable nitrogen in two tropical soil types. *Journal of agricultural and food chemistry*, *52*(24), 7370-7376.

Mia, R., Selim, M., Shamim, A. M., Chowdhury, M., Sultana, S., Armin, M., ... & Naznin, H. (2019). Review on various types of pollution problem in textile dyeing & printing industries of Bangladesh and recommandation for mitigation. *Journal of Textile Engineering & Fashion Technology*, *5*(4), 220-226.

Miller, G. T. 2004: Sustaining the Earth, 6th edition. Thompson learning, Inc. Pacific Grove, California. 9:211-216.

Mills, K., & Kegley, S. (2006). Air Monitoring for Chlorpyrifos in Lindsay, California June-July 2004 and July-August 2005. Pesticide Action Network North America. July 14, 2006.

Mineau P (2003) Avian species. In: Plimmer JR, Gammon DW, Ragsdale NN (eds) Encyclopedia of agrochemicals. Wiley, New York, pp 1–27

Mineau P, Tucker KR (2002b) Improving detection of pesticide poisoning in birds, part II. J Wildl Rehabil 25(3):4–12

Mishra, S., Zhang, W., Lin, Z., Pang, S., Huang, Y., Bhatt, P., & Chen, S. (2020). Carbofuran toxicity and its microbial degradation in contaminated environments. *Chemosphere*, *259*, 127419.

Mittal, S., Kaur, G., & Vishwakarma, G. S. (2014). Effects of environmental pesticides on the health of rural communities in the Malwa Region of Punjab, India: a review. *Human and Ecological Risk Assessment: An International Journal*, *20*(2), 366-387.

Mohammad, F. K., Garmavy, H. M. S., Mohammed, A. A., & Rashid, H. M. (2023). First meta-analysis study of cholinesterase inhibition in experimental animals by organophosphate or carbamate insecticides under the influence of diphenhydramine, Veterinary World, 16 (1): 118–125. Abstract.

Mohanta, D., & Ahmaruzzaman, M. (2021). Facile fabrication of novel Fe_3O_4-SnO_2-g-C_3N_4 ternary nanocomposites and their photocatalytic properties towards the degradation of carbofuran. *Chemosphere*, *285*, 131395.

Morin-Crini, N., Lichtfouse, E., Liu, G., Balaram, V., Ribeiro, A. R. L., Lu, Z., ... & Crini, G. (2022). Worldwide cases of water pollution by emerging contaminants: a review. *Environmental Chemistry Letters*, *20*(4), 2311-2338.

Mu, J., Chen, B., Zhang, M., Guo, Z., Zhang, P., Zhang, Z., ... & Liu, Y. (2012). Enhancement of the visible-light photocatalytic activity of In_2O_3–TiO_2 nanofiber hetero-architectures. *ACS applied materials & interfaces*, *4*(1), 424-430.

Mubushar, M., Aldosari, F. O., Baig, M. B., Alotaibi, B. M., & Khan, A. Q. (2019). Assessment of farmers on their knowledge regarding pesticide usage and biosafety. *Saudi journal of biological sciences*, *26*(7), 1903-1910.

Muhamad, S. G. 2010. Kinetic Studies of Catalytic Photodegradation of Chlorpyrifos Insecticide in Various Natural Waters. Arab. J. Chem. 3 (2), 127–133

Muhammad, N., Zia-ul-Haq, M., Ali, A., Naeem, S., Intisar, A., Han, D., ... & Wei, B. (2021). Ion chromatography coupled with fluorescence/UV detector: A comprehensive review of its applications in pesticides and pharmaceutical drug analysis. *Arabian Journal of Chemistry*, *14*(3), 102972.

Mundu, P. A., Kumar, M., Satapathy, R. P., & Mitra, J. K. (2019). Organophosphate induced delayed neuropathy: A case report. *Int J Contemp Med Res*, *3*, 2289-91.

Murphy, M. W., Sanderson, W. T., Birch, M. E., Liang, F., Sanyang, E., Canteh, M., ... & Murphy, S. C. (2012). Type and toxicity of pesticides sold for community vector control use in the Gambia. *Epidemiology Research International*, *2012*.

Muszkat, L., Feigelson, L., Bir, L., & Muszkat, K. A. (2002). Photocatalytic degradation of pesticides and bio-molecules in water. *Pest Management Science: formerly Pesticide Science*, *58*(11), 1143-1148.

Nguyen-Phan, T.-D.; Pham, V.H.; Shin, E.W.; Pham, H.-D.; Kim, S.; Chung, J.S.; Kim, E.J.; Hur, S.H. The role of graphene oxide content on the adsorption-enhanced photocatalysis of titanium dioxide/graphene oxide composites. *Chem. Eng. J.* **2011**, *170*, 226–232.
Ohgaki, S., Fukushi, K., Katayama, H., Takizawa, S., & Polprasert, C. (Eds.). (2005). *Southeast Asian Water Environment 1*. IWA Publishing.

Ojha, A., Yaduvanshi, S. K., Pant, S. C., Lomash, V., & Srivastava, N. (2013). Evaluation of DNA damage and cytotoxicity induced by three commonly used organophosphate pesticides individually and in mixture, in rat tissues. *Environmental Toxicology*, *28*(10), 543-552.

Ollera S., Malatoa J. and Sánchez-Pérezb. A. 2011. Combination of Advanced Oxidation Processes and biological treatments for wastewater decontamination—A review. Science of the Total Environment. 409 (20), 15, 4141-4166. https://doi.org/10.1016/j.scitotenv.2010.08.061

Ollis, D.F., Pelizzetti, E. and Serpone, N. (1991) Photo-catalyzed Destruction of Water Contaminants. Environmental Science & Technology, 25, 1522-1529

Ong, W. J., Tan, L. L., Ng, Y. H., Yong, S. T., & Chai, S. P. (2016). Graphitic carbon nitride (g-C3N4)-based photocatalysts for artificial photosynthesis and environmental remediation: are we a step closer to achieving sustainability?. *Chemical reviews*, *116*(12), 7159-7329.

Orts, F., Del Río, A. I., Molina, J., Bonastre, J., & Cases, F. (2018). Electrochemical treatment of real textile wastewater: Trichromy Procion HEXL®. *Journal of Electroanalytical Chemistry*, *808*, 387-394.

Oskoei, V., Dehghani, M. H., Nazmara, S., Heibati, B., Asif, M., Tyagi, I., ... & Gupta, V. K. (2016). Removal of humic acid from aqueous solution using UV/ZnO nano-photocatalysis and adsorption. *Journal of Molecular Liquids*, *213*, 374-380.

Otieno, P. O., Lalah, J. O., Virani, M., Jondiko, I. O., & Schramm, K. W. (2011). Carbofuran use and abuse in Kenya: residues in soils, plants, water courses and the African white-backed vultures (Gyps africanus) found dead. *The Environmentalist*, *31*, 382-393.

Otieno, P. O., Lalah, J. O., Virani, M., Jondiko, I. O., & Schramm, K. W. (2010). Carbofuran and its toxic metabolites provide forensic evidence for Furadan exposure in vultures (Gyps africanus) in Kenya. *Bulletin of environmental contamination and toxicology*, *84*, 536-544.

Padmaja, R., Amar, R., Nayak, V. C., Bakkannavar, S. M., Smitha, N., & Anjana, R. (2014). Profile of organophosphorus insecticides poisoning in Kasturba Hospital, Manipal, South India. *Journal of Pharmaceutical and Scientific Innovation (JPSI)*, *3*(1), 73-77.

Palmisano, R., Campanella, L., & Ambrosetti, B. (2015). Photo-degradation of amoxicillin, streptomycin, erythromycin and ciprofloxacin by UV and UV/TiO_2 processes. Evaluation of toxicity changes using a respirometric biosensor. *J Environ Anal Chem*, *2*(143), 2.

Panda, S.; Rout, T.K.; Prusty, A.D.; Ajayan, P.M.; Nayak, S. Electron Transfer Directed Antibacterial Properties of Graphene Oxide on Metals. *Adv. Mater.* **2018**, *30*, 1702149.

Pang, N.; Lin, H.; Hu, J. Photodegradation of fluazaindolizine in aqueous solution with graphitic carbon nitride nanosheets under simulated sunlight illumination. *Ecotoxicol. Environ. Saf.* **2019**, *170*, 33–38.

Pang, N.; Wang, T.; Cui, Y.; Hu, J. New dispersive solid phase extraction sorbent of graphitic carbon nitride for field evaluation and dissipation kinetics of pesticides in wheat ecosystem by liquid chromatography tandem mass spectrometry. *Int. J. Environ. Anal. Chem.* **2016**, *96*, 1156–1169.

Park, C. H., Zhang, S. B., & Wei, S. H. (2002). Origin of p-type doping difficulty in ZnO: The impurity perspective. *Physical Review B*, *66*(7), 073202.

Parra, S., Olivero, J. and Pulgarin, C., 2002. Relationships between physicochemical properties and photoreactivity of four biorecalcitrant phenylurea herbicides in aqueous TiO_2 suspension. Appl. Catal. B: Environ.36, 75-85.

Parra-Arroyo, L., González-González, R. B., Castillo-Zacarías, C., Martínez, E. M. M., Sosa-Hernández, J. E., Bilal, M., ... & Parra-Saldívar, R. (2022). Highly hazardous pesticides and related pollutants: Toxicological, regulatory, and analytical aspects. *Science of The Total Environment*, *807*, 151879.

Pathan, A.A.; Desai, K.R.; Bhasin, C. Synthesis of La_2O_3 Nanoparticles using Glutaric acid and Propylene glycol for Future CMOS Applications. Int. J. Nanomater. Chem. 2017, 3, 21–25.

Pawar, R. R., Gosavi, N. R., Pandhare, A. T., More, B. P., Rewatkar, L. B., Kapdnis, R. H., & Doundkar, B. B. (2015). A statistical study of insecticidal poisoning in Nasik region a comparative study. *World J Pharm Res*, *4*(946), e951.

Pearce, C. I., Lloyd, J. R., & Guthrie, J. T. (2003). The removal of colour from textile wastewater using whole bacterial cells: a review. *Dyes and pigments*, *58*(3), 179-196.

Pedersen, TL (June 1997), Pesticide residues in drinking water. extoxnet.orst.edu. Retrieved on 15 September 2007).

Pedroso, T. M. A., Benvindo-Souza, M., de Araújo Nascimento, F., Woch, J., Dos Reis, F. G., & de Melo e Silva, D. (2022). Cancer and occupational exposure to pesticides: a bibliometric study of the past 10 years. *Environmental Science and Pollution Research*, 1-12.

Peng, W. C., & Li, X. Y. (2014). Synthesis of MoS_2/ g-C_3N_4 as a solar light-responsive photocatalyst for organic degradation. *Catalysis Communications*, *49*, 63-67.

Pham, V. V., Truong, T. K., Hai, L. V., La, H. P. P., Nguyen, H. T., Lam, V. Q., ... & Cao, T. M. (2022). S-Scheme α-Fe_2O_3/ g-C_3N_4 nanocomposites as heterojunction photocatalysts for antibiotic degradation. *ACS Applied Nano Materials*, *5*(3), 4506-4514.

Phung, D. T., Connell, D., Miller, G., & Chu, C. (2012). Probabilistic assessment of Chlorpyrifos exposure to rice farmers in Viet Nam. *Journal of exposure science & environmental epidemiology*, *22*(4), 417-423.

Pink, R. M. (2016). Water Rights in China and India: A Human Security Perspective. *Asian Affairs: An American Review*, *43*(2), 19-35.

Pirsaheb, M., Hossini, H., Asadi, F., & Janjani, H. (2017). A systematic review on organochlorine and organophosphorus pesticides content in water resources. *Toxin reviews*, *36*(3), 210-221.

Pouretedal, H. R. and Hasanali, M. A. 2013. Photocatalytic degradation of some βlactam antibiotics in aqueous suspension of ZnS nanoparticles, Desalination and Water Treatment. 51:13-15, 2617-2623, DOI:10.1080/19443994. 2012.749197

Prakash, A., Khan, S., Aggarwal, M., Telang, A. G., & Malik, J. K. (2009). Chlorpyrifos induces apoptosis in murine thymocytes. *Toxicology Letters*, (189), S83.

Prakash, K., Kumar, J. V., Latha, P., Kumar, P. S., & Karuthapandian, S. (2019). Fruitful fabrication of CDs on GO/g-C3N4 sheets layers: a carbon amalgamation for the remediation of carcinogenic pollutants. *Journal of Photochemistry and Photobiology A: Chemistry*, *370*, 94-104

Preeyanghaa M, Vinesh V, Neppolian B. Construction of Scheme 1D/2D rod-like g-C_3N_4/V_2O_5 heterostructure with enhanced sonophotocatalytic degradation for Tetracycline antibiotics. Chemosphere 2022;287:132380.

Pujeri,U.S., M.I., Punjar, A.S., Hiremath,S.C. and Yadave, M.S.(2011). Analysis of pesticide residue in Kummargi, Baratagi and Katral lakes of Bijapur, Karnataka. J.Pharma.Biomed. Sci.,6(07), 1-4.

Qamar, A., Asi, R., Iqbal, M., Nazir, A., & Arif, K. (2017). Survey of Residual Pesticides in Various Fresh Fruit Crops: A Case Study. *Polish Journal of Environmental Studies*, *26*(6).

Qi, K., Li, Y., Xie, Y., Liu, S. Y., Zheng, K., Chen, Z., & Wang, R. (2019). Ag loading enhanced photocatalytic activity of g-C3N4 porous nanosheets for decomposition of organic pollutants. *Frontiers in Chemistry*, *7*, 91.

Qu, L., Zhu, G., Ji, J., Yadav, T. P., Chen, Y., Yang, G., ... & Li, H. (2018). Recyclable visible light-driven Og-C_3N_4/graphene oxide/N-carbon nanotube membrane for efficient removal of organic pollutants. *ACS Applied Materials & Interfaces*, *10*(49), 42427-42435.

Quintana, M. A., Solís, R. R., Martín-Lara, M. Á., Blázquez, G., Calero, F. M., & Muñoz-Batista, M. J. (2022). Enhanced boron modified graphitic carbon nitride for the selective

photocatalytic production of benzaldehyde. *Separation and Purification Technology*, *298*, 121613.

Quiroz, M. A., Bandala, E.R. and Martínez-huitle. C.A. 2007. Advanced Oxidation Processes (AOPs) for Removal of Pesticides from Aqueous Media. Pesticides - Formulations, Effects, Fate. www.intechopen.com.

Racke, K. D., Steele, K. P., Yoder, R. N., Dick, W. A., & Avidov, E. (1996). Factors affecting the hydrolytic degradation of Chlorpyrifos in soil. *Journal of Agricultural and Food Chemistry*, *44*(6), 1582-1592.

Ragnarsdottir, K. V. (2000). Environmental fate and toxicology of organophosphate pesticides. *Journal of the Geological Society*, *157*(4), 859-876.

Răileanu, M., Crişan, M., Niţoi, I., Ianculescu, A., Oancea, P., Crişan, D., & Todan, L. (2013). TiO_2-based nanomaterials with photocatalytic properties for the advanced degradation of xenobiotic compounds from water. A literature survey. *Water, Air, & Soil Pollution*, *224*, 1-45.

Raizada, P.; Sudhaik, A.; Saini, A.K.; Singh, P. Graphitic carbon nitride base metal free nanocomposite for pesticide degradation and bacteria disinfection. India Patent IN201811023694, 27 December 2019.

Rani, M., & Shanker, U. (2018). Degradation of traditional and new emerging pesticides in water by nanomaterials: recent trends and future recommendations. *International Journal of Environmental Science and Technology*, *15*, 1347-1380.

Rasmussen, J. J., Wiberg-Larsen, P., Baattrup-Pedersen, A., Cedergreen, N., McKnight, U. S., Kreuger, J., ... & Friberg, N. (2015). The legacy of pesticide pollution: an overlooked factor in current risk assessments of freshwater systems. *Water Research*, *84*, 25-32..

Rathore, H. S., & Nollet, L. M. (Eds.). (2012). *Pesticides: evaluation of environmental pollution*. CRC press.

Rauf, M. A., Bukallah, S. B., Hamadi, A., Sulaiman, A., & Hammadi, F. (2007). The effect of operational parameters on the photoinduced decoloration of dyes using a hybrid catalyst V_2O_5/TiO_2. *Chemical Engineering Journal*, *129*(1-3), 167-172.

Rauh, V. A., Perera, F. P., Horton, M. K., Whyatt, R. M., Bansal, R., Hao, X., ... & Peterson, B. S. (2012). Brain anomalies in children exposed prenatally to a common organophosphate pesticide. *Proceedings of the National Academy of Sciences*, *109*(20), 7871-7876.

RAY, A. K., & GHOSH, M. C. (2006). Aquatic toxicity of carbamates and organophosphates. In *Toxicology of Organophosphate & Carbamate Compounds* (pp. 657-672). Academic Press.

Reddy, K.R., Reddy, C.H.V., Nadagouda, M.N., Shetti, N.P., Jaesool, S., Aminabhavi, T.M., 2019. Polymer graphitic carbon nitride (g-C3N4)-based semiconducting nanostructured materials: synthesis methods, properties and photocatalytic applications. J. Environ. Manag. 238, 25–40.

Rehana, Z., Malik, A., & Ahmad, M. (1995). Mutagenic activity of the Ganges water with special reference to the pesticide pollution in the river between Kachla to Kannauj (UP), India. *Mutation Research/Genetic Toxicology*, *343*(2-3), 137-144.

Reigart, J. R., & Roberts, J. R. (2001). Pesticides in children. *Pediatric Clinics of North America*, *48*(5), 1185-1198.

Reynolds, J. G., & Reynolds, C. L. (2014). Progress in ZnO acceptor doping: what is the best strategy?. *Advances in Condensed Matter Physics*, *2014*.

Rezg, R., Mornagui, B., El-Fazaa, S., & Gharbi, N. (2010). Organophosphorus pesticides as food chain contaminants and type 2 diabetes: a review. *Trends in food science & technology*, *21*(7), 345-357.

Righetto, M., Meggiolaro, D., Rizzo, A., Sorrentino, R., He, Z., Meneghesso, G., ... & Lamberti, F. (2020). Coupling halide perovskites with different materials: From doping to nanocomposites, beyond photovoltaics. *Progress in Materials Science*, *110*, 100639.

Risher, J. F., Mink, F. L., & Stara, J. F. (1987). The toxicologic effects of the carbamate insecticide aldicarb in mammals: a review. *Environmental health perspectives*, *72*, 267-281.

Risher, J., & Navarro, H. A. (1997). Toxicological profile for chlorpyrifos.

Robert, D., & Malato, S. (2002). Solar photocatalysis: a clean process for water detoxification. *Science of the total environment*, *291*(1-3), 85-97.

Romeh, A. A., & Hendawi, M. Y. (2013). Chlorpyrifos insecticide uptake by plantain from polluted water and soil. *Environmental chemistry letters*, *11*, 163-170.

Salazar-Arredondo, E., de Jesús Solís-Heredia, M., Rojas-García, E., Hernández-Ochoa, I., & Quintanilla-Vega, B. (2008). Sperm chromatin alteration and DNA damage by methyl-parathion, chlorpyrifos and diazinon and their oxon metabolites in human spermatozoa. *Reproductive Toxicology*, *25*(4), 455-460..

Saleh, I. A., Zouari, N., & Al-Ghouti, M. A. (2020). Removal of pesticides from water and wastewater: Chemical, physical and biological treatment approaches. *Environmental Technology & Innovation*, *19*, 101026.

Samsudin, E. M., Goh, S. N., Wu, T. Y., Ling, T. T., Hamid, S. A., & Juan, J. C. (2015). Evaluation on the photocatalytic degradation activity of reactive blue 4 using pure anatase nano-TiO_2. *Sains Malaysiana*, *44*(7), 1011-1019.

Sánchez-Montes, I., Doerenkamp, J. C., Núñez-de la Rosa, Y., Hammer, P., Rocha-Filho, R. C., & Aquino, J. M. (2023). Effective Fenton-like degradation of the tebuthiuron herbicide by ferrocene functionalized g-C_3N_4. *Journal of Photochemistry and Photobiology A: Chemistry*, *435*, 114276.

Sandal, S., & Yilmaz, B. (2011). Genotoxic effects of chlorpyrifos, cypermethrin, endosulfan and 2, 4-D on human peripheral lymphocytes cultured from smokers and nonsmokers. *Environmental Toxicology*, *26*(5), 433-442.

Sanghi, R., Pillai, M. K., Jayalekshmi, T. R., & Nair, A. (2003). Organochlorine and organophosphorus pesticide residues in breast milk from Bhopal, Madhya Pradesh, India. *Human & experimental toxicology*, *22*(2), 73-76.

Saquib, Q., Siddiqui, M. A., Ansari, S. M., Alwathnani, H. A., & Al-Khedhairy, A. A. (2021). Carbofuran cytotoxicity, DNA damage, oxidative stress, and cell death in human umbilical vein endothelial cells: Evidence of vascular toxicity. *Journal of Applied Toxicology*, *41*(5), 847-860.

Saratale, R. G., Saratale, G. D., Chang, J. S., & Govindwar, S. P. (2011). Bacterial decolorization and degradation of azo dyes: a review. *Journal of the Taiwan institute of Chemical Engineers*, *42*(1), 138-157.

Sarkar, S. K., Bhattacharya, B. D., Bhattacharya, A., Chatterjee, M., Alam, A., Satpathy, K. K., & Jonathan, M. P. (2008). Occurrence, distribution and possible sources of organochlorine pesticide residues in tropical coastal environment of India: an overview. *Environment International*, *34*(7), 1062-1071.

Sasikala, C., Jiwal, S., Rout, P., & Ramya, M. (2012). Biodegradation of chlorpyrifos by bacterial consortium isolated from agriculture soil. *World Journal of Microbiology and Biotechnology*, *28*, 1301-1308.

Science Daily, 3 Feb 2006

Sebby, K. (2010). The green revolution of the 1960's and its impact on small farmers in India.

Serpone, N., Sauvé, G., Koch, R., Tahiri, H., Pichat, P., Piccinini, P., ... & Hidaka, H. (1996). Standardization protocol of process efficiencies and activation parameters in heterogeneous photocatalysis: relative photonic efficiencies ζr. *Journal of photochemistry and photobiology A: Chemistry*, *94*(2-3), 191-203.

Shah, Z. U., & Parveen, S. (2021). Pesticides pollution and risk assessment of river Ganga: A review. *Heliyon*, *7*(8), e07726.

Shan, M., Fang, H., Wang, X., Feng, B., Chu, X. Q., & Yu, Y. L. (2006). Effect of chlorpyrifos on soil microbial populations and enzyme activities. *Journal of Environmental Sciences*, *18*(1), 4-5.

Shan, X., Guo, X., Yin, Y., Miao, Y., & Dong, H. (2017). Surface modification of graphene oxide by goethite with enhanced tylosin photocatalytic activity under visible light irradiation. *Colloids and Surfaces A: Physicochemical and Engineering Aspects*, *520*, 420-427.

Sharma, A., Kumar, V., Shahzad, B., Tanveer, M., Sidhu, G. P. S., Handa, N., ... & Thukral, A. K. (2019). Worldwide pesticide usage and its impacts on ecosystem. *SN Applied Sciences*, *1*, 1-16.

Sharma, A., Shukla, A., Attri, K., Kumar, M., Kumar, P., Suttee, A., ... & Singla, N. (2020). Global trends in pesticides: A looming threat and viable alternatives. *Ecotoxicology and Environmental Safety*, *201*, 110812.

Sharma, A., Shukla, A., Attri, K., Kumar, M., Kumar, P., Suttee, A., ... & Singla, N. (2020). Global trends in pesticides: A looming threat and viable alternatives. *Ecotoxicology and Environmental Safety*, *201*, 110812.

Sharma, G., Kumar, A., Naushad, M., Sharma, S., Ghfar, A. A., Ahamad, T., ... & Stadler, F. J. (2019). Graphene oxide supported La/Co/Ni trimetallic nano-scale systems for photocatalytic remediation of 2-chlorophenol. *Journal of Molecular Liquids*, *294*, 111605.

Sidhu, G. K., Singh, S., Kumar, V., Dhanjal, D. S., Datta, S., & Singh, J. (2019). Toxicity, monitoring and biodegradation of organophosphate pesticides: a review. *Critical reviews in environmental science and technology*, *49*(13), 1135-1187.

Singh, B. K., Walker, A., Morgan, J. A. W., & Wright, D. J. (2004). Biodegradation of chlorpyrifos by Enterobacter strain B-14 and its use in bioremediation of contaminated soils. *Applied and environmental microbiology*, *70*(8), 4855-4863.

Singh, B., & Gupta, A. (2002). Monitoring of pesticide residues in farmgate and market samples of vegetables in a semiarid, irrigated area. *Bulletin of environmental contamination and toxicology*, *68*(5), 747.

Singh, B., & Unnikrishnan, B. (2006). A profile of acute poisoning at Mangalore (South India). *Journal of clinical forensic medicine*, *13*(3), 112-116.

Singh, G., & Khurana, D. (2009). Neurology of acute organophosphate poisoning. *Neurology India*, *57*(2), 119.

Sivakumar V., Jayaram P., Sankaran M, "Removal of Chlorpyrifos, an insecticide using metal-free heterogeneous graphitic carbon nitride (g-C_3N_4) incorporated chitosan as a catalyst: Photocatalytic and adsorption studies" International Journal of Biological Macromolecules,**132**,289-199 (2019).

Sivaperumal, P., Thasale, R., Kumar, D., Mehta, T. G., & Limbachiya, R. (2022). Human health risk assessment of pesticide residues in vegetable and fruit samples in Gujarat State, India. *Heliyon*, *8*(10), e10876.

Slotkin, T. A. (2004). Guidelines for developmental neurotoxicity and their impact on organophosphate pesticides: a personal view from an academic perspective. *Neurotoxicology*, *25*(4), 631-640.

Slotkin, T. A., Cooper, E. M., Stapleton, H. M., & Seidler, F. J. (2013). Does thyroid disruption contribute to the developmental neurotoxicity of chlorpyrifos?. *Environmental toxicology and pharmacology*, *36*(2), 284-287.

Smegal, D. C. (2000). Human health risk assessment chlorpyrifos. *US Environmental Protection Agency, Office of Prevention, Pesticides and Toxic Substances, Office of Pesticide Programs, Health Effects Division, US Government Printing Office: Washington, DC*, 1-131.

Sobczyński, D. A. 2001. Water purification by photocatalysis on semiconductors. Polish Journal of Environmental Studies. 10(4):195-205.

Soderlund, D. M. (2012). Molecular mechanisms of pyrethroid insecticide neurotoxicity: recent advances. *Archives of toxicology*, *86*, 165-181.

Sogorb, M. A., & Vilanova, E. (2002). Enzymes involved in the detoxification of organophosphorus, carbamate and pyrethroid insecticides through hydrolysis. *Toxicology letters*, *128*(1-3), 215-228.

Sogorb, M. A., Vilanova, E., & Carrera, V. (2004). Future applications of phosphotriesterases in the prophylaxis and treatment of organophosporus insecticide and nerve agent poisonings. *Toxicology letters*, *151*(1), 219-233.

Sousa, J. M., Macedo, G., Pedrosa, M., Becerra-Castro, C., Castro-Silva, S., Pereira, M. F. R., ... & Manaia, C. M. (2017). Ozonation and UV254 nm radiation for the removal of microorganisms and antibiotic resistance genes from urban wastewater. *Journal of Hazardous Materials*, *323*, 434-441.

Srinivas Rao, C. H., Venkateswarlu, V., Surender, T., Eddleston, M., & Buckley, N. A. (2005). Pesticide poisoning in south India: opportunities for prevention and improved medical management. *Tropical Medicine & International Health*, *10*(6), 581-588.

Su, Y., Chen, P., Wang, F., Zhang, Q., Chen, T., Wang, Y., ... & Liu, G. (2017). Decoration of TiO_2/g-C_3N_4 Z-scheme by carbon dots as a novel photocatalyst with improved visible-light photocatalytic performance for the degradation of enrofloxacin. *Rsc Advances*, *7*(54), 34096-34103.

Subash, S. P., Chand, P., Pavithra, S., Balaji, S. J., & Pal, S. (2017). Pesticide use in Indian agriculture: trends, market structure, and policy issues.

Subash, S.P., Chand, P., Pavithra, S., Balaji, S.J., Pal, S., (2018). Pesticide use in Indian agriculture: Trends, market structure and policy issues

Sudhaik, A., Raizada, P., Thakur, S., Saini, R. V., Saini, A. K., Singh, P., ... & Asiri, A. M. (2020). Synergistic photocatalytic mitigation of imidacloprid pesticide and antibacterial activity using carbon nanotube decorated phosphorus doped graphitic carbon nitride photocatalyst. *Journal of the Taiwan Institute of Chemical Engineers*, *113*, 142-154.

Sultan, M., Hamid, N., Junaid, M., Duan, J. J., & Pei, D. S. (2023). Organochlorine pesticides (OCPs) in freshwater resources of Pakistan: A review on occurrence, spatial distribution and associated human health and ecological risk assessment. *Ecotoxicology and Environmental Safety*, *249*, 114362.

Sun, L., Du, T., Hu, C., Chen, J., Lu, J., Lu, Z., & Han, H. (2017). Antibacterial activity of graphene oxide/g-C3N4 composite through photocatalytic disinfection under visible light. *ACS Sustainable Chemistry & Engineering*, *5*(10), 8693-8701.

Sun, M., Zhao, Q., Du, C., & Liu, Z. (2015). Enhanced visible light photocatalytic activity in BiOCl/SnO_2: heterojunction of two wide band-gap semiconductors. *Rsc Advances*, *5*(29), 22740-22752.

Swedha, M., Alatar, A. A., Okla, M. K., Alaraidh, I. A., Mohebaldin, A., Aufy, M., ... & Khan, S. S. (2022). Graphitic carbon nitride embedded Ni_3 (VO_4) 2/$ZnCr_2O_4$ Z-scheme photocatalyst

for efficient degradation of p-chlorophenol and 5-fluorouracil, and genotoxic evaluation in Allium cepa. *Journal of Industrial and Engineering Chemistry*, *112*, 244-257.

Syafrudin, M., Kristanti, R. A., Yuniarto, A., Hadibarata, T., Rhee, J., Al-Onazi, W. A., ... & Al-Mohaimeed, A. M. (2021). Pesticides in drinking water—a review. *International journal of environmental research and public health*, *18*(2), 468.

Tang, M., Ao, Y., Wang, C., & Wang, P. (2020). Facile synthesis of dual Z-scheme g-C_3N_4/Ag_3PO_4/AgI composite photocatalysts with enhanced performance for the degradation of a typical neonicotinoid pesticide. *Applied Catalysis B: Environmental*, *268*, 118395.

Tang, R., Gong, D., Deng, Y., Xiong, S., Zheng, J., Li, L., ... & Zhao, J. (2022). π-π stacking derived from graphene-like biochar/g-C_3N_4 with tunable band structure for photocatalytic antibiotics degradation via peroxymonosulfate activation. *Journal of Hazardous Materials*, *423*, 126944.

Teramura, K., Tanaka, T., Kani, M., Hosokawa, T., & Funabiki, T. (2004). Selective photo-oxidation of neat cyclohexane in the liquid phase over V_2O_5/Al_2O_3. *Journal of Molecular Catalysis A: Chemical*, *208*(1-2), 299-305.

The Hindu, 27 july,2020 https://www.thehindu.com/news/national/telangana/centre-urged-to-rethink-on-ban-of-pesticides/article32203800.ece

The Hindu, 25 Jan 2020) https://www.thehindu.com/business/pesticide-sector-hit-by-input-issues/article31043301.ece

The Hindu,16 Nov 2021, https://www.thehindu.com.

The Hindu,2005, https://www.thehindu.com

Theriot, C. M., & Grunden, A. M. (2011). Hydrolysis of organophosphorus compounds by microbial enzymes. *Applied Microbiology and Biotechnology*, *89*, 35-43.

Thrasher, J. D., Heuser, G., & Broughton, A. (2002). Immunological abnormalities in humans chronically exposed to chlorpyrifos. *Archives of Environmental Health: An International Journal*, *57*(3), 181-187.

Tiwari, D. K., Behari, J., and Sen, P. 2008. Application of nanoparticles in wastewater treatment. World Applied Sciences Journal. 3(3):417-433.

TOBIN, J. S. (1970). Carbofuran: a new carbamate insecticide. *Journal of Occupational Medicine*, *12*(1), 16-19.

Toole, G. and Toole, S. 1995 Understanding biology. 3rd ed. Stanley Thomes, Cheltenham, UK.

Ullah, I., Ali, S., Hanif, M. A., & Shahid, S. A. (2012). Nanoscience for environmental remediation: A Review. *International Journal of Chemical and Biochemical Sciences*, *2*(1), 60-77.

Ündeger, U. and Basaran N. 2005. Effects of pesticides on human peripheral lymphocytes in vitro: induction of DNA damage. Arch Toxicol. 79: 169-76

Vale, A., & Lotti, M. (2015). Organophosphorus and carbamate insecticide poisoning. *Handbook of clinical neurology*, *131*, 149-168.

Varma, R., & Varma, D. R. (2005). The Bhopal disaster of 1984. *Bulletin of Science, Technology & Society*, *25*(1), 37-45.

Vellaichamy, B., Periakaruppan, P., Arumugam, R., Sellamuthu, K., & Nagulan, B. (2018). A novel photocatalytically active mesoporous metal-free PPy grafted MWCNT nanocomposite. *Journal of colloid and interface science*, *514*, 376-385.

Verma, N., & Bhardwaj, A. (2015). Biosensor technology for pesticides—a review. *Applied biochemistry and biotechnology*, *175*, 3093-3119.

Vignesh, S., Suganthi, S., Srinivasan, M., Tamilmani, A., Sundar, J. K., Gedi, S., ... & Raza, M. K. (2022). Investigation of heterojunction between α-Fe_2O_3/V_2O_5 and g-C_3N_4 ternary nanocomposites for upgraded photo-degradation performance of mixed pollutants: efficient dual Z-scheme mechanism. *Journal of Alloys and Compounds*, *902*, 163705.

Vigneshwaran, S., Preethi, J., & Meenakshi, S. (2019). Removal of chlorpyrifos, an insecticide using metal free heterogeneous graphitic carbon nitride (g-C_3N_4) incorporated chitosan as

catalyst: Photocatalytic and adsorption studies. *International journal of biological macromolecules*, *132*, 289-299..

Vora, J. J., Chauhan, S. K., Parmar, K. C., Vasava, S. B., Sharma, S., & Bhutadiya, L. S. (2009). Kinetic study of application of ZnO as a photocatalyst in heterogeneous medium. *E-Journal of Chemistry*, *6*(2), 531-536.

Vyas, N. B., Spann, J. W., Hulse, C. S., Bauer, W., & Olson, S. (2005). From the Field: Carbofuran detected on weathered raptor carcass feet. *Wildlife Society Bulletin*, *33*(3), 1178-1182.

Wachter, N., Aquino, J. M., Denadai, M., Barreiro, J. C., Silva, A. J., Cass, Q. B., ... & Bocchi, N. (2019). Optimization of the electrochemical degradation process of the antibiotic ciprofloxacin using a double-sided β-PbO_2 anode in a flow reactor: kinetics, identification of oxidation intermediates and toxicity evaluation. *Environmental Science and Pollution Research*, *26*, 4438-4449.

Waghmare, C. S., Nigam, M., Mishra, P. K., & Patel, S. (2014). The Study of Investigational Profile of Common Pesticide Poisoning Cases admitted at SAIMS, Indore. *Journal of Indian Academy of Forensic Medicine*, *36*(1), 52-54.

Waheed, A., Baig, N., Ullah, N., & Falath, W. (2021). Removal of hazardous dyes, toxic metal ions and organic pollutants from wastewater by using porous hyper-cross-linked polymeric materials: A review of recent advances. *Journal of Environmental Management*, *287*, 112360.

Wan, Y., Tran, T. M., Nguyen, V. T., Wang, A., Wang, J., & Kannan, K. (2021). Neonicotinoids, fipronil, chlorpyrifos, carbendazim, chlorotriazines, chlorophenoxy herbicides, bentazon, and selected pesticide transformation products in surface water and drinking water from northern Vietnam. *Science of the Total Environment*, *750*, 141507.

Wang, A., Cockburn, M., Ly, T. T., Bronstein, J. M., & Ritz, B. (2014). The association between ambient exposure to organophosphates and Parkinson's disease risk. *Occupational and environmental medicine*, *71*(4), 275-281.

Wang, D. M. (2016). Environmental protection in clothing industry. In *Sustainable development: proceedings of the 2015 International Conference on sustainable development (ICSD2015)* (pp. 729-735).

Wang, F., Xu, J., Wang, Z., Lou, Y., Pan, C., & Zhu, Y. (2022). Unprecedentedly efficient mineralization performance of photocatalysis-self-Fenton system towards organic pollutants over oxygen-doped porous g-C_3N_4 nanosheets. *Applied Catalysis B: Environmental*, *312*, 121438.

Wang, G., Chen, Q., Liu, Y., Ma, D., Xin, Y., Ma, X., & Zhang, X. (2018). In situ synthesis of graphene/WO_3 co-decorated TiO_2 nanotube array photoelectrodes with enhanced photocatalytic activity and degradation mechanism for dimethyl phthalate. *Chemical Engineering Journal*, *337*, 322-332..

Wang, H., Casalongue, H. S., Liang, Y., & Dai, H. (2010). Ni (OH) 2 nanoplates grown on graphene as advanced electrochemical pseudocapacitor materials. *Journal of the American Chemical Society*, *132*(21), 7472-7477.

Wang, H., Liang, Y., Liu, L., Hu, J., & Cui, W. (2018). Highly ordered TiO_2 nanotube arrays wrapped with g-C_3N_4 nanoparticles for efficient charge separation and increased photo electrocatalytic degradation of phenol. *Journal of hazardous materials*, *344*, 369-380..

Wang, J. Li, L. Wu, et al., MnO_2 and carbon nanotube co-modified C_3N_4 composite catalyst for enhanced water splitting activity under visible light irradiation, Int. J. Hydrogen Energy 41 (48) (2016) 22743–22750.

Wang, J., & Zhuan, R. (2020). Degradation of antibiotics by advanced oxidation processes: An overview. *Science of the Total Environment*, *701*, 135023.

Wang, J., Cong, J., Xu, H., Wang, J., Liu, H., Liang, M., ... & Yao, J. (2017). Facile gel-based morphological control of Ag/g-C_3N_4 porous nanofibers for photocatalytic hydrogen generation. *ACS Sustainable Chemistry & Engineering*, *5*(11), 10633-10639.

Wang, J., Zhuan, R., & Chu, L. (2019). The occurrence, distribution, and degradation of antibiotics by ionizing radiation: an overview. *Science of the Total Environment*, *646*, 1385-1397.

Wang, J.; Feng, H.; Tang, L.; Zeng, G.; Chen, H.; Yu, M.; Zhang, H. Chapter 6-Nanohybrid Photocatalysts for Recalcitrant Organic Pollutant Degradation. In *Nanohybrid and*

Nanoporous Materials for Aquatic Pollution Control; Tang, L., Ed.; Elsevier: Amsterdam, The Netherlands, 2019; pp. 155–200.

Wang, M., Liu, J., Guo, C., Gao, X., Gong, C., Wang, Y., ... & Sun, L. (2018). Metal–organic frameworks (ZIF-67) as efficient cocatalysts for photocatalytic reduction of CO_2: the role of the morphology effect. *Journal of Materials Chemistry A*, *6*(11), 4768-4775.s

Wang, N., Li, J., Wu, L., Li, X., & Shu, J. (2016). MnO2 and carbon nanotube co-modified C_3N_4 composite catalyst for enhanced water splitting activity under visible light irradiation. *International Journal of Hydrogen Energy*, *41*(48), 22743-22750.

Wang, Q., Chen, X., Tian, J., Wei, L., Liu, Y., & Yang, C. (2020). The preparation of S-SnO_2/ g-C_3N_4 heterojunction and its photocatalytic degradation of phenol and trichlorophenol. *Journal of Materials Science: Materials in Electronics*, *31*, 16991-17002.

Wang, Q., Yang, J., Li, C., Xiao, B., & Que, X. (2013). Influence of initial pesticide concentrations in water on Chlorpyrifos toxicity and removal by Iris pseudacorus. *Water Science and Technology*, *67*(9), 1908-1915.

Wang, W., Fang, J., Shao, S., Lai, M., & Lu, C. (2017). Compact and uniform TiO_2@ g-C_3N_4 core-shell quantum heterojunction for photocatalytic degradation of tetracycline antibiotics. *Applied Catalysis B: Environmental*, *217*, 57-64.

Wang, W., Wang, J., Wang, Z., Wei, X., Liu, L., Ren, Q., ... & Shi, H. (2014). p–n junction CuO/$BiVO_4$ heterogeneous nanostructures: synthesis and highly efficient visible-light photocatalytic performance. *Dalton Transactions*, *43*(18), 6735-6743.

Wang, X. J., Yang, W. Y., Li, F. T., Xue, Y. B., Liu, R. H., & Hao, Y. J. (2013). In situ microwave-assisted synthesis of porous N-TiO_2/ g-C_3N_4 heterojunctions with enhanced visible-light photocatalytic properties. *Industrial & Engineering Chemistry Research*, *52*(48), 17140-17150.

Wang, X., Blechert, S., Antonietti, M., 2012. Polymeric graphitic carbon nitride for heterogeneous photocatalysis. ACS Catal. 2, 1596–1606.

Wang, X., Liu, G., Chen, Z. G., Li, F., Lu, G. Q. M., & Cheng, H. M. (2009). Efficient and stable photocatalytic H_2 evolution from water splitting by (Cd0. 8Zn0. 2) S nanorods. *Electrochemistry communications*, *11*(6), 1174-1178.

Wang, X., Maeda, K., Chen, X., Takanabe, K., Domen, K., Hou, Y., ... & Antonietti, M. (2009). Polymer semiconductors for artificial photosynthesis: hydrogen evolution by mesoporous graphitic carbon nitride with visible light. *Journal of the American Chemical Society*, *131*(5), 1680-1681.

Wang, X., Maeda, K., Thomas, A., Takanabe, K., Xin, G., Carlsson, J.M., Domen, K., Antonietti, M., 2009. A metal-free polymeric photocatalyst for hydrogen production from water under visible light. Nat. Mater. 8, 76–80.

Wang, Y., Qiu, L., Ranson, H., Lumjuan, N., Hemingway, J., Setzer, W. N., ... & Chen, L. (2008). The structure of an insect epsilon class glutathione S-transferase from the malaria vector Anopheles gambiae provides an explanation for the high DDT-detoxifying activity. *Journal of structural biology*, *164*(2), 228-235.

Watts, M. (2012). Chlorpyrifos as a possible global POP. *Pesticide Action Network North America, Oakland, CA. www. Pan-Europe. info/News/PR/121009_Chlorpyrifos_as_POP_final. pdf*.

Wei, H., Zhang, Q., Zhang, Y., Yang, Z., Zhu, A., & Dionysiou, D. D. (2016). Enhancement of the Cr (VI) adsorption and photocatalytic reduction activity of g-C_3N_4 by hydrothermal treatment in HNO_3 aqueous solution. *Applied Catalysis A: General*, *521*, 9-18.

Wei, M.; Gao, L.; Li, J.; Fang, J.; Cai, W.; Li, X.; Xu, A. Activation of peroxymonosulfate by graphitic carbon nitride loaded on activated carbon for organic pollutants degradation. *J. Hazard. Mater.* **2016**, *316*, 60–68.

Wei, W. D., Liu, X. Y., Cui, S. C., & Liu, J. G. (2017). Loading of Co_3O_4 onto Pt-modified nitrogen-doped TiO_2 nanocomposites promotes photocatalytic hydrogen production. *RSC advances*.

Wei, X., Wu, H., He, G., & Guan, Y. (2017). Efficient degradation of phenol using iron-montmorillonite as a Fenton catalyst: Importance of visible light irradiation and intermediates. *Journal of Hazardous Materials*, *321*, 408-416.

Wei, Z., Xinyue, T., Xiaomeng, W., Benlin, D., Lili, Z., Jiming, X., ... & Fengxia, Z. (2019). Novel pn heterojunction photocatalyst fabricated by flower-like $BiVO_4$ and Ag_2S nanoparticles: Simple synthesis and excellent photocatalytic performance. *Chemical Engineering Journal*, *361*, 1173-1181.

Wiklund, K., Dich, J., & Holm, L. E. (1987). Risk of malignant lymphoma in Swedish pesticide appliers. *British Journal of Cancer*, *56*(4), 505-508.

Wu, T., He, Q., Liu, Z., Shao, B., Liang, Q., Pan, Y., ... & Gong, S. (2022). Tube wall delamination engineering induces photogenerated carrier separation to achieve photocatalytic performance improvement of tubular g-C_3N_4. *Journal of Hazardous Materials*, *424*, 127177.

Xia, X., Xie, C., Xu, B., Ji, X., Gao, G., & Yang, P. (2022). Role of B-doping in g-C_3N_4 nanosheets for enhanced photocatalytic NO removal and H2 generation. *Journal of Industrial and Engineering Chemistry*, *105*, 303-312.

Xiaoqiang, C. H. U., Hua, F. A. N. G., Xuedong, P. A. N., Xiao, W. A. N. G., Min, S. H. A. N., Bo, F. E. N. G., & Yunlong, Y. U. (2008). Degradation of chlorpyrifos alone and in combination with chlorothalonil and their effects on soil microbial populations. *Journal of Environmental Sciences*, *20*(4), 464-469.

Xu, H., Xu, Y., Li, H., Xia, J., Xiong, J., Yin, S., ... & Wan, H. (2012). Synthesis, characterization and photocatalytic property of AgBr/BiPO 4 heterojunction photocatalyst. *Dalton transactions*, *41*(12), 3387-3394.

Xu, H., Yan, J., Xu, Y., Song, Y., Li, H., Xia, J., ... & Wan, H. (2013). Novel visible-light-driven AgX/graphite-like C3N4 (X= Br, I) hybrid materials with synergistic photocatalytic activity. *Applied Catalysis B: Environmental*, *129*, 182-193.

Xu, L., Huang, W. Q., Wang, L. L., Tian, Z. A., Hu, W., Ma, Y., ... & Huang, G. F. (2015). Insights into enhanced visible-light photocatalytic hydrogen evolution of g-C_3N_4 and highly reduced graphene oxide composite: the role of oxygen. *Chemistry of Materials*, *27*(5), 1612-1621.

Xue, J., Luo, Z., Li, P., Ding, Y., Cui, Y., & Wu, Q. A residue-free green synergistic antifungal nanotechnology for pesticide thiram by ZnO nanoparticles (2014). *Scientific Reports*, *4*.

Yadav, I. C., Devi, N. L., Syed, J. H., Cheng, Z., Li, J., Zhang, G., & Jones, K. C. (2015). Current status of persistent organic pesticides residues in air, water, and soil, and their possible effect on neighboring countries: a comprehensive review of India. *Science of the Total Environment*, *511*, 123-137.

Yadav, M., Shukla, A. K., Srivastva, N., Upadhyay, S. N., & Dubey, S. K. (2016). Utilization of microbial community potential for removal of chlorpyrifos: a review. *Critical reviews in biotechnology*, *36*(4), 727-742.

Yahiaoui, I., Aissani-Benissad, F., Fourcade, F., & Amrane, A. (2013). Removal of tetracycline hydrochloride from water based on direct anodic oxidation (Pb/PbO_2 electrode) coupled to activated sludge culture. *Chemical engineering journal*, *221*, 418-425.

Yang, Y., Guo, Y., Liu, F., Yuan, X., Guo, Y., Zhang, S., ... & Huo, M. (2013). Preparation and enhanced visible-light photocatalytic activity of silver-deposited graphitic carbon nitride plasmonic photocatalyst. *Applied Catalysis B: Environmental*, *142*, 828-837.

Ye, J., Yang, D., Dai, J., Li, C., Yan, Y., & Wang, Y. (2022). Strongly coupled cobalt/oxygen co-doped porous g-C_3N_4 heterostructure with abundant oxygen vacancies modulated the peroxymonosulfate activation pathway. *Chemical Engineering Journal*, *431*, 133972.

Yeganeh, M., Azari, A., Sobhi, H. R., Farzadkia, M., Esrafili, A., & Gholami, M. (2023). A comprehensive systematic review and meta-analysis on the extraction of pesticide by various solid phase-based separation methods: a case study of malathion. *International Journal of Environmental Analytical Chemistry*, *103*(5), 1068-1085.

Yu, C., Hou, J., Zhang, B., Liu, S., Pan, X., Song, H., ... & Xin, Y. (2022). In-situ electrodeposition synthesis of Z-scheme rGO/ g-C_3N_4/TNAs photoelectrodes and its degradation mechanism for oxytetracycline in dual-chamber photo electrocatalytic system. *Journal of Environmental Management*, *308*, 114615.

Yu, X., Wu, P., Qi, C., Shi, J., Feng, L., Li, C., & Wang, L. (2017). Ternary-component reduced graphene oxide aerogel constructed by g-C_3N_4/BiOBr heterojunction and graphene oxide with enhanced photocatalytic performance. *Journal of Alloys and Compounds*, *729*, 162-170.

Zangiabadi, M.; Saljooqi, A.; Shamspur, T.; Mostafavi, A.; Mehrabi, F.; Mohamadi, M. Efficient Degradation of Fenitrothion Pesticide and Reaction Mechanism with GO-Fe_3O_4/TiO_2 Mesoporous Photocatalyst under Visible Light Irradiation. *Pistachio Health J.* **2019**, *2*, 10–21.

Zeng, G., He, Z., Wan, T., Wang, T., Yang, Z., Liu, Y., ... & Pu, S. (2022). A self-cleaning photocatalytic composite membrane based on g-C_3N_4@ MXene nanosheets for the removal of dyes and antibiotics from wastewater. *Separation and Purification Technology*, *292*, 121037.

Zhang X, Jia X, Duan P, Xia R, Zhang N, Cheng B, et al. V_2O_5/P g-C_3N_4 Z-scheme enhanced heterogeneous photocatalytic removal of methyl orange from water under visible light irradiation. Colloids Surf A Physicochem Eng Asp 2021;608:125580

Zhang, A., Luo, W., Sun, J., Xiao, H., & Liu, W. (2015). Distribution and uptake pathways of organochlorine pesticides in the greenhouse and conventional vegetables. *Science of the Total Environment*, *505*, 1142-1147.

Zhang, C., Fei, W., Wang, H., Li, N., Chen, D., Xu, Q., ... & Lu, J. (2020). pn Heterojunction of BiOI/ZnO nanorod arrays for piezo-photocatalytic degradation of bisphenol A in water. *Journal of Hazardous Materials*, *399*, 123109.

Zhang, C., Jia, M., Xu, Z., Xiong, W., Yang, Z., Cao, J., ... & Jing, Y. (2022). Constructing 2D/2D N-ZnO/ g-C_3N_4 S-scheme heterojunction: Efficient photocatalytic performance for norfloxacin degradation. *Chemical Engineering Journal*, *430*, 132652.

Zhang, F., Wang, X., Liu, H., Liu, C., Wan, Y., Long, Y., & Cai, Z. (2019). Recent advances and applications of semiconductor photocatalytic technology. *Applied Sciences*, *9*(12), 2489.

Zhang, G., Wang, P., Lu, W. T., Wang, C. Y., Li, Y. K., Ding, C., ... & Cao, F. F. (2017). Co nanoparticles/Co, N, S tri-doped graphene templated from in-situ-formed Co, S Co-doped g-C_3N_4 as an active bifunctional electrocatalyst for overall water splitting. *ACS applied materials & Interfaces*, *9*(34), 28566-28576.

Zhang, W., Jiang, F., & Ou, J. (2011). Global pesticide consumption and pollution: with China as a focus. *Proceedings of the international academy of Ecology and environmental sciences*, *1*(2), 125.

Zhang, W., Zhou, L., Shi, J., & Deng, H. (2017). Fabrication of novel visible-light-driven AgI/g-C_3N_4 composites with enhanced visible-light photocatalytic activity for diclofenac degradation. *Journal of colloid and interface science*, *496*, 167-176.

Zhang, X., & Zhang, M. (2011). Modeling effectiveness of agricultural BMPs to reduce sediment load and organophosphate pesticides in surface runoff. *Science of the Total Environment*, *409*(10), 1949-1958.

Zhang, L., Du, L., Yu, X., Tan, S., Cai, X., Yang, P., ... & Mai, W. (2014). Significantly enhanced photocatalytic activities and charge separation mechanism of Pd-decorated ZnO–graphene oxide nanocomposites. *ACS applied materials & interfaces*, *6*(5), 3623-3629.

Zhang, Y., Hou, Y., Chen, F., Xiao, Z., Zhang, J., & Hu, X. (2011). The degradation of chlorpyrifos and diazinon in aqueous solution by ultrasonic irradiation: effect of parameters and degradation pathway. *Chemosphere*, *82*(8), 1109-1115.

Zhang, Y., Pan, Q., Chai, G., Liang, M., Dong, G., Zhang, Q., & Qiu, J. (2013). Synthesis and luminescence mechanism of multicolor-emitting g-C_3N_4 nanopowders by low-temperature thermal condensation of melamine. *Scientific reports*, *3*(1), 1-8.

Zhang, Y., Wu, J., Deng, Y., Xin, Y., Liu, H., Ma, D., & Bao, N. (2017). Synthesis and visible-light photocatalytic property of Ag/GO/ g-C_3N_4 ternary composite. *Materials Science and Engineering: B*, *221*, 1-9.

Zhang, Y.; Zhang, N.; Tang, Z.-R.; Xu, Y.-J. Graphene Oxide as a Surfactant and Support for In-Situ Synthesis of Au–Pd Nanoalloys with Improved Visible Light Photocatalytic Activity. *J. Phys. Chem. C* **2014**, *118*, 5299–5308.

Zhao, Z., Sun, Y., & Dong, F. (2015). Graphitic carbon nitride-based nanocomposites: a review. *Nanoscale*, *7*(1), 15-37.

Zheng, Q.; Durkin, D.P.; Elenewski, J.E.; Sun, Y.; Banek, N.A.; Hua, L.; Chen, H.; Wagner, M.J.; Zhang, W.; Shuai, D. Visible-Light-Responsive Graphitic Carbon Nitride: Rational Design and Photocatalytic Applications for Water Treatment. *Environ. Sci. Technol.* **2016**, *50*, 12938–12948.

Zhong, J., Huang, J., Liu, Y., Li, D., Tan, C., Chen, P., ... & Liu, G. (2022). Construction of double-functionalized g-C_3N_4 heterojunction structure via optimized charge transfer for the

synergistically enhanced photocatalytic degradation of sulfonamides and H_2O_2 production. *Journal of Hazardous Materials*, *422*, 126868.

Zhu, M., Chen, P., & Liu, M. (2011). Graphene oxide enwrapped Ag/AgX (X= Br, Cl) nanocomposite as a highly efficient visible-light plasmonic photocatalyst. *ACS nano*, *5*(6), 4529-4536.

Zhu, Q., Xu, Z., Qiu, B., Xing, M., & Zhang, J. (2021). Emerging cocatalysts on g-C_3N_4 for photocatalytic hydrogen evolution. *Small*, *17*(40), 2101070.

Zhuang, X. D., Chen, Y., Liu, G., Li, P. P., Zhu, C. X., Kang, E. T., ... & Li, Y. X. (2010). Conjugated-polymer-functionalized graphene oxide: synthesis and nonvolatile rewritable memory effect. *Advanced Materials*, *22*(15), 1731-1735.

Zou, X., Dong, Y., Li, S., Ke, J., Cui, Y., & Ou, X. (2018). Fabrication of V_2O_5/ g-C_3N_4 heterojunction composites and its enhanced visible light photocatalytic performance for the degradation of gaseous ortho-dichlorobenzene. *Journal of the Taiwan Institute of Chemical Engineers*, *93*, 158-165.

Zou, Y., Wang, X., Ai, Y., Liu, Y., Ji, Y., Wang, H., ... & Wang, X. (2019). Correction: β-Cyclodextrin modified graphitic carbon nitride for the removal of pollutants from aqueous solution: experimental and theoretical calculation study. *Journal of Materials Chemistry A*, *7*(18), 11539-11540.

Annexure

List of Publications

1. **Tabasum, S.,** Rani, S., Sharma, A., Dhupar, N., Singh, P. P., Bagri, U., & Kumar, D. (2023). Efficient Photocatalytic Degradation of Chlorpyrifos Pesticide from Aquatic Agricultural Waste Using g-C_3N_4 Decorated Graphene Oxide/V_2O_5 Nanocomposite. *Topics in Catalysis*, 1-12.
2. **Tabasum, S.,** Sharma, A., Rani, S., Chaudhary, S., Malik, A. Q., Kumar, D., & Deshpande, T. (2023). PROLIFIC FABRICATION OF LANTHANUM OXIDE WITH GRAPHITIC CARBON/GRAPHENE OXIDE FOR ENHANCING PHOTOCATALYTIC DEGRADATION OF CARBOFURAN FROM AQUEOUS SOLUTION. *Rasayan Journal of Chemistry*, *16*(2).
3. **Tabasum, S**., Rani, S., Thakur, A., Sindhu, M., Maan, K. S., Upasana, U., ... & Sharma, A. K. (2023, September). Photo-catalytic detoxification of chlorpyrifos pesticide from the aquatic environment using g-C_3N_4 doped with GO nano-composite. In *AIP Conference Proceedings* (Vol. 2800, No. 1). AIP Publishing.
4. Rani, S., Sharma, A., **Tabasum, S**., Malik, A. Q., Chaudhary, S., Kumar, D., ... & Singh, P. P. (2023). Highly Efficient Photocatalytic Properties of La-Doped ZnO over Pristine ZnO for Degradation of 2-Chlorophenol from Aquatic Agriculture Waste. *Chemistry Africa*, 1-10.
5. Rani, S., **Tabasum, S**., Sharma, A., Singh, P., Singh, P. P., Reehl, P., ... & Singh, H. (2023). Effects of Cu substitution on photocatalytic performance of ZnO nanorods synthesised via hydrothermal route for the degradation of chlorobenzene. *International Journal of Environmental Analytical Chemistry*, 1-13.
6. Malik, A. Q., **Tabasum, S.,** Rani, S., Lokhande, P., Singh, P. P., Mooney, J., ... & Kumar, D. (2023). Fluorescent CdS QDs Modified with Molecular Imprinted Polymer for the Photodegradation of Imidacloprid and Buprofezin Pesticides Under Visible Light. *Journal of Inorganic and Organometallic Polymers and Materials*, 1-17.

7. Vishwakarma, N., Sindhu, M., Maan, K. **S., Tabasum**, S., Rani, S., Patel, V., ... & Sharma, A. K. (2023, September). Preparation of vanadium oxide from various route of synthesis process for energy storage application. In *AIP Conference Proceedings* (Vol. 2800, No. 1). AIP Publishing.

Communicated:

1. **Sahima Tabasum**, Ajit Sharma, Suman Rani, E. Lokhande, Tushar Deshpandes: Synthesis and evaluation the performance of g-C_3N_4/GO/La_2O_3 photocatalyst for the efficient removal of insecticide using Continuous reactor, *Journal of Material Science: Materials in Electronics*

Presentation (Oral/Posters):

1. Poster presentation on topic 'Solar-catalytic Induced g-C_3N_4 with V_2O_5 Nanocomposite for Photocatalytic Mineralization of Chlorpyrifos from Agricultural Aquatic Waste' organized by CSIR-CSIO on 9-11-Oct-2022
2. Oral presentation on the Topic 'Light-driven photocatalytic degradation of Carbofuran using g-C_3N_4 doped with V_2O_5 nanocomposite' organized by Water innovation center: Technology, Research and Education and Asian Universities Alliance on December 1-2, 2022.
3. Oral presentation on the Topic 'photocatalytic detoxification of Chlorpyrifos using g-c3n4 doped with GO nanocomposite' Organized by department of Research Impact and Outcome, Lovely Professional University, on February 18-19,2022.
4. Poster presentation on topic 'Photo-catalytic induced g-C_3N_4 with V_2O_5 Nanocomposite for Photocatalytic Mineralization of Chlorpyrifos from Agricultural Aquatic Waste' Organized by International Association of Advanced of Materials on December 12-14,2022.
5. Poster presentation on topic Nano-structural modification of g-C_3N_4 with La_2O_3 nanocomposite for solar light induced photocatalytic mineralization of pesticides

organized by School of chemical Engineering and Physical Sciences, Lovely Professional University, on June 25-26 2021.

Workshops and Conferences (Participated/Attended):

1. Two days CSIR-NEERI Online skill/Training Program on Water Quality Monitoring and Management, organized by CSIR-National Environmental Engineering Research Institute (NEERI).
2. Worked on the Interdisciplinary School for Environmental Crisis (ISEC-2) project on Energy Production from Micro-Nuclear Reactor (20 MW) in **Euboea, Greece, Europe**